A MIXED INTEGER LINEAR UNIT COMMITMENT AND ECONOMIC DISPATCH MODEL FOR THERMO-ELECTRIC AND VARIABLE RENEWABLE ENERGY GENERATORS WITH COMPRESSED AIR ENERGY STORAGE: VERIFICATION AND APPLICATION USING DATA FROM THE IRISH GRID

Thomas Nikolakakis

Submitted in partial fulfillment of the requirements for the degree of Doctor of Philosophy in the Graduate School of Arts and Sciences

COLUMBIA UNIVERSITY
2017

ABSTRACT

A MIXED INTEGER LINEAR UNIT COMMITMENT AND ECONOMIC DISPATCH MODEL FOR THERMO-ELECTRIC AND VARIABLE RENEWABLE ENERGY GENERATORS WITH COMPRESSED AIR ENERGY STORAGE: VERIFICATION AND APPLICATION USING DATA FROM THE IRISH GRID

Thomas Nikolakakis

The objective of this PhD thesis is to create a Unit Commitment and Economic Dispatch (UCED) modelling tool that can used to simulate the deterministic performance of a power system with thermal and renewable generators and energy storage technologies. The model was formulated using mixed integer programing (MIP) on GAMS interface. A robust commercial solver by IBM (CPLEX) is used as solver. Emphasis on the development of the tool has been given on the following aspects.

a) Technical impacts of Variable Renewable Energy (VRE) integration. The UCED model developed in this thesis is a high resolution short-term dispatch model. It captures the variability of VRE power on the intra-hour level. In addition the model considers a large number of important real world, system, unit and policy constraints. Detailed representation of a power system allows for a realistic estimation of maximum penetration levels of VRE and the related technical impacts like cycling of generators (part-loading and number of start-ups).

b) CO2 emissions. High levels of VRE penetration can potentially increase consumption of fuel in thermal units per unit of electricity produced due to

increased thermal cycling. The dispatch of units in the UCED model is based on minimizing systemwide operational costs the most important of those being fuel, start-up costs and the cost of carbon. Fuel consumption is calculated using technical data from Input/Output curves of individual generators. The start-up cost is calculated based on times the generator units have been off and the energy requirement to bring the unit back to hot state. Thus dynamic changes on fuel consumption can be captured and reported.

c) Technical solutions to facilitate VRE integration. VRE penetration can be facilitated if appropriate solutions are implemented. Energy storage is an effective way to reduce the impact of RE variability. The UCED model includes an integrated Mixed Integer Linear (MILP) compressed air energy storage (CAES) simulation sub-model. Unlike existing CAES models, the new "Thermo-Economic" (TE) CAES model developed in this thesis uses technical data from major CAES manufacturers to model the dynamic effect of cavern pressure on both the compression and expansion sides during CAES operation. More specifically the TE model takes into account that a) a compressor discharges at a pressure equal to the back-pressure developed in the cavern at each moment, b) the speed of charging can be regulated through inlet guide vanes; higher charging speed can take place at the expense of additional power consumption, c) the maximum power output during expansion can be limited by the levels of cavern pressure; there is a threshold pressure level below which the maximum output decreases linearly with pressure.

Since it uses actual power curves to simulate CAES operation, the TE model can be assumed to be more accurate than conventional Fixed Parameter (FP) models that don't model dynamic effects of cavern pressure on CAES operation. The TE model in this thesis is compared with conventional FP models using historical market prices from the Irish electricity market. The comparison was based on the ability of a CAES unit to arbitrage energy for making profit in the Irish electricity market. More specifically a “Base” scenario was created that included the operation of a 270MW CAES unit with technical characteristics obtained from a major CAES manufacturer and assumed discharge time of 13hr. Various sensitivities on discharge time, natural gas prices and system marginal prices (SMPs) were modeled. An additional scenario was created to show the benefit on CAES profitability if the unit participated in both the energy and ancillary services markets. All scenarios were modeled using both the TE and FP CAES models.

The results showed that the most realistic TE model returns around 15% less profitability across more scenarios. The reduction in profitability grows to around 30% when the cavern volume (discharge time) is reduced to half (6 hours). The latter is related to the sensitivity of the TE model on cavern pressure that is being built faster when the volume is reduced. A CAES unit won’t get a positive net present value (NPV) in Ireland under any scenario unless SMPs are greatly increased. Thus, it was shown that that existing FP CAES models overestimate CAES profitability. More accurate models need to be used to estimate CAES profitability in deregulated markets. Additionally, it might deem necessary to create additional markets for energy storage units and increase the possible revenue sources and magnitude to facilitate an increase of storage capacity worldwide.

The second step of analysis involved the integration of the CAES and UCED models. The UCED model developed in this thesis was validated and applied using data from the Irish grid, a power system with more than 50 thermal generators. A vast of existent data was used to create a mathematical model of the Irish system. Such data include technical specifications and variables of thermal generators, maintenance schedules and historical solar, wind and demand data. The validation exercise was deemed successful since the UCED model simulated utilization factors of 45 out of 52 generators with an absolute difference between modeled and actual results on utilization factors of less than 6% (the absolute differences are called Delta in this thesis). In addition the results of validation exercise were compared with the results of a similar exercise where PLEXOS was the modelling tool and it was found that the results of the two models were similar for the vast majority of generators. More specifically, the PLEXOS model results showed higher deltas for the coal-fired generators compared to the UCED model. On the other hand the UCED model, reported higher delta values for peat-fired generators. The results of the PLEXOS model were slightly better for the gas-fired generators while both models reported deltas nearly zero for all oil and distillate-fired generators.

Finally the model was applied to study the benefits of energy storage in Ireland in 2020 when wind penetration is expected to reach 37% of total demand. The analysis involved the development of two groups of 3 scenarios each. In the first group the main scenario also called the “Reference” was used to simulate the short-term unit (30 min step) commitment within the Irish system without storage. The results of the reference scenario were compared with two additional scenarios that assumed the existence of one 270MW

CAES unit in Northern Ireland by 2020 (again the first scenario involved the TE and the second the FP CAES model). The results showed –when using the TE model- that the inclusion of one 270MW CAES unit in AI can help reduce wind curtailment by 88GWh, CO_2 emissions by 150,000 tonnes and system costs by €6 million per year. If an FP model had been used instead the reductions would be: wind curtailment by 108GWh, CO_2 emissions by 270,000 tonnes and annual system costs by €13 million. Two main conclusions can be obtained from the specific set of results. The first conclusion is that storage units have a financial benefit over the whole system. Thus, when a CAES unit operates to minimize the costs of the whole system can incur substantially more benefits compared to if the CAES unit operated to maximize the individual unit's profits as in the case presented earlier. The benefits of storage over the whole system should be accounted to make policy decisions and create incentives for investors to increase energy storage capacity in national grids. The second important conclusion is that existing CAES FP models overestimate the ability of a CAES unit to facilitate VRE penetration. More accurate TE models should be used to assess a unit's capability to increase system flexibility.

A second group of scenarios was created to simulate the benefit of CAES at even higher VRE penetration levels. In the second group the "Reference" scenario again, assumed no storage however, wind production was increased by 25%. Again the "Reference" was compared with two additional scenarios that assumed integration of 3x270MW=810MW of storage capacity in AI (one scenario used the TE model and the other the FP). The results for the TE model show that each of the 3 CAES units reduces wind curtailment by

188,000MWh, total system costs by €29 million and CO_2 emissions by 180,000 tonnes. The same reductions for the FP model are 217,000MWh of wind curtailment, €25.6 million on total system costs and 180,000 tonnes of CO_2. Thus, the results of the second group of scenarios show that as the installed capacity of both CAES and wind increases in Ireland a) the system-wide benefits of CAES increase and b) the differences on results between the TE and FP models become much smaller.

Table of Contents

LIST OF FIGURES

LIST OF TABLES

ACRONYMS

AI: All-Ireland

BETTA: British Electricity Trading and Transmission Arrangements

EDC: Economic Dispatch Calculation

CAISO: California Independent System Operator

CER: Commission for Energy Regulation

GB: Great Britain

IA: Interconnector Administrator

IWEA: Irish Wind Energy Association

IUs: Interconnector Units

LR: Lagrange Relaxation

MIP: Mixed Integer Programming

MISO: Midcontinent Independent System Operator

MSQ: Market Scheduled Quantity (MSQ)

NI: North Ireland

NIAUR: North Ireland Authority for Utility Regulation

NYISO: New York Independent System Operator

RoI: Republic of Ireland

SCED: Security Constrained Economic Dispatch

SEM: Single Electricity Market

SEMO: Single Energy Market Operator

SNSP: System Non-Synchronous Penetration

SRMC: Short-Term Marginal Cost

SMP: System Marginal Price

TSC: Trading and Settlement Code

TSO: Transmission System Operator

UC: Unit Commitment

Acknowledgements

First and foremost I would like to express my gratitude to my supervisor -professor Fthenakis- for his mentorship, encouragement and guidance as well as for offering me the opportunity to do research at the Center of Life Cycle Analysis and to walk through a long and wonderful experience that made me a better professional and person. This PhD thesis was funded by the Center of Life Cycle Analysis at Columbia University; additional support was provided by the Onassis and Gerontelis foundations. I am also grateful for the support of the members of my PhD defense committee Dr. Peter Schlosser (EEE), Dr. Robert Farrauto (EEE), Dr. Matthias Preindl (EE) and Dr. Li Ku (New York Power Authority).

I would also like to thank my colleagues at Columbia Rob Van Haaren, Marc Perez, Brendan Cleary, Thanasis Bourtsalas, Constantine Spanos and Angela Zheng for accompanying me into this journey, for being real friends and for giving me their constructive inputs throughout the PhD process. I also owe a big thank you to my friends Kostas and Sofia Alexandrou and Pantelis Pantelidis for being next to me during difficult and happy moments. A lot of gratitude I also feel for my supervisor at the World Bank, Debabrata Chattopadhyay for teaching me secrets of power systems planning and for being supportive during the period I was a professional and a student at the same time.

Last but most importantly, I would like to thank my parents and my brother. My family has supported me to every step of my life so far.

Dedication

I dedicate my thesis to my beloved grandmother Eleni, who passed away while I was a student and to my other grandmother Afrodite who is standing by me at the moment I am writing those words

Chapter 1 : Introduction

Solar and wind technologies have experienced significant cost reductions due to technology advances and economies of scale. At the moment 183 countries have RE generation targets and the PV and wind contributions in the global energy mix are only expected to grow. However, integrating relatively high levels of solar and wind based generation is challenging because both power sources introduce into a power system higher levels of a) demand variability and b) uncertainty. More specifically very high levels of PV and wind power can affect the economics of producing electricity as well as power system operations and system security, in the following manner:

1. Can disturb system marginal prices of electricity through a) bringing on line more expensive units (usually gas or oil fired) to balance demand variability and b) bringing on line units that are not necessarily the most economic just to ensure the power flows within the transmission network satisfy system constraints and reliability criteria (avoid overloading lines, maintain voltage within acceptable limits, deal with uncertainty related to forecasts of outputs from solar and wind).
2. Can increase system OPEX costs forcing thermal units operate away from their optimal generating points.
3. Can affect system CAPEX costs because additional investments are required for increased ancillary services requirements due to increased uncertainty levels.

However, there are technical solutions for dealing with VRE variability and uncertainty. One way is to reduce net-load variability and uncertainty by dispersing geographically PV and wind, taking advantage of PV and wind synergy at specific locations through implementing Demand Side Management (DSM) programs, and investing on smart grids. Another way to facilitate VRE integration is increasing grid flexibility through investing into more flexible generation like gas-fired units and investing on transmission projects to interconnect different grids or parts of the same grid to allow for a larger balance zone. Finally, there are hybrid solutions like energy storage. The solution choices depend on the characteristics of each power system, the time scale of operation of each solution and of course, on economics.

In this doctoral thesis a steady-state Unit Commitment and Economic Dispatch (UCED) model that simulates half-hourly grid operation and can be used to study the impacts of PV and wind integration on a power system is presented. More specifically, the thesis includes the development of a Mixed Integer Linear Optimization model on GAMS platform that uses the IBM CPLEX algorithm to optimize Unit Commitment of thermoelectric systems with renewable energy generation and energy storage solutions. It optimizes system operation having as an objective the minimization of the operational cost of the system considering a set of constraints like, reserve margin requirement, DC approximation for transmission power flows, ramp up/down and minimum up/down constraints, start-up costs, carbon pricing and carbon cap schemes. The model also uses a piece-wise linear approximation approach to simulate the Input/Output characteristics of thermal generators considering the effects of part-load operation on unit efficiency. The modeling approach is very similar to the approach used by major commercial power system planning models like PLEXOS and PSR that both use CPLEX as the underlying Mixed Integer Programming (MIP solver as well). The UCED model however, is the first that simulates thermo-economic operation of compressed air energy storage (CAES) units. It uses actual power curves from a major CAES manufacturer and a MIP approach to simulate the thermal characteristics of the compressor and expansion units. Thus it is possible to capture the economics or technical inefficiencies related to part-load operation of the compressor or due to built-up of significant levels of back-pressure in the cavern. The model optimizes CAES operation adjusting inlet guide vane valves to charge or discharge as fast as needed so that the whole system costs are minimized. A list of outputs of the model include: Hourly or half-hourly System Marginal Prices (SMPs), Power output per unit, fuel consumption, and CO2 emissions and operational and start-up costs. Finally, the model is applied using data from the Irish grid. The case of Ireland was chosen because of a) the existence of an aggressive VRE portfolio, b) the plans for integration of a CAES unit and c) the availability of relevant data needed for the validation and application of a UCED model.

This thesis is organized in the following manner:

- **In chapter 2**, basics of conventional power system operations like demand supply balancing and provision of ancillary services are introduced. Additional topics include basic characteristics of VRE technologies like variability and uncertainty of the output. The discussion focuses on impacts VRE integration introduces into power systems as well as most suitable technical solutions. Special focus is being given on CAES as an energy storage technology for mitigating impacts of VRE integration.

- **In chapter 3,** the MIP formulation of a CAES model that simulates operation based on power curves from a major CAES manufacturer for both the expansion and compression sides in introduced. The CAES model that was named "Thermo-Economic CAES" is integrated into a steady-state deterministic MIP UCED model the mathematical formulation of which is also introduced in the same chapter.
- **In Chapter 4** the context of Irish power sector is described together with historical and current demand growth and supply options. Additional topics include the structure and basic operations of the Single Electricity Market (SEM) of Ireland, the high voltage transmission network and most important active policy targets the Republic of Ireland (RoI) and North Ireland need to comply with.
- **In Chapter 5** I use data published by the Irish Commission for Energy Regulation (CER) to reproduce historical commitment of the Irish power fleet in order to validate the UCED model. Data used include, technical information of thermal generators, historical demand, wind and hydro data, historical generator availability data, historical power flows as well as historical system shadow prices all on a per half hourly basis.
- **In Chapter 6** historical Irish system marginal prices (SMPs) and operational reserve payment data are used to research the financial viability of a CAES unit performing energy arbitrage and providing reserve capacity in the SEM. The Thermo-Economic (TE) CAES model is compared with a conventional "Fixed Parameter" model (FP) that –unlike the TE model- does not consider constraints on

CAES operation imposed by the effect of cavern pressure on the turbine and compressor operation.

- **In Chapter 7** data from the CER and the Irish system operators EIRGRID and SONI are used to create a UCED model that represents the Irish power system in 2020. The model is applied to research the impact of an existing policy target for 40% wind penetration by 2020 on the power system. The analysis focuses on the levels of wind curtailment required for the system to operate safely and research if VRE integration impacts can be reduced if one or more CAES units are added into the system.

Chapter 2 : Impact of VRE on Power Systems

2.1Chapter introduction

The rapid development of wind- and solar- generating capacity is driven mainly by 1) government support of various policy goals such as environmental sustainability and energy diversity and 2) cost decline of PV and wind technologies. However, the integration of renewables comes with some challenges that need to be overcome. The challenges are related to the inherent characteristics of wind and solar resources namely intermittency and uncertainty. Such characteristics render power system operations more challenging. Thankfully there is a number of technical solutions that can be implemented to successfully integrate large amounts of variable sources into power systems.

2.2Main characteristics of VRE sources

Integrating very high-levels of PV and wind is challenging due to the characteristics of solar and wind resource. The main characteristics of VRE resources are:

- Resource variability: wind and solar electricity production only occurs when wind and solar resources are available. Solar and wind power outputs at a specific location cannot be controlled at will (non-dispatchable electricity) the same way as fossil fueled power which is highly controllable (dispatchable electricity).
- Uncertainty: Both wind and solar short-term resource variations cannot be perfectly predicted. There is always uncertainty on the amount of energy to be delivered from those sources over the next hour or next day (see figure 2-1).

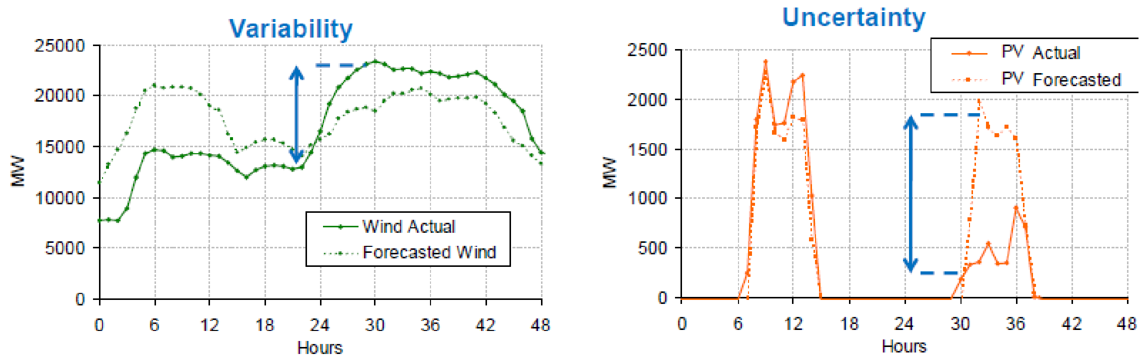

Figure 2-1: The figure above shows how wind and solar output can vary throughout a period of two days. The left picture gives emphasis on wind variability while the right on uncertainty of solar power. Wind resource can be indeed forecasted with a higher level of certainty. However it should be noted that PV variability can be more extreme when there are clouds in the sky(Source **[1]**)

Variability and unpredictability are very low in conventional systems since the output of thermal generation is controllable. At the same time power supply in a power system must match the demand at all times. This means that aggregated generation (VRE+thermal) must be "totally controllable" as a whole. For that reason solar and wind variability needs to be managed by the thermal generation fleet –and other resources in the system such as transmission and demand response, or storage– which adjusts their output to produce a controllable aggregated output. This process is managed by a number of grid operations. To explain the impact of VRE in a power system it is important to give some overview of basics of power system operations.

2.3 Basics of grid operation

Even though, the generation part of conventional grids is controllable there is uncertainty related to the load[1] that changes with time. There is also uncertainty in the availability of other elements in the grids. Generator and transmission lines can fail and systems are

---

[1] :The term demand or "load" defines the amount of electric power delivered or required at any specified point or points in a power system (see figure **3**)

generally design to deal with these situation. Variability of wind and solar adds to the complexity of operating interconnected power systems.

In its simplest form operating an interconnected power system can be reduced to a few tasks [2]:

1. Balance aggregate generation to aggregate load at all times maintaining frequency
    - Under normal conditions
    - Under contingency[2] conditions
2. Maintain voltages throughout the power system
    - Under normal conditions
    - Under contingency conditions
3. Avoid overloading system elements (transmission lines, generators, transformers)
4. Restart the system if it unavoidably collapses

The above tasks are being implemented through various system functions that can be largely grouped into two distinctive types of grid operations namely a) Energy operations and b) Ancillary services operations. Both types of operations occur along a multitude of time scales from seconds[3] to hours or even days.

Energy operations (or unit commitment and economic dispatch) have a role to balance energy supply and energy demand at all times. Since load is time dependent, the

---

[2] : A contingency is a sudden, unexpected loss of a generator or transmission element

[3] : It should be noted that names of different types of operations might be different in different power systems. Also, some systems might not incorporate all types of operations described in the section below. For example in some systems real-time energy operations are used for load following services and both-terms have the same meaning.

generating mix of a power system must incorporate flexible units with capabilities to fluctuate their output on a controllable way and track the varying part of the load (see figure 2-2).

The daily profile of the energy demand, also called the load, is composed of a constant and a variable part. The constant part defined by the minimum daily demand is called base-load and is met by a set of generators that run 24/7 at near rated power output. Base load generators have high capital and start-up costs and low operational costs and are usually, coal, nuclear and hydro generators. Another notable characteristic of base load generators is that they are technically constrained in their ability to vary their output (inflexible generators). The variable part of the demand can be split into an intermediate and a peak part. It is met by flexible generators able to track changes in demand (also called load-following units). Intermediate and peak generators have relatively low start-up and capital costs and higher operational costs. Such generators are usually gas, oil and hydro generators.

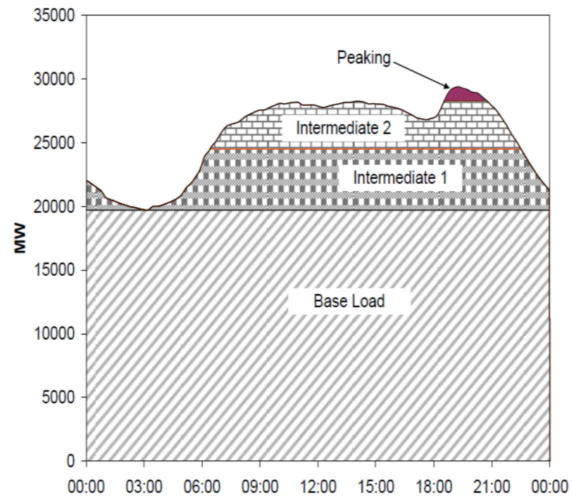

Figure 2-2*:* Explanation of base, intermediate and peak demand (source: **[2]**).

Given a power system with an existing generation fleet, energy operations schedule a) which power units will operate to supply base and variable demand and b) what will be the time varying power output of each unit thru the day. The former process is called Unit Commitment (UC) while the later Economic Dispatch (ED). Due to time varying nature of load, energy scheduling takes place during various time frames to manage uncertainties related to load forecasting. The largest portion of the demand that can be predicted with high accuracy is scheduled the day before (day-ahead dispatch). In addition to day-ahead services, some power systems also operate real-time energy markets to balance unanticipated differences (see ancillary services section). In vertically integrated power systems, energy dispatch is optimized through the use of sophisticated computing methods (see figure 2-3). In deregulated energy market generators bid for a least-cost participation in the energy planning process.

The unit commitment (UC) and economic dispatch (ED) algorithm decides the most economic day-ahead schedule of generators. It takes into account operational costs of generators like fuel cost and operational variable costs as well as start-up costs (transition costs). Additionally, the algorithm considers generator constraints-like the ramping capabilities, minimum amount of time required to start-up and allowable operational range- and transmission constraints. As an example, steam based coal fired generators require substantial amounts of energy to heat water to start from a cold state as opposed to SCGT that have higher operational but lower start-up costs. Thus the algorithm will schedule a coal power plant to supply base power while a SCGT for peak generation.	$Min \sum(operational\ cost_{jk} +\ transition\ cost_{jk})$ subject to $\sum_j generation_{jk} = demand_k$ $technical\ generator\ and\ transmission\ congestion\ constraints\ included$ where: j and k represent technology and time period

Figure 2-3: Explanation of least-cost thermal unit scheduling

Ancillary services have a role to provide the system operator with the resources needed to balance instantaneous generation and to ensure power system stability. Power system stability is the ability of an electric power system to regain a state of operating equilibrium-e.g. bring system voltage and frequency fast at acceptable levels- after a generator or transmission line fails.

1. **Frequency regulation**: Even a small mismatch between the actual and forecasted load can disturb the frequency of the grid that has to be maintained nearly constant to avoid mechanical damage of generators and transformers. Frequency regulation is being performed by a set of very fast responding oil and gas units that increase or decrease their output according to central signaling to balance real-time mismatch not captured by energy operations.
2. **Load Following**: It is an ancillary service used to ensure generation meets the varying portion of demand. Like in regulation, balancing occurs through an automated generator control (AGC) system. While both frequency regulation and

load following deal with forecasting errors, their fundamental differences is the time frame of operation. The former responds to rapid load fluctuations in the order of one minute or less, while the latter to slower changes in the order of 5 to 30 minutes (see figure 2-5). Another notable distinction is between load following and real-time energy operations. Both services operate at similar time frames. However, energy markets balance the difference between actual generation and day-ahead scheduled generation while the load following function ensures balancing the difference between actual generation and the demand.

3. **Contingency reserves**: In case of a contingency such as the loss of a large generator, a set of generation units must respond fast and for that reason they are synchronized with the grid (spinning) ready for action. The so-called spinning reserves are required to respond within a few minutes (usually 10 minutes) after a contingency occurs. Another set of fast responding units are unloaded (not synchronized) and are to respond within 10 minutes after a contingency and after spinning reserves have jumped in. Such units are called non-spinning reserves. Spinning and non-spinning reserves are also called contingency reserves. It is important to note that under normal conditions contingency reserves supply the system with available capacity, not with energy.

4. **Other services**: Other ancillary services include voltage control and black start. System frequency is regulated through real power injection while system voltage through reactive power injection. Voltage control equipment provides reactive power when necessary- for example after a generator fails. Black start service is being provided by generators that can start-up quickly without an external

electricity source. Their role is to restart the system fast in case of a major blackout.

Figure 2-4 shows how the energy and ancillary operations can be viewed from an energy and a capacity viewpoint. The energy example shows how the daily varying load is being balanced by the energy and load following operations. The day-ahead operations supply the largest portion and highly predictable energy demand. Load-following units, being more flexible supply intermediate demand. To avoid confusion it should be noted that base-load and peak energy generation is scheduled by energy operations. The instant forecasting error is being balanced by the units providing frequency regulation. The right figure shows the capacity required at a snapshot in time (peak hour) in that case. Contingency reserve units only provide available capacity and they are used only in the case of a contingency.

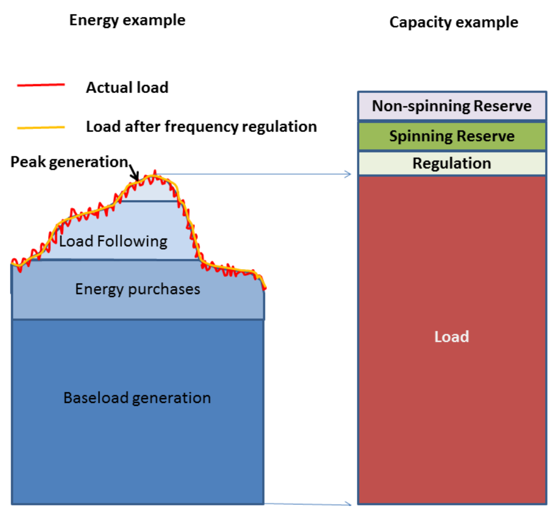

Figure 2-4: Energy and ancillary services from an energy and a capacity standpoint.

2.4 Impact of VRE integration on power system operations

The integration of VRE sources in a power system can be visualized as a reduction in the load, also called the net-load. Like in a conventional system, the net-load has to be managed by grid operations with the only difference that it is more variable and less predictable than the actual load (see figure 2-5).

Figure 2-5 shows the net-load (net load=actual load-VRE production) over a two week period using 2005 load data and 15GW spatially diverse wind data in the ERCOT. After wind penetration, system operations have to manage the net-load instead of the actual load. Wind integration increases a) the ramping rate, or the speed at which load following units must increase and increase their output, b) the ramping range, or the difference between minimum and maximum demand on daily basis and c) forecasting uncertainty.

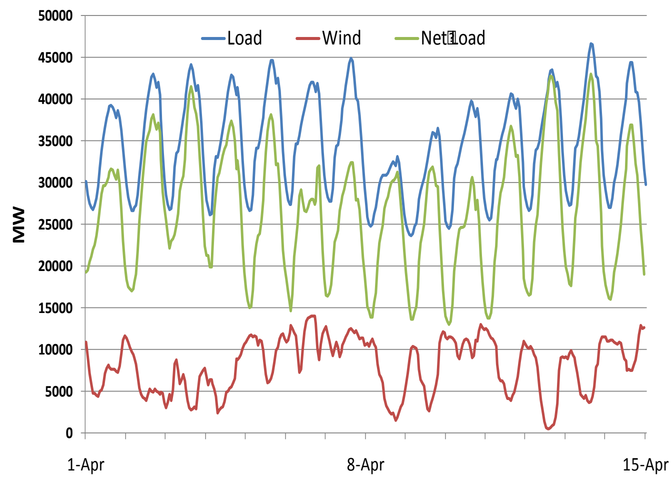

Figure 2-5: Impact of net-load from increased use of renewable energy (Source: **[3]**).

In general, the increased variability and unpredictability introduced into the system makes more challenging the task of the operator to balance supply and demand, maintain system reliability and stability. More specifically, large-scale VRE integration can cause:

- Increased need for flexible generation to provide operating reserves. This results to less efficient short-term dispatch because load-following and regulation units operate at part-load conditions potentially displacing more efficient and cheaper to operate base-load units.
- Increased need for contingency reserve capacity to deal with increased uncertainty and associated risks.
- Continuous cycling of intermediate, peak and in some cases base-load generators. Cycling causes wear and tear of mechanical equipment and results to reduced fuel efficiency.

- Frequent start-ups of peak and intermediate units.
- Large-scale concentrated injection of variable power. This can overload transmission lines and raise transmission upgrade issues.

The resulting total impact on the grid translates into additional cost to account for greater flexibility, ramping capability, operating reserves and transmission upgrades in the system.

This figure shows the impact of solar and wind penetration on a small system where the variable portion is being supplied by two Oil, two SCGT[4] and two CCGT[5] generators. The top figure shows the most economic dispatch schedule for one week. The variable section of the demand is being supplied mainly by the most economic CCGTs and only for a few hours, the less efficient gas generators jump in to supply peak demand. The bottom picture shows the same week where now PV and wind supply 49% of the variable portion of energy. The UC algorithm (see figure 4) now considers the net-load instead of the actual load. The resulting schedule is more expensive and less efficient than the no VRE scenario. Now CCGTs supply a much smaller portion of the demand due to technical/flexibility constraints. Gas generators supply a considerable portion of electricity while the oil generators- having the highest carbon footprint- jump in for a few hours. In general, PV and wind variability (black color in graph) causes frequent cycling of thermal generators and increases the number of start-ups.

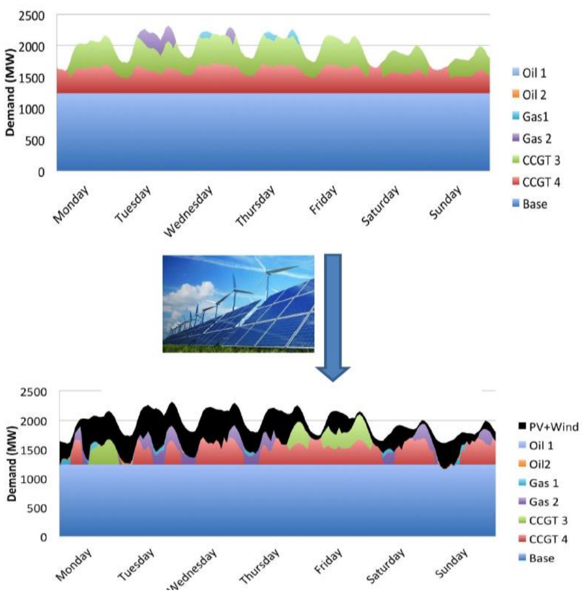

Figure 2-6: Impact of solar and wind variability on a small grid (Source: **[4]**).

[4] SCGT stands for Single Cycle Gas Turbine. SCGTs are conventional gas turbines. A typical efficiency of a SCGT is about 34%. SCGT are flexible and have low start-up costs. Thus, they are well suited for intermediate and peak generators.

[5] CCGT stands for Combined Cycle Gas Turbine: CCGT utilize the hot gas output to heat water and run a steam turbine. The result is increased thermal efficiency. CCGT can reach efficiencies of 60%. They are more expensive to start-up and less flexible than SCGT and thus they are used as base-load and intermediate generators.

2.5The path towards large scale VRE deployment

From the previous discussion it is clear that controlling/minimizing net load variability is an effective way to reduce the impact of VRE integration and its associated costs. Complementary solutions increase conventional system capabilities to balance the net-load.

1. **Reducing net-load variability**: Since *net load=actual load-VRE production*, one way to reduce net-load variability can happen through controlling the profile of the actual load through Demand Side Management (DSM). Another way is to reduce VRE profile variability. This can be done through geographic dispersion of VRE sources, combining solar and wind to take advantage of synergies, implementing ramp rate controls for PV and wind systems, implementing smart grids or simply by curtailing VRE (a more detailed explanation of all solutions is provided on next section).
2. **Increase system capabilities to balance net-load:** One way to do this is to increase the supply side flexibility of conventional generation (e.g. adding more hydro and gas units). Additional solutions include transmission expansion to connect neighboring grids and their operations to increase operational resources and thus the ability of system operators to dispatch units reliably and
3. **Solutions that fall within:** Energy storage is a very effective, yet still expensive, solution that fits both categories mentioned above. Also, smart grids include functions that fall in the region within.

From the discussion around the impact of VRE on grid operations three facts become eminent.

a) The first is that power systems vary. Every power system has its own capabilities to manage VRE integration. As a fact, larger power systems have more available options to increase their demand side and supply side flexibilities and thus more capable of dealing with high levels of VRE penetration. For example geographic dispersion of VRE is not a feasible form of action for a small isolated grid; similarly, it's not possible to add hydro if the resource is not available at the region.

b) The second fact is actions should be chosen following the most economic path according to figure 2-8. Currently, there are few countries with PV and wind penetration combined higher than 10%. However, as VRE penetration increases and power systems start feeling the impact, the cheapest solutions will be chosen first; those include DSM, geographic dispersion of PV and wind, and supply and reserve sharing. Such solutions are more proactive and increase a system's flexibility with minimum additions of new technical equipment. Increasing supply side flexibility and energy storage are more expensive solutions more appropriate at high levels of VRE integration.

c) The third fact is there is no single global solution to deal with VRE variability. Power system operations have their own response timeframes and so do solutions. Regulation units have to respond within seconds, load following within minutes while economic dispatch is scheduled hours before. PV systems are known to experience very sharp decreases of their output within seconds when a cloud passes over. Thus, large-scale PV integration can potentially impact very short term operations, like frequency regulation. Appropriate solutions would need to be able to either minimize very short-term net-load variability or increase system capabilities to respond within seconds. On the other hand, the short-term variation of wind would most likely impact load following operations. As an example, flywheels is a very fast energy storage technology appropriate for frequency regulation while pumped hydro is much better suited for load following but the opposite is not true. Thus, a set of solutions should be chosen depending on the needs of each system (see figure 2-8).

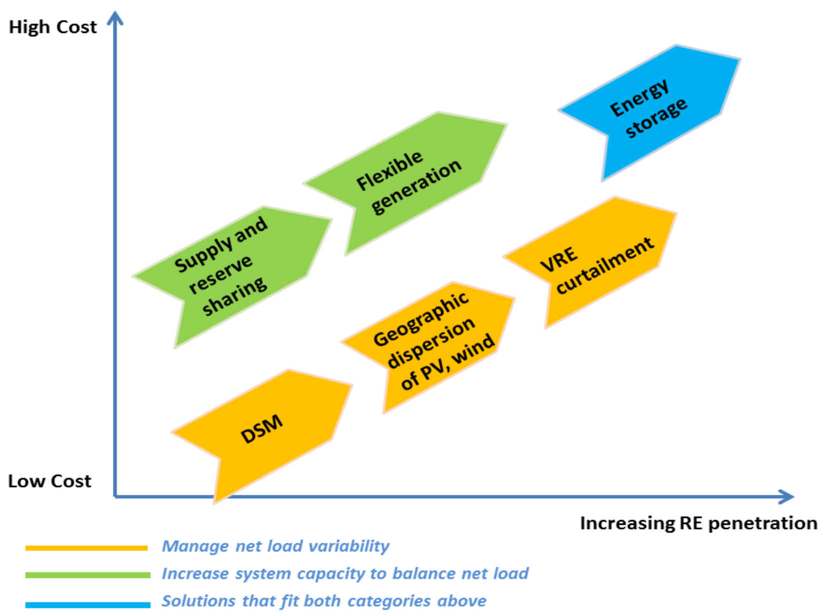

Figure 2-7: Solutions to the problem of VRE variability ranked from cheapest to most expensive (Source: **[3]**).

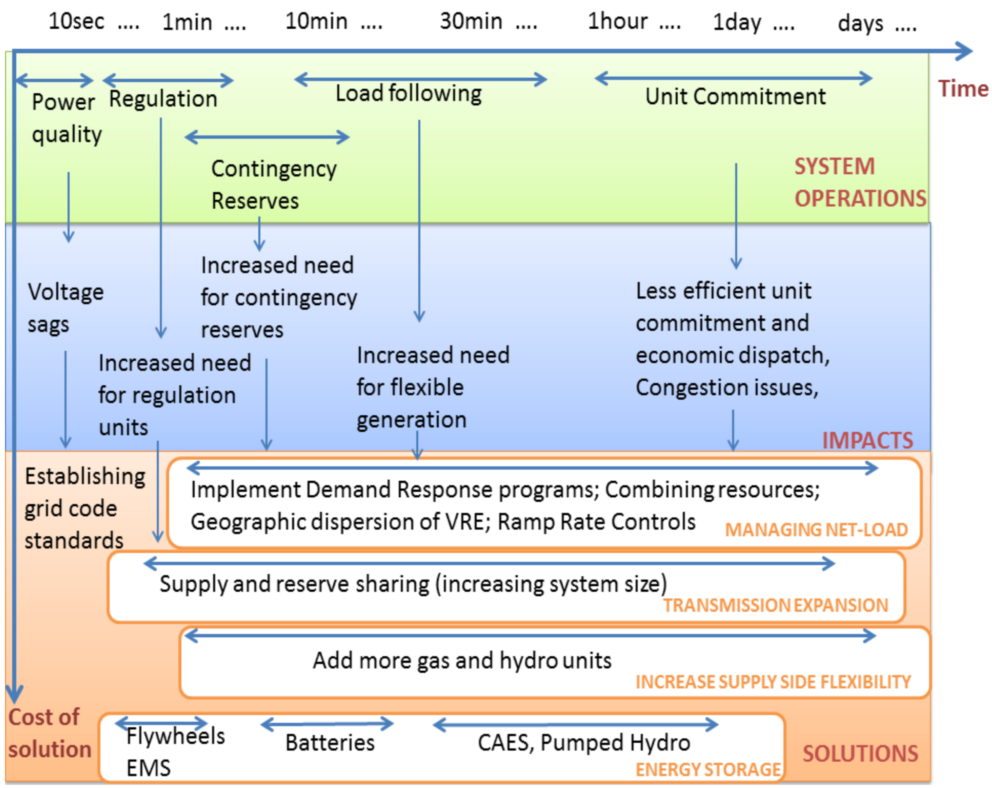

Figure 2-8: Solutions to the problem of VRE variability based on their operation timescale and cost of implementation. The green area highlights the time frames of system operations. The blue section shows the impacts of VRE integration on different system operations. Finally the orange area shows the time-scale of specific solutions while ranking them based on their cost. As an example adding pumped hydro power in a system can increase system flexibility and thus improve its ability for providing load-following and committing more efficiently its thermal units. Increasing system size through transmission expansion some-times can be a cheaper way to share supply and reserve assets that operate within the whole time spectrum (Source: Author).

An overview of all available solutions is given on the next section.

2.6 Technical solutions to facilitate VRE integration

2.6.1 Smart Grids

There is no global definition for a smart grid. It is a grid that incorporates smart solutions to achieve targeted sector goals that are specific to regional needs. Such a need can be VRE integration. A smart grid incorporates many of the solutions mentioned above. In general, it refers to an electricity network that uses digital and other advanced technologies to enable central control of various grid components as well as costumer participation. In conventional grids, utilities have had to send workers out to read meters, measure voltage and gather other types of useful data. In a smart grid, the components of the grid –variable and thermal generators, loads, wires, substations, transformers, even consumer appliances- have integrated sensors that carry data as well as two-way communication capabilities between the device and the utility's operations center. That way, the utility can adjust and control each device or millions of devices from a central location. Implementation of smart grids requires implementation of *grid codes/standards* to ensure VRE and other parts of grid quality and synergistic operation. Smart grids increase the efficiency, flexibility and intelligence of a power system and thus can help enable higher levels of VRE within a system. Some ways that smart grids can help VRE integration are [5]:

- Smart grids require implementation of grid codes/standards to ensure synergistic operations among grid components. Such codes promote manufacturing of reliable and smart PV and wind equipment that ensure safe and non-disruptive flow to the network while supporting system operations. As an example grid codes in Germany demand that medium voltage PV systems should be able to provide reactive control (voltage control) during a fault as well as reduce their output when the frequency is above 50.2 Hz.
- Increase supply side flexibility through promoting greater use controllable distributed generation like small-scale distributed PV with smart controls. Examples include reducing output or even disconnecting systems or tighter voltage

control to ensure reliability. Another example is controlling fast-changing outputs of PV systems that can violate ramping limits set by utilities (*ramp –rate control systems*).

- Increase demand side-flexibility through *demand response* (DR) programs. DR can be achieved through direct load control (DLC) or voluntary load reduction. In the latter case costumers can act synergistically with VRE to match supply and demand accurately. Another example of DLC enabling VRE is smart increase of the thermostat levels of a number of consumers in a cold night with very high wind penetration. In that case the extra wind power will be absorbed by heat loads instead of forcing base-load generators operate at non-optimal levels.
- Reduce operational impacts of VRE through incorporating short-term *solar and wind forecasting*. Day ahead and shorter term forecasting is already incorporated on large systems with renewables. Smart wind turbines incorporate very short-term (millisecond) wind forecasting (also called nowcasting) to optimize power output through dynamically adjusting the pitch of turbine blades. Short-term solar forecasting includes ground-based sky imaging to measure cloud speed and short-term output. In general, increasing a grid's forecasting capabilities can lead to *faster energy markets* and more flexible day-ahead and real-time dispatch [5].

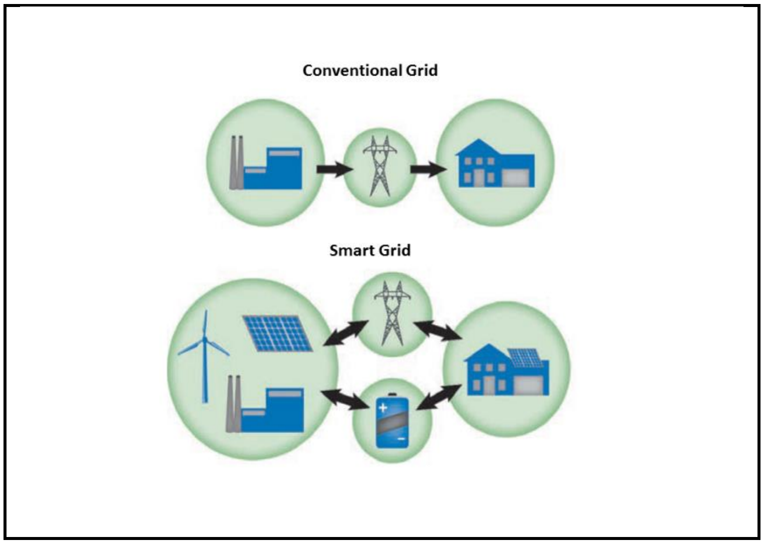

Figure 2-9: Conventional versus Smart Grid.

2.6.2 Reducing variability by combining different resources (the example of PV and wind synergy)

In many cases, there is a negative correlation between PV and wind resources: during night time and/or when the sky is cloudy, winds tend to be stronger, and solar power peaks in the summer while wind tends to peak in the winter. On the other hand, solar power peaks during the day, while wind tends to peak in the afternoon and night time. Thus, it is possible to combine appropriate capacities of wind and solar so that the combined power output will fluctuate around an average that resembles the demand curve. This is natural balancing.

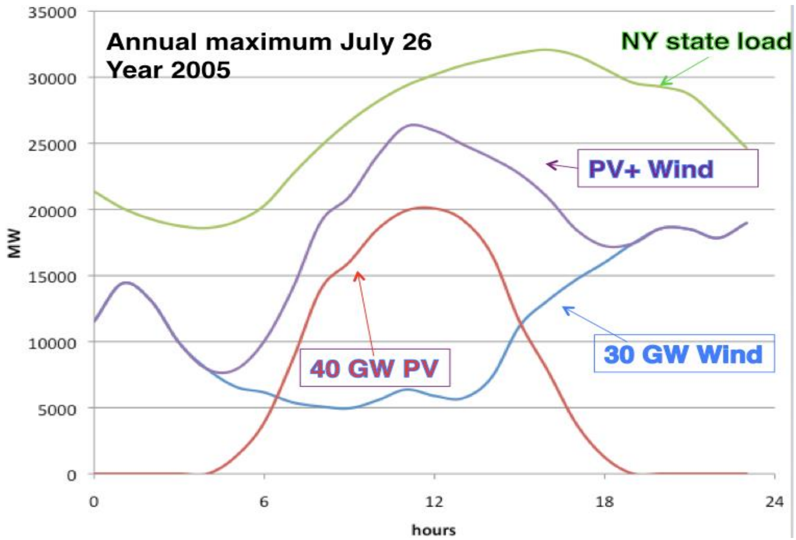

Figure 2-10. An example of how the combined output of PV and wind would match the load compared to if PV or wind would operate individually during the peak demand day of year 2005 in New York state (Source [4]).

2.6.4 Transmission expansion

The richest solar and wind renewable energy sites are often disperse across multiple locations that are also far away from consumption centers or existing transmission networks. Unlike power sources based on fossil fuels where planners have discretion on location, moving renewable plant sites reduces the quality of the resource. Therefore, renewable energy sources are very much site-constrained and, for this reason, transmission[6] networks need to be expanded to reach them (add source). In addition, transmission infrastructure is required to achieve geographic aggregation of VRE output. Detailed studies have shown that geographic dispersion of PV and wind can dramatically reduce the costs of their integration because the aggregated output is much less variable [6]. The

[6] This includes sub-transmission infrastructure as well. In some cases, like that of Brazil, both transmission and sub-transmission level investments are needed to connect renewables to the grid.

physical expansion of a grid (or interconnection with neighboring grids) can increase its flexibility through increasing its operational resources and capabilities.

2.6.5 Adding flexible generation

The speed at which energy can be delivered to the costumer is constrained by the limited ability of the mechanical equipment comprising power plants to ramp power -up or -down. The flexibility of a power system, that is, its ability to vary its output to meet the demand, depends on the mix of its generators. Most types of thermal generators heat water to produce steam and run power generating turbines. However natural gas turbines use air as the working fluid. Air can be heated faster than water and for that reason gas turbines can ramp-up and -down faster than most thermal types of generators. The same is true for hydro units that can increase and decrease their output fast through regulating pressure valves. Both types of units are appropriate for providing ancillary services or balancing the net-load and their deployment adds to the flexibility to the grid.

2.6.6 Energy storage

Energy storage can be used to enhance grid operations due to their very fast response times and high part-load efficiencies. Electric-storage technologies are differentiated by various attributes, such as rated power and discharge time. In general, there are three major categories of large-scale energy storage technologies: Power quality; bridging power; and energy management. Each category has specific application on grid operations based on its operation timescale as shown in table 1. In addition to enhancing grid operations, energy storage can be used to increase supply side flexibility. As an example Compressed Air Energy Storage (CAES) and pumped hydro can be used to store high wind output at night time when the demand is low and use it during peak hours to avoid running base-load generation at non-optimal levels and reduce need for peak generation. When directly coupled with VRE systems can help firm their output to a less variable one or even constant output.

Table 2-1: Categories of Electricity Storage Technologies (Sources: **[7]**, **[8]**).

Categories	**Applications**	**Operation Timescale**	**Technologies**
Power Quality	Frequency Regulation, Voltage Stability	Seconds to Minutes	Flywheels, Capacitors, Superconducting Magnetic Storage, Batteries
Bridging Power	Contingency Reserves, Ramping	Minutes to ~1 Hour	High Energy Density Batteries
Energy Management	Load Following, Capacity, Transmission &Distribution Deferral	Hours to Days	CAES, Pumped Hydro, High Energy Batteries

2.6.6.1 Compressed Air Energy Storage

In this thesis, increased focus is being given on modelling of compressed air energy storage technologies (CAES). CAES coverts grid electricity to mechanical energy in the form of compressed air stored in underground (or surface) reservoirs. The source of input energy can excess off-peak electricity, or renewable electricity coming from wind or solar farms. To convert stored energy back to electricity, the compressed air is released through a piping system into a turbine generator system after having been heated. When compression and expansion are rapid, the processes are near adiabatic; heat is generated during compression, and cooling occurs during expansion. The first is associated with large energy losses as compression to 70 atm can produce temperatures of about 1000oC, so necessitating cooling. For large CAEES plants, a large storage volume is required and underground reservoirs are the most economically viable solution. Such reservoirs can be a salt formation, an aquifer, or depleted natural gas field. When the volume confining the air is constant, pressure fluctuates throughout the compression cycle. Constant pressure operation in hard rock mined caverns is achievable by using a head of water applied by an aboveground reservoir. For smaller CAES plants (e.g., <5MW), air can be stored in above-ground metallic tanks or large onsite pipes, such as those designated for carrying natural gas under high pressure. A typical CAES power plant comprises a compression and a generation train connected through a motor/generator device. During the compression mode, electricity runs dynamic compressors that compress that compress air at pressures of 70 bars or more. Because of the high pressure ratio required, compression takes place in a series of stages separated by cooling periods. Cooling the air is necessary to reproduce power consumption and meet the cavern's volume requirements. The higher the number of stages, the greater the efficiency attained; however, this increases the cost of the system. During the expansion mode, motor operation stops and clutches engage the generation drive. Air is released to run the expanders after having first being heated in properly designed combustors. Heating the air assures high efficiency and avoids damaging of the turbomachinery due to low temperatures resulting from the rapid expansion of air and the Joule-Thompson effect. A recuperator sited after the exit from the expanders recovers some of the energy of the heated air before it is released to the atmosphere. Even though fuel is needed to run a CAES power plan, the input for a certain power capacity is around 65% less than the amount required to run a GT because around two-thirds of the energy produced by a GT is used to run its compressor. Thus, when the compressors are fed by renewable electricity, the emissions of a CAES power plant are 35% of those produced by a GT of the same capacity. Figure 2-12 is scheme of a typical CAES power plant.

Currently, two CAES power plants are operating. The world's first facility is the Huntorf CAES plant that has operated since 1978 in Bremen, Germany. It is a 290MW facility, designed to provide black-start services to nuclear power plants located nearby, along with spinning reserves and VAR support as well as cheap off-peak electricity. It stores up to 1000ps (68atm) in two depleted salt caverns located 2100 and 2600 feet under the ground; it offers up to 4h of power generation. The second CAES plant is an 110MW power plant operating in McIntosh, Alabama, since 1991. It pressurizes air up to 1100psi (75atm) and has electricity generation cycle of up to 26h between full charges. The McIntosh plant also has a heat recuperator in the expansion train that reduces fuel consumption by 25% compared to Huntorf plant that does not include recuperation.

Deregulation and the current structure of electricity markets now allow storage technologies to participate in the market and profit from their operation. As an example, the NYISO includes markets for installed capacity, energy, ancillary services, and transmission congestion contracts [9]. Two specific advantages of CAES power pants make them suitable for large scale, diurnal, multi-day and seasonal energy storage: a) CAES and pumped hydro are the only storage technologies that offer the high capacities (>100MW) for long periods and b) CAES has an approximately flat heat rate at part-load conditions.

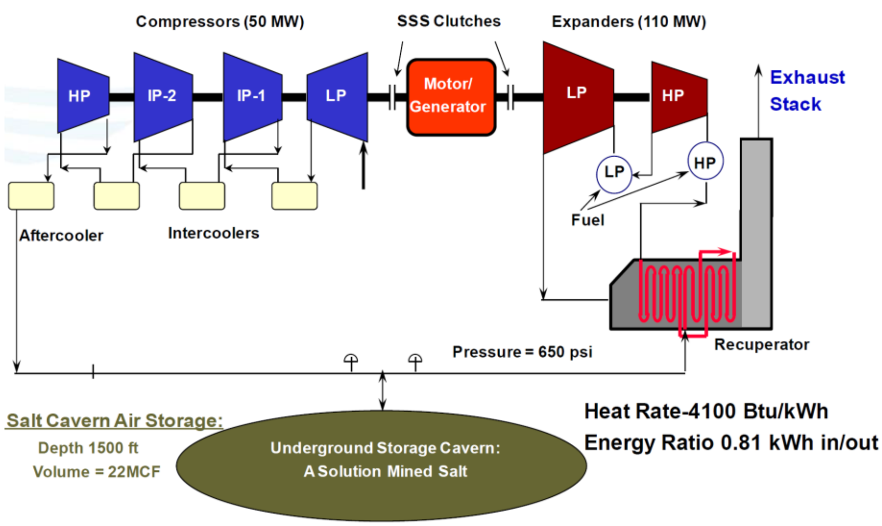

Figure 2-11: Mechanical parts of a typical CAES plant. Source: Energy Storage and Power LLC, presentation at CAES workshop at Columbia University, 2010.

Chapter 3 : Mathematical Formulation of a Deterministic Short-Term Unit Commitment Model for a Power System with Compressed Air Energy Storage (CAES)

This chapter presents the mathematical formulation of a Unit Commitment (UC) model with Compressed Air Energy Storage being part of the generation fleet. More specifically it describes the following:

- The mathematical formulation and solution strategies of a MIP deterministic unit commitment (UC) model for a thermal power system with solar, wind and hydro generators.
- Modeling generator flexibility in the UC model, taking into account changes into efficiency of generators at part load conditions.
- A “Fixed Parameter” (FP) MIP model of a Compressed Air Energy Storage (CAES) unit with constant electrical and thermal efficiencies performing energy arbitrage as well as providing ancillary services (reserve capacity).
- A “Thermo-Economic” (TE) MIP model of a CAES unit with variable electrical efficiency performing energy arbitrage. Unlike other existing CAES models, the model developed in this thesis uses technical information from a major CAES manufacturer to describe the effect of cavern pressure on the compression and expansion sides of the CAES unit. The TE model also has an objective or maximize its profit through energy arbitrage and providing ancillary services.

- An integration of the UC and "Thermo-Economic" CAES models to produce a least-cost short-term dispatch MIP model for a deterministic system with thermal units, renewables and "Thermo-Economic CAES. The CAES unit supports the system in its operation and the objective of the model is to minimize the total system costs. Unlike the arbitrage model the CAES unit does not operate to maximize its individual profit taking advantage electricity price differences but rather for the economic welfare of the whole system. The operation of CAES supports a) peak shaving through storing cheap base-load electricity to replace expensive peak load units, b) penetration of renewables through smoothening variability of wind and solar electricity and minimizing the need for expensive curtailment and c) system reliability through minimizing the risk of existence of unmet demand.

The verification of the UC-CAES model using data from the Irish system is discussed in chapter 5 and case studies are discussed in chapter 7.

3.1. Introduction

Since generators cannot turn-on instantly to produce power their operation needs to be scheduled ahead of time. Such scheduling usually takes place in advance of the operating day. In modern utilities, the scheduling of generators is calculated with making use of optimization software that solves the so called Unit Commitment and Economic Dispatch (UCED).

The goal of the UCED problem is to choose a control strategy to minimize economic losses or maximize profit subject to a set of system constraints. UCED scheduling is a short-term power system planning/optimization strategy as shown in figure 3.1 below. The algorithms presented in this thesis represent steady state operation. The time step changes in the system are of the order of 30 minutes and the optimization period one week. The operational times have been chosen based on data availability for the model application described in chapters 5, 6 and 7. Very short-term changes in the system in the order of a few seconds (or less) are handled by dynamic and transient systems controls. Dynamic modeling is beyond the scope of this PhD thesis. The UCED is a combination of two calculations to be discussed below, the Economic Dispatch Calculation (EDC) and the Unit Commitment calculation (UC).

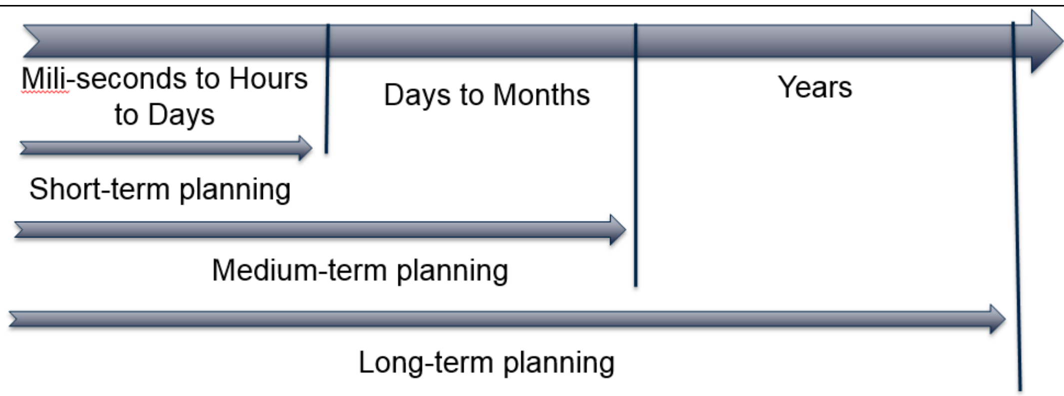

Short-term utility planning:

- Deals with day ahead operations like energy scheduling (security constrained dispatch) and ancillary service (load following, frequency regulation, contingency reserves etc)

Medium-term utility planning:

- Set of decisions that affect short-term planning but are taken before the setting of day ahead planning. Examples of such decisions can be maintenance schedules for generation and transmission, best use of technology with limited use (e.g subject to environmental rules), pooling with neighboring grids etc

Long-term utility planning:

- Generation and transmission expansion to meet growing demand over a large period of time subject to cost minimization and reliability

Figure 3-1: Types of power systems planning based on optimization cycle length.

3.2. The Economic Dispatch (ED) problem

The economic dispatch calculation (EDC) is performed to schedule a set of online generating units[7]. Unlike the UC problem, the EDC calculation is a snapshot in time and it assumes the scheduling of the units has already decided. The output of the calculation is the amount of power that each unit needs to produce at a specified point in time to balance the demand but not which units will operate (assuming a generation fleet). As the electricity demand changes with time the EDC calculation is performed multiple times to adjust the output of the units for the minimum impact on generation costs. The ECD is a mathematical optimization calculation with a specific objective. The objective of the EDC calculation depends on the electricity market environment. In a monopolistic environment, the utility performs the EDC for the entire area by itself having an objective to minimize operational costs subject to operational constraints. In a decentralized market the objective depends on the market structure. It might be taking place by a specific GENCO having an objective to maximize its profits given the prices, demands and costs. In a power pool the ISO (or other central unit) will be performing the EDC calculation to centrally dispatch generation from many GENCOs. Depending on market rules the generation costs might be masked and a bidding process would decide dispatching. Some of the most important inputs of the EDC calculation are listed below [10]:

[7] The key word in the sentence is “online”. The ED calculation only decides scheduling of units that has already decided to be online at a specific hour.

1. The electricity demand.

The electricity of generated at each moment needs to be equal to the electricity consumed plus any transmission losses according to the laws of physics. The instant electricity demand is an input for the EDC. In monopolies, utilities have to serve the whole demand within their territory. In competitive markets, a generating company (GENCO) can decide whether to sign bilateral contracts with specific clients, and/or to supply any additional demand through participating into the whole electricity market or to provide ancillary services when the opportunity arises. In the former case the output is not a subject to any calculation but has been decided already. Outside bilateral contracts the objective of economic dispatch can vary (e.g. cost minimization, profit maximization, reliability).

2. Technical limitations

The EDC needs to consider all technical limitations arising from the need for reliable operation of power systems as explained in chapter 2. The most technical important limitations considered in the EDC are the operational limits of generators and the transmission constraints. The first has to do with the inability of a generator to produce more electricity that its maximum allowable generation limit and less than the minimum. The second is related to transmission constraints. There might be apparent bottlenecks in the system that constraint adequate amounts of power reaching a load. The EDC calculation needs to consider the transmission system as well and include power flow equations to dispatch generators without overloading transmission lines and risking line failures and overall system reliability.

3. The operational cost of electricity production

The most important OPEX cost of thermal generators is fuel costs. The fuel cost curve of thermal generators can be derived from the Input/Output (I/O) curve of thermal generators. In the engineering world, I/O represent the power output of thermal generators as a function of thermal input and they are derived through actual measurements where fuel consumption is measured while increasing power output (figure 3-2). When the thermal input is multiplied with cost of fuel the fuel cost curve is derived. Fuel cost curves of generators are usually of convex and of quadratic form. In some generators like the one presented in figure 3-3 the I/O curve is nearly linear. Convexity, of fuel curves is an important mathematical characteristic since existing non-linear optimization models can obtain a global optimum if the problem is convex as will be discussed in section 3.3.3. However, large multi-valve steam turbines exhibit non-convex, non-quadratic characteristics that increase the complexity of the UC problem.

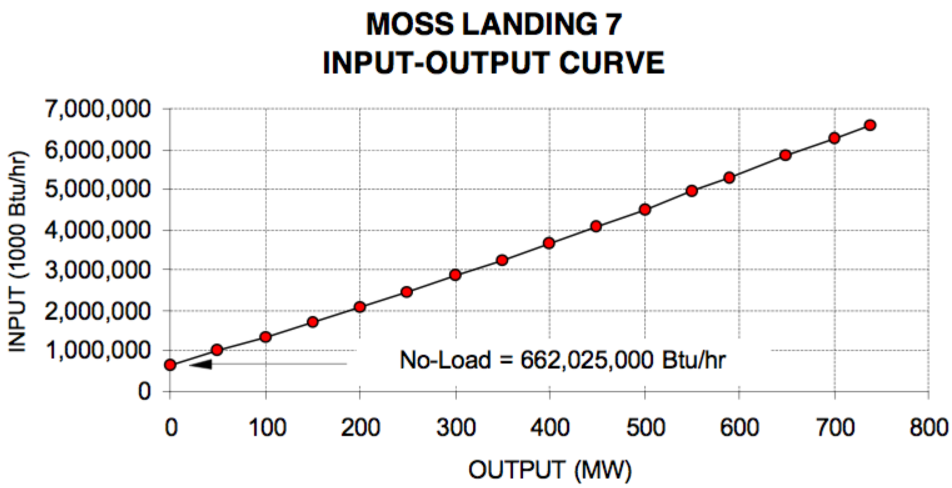

Figure 3-2: Input/Output curve for Moss Landing 7 gas fired unit (Source: **[11]**).

3.2.1. Mathematical formulation of the EDC problem

The EDC is an optimization problem that can be solved if the objective of the ED problem is cost minimization then it can be solved with the method of Lagrange multipliers according to the following mathematical formulation:

$$Minimize\ L = \sum_{g=g1}^{NG} (F_g) + \lambda_g \cdot \left(D - \sum_{g=g1}^{NG} P_g \right) \qquad [eq.3-1]$$

Where:

$$F_g = a \cdot P_g^2 + b \cdot P_g + c \text{ [8]} \qquad [eq.3-2]$$

[8] If the I/O curve is linear the quadratic coefficient is equal to zero.

$$P_g^{min} \leq P_g \leq P_g^{max} \qquad [eq.3-3]$$

where:

$g: set\ of\ generators\ of\ total\ number\ NG\ \ [MW]$

$L: Langrangian\ cost\ function\ \ [MW]$

$P_g: Power\ output\ of\ generator\ g\ \ [MW]$

$F_g = a \cdot P_g^2 + b \cdot P_g + c$ is the fuel cost function of generator g [$]

$\alpha: quadratic\ coefficient\ \left[\frac{\$}{MW^2}\right]$

$b: linear\ coefficient\ \left[\frac{\$}{MW}\right]$

$c: coefficient$ [$]

$D: Demand\ [MW]$

$\lambda_g =: The\ marginal\ cost\ of\ electricity\ production\ of\ unit\ g\ \ \left[\frac{\$}{MWh}\right]$

3.2.2. Solution algorithms of the EDC problem

The analytical solution of optimization problem described by equations 3-1 to 3-3 using the Lagrange multipliers method will yield a global minima when all units produce electricity at the same marginal cost (e.g.$\lambda_1 = \lambda_2 = \lambda_3 = \cdots \lambda_{NG} = \lambda$). In that case λ is the marginal cost of the electricity production for the system. As the number of constraints involved (especially when they introduce non-linearities) and the complexity of the EDC grow it becomes necessary to use iterative search techniques. Methods to solve the EDC problem are discussed by [12]. "The Traditional methods include Newton- Raphson method, Lambda Iteration method, Base Point and Participation Factor method, Gradient method, etc. However, these classical dispatch algorithms require the incremental cost curves to be monotonically increasing. Practically the input to output characteristics of the generating units are highly non-linear, non-smooth and discrete in nature owing to prohibited operating zones and multi-fuel effects. Thus the resultant ELD becomes a challenging non-convex optimization problem, which is difficult to solve using the traditional methods. Methods like dynamic programming, genetic algorithm, evolutionary programming, artificial intelligence, and particle swarm optimization solve non-convex optimization problems efficiently and often achieve a fast and near global optimal solution. Although these heuristic methods do not always guarantee the global optimal solution, they generally provide a fast and reasonable solution (sub optimal or near global optimal)". When a system is very large, it might not be efficient to maintain the quadratic form of the objective function and/or constraints. In such cases it is more efficient to break the fuel cost curves (and/or other constraints) of thermal generators into piece-wise linear segments and formulate the problem as a linear program. This method is being applied for the formulation of UC problem in this thesis as discussed later in this chapter. Some well-known methods to solve LPs are the simplex, the ellipsoid and the interior point. More information on EDC solution methods can be found at [13].

3.3. The Unit Commitment (UC) Problem

The Unit Commitment (UC) problem is defined as the scheduling of operation of a number of units over a specified period of time (usually one day or 1 week)[9]. While the EDC problem only decides the optimal power production of a set of online units, the UC problem decides both the output and the operational status (on/off) of the whole generation fleet over the specified optimization period. In that sense the EDC is an inherent part of the UC problem and for that reason the UC is also called Unit Commitment and Economic Dispatch problem (UCED)[10]. It should be noted that from now and on in this thesis UC and UCED will refer to the same problem for avoidance of any confusion.

The UC is a combinatorial problem meaning the best solution is obtained from a finite set of problems each of them having its own solution. Each of those problems involves the EDC problem as an inherent part that needs to be solved (see figure 3.3). The UC problem grows exponentially with a) the number of generators involved and b) with the number of steps comprising and optimization cycle. For a single hour the total number of combinations to be checked are 2^{NG}-1 where NG is the total number of generators. If we account for the dimension of time the formula becomes $(2^{NG}-1)^{NT}$. Assuming a 10 generator system and an hourly optimization cycle of 1 day (day ahead UC) there are $(2^{10}-1)^{24} \cong 10^{72}$ combinations to be tested. It would take thousands of years even the most advanced super computer to come with a solution. For that reason, we use methods that skip solutions that

[9] Unlike the EDC problem –which defines the operation of online units at a snapshot in time- the unit commitment problem includes the element of time

[10] Or Security Constrained Unit Commitment (SCUC) if the EDC part of the UC problem includes power flow equations

are far from the optimum one and diverge fast towards the best solution depending the solution method used.

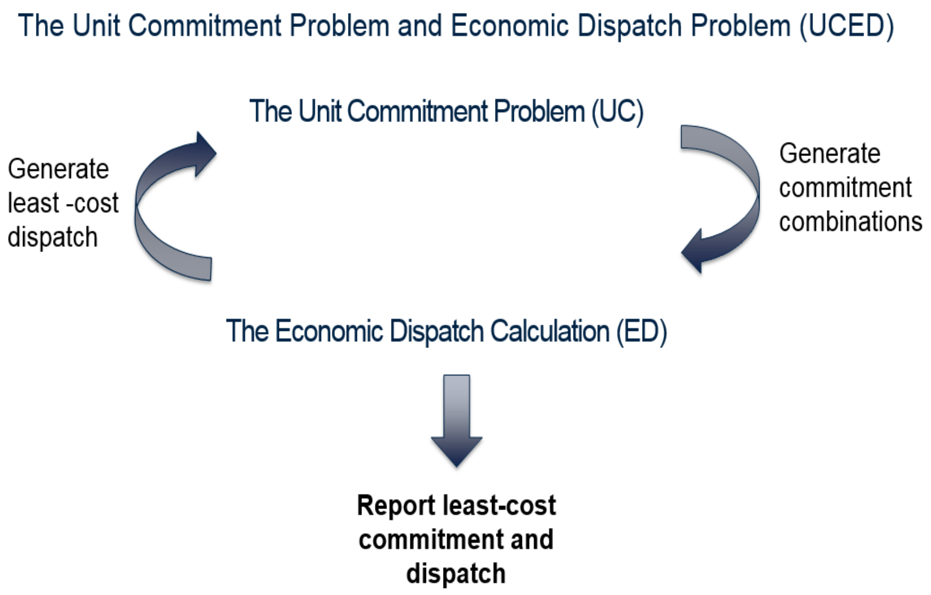

Figure 3-3: Schematics on the way the UCED problem is solved.

As explained in section 3-2 the objective of the UC can vary. For a GENCO bidding on a competitive market the objective is profit maximization. For a vertical integrated utility the objective would be operational cost minimization. While both the EDC and UC calculations focus on short-term variable operational costs, the UC also includes transitional costs, aka start-up costs being part of the objective function.

In its simplest form the objective function of the UC optimization problem is:

$$Minimize \sum_{g=g1}^{NG} \sum_{t=t1}^{NT} \sum_{f=f1}^{NF} \left(Cost_{StartUp}\, g,t + Cost_{VAR}\, g,f,t \right) \qquad [eq. 3-4]$$

Where:

t: Time increments [e.g half hrs] $t_1 < \mathrm{t} < t_{NT}$
g: Generator $g_1 < \mathrm{g} < g_{NG}$
f: Fuel $f_1 < \mathrm{f} < f_{NF}$

and

NT: Total number of time steps comprising an optimization cycle
NG: Total number of generators
NF: Total number of fuels burned by each generator

$\mathrm{Cost}_{\mathrm{StartUp}}$ g, t: Start Up cost incurred if a generator started up at time t[$]
$\mathrm{Cost}_{\mathrm{VAR}}$ g, f, t: variable cost per generator per fuel consumed during increment t (includes fuel,VOM and if applicable carbon costs)[$]

3.3.1. Start-Up cost models for the UC problem

The fuel cost functions of thermal generators and their usefulness on calculation of operational costs has been discussed in section 3.2.1. The start-up costs of thermal generators are not fixed, but rather depend on the time the unit has been off. The effect of time a unit being off is much more important for generators running on a steam cycle because it requires large amounts of thermal energy to heat cold water. In literature there are three widely used models for estimation of thermal generator start-up costs [14]. The first model called also called cooling model, is exponential and is mostly used to calculate cold start-up costs. The second model assumes linear connection between time and energy requirements to bring the unit to operational temperature. The slope of the linear curves decreases as we pass from hotter to colder regimes. The third model assumes fixed start-up cost within each of the hot, warm, cold bands (see figure 3-4).

1. Cooling model

$$Cost_{StUp_{Cold}}(t) = \left(1 - e^{\frac{-t}{a}} +\right) \cdot Cost_{fuel} + C_f \qquad [eq.3-5]$$

Where:

$\mathrm{C_f}$: Fixed cost of (included crew cost, maintenance costs)[\$]
$\mathrm{Cost_{fuel}}$: Cost of fuel $\left[\frac{\$}{\mathrm{GJ}}\right]$
t : time after unit shut – down [hrs]
a : thermal time constant specific for the unit [hrs]
$\mathrm{Cost_{StUp_{Cold}}}$: Cold start up costs [\$]

2. Piece wise linear model

$$Cost_{StUp_{Hot}}(t) = (\tan(\beta_{Hot}) \cdot t) \cdot Cost_{fuel} + C_f \quad \forall \quad 0 \leq t < \Delta t_{Hot} \qquad [Eq.\ 3-6]$$

$$Cost_{StUp_{Warm}}(t) = (\tan(\beta_{Warm}) \cdot (t - \Delta t_{Hot}) + C_1\ ) \cdot Cost_{fuel} + C_f$$
$$\forall \quad \Delta t_{Hot} \leq t < \Delta t_{Hot} + \Delta t_{Warm} \qquad [Eq.\ 3-7]$$

$$Cost_{StUp_{Cold}}(t) = Cost_{fuel} \cdot C_C + C_f \qquad \forall \quad \Delta t_{Hot} + \Delta t_{Warm} \leq t \qquad [Eq.\ 3-8]$$

Where:
$\Delta \mathrm{t_{Hot}}$: Time band a unit is in hot state [hrs]
$\Delta \mathrm{t_{Warm}}$: Time band a unit is in warm state [hrs]
$\mathrm{C_1}$: Heat requirement to bring the unit to operational status when $\mathrm{t = \Delta t_{Hot}}$ [GJ]
$\mathrm{C_C}$: Heat requirement to bring the unit to cold start up [GJ]
β_{Hot}:Angle of the linear curve within the hot band [rad]

β_{Warm}: Angle of the linear curve within the warm band [rad]

3. Step model

$$Cost_{StUp_{Hot}}(t) = C_H \cdot Cost_{fuel} + C_f \quad \forall \quad 0 \le t < \Delta t_{Hot} \qquad [Eq.\ 3-9]$$

$$Cost_{StUp_{Warm}}(t) = C_W \cdot Cost_{fuel} + C_f$$
$$\forall\ \Delta t_{Hot} \le t < \Delta t_{Hot} + \Delta t_{Warm} \qquad [Eq.\ 3-10]$$

$$Cost_{StUp_{Cold}}(t) = C_C \cdot Cost_{fuel} + C_f \qquad \Delta t_{Hot} + \Delta t_{Warm} \le t \qquad [Eq. 3-11]$$

Where:

C_H: Heat requirement to bring the unit to operational level when still hot (step model) [GJ]
C_W: Heat requirement to bring the unit to operational level when warm (step model) [GJ]

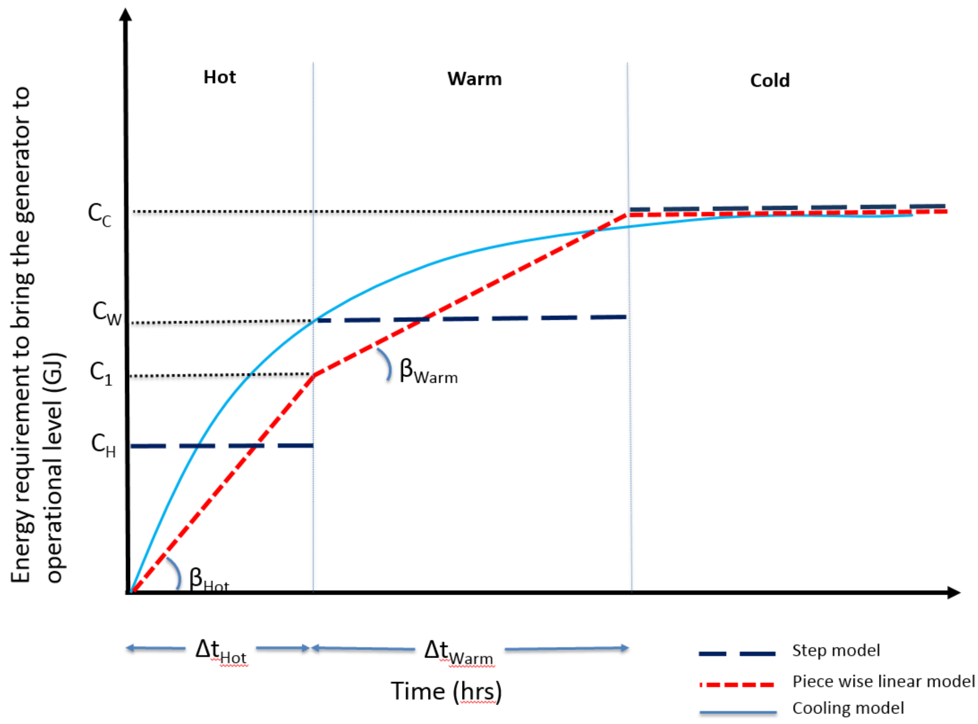

Figure 3-4: Three different models for thermal generator start-up heating requirement.

3.3.2. Constraints of the UC model

As explained earlier the objective function of the UC problem depends on fuel and start-up costs. At the same time the UC optimization problem is subject to a set of constraints that represent laws of physics, technical limitations, fuel reserve limitation and policies specific to the power system to be studied. Such constraints can be broken down into a) system constraints and b) unit constraints and c) policy constraints.

- **List of System Constraints**
  - **Demand/Supply balance**. At each moment, the power generated must be equal to power consumed plus any transmission and generation losses. Depending on the model used (transport, DC, AC) the demand balance equations represent the power flows in the system (see section 3.2.2.1).
  - **System reserve requirements**. At each moment there needs to be some available capacity for ancillary services (spinning reserves) to minimize the probability of an outage. The reserve is considered to be a predetermined amount or a given percentage of the forecasted demand
  - **Fuel reserve constraints**: The available capacity of a system might be limited by fuel availability. Fuel reserve constraints are used to distinguish among de-rated capacity and actually available capacity after considering fuel availability.
  - **Transmission constraints**: Have already been discussed in section 3.2.2.1.

- **List of Unit Constraints**
    - **Initial conditions:** The final conditions of the last optimization cycle need to be the initial conditions of the upcoming cycle. Initial conditions depend the on/off status of the units and the amount of time a unit has been continuously on or off when the new cycle begins. The initial conditions are involved in the determination of ramp rates and minimum up times (MUT) and minimum down times (MDT) as explained below.
    - **Ramp rates:** Thermal units are technically limited on their ability to increase and/or decrease their power output. Ramp rate constraints are used to account for flexibility in a power system.
    - **Minimum Up and Down times.** MUT and MDT constraints are used to account for the technical ability of thermal units to turn on and/or shut down within a specified time. MUT defines the minimum amount of time a unit needs to operate after it was initially turned on. MDT defines the minimum amount of time a unit needs to stay off after it was initially turned off.
    - **Unit operational range constraints:** Thermal units can only operate within a specified range. The specific fuel consumption within this range is described by the I/O curves. This type of constraint is inherent in the EDC and has been discussed in section 3.2.
    - **Must run constraints:** The dispatch of some units might be mandatory, dictated by technical rather than economic rules. For example combined

heat and power plants are dispatched on winter months to supply heating demand together with electricity.

- **Policy constraints** represent constraints imposed by government regulations or utility policies specific to the power system to be studied. Such constraints might be **carbon constraints** if there is some carbon cap active. Other types of policy constraints are variable renewable energy **(VRE) penetration targets** expressed as percentage of total installed capacity of total energy produced other **emissions constraints**.

3.3.3. Solution methods for the UC problem

The objective of the UC problem varies from utility to utility and the complexity depends on the number and type of units and the constraints imposed. Therefore, there are various approaches to solve the UC problem. Based on previous discussion the main issues in the UC problem are: complexity of search space (high dimensionality), generation of initial feasible schedules, MUD/MDT ramping and spinning reserve constraints, handling of sometimes non-linear and/or non/convex EDC sub problem. Some of them are deterministic, some are stochastic and some hybrid methods. Many modern solution methods use heuristics to reduce dimensionality. When the fuel curves of generators are convex it is common to apply iterative techniques like the Newton and the lambda-iteration methods. Dynamic programming (DP) and mixed integer programming (MIP) are solution methods that can address issues with non-linearity/ non convexity related to fuel curves, ramping constraints and MUT/MDT constraints. However, DP and MIP suffer from the curse of dimensionality especially as the number of generators increases. More recent artificial intelligence (AI) techniques like the genetic algorithm (GA) can handle well non-linearities common on power system optimization problems. However, such techniques even though time efficient cannot guaranty optimal results. A detailed comparison of solution methods is beyond the purpose of this PhD thesis. The reader can refer to [15] [16] and [17] for a comprehensive literature review/comparison of the latest solution methods.

The UCED problem in this thesis is formulated as a mixed integer linear program (MILP)[11] and solved with a commercial MIP solver as will be discussed later. The branch and bound (B&B) method is the most widely used in MIP nowadays. B&B begins by finding the optimal solution to the "relaxation" of the problem without integer constraints (via standard linear methods or non-linear methods[12]). If the decision variables with integer constraints have integer values, then no further work is required. If one or more integer variables have non-integral solutions, the Branch and Bound method chooses one such variable and "branches," creating two new sub problems where the value of that variable is more tightly constrained. These sub problems are solved and the process is repeated, until a solution that satisfies all of the integer constraints is found[13].

[11] It is beyond the purpose of this thesis to discuss other optimization methods techniques like quadratic programming (QP) and non-linear programming (NLP).

[12] The linear programming (LP)-based technique is used to formulate many mathematical optimization problems. Some of the main advantages of the LP approach are: a) reliability especially with regards to convergence properties, b) it can quickly identify infeasibilities and c) it accommodates a large variety of power system operating limits, including the very important contingency constraints. The main disadvantage of LP based models is lower accuracy compared to more accurate nonlinear power system model. However, LP techniques generally meet the requirements of engineering precision and are widely used for simple UCED problems

[13] Source: www.solver.com

The decision to use MIP for the UC formulation and solution in this thesis is based on access to a) cplex of IBM a robust commercial MIP solver that has been tested on MIP problems with millions of variables and constraints b) GAMS a modeling system for formulating and solving optimization problems with the option to use cplex as the underlying solver engine.

3.3.4. The General Algebraic Modeling System (GAMS)[14]

We chose the General Algebraic Modeling System (GAMS) as the platform for formulating our MIP models in this thesis. GAMS is a modeling system for mathematical programming and optimization. It consists of a language compiler and a stable of integrated high-performance solvers. GAMS is tailored for complex, large scale modeling applications, and allows someone to build large maintainable models that can be adapted quickly to new situations.

GAMS model types include Linear Programming (LP), Mixed Integer Programming (MIP), Mixed Integer Non-Linear Programming (MINLP), and different forms of Non-Linear Programs (NLPs). The Unit Commitment problem must make on/off decisions for each unit. Structuring of such problem requires the use of integer decision variables as shown in Chapter 2. Thus the Unit Commitment problem cannot be solved as a Linear Program. Within GAMS the user can choose among a number of solvers capable of

[14] General information about GAMS presented on this section have been obtained mainly from GAMS website : https://www.gams.com/docs/intro.htm

handling MIP programs[15]. I used CPLEX for this thesis. The IBM ILOG CPLEX Optimizer solves integer programming problems, very large linear programming problems using either primal or dual variants of the simplex method or the barrier interior point method, convex and non-convex quadratic programming problems, and quadratic convex problems (solved via second-order cone programming, or SOCP) [18].

3.4 Development of a short-term UC for a thermal system with renewables (solar, wind and hydro) and CAES

In this section I present the basic features as well as a MILP mathematical representation of the UC problem for a deterministic power system with thermal generators, renewables and energy storage technologies. Additionally, I formulate a MIP representation of a CAES unit performing energy arbitrage called "Fixed Parameter" model. The CAES unit is modeled having fixed technical characteristics. As a next step I introduce a "Thermo-Economic" CAES model where the compression and expansion parts of the CAES unit are modelled using power curves from a major CAES manufacturer. Finally I incorporate the "Thermo-Economic" CAES model into the UC model to create a short-term least-cost dispatch model for a thermal system with renewables and CAES.

[15] A complete list of embedded commercial GAMS is using can be found on: https://www.gams.com/help/index.jsp?topic=%2Fgams.doc%2Fsolvers%2Findex.html&anchor=SOLVERS_MODEL_TYPES

3.4.1 A deterministic UC model of a thermal system with renewables

Section 3.4.1 presents the basic features as well as a MILP mathematical representation of the UC problem for a deterministic power system with thermal generators, renewables and energy storage technologies. Section 3.4.2 shows a formulation of a common MIP representation of a CAES unit performing energy arbitrage which I call "Fixed Parameter" model. In the next step I introduce a "Thermo-Economic" CAES model where I modeled the compression and expansion parts of the CAES unit using power curves from a major CAES manufacturer. Finally I incorporate the "Thermo-Economic" CAES model into the UC model to create a short-term least-cost dispatch model for a thermal system with renewables and CAES.

The UC model to be formulated on next section has the following basic features:

- **Demand**: The electricity demand is an input in the model in an excel format. The user is entering the total demand per time step and the load contribution at each bus. The time step can be decided by the user. The smaller the time step the larger the number of time steps and it takes longer for the code to converge. The model that has been developed in this thesis operates using a time step of 30 minutes and an optimization period of 1 week (336 steps per optimization cycle). The model was tested on a three node system with 56 thermal generators. The time to run one week is around 5 minutes using GAMS as the main solver on an Inter i7 2.8GHz PC.
- **Renewables**: In the "renewables" category we include, photovoltaics, wind power, hydro power, biomass and waste power. Waste and biomass power plants are

treated similarly as the rest of thermal generators. PV, wind and hydro are treated deterministically, with their production being an input into the model. We use historical production data from PV, wind and hydro sources under the assumption that production will be similar in the future. When the future installed capacity of VRE sources is expected to grow, the output needs to be scaled up accordingly. With climate change looming, the annual variation of hydro may be considerable. For that reason when hydro represents a significant fraction of the total generation is it is advisable to apply sensitivity analysis using data from both low and high hydrological years. After the demand and temporal production of all VRE sources have been entered as inputs, the model calculates the net-load. As penetration from VRE increases so does variability as discussed in chapter 2. In the UCED model high VRE penetration activates specific constraints like, ramping rate limitations and starting up/shutting down restrictions and makes balancing more challenging. Since VRE production has very low production costs, VRE generators have almost always priority over thermal generators. However, the model decides if VRE curtailment is needed due to technical infeasibilities or just being more economic in exchange for a VRE curtailment penalty to the system. VRE output is entered in excel format.

- **Outage rates**: The model requires as input the capacity availability of each unit in each optimization time-step. For example if a power plant is composed of 5 units of 100MW each, and one unit is being maintained during a day, the availability of the power station is declared as 400MW for the specified period. The model in that case will only allow a maximum output of 400MW from the specified power plant. Generator availability data are entered in excel format.

- **Carbon cap**: The model includes two policy constraints, a) carbon cap and b) carbon pricing. With regards to carbon cap the user needs to specify the maximum amount of carbon allowed per optimization period. The optimization period is one month and the carbon cap is defines as metric tonnes (tones) of CO2. The user needs to specify the emissions intensity of each fuel in kg of CO2 per GJ of thermal input. The output emissions rates (tones CO2 per MWh-e) is different for each generator and depends on its individual I/O characteristics.
- **Carbon pricing**: When the carbon pricing constraint is active there is a price on carbon included for every tonne of CO2 emitted. The used needs to specify the carbon price ($/MW) in addition to the emissions intensity.
- **System constraints**: The system constraints are a) transmission constraints, b) fuel reserve constraints, c) reserve capacity.
- **Unit constraints**: Unit constraints included in the model are: minimum up times (MUT), minimum down times (MDT), ramping, operation range, and "must run" constraints. (MUT/MDT constraints are related to the time unit needs to stay on or off after is started or turned off respectively. Must-run units, are generators that operate even if not being the most economical due to system requirements (for example CHPs operating to provide district heating).
- **Start-up costs**: I have included the step model (see section 3.3.1) for calculation of start-up costs. The user needs to identify the energy requirements (in GJ) for a hot, warm and cold start up as well as the time frame that defines each segment.

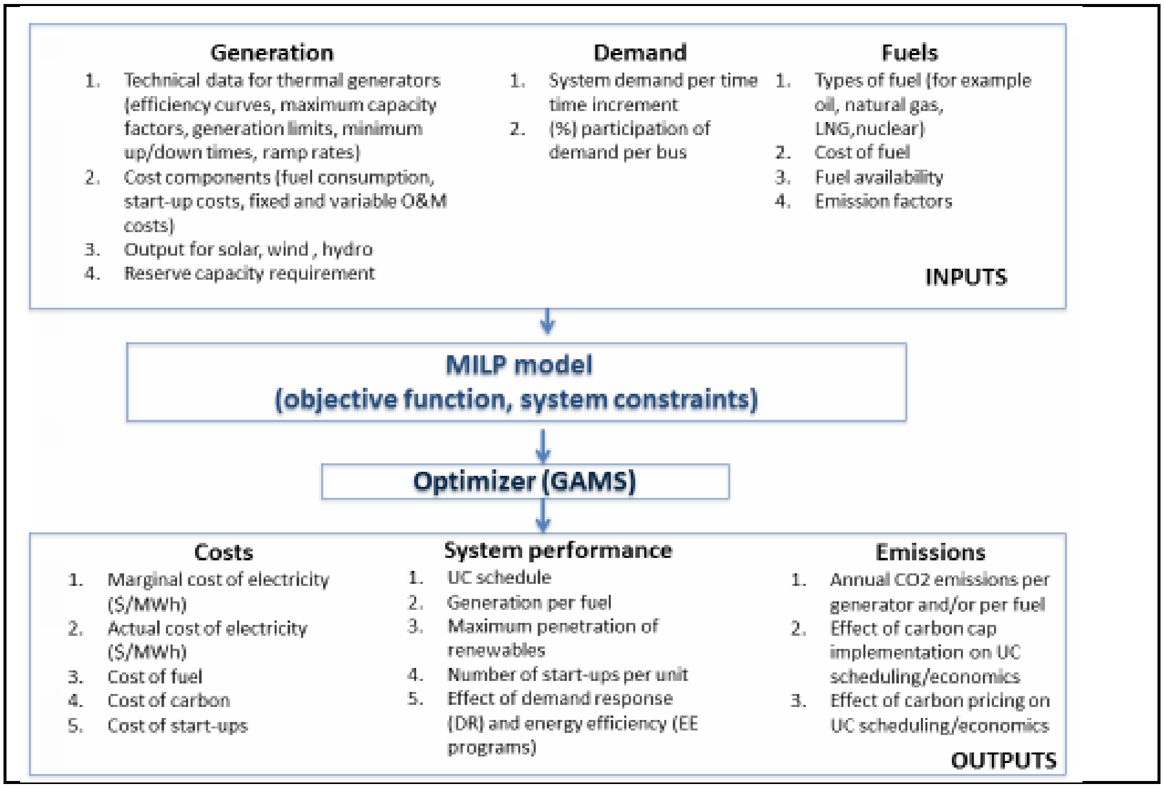

Figure 3-5: UC model structure.

3.4.2 MIP Formulation of the UC Problem for a thermal system with renewables

Before we present the formulation of the objective function and model constraints we present the model sets, variables and parameters.

Sets

g: Generators $\quad g_1 \leq g \leq g_{NG}$

t: Time steps $t_1 \leq t \leq t_{NT}$

f: Fuel $f_1 \leq f \leq t_{NF}$

i: Buses $i_1 \leq i \leq i_{NI}$

l: Power segments of fuel cost function $l_1 \leq l \leq l_{NL}$

G(i): the subset of generators that is connected to bus i

F(g): the subset of fuels that are used by generator g

where:

NG: Total number of generators

NT: Total number of time steps comprising one optimization cycle

NF: Total number of fuels

NI: Total number of buses

NL: Total number of power segments to break down the power curves of generators

Decision binary variables

$\boldsymbol{u}(\boldsymbol{g},\boldsymbol{y})$: Unit g operates at time t (1: YES, 0: NO)

$\boldsymbol{uStUp}(\boldsymbol{g},\boldsymbol{y})$: Unit g started up at time t (1: YES, 0: NO)

$\boldsymbol{uShDn}(\boldsymbol{g},\boldsymbol{y})$: Unit g shut down at time t (1: YES, 0: NO)

Decision variables

$\mathbf{FC}\ (\mathbf{g}, \mathbf{f}, \mathbf{t})$: Fuel cost by generator g, during time increment t, due to burning fuel f $[\frac{\$}{\text{time increment}}]$

$\mathbf{P}\ (\mathbf{g}, \mathbf{f}, \mathbf{t})$: Power produced by generator g, during time increment t, due to burning fuel f [MW]

$\mathbf{P\ l}(\mathbf{l}, \mathbf{g}, \mathbf{t})$: Power per piece wise linear segment of the input − output curve by generator g, during time increment t, due to burning fuel f [MW]

$\mathbf{Pmax}\ (\mathbf{g}, \mathbf{t})$: Maximum power output of generator g, during time increment t [MW] (depends on ramp rates and future state of unit g, (see eq. 13)

$\boldsymbol{P_{W\_curt}}(\mathbf{i}, \mathbf{t})$: Curtailed wind power at bus i and time t [MW]

$\boldsymbol{P_{PV\_curt}}(\mathbf{i}, \mathbf{t})$: Curtailed PV power at bus i and time t [MW]

$\mathbf{UNMET}(\mathbf{i}, \mathbf{t})$: Unmet demand during time increment t [MW]

Model parameters (inputs)

$\mathbf{Cap}\ (\mathbf{g})$: Rated capacity of generator g [MW]

$\boldsymbol{CarbonPrice}$: Cost of CO2 emissions $\left[\frac{\$}{\text{kg}}\right]$

$\boldsymbol{CarbonCap}$: Maximum number of tonnes of CO2 alowed during the optimization cycle[16] $\left[\frac{\$}{\text{kg}}\right]$

$\boldsymbol{CoUE}$: Cost of Unserved Energy $\left[\frac{\$}{\text{MWhr}}\right]$

$\boldsymbol{Cost_W}$: Cost of curtailed wind energy $\left[\frac{\$}{\text{MWhr}}\right]$

$\boldsymbol{Cost_{PV}}$: Cost of curtailed PV energy $\left[\frac{\$}{\text{MWhr}}\right]$

$\mathbf{Dn}\boldsymbol{T}^{\mathbf{0}}(\mathbf{g})$: Number of hours the unit was down since last shut down [hr]

$\boldsymbol{ER(f)}$: Emissions rate of fuel f $\left[\frac{kg\ CO2}{GJ}\right]$

$\boldsymbol{FuelCost(f)}$: Cost of fuel f $[\frac{\$}{\text{GJ}}]$

$\boldsymbol{FuelLim(f)}$: Maximum daily fuel reserve of fuel f during year y $\left[\frac{MMBTU}{day}\right]$

$\boldsymbol{HRNL(g)}$: No Load Heat Requirement of generator g $[\frac{\text{GJ}}{\text{hr}}]$

$\boldsymbol{HRINC0(g)}$: Incremental heat requirement of generator g from no load to LP1 $[\frac{\text{GJ}}{\text{hr}}]$

$\boldsymbol{HRINCl(g)}$: Incremental heat requirement of generator g from LPl to LPl + 1 $\left[\frac{\text{GJ}}{\text{hr}}\right]$ $1 \leq \text{l} \leq 4$

LoadPart(i): Load participation at bus i. It is the percentage of total load allocated at each bus [%]

$\boldsymbol{LPx(g)}$: Load point x of generator g [MW], $1 \leq \text{x} \leq 5$

MinDnT (g): Minimum down time of generator g [hr]

MinUpT (g): Minimum up time of generator g [hr]

$\mathbf{PF}\ (\mathbf{i}, \mathbf{j}, \mathbf{t})$: Power flow from bus i to bus j at time t [MW]

$\mathbf{Pmin}\ (\mathbf{g})$: Minimum power output of generator g [MW]

$\mathbf{RunDn}\ (\mathbf{g})$: The ramp down rate of generator g during shut down $[\frac{\mathrm{MW}}{\mathrm{hr}}]$

$\mathbf{RunUp}(\mathbf{g})$: The ramp up rate of generator g during start up $[\frac{\mathrm{MW}}{\mathrm{hr}}]$

$\mathbf{RampDn}\ (\mathbf{g})$: The ramp down rate of generator g during normal operation $[\frac{\mathrm{MW}}{\mathrm{hr}}]$

$\mathbf{RampUp}\ (\mathbf{g})$: The ramp up rate of generator g during normal operation $[\frac{\mathrm{MW}}{\mathrm{hr}}]$

$\boldsymbol{S}(\boldsymbol{g}, \boldsymbol{l})$: Maximum power of piece wise linear segment l of generator g [MW]

$\boldsymbol{SL}$: Time length of one time step [hr]

$\boldsymbol{S}(\boldsymbol{g}, \boldsymbol{l})$: Maximum power of piece wise linear segment l of generator g [MW]

$\boldsymbol{StUpCost}(\boldsymbol{g})$: Start up cost of generator g $\left[\frac{\$}{MWh}\right]$

$\boldsymbol{TL}(\boldsymbol{i}, \boldsymbol{j})$: Transmission losses from bus i to bus j [%]

$\mathbf{Up}\boldsymbol{T}^{\mathbf{0}}(\mathbf{g})$: Number of hours the unit was up since last start up [hr]

$\boldsymbol{VOM}(\boldsymbol{g})$: Variable O&M cost of generator g $\left[\frac{\$}{MWh}\right]$

Mathematical formulation of the problem is presented below:

Objective function

As per equation 3-4 presented earlier, the objective of a least-cost UC problem is to minimize fixed and variable costs:

$$\boldsymbol{Minimize}\ \sum_{g=g1}^{gNG}\sum_{t=t1}^{tNT}\sum_{f=f1}^{fNF}\sum_{i=i1}^{NI}\Big(\boldsymbol{Cost_{Fuel}}(\boldsymbol{g},\boldsymbol{f},\boldsymbol{t})+\boldsymbol{Cost_{VOM}}(\boldsymbol{g},\boldsymbol{f},\boldsymbol{t})$$

$$+\boldsymbol{Cost_{CO2}}(\boldsymbol{g},\boldsymbol{f},\boldsymbol{t})+\ \boldsymbol{Cost_{Start\ Up}}(\boldsymbol{g},\boldsymbol{t})+\boldsymbol{Cost_{UNMET}}(\boldsymbol{i},\boldsymbol{t})$$

$$+\boldsymbol{Cost_{VRE_{Curtailment}}}(\boldsymbol{i},\boldsymbol{t})\Big) \qquad [\boldsymbol{eq}\ \mathbf{3-12}]$$

where:

$\boldsymbol{Cost_{Fuel}}$: Operational cost of fuel for each generator [$] (see figure 3-7)

$$\boldsymbol{Cost_{Fuel}}(\boldsymbol{g},\boldsymbol{f},\boldsymbol{t})$$

$$=\left[\mathbf{HRNL}\ (\mathbf{g})\cdot\mathbf{u}(\mathbf{g},\mathbf{t})+\mathbf{LP1}(\mathbf{g})\cdot\mathbf{HRINC0}(\mathbf{g})\cdot\mathbf{u}(\mathbf{g},\mathbf{t})+\sum_{\boldsymbol{l}=1}^{\boldsymbol{NL}}(\boldsymbol{S}(\boldsymbol{g},\boldsymbol{l})\right.$$

$$\left.\cdot\ \mathbf{HRINC(g,l)})\right]\cdot\big(\mathbf{FuelCost(f)}\big)$$

$$\cdot\ \boldsymbol{SL} \qquad [\boldsymbol{eq}.\mathbf{3-13}]$$

$\boldsymbol{Cost_{VOM}}$: Variable O&M cost for each generator [$]

$$\boldsymbol{Cost_{VOM}}(\boldsymbol{g},\boldsymbol{t})\ =\ \big(\mathbf{P}(\mathbf{g},\mathbf{f},\mathbf{t})\big)\cdot\mathbf{VOM}(\mathbf{g}))\ \times\mathbf{SL}$$

$$[\boldsymbol{eq}.\ \mathbf{3-14}]$$

$\boldsymbol{Cost_{StartUp}}$: Start Up cost for each generator at time t [$]

$$\boldsymbol{Cost_{StartUp}}(\boldsymbol{g},\boldsymbol{t})\ =\ \mathbf{uStUp}(\mathbf{g},\mathbf{t})\cdot\mathbf{StUpCost}(\mathbf{g})$$

$$[\boldsymbol{eq}.\ \mathbf{3-15}]$$

$\boldsymbol{Cost_{C02}}$: Cost of carbon [$]

$$\boldsymbol{Cost_{C02}\ (g,f,t)}$$

$$= \left[\mathbf{HRNL\ (g) \cdot u(g,t) + LP1(g) \cdot HRINC0(g) \cdot u(g,t)} + \sum_{\boldsymbol{l=1}}^{\boldsymbol{NL}} (\boldsymbol{S(g,l)}\right.$$

$$\left. \cdot\ \mathbf{HRINC(g,l)})\right] \times (\mathbf{ER(f)} \cdot \boldsymbol{Carbon\ Price}) \times \boldsymbol{SL} \quad \boldsymbol{f \in F(g)}$$

$$[\boldsymbol{eq.\ 3-16}]$$

$\boldsymbol{Cost_{USE}}$: Cost of unused energy [$]

$$\boldsymbol{Cost_{USE}\ (i,t)} \ = \ \mathbf{UNMET(i,t)} \times \mathbf{CoUE} \times \boldsymbol{SL} \qquad [\boldsymbol{eq.3-17}]$$

$\boldsymbol{Cost_{VRE\_Curt}}$: Cost of curtailed VRE energy [$]

$$\boldsymbol{Cost_{VRE_{Curt}}\ (i,t)} = \left[\boldsymbol{P_{W\_Curt}}(\mathbf{i,t}) \times \mathbf{CostW} + \boldsymbol{P_{PV\_Curt}}(\mathbf{i,t}) \times\right.$$

$$\left.\mathbf{CostPV}\right] \cdot \boldsymbol{SL} \qquad [\boldsymbol{eq.3-18}]$$

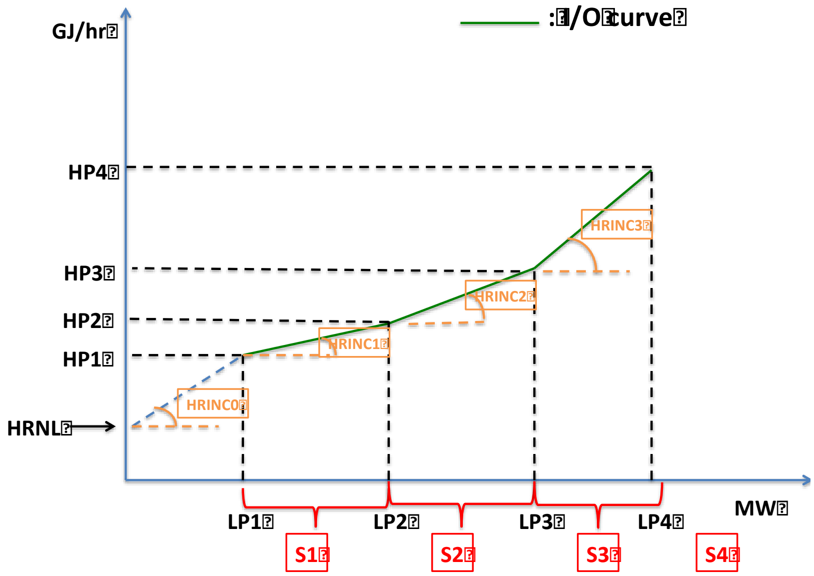

Figure 3-6: A hypothetical Input/Output (I/O) curve of a thermal generator. An I/O curve represents the heat requirement as a function of power output. In this example the curve is represented as a set of 3 piece wise linear segments defined by four load points, LP1, LP2, LP3 and LP4. The horizontal length of each segment is denoted with letter S. Each generator requires a minimum heat input known as the no load heat requirement (HRNL). The tangent of the angles defined by a linear segments and its horizontal mapping S represent the incremental hear rates of each segment (HRINC). My model returns correct results only when the I/O curves of thermal generators are convex.

System Constraints

SYSTEM CONSTRAINTS	
Fuel reserve constraint (Fuel limit is defined in MMBTU per day)	$\sum_{g=g1}^{gNG}\sum_{t=t1}^{tNT}[\mathrm{HRNL}(g)\times u(g,t)+\mathrm{LP1}(g)\times \mathrm{HRINC0}(g)\times u(g,t)+\sum_{l=1}^{NL}(S(l)\cdot \mathrm{HRINC}(g,l))]\cdot\left(\frac{NT}{24}\right)\le FL(f)\cdot\left(\frac{1}{0.97}\right)$ [eq. 3-19]
Supply/Demand balance (transport model)	$\sum_{g=g1}^{gNG}\sum_{f=f1}^{fNF}[P(g,f,t)]+UNMET(i,t)+P_w(i,t)+P_{PV}(i,t)+P_H(i,t)+\sum_{j=j1}^{jNJ}[PF(j,i,t)\cdot(1-TL(j,i))]-\sum_{j=j1}^{jNJ}[PF(i,j,t)]=Demand(i,t)\cdot LoadPart(i)\quad g\in G(i),\quad f\in F(g)$ $[eq.3-20]$

Reserve Margin	$\sum_{g=g1}^{gNG}\left[u(g,t)\cdot Gmax(g)-\sum_{f}P(g,f,t)\right] \leq ResMarg\cdot Demand(t) \quad [eq.3-21]$
UNIT CONSTRAINTS	
Total power output equal to sum of partials	$\sum_{f}P(g,f,t) \leq \sum_{l=l1}^{lNL}(Pl(l,g,t))+LP1\cdot u(g,t) \quad \boldsymbol{f} \in \boldsymbol{F'}(\boldsymbol{g}) \quad [eq.3-22]$
Power output per segment	$0 \leq Pl(l,g,t) \leq LP_{l+1}(g) - LP_{l}(g) \quad [\mathrm{eq}.3-23]$
Maximum generation constraint	$\sum_{f}P(g,f,t) \leq Pmax(g,t) \quad \boldsymbol{f} \in \boldsymbol{F'}(\boldsymbol{g}) \quad [eq.3-24]$
Minimum generation constraint	$\sum_{f}P(g,f,t) \geq Pmin(g) \quad \boldsymbol{f} \in \boldsymbol{F'}(\boldsymbol{g}) \quad [eq.3-25]$
Maximum power output dependence on Run Down Time	$Pmax(g,f,t) \leq Cap(g)\cdot\left(u(g,t)-uShDn(g,t+1)\right)+RunDn(g)\cdot uShDn(g,t+1) \quad [eq.3-26]$
Start-Up / Shut –Down binary variables related	$uStUp(g,t)-uShDn(g,t) = u(g,t)-u(g,t-1) \quad [eq.3-27]$
Unit cannot-start up and shut-down at the same hour	$uStUp(g,t)+uShDn(g,t) \leq 1 \quad [eq.3-28]$
Min Up Time constraint for t ≤ Lg	$\sum_{t=1}^{Lg}(1-u(g,t))=0 \quad \forall\ g\in G,\ \forall\ t\in 1,\dots L_g \quad [eq.3-29]$ $Lg = Number\ of\ time\ steps\ the\ unit\ has\ to\ stay\ on\ when\ the\ optimization\ cycle$ $Lg\ depends\ on\ how\ many\ hours\ before\ the\ optimization\ cycle\ the\ unit\ start$ $Lg=\min\{\Theta,(MinUpT(g)-UpT^{0})\times u(g,0)\}$
Minimum Up Time constraint for t > Lg and t ≤ NT − MinUpT(g) + 1	$\sum_{\tau=t}^{T1}u(g,\tau) \geq MinUpT(g)*uStUp(g,t),\ \forall\ g\in G,\ \forall\ t \in L_g+1\dots.\mathrm{NT}-MinUpT(g)+1 \quad [eq\ 3-30]$

Minimum Up Time constraint for t > NT − MinUpT (g) + 1	$\sum_{\tau=t}^{NT}(u(g,\tau) - uStUp\,(g,t)) \geq 0 \;\; \forall \;\; t \in \mathrm{NT} - MinUpT\,(g) + 2 \ldots NT [eq\ 3-31]$
Min Down Time constraint for t ≤ Kg	$\sum_{t=1}^{Kg} u(g,t) = 0 \quad \forall \;\; g \in G, \; \forall \;\; t \in 1, \ldots K_g \qquad [eq.\ 3-32]$ Kg $= Number\ of\ time\ steps\ the\ unit\ has\ to\ stay\ off\ when\ the\ optimization\ cycl$ $Kg\ depends\ on\ how\ many\ hours\ before\ the\ optimization\ cycle\ the\ unit\ shut$ $Kg = \min\{\mathrm{NT}, (MinDnT\,(g) - DnT^{\,0}) \times (1 - u(g,0))\}$
Minimum Down Time constraint for t > Kg and t ≤ NT − MinDnT (g) + 1	$\sum_{\tau=t}^{T2}(1 - u(g,\tau)) \geq MinDnT\,(g) * uShDn\,(g,t), \forall \;\; g \in G, \forall \;\; t \in K_g \; + 1 \ldots . \mathrm{NT} -$ $MinDnT\ (g) + 1 \qquad [eq.3-33]$
Minimum Down Time constraint for t > NT − MinDnT (g) + 1	$\sum_{\tau=t}^{NT}(1 - u(g,\tau) - uShDn(g,t)) \geq 0 \;, \forall \;\; g \in G,$ $\forall \;\; t$ $\in \mathrm{NT} - MinUpT\,(g) + 2 \ldots NT \qquad [eq\ 3-34]$
Ramp Up Constraint	$Pmax\,(g,f,t) \leq \sum_{f} P(g,f,t-1) \; + RampUp\,(g) \times u(g,t-1) + RunUp(g)$ $\times\ uStUp\,(g,t) \qquad \boldsymbol{f} \in \boldsymbol{F}'(\boldsymbol{g}) \qquad [eq.\ 3-35\ ]$
Ramp Down Constraint	$\sum_{f}(P(g,f,t-1) - P(g,f,t-1))$ $\leq RampDn(g) \times u(g,t) + RunDn(g) \times uShDn(g,t) \quad \boldsymbol{f}$ $\in \boldsymbol{F}'(\boldsymbol{g}) \qquad [eq.3-36\ ]$
Must Run Units operate continuously	$\sum_{g} u(g,t) = NT \;\; \boldsymbol{g} \in \boldsymbol{G}' \qquad [eq.3-37]$
POLICY CONSTRAINTS	
Carbon Cap Constraint	$\sum_{g=g1}^{gNG} \sum_{t=t1}^{tNT}(\mathrm{HRNL}\ (\mathrm{g}) \times \mathrm{u}(\mathrm{g,t}) + \mathrm{LP1}(\mathrm{g}) \times \mathrm{HRINC0}(\mathrm{g}) \times \mathrm{u}(\mathrm{g,t}) + \sum_{l=1}^{NL}(S(l)$ $\times\ \mathrm{HRINC}(\mathrm{g,l}))) \cdot ER \cdot SL \cdot NT \cdot 0.001 \leq CarbonCap$ [eq. 3-38]

3.4.3 Mathematical Formulation of a CAES system performing energy arbitrage

3.4.3.1 Formulation of a "Fixed Parameter" CAES model for energy arbitrage

This section is an introduction on modeling a Compressed Air Energy Storage (CAES) unit. The CAES device is performing energy arbitrage and is modeled having constant thermal characteristics (compressor efficiency, expander heat rate, energy ratio). I have named this simple representation of a CAES device "Fixed Parameter" model. The formulation of the Fixed Parameter model is a first step towards building a more complicated thermodynamic CAES model for more accurate modeling of the economics and technical benefits of CAES on power systems.

Energy arbitrage is the process of storing energy at valley hours when price is low and selling at peak hours to maximize profit. Thus the objective of energy arbitrage is profit maximization of the CAES device assuming that the market prices are perfectly known ahead of time. It should be noted that unlike the unit commitment model presented earlier we don't optimize the whole generation fleet but rather the CAES units only. In that respect electricity prices are an endogenous input in the model. Such an assumption simplifies the problem however it is only valid in large systems where the peak shaving performed by a storage device doesn't have a big impact on marginal system prices. In reality CAES being a part of the system has an effect on marginal prices (it most of the time reduces marginal prices through peak shaving). Before we proceed with the mathematical formulation we give below the model parameter and continuous and binary variables of the model.

Sets

c: CAES units, $c_1 \leq \mathrm{c} \leq c_N$

t: time steps $t_1 \leq \mathrm{c} \leq t_N$

Where:

$\boldsymbol{c_N}$: $Total\ number\ of\ CAES\ units$

$\boldsymbol{t_N}$: Total number of time steps

Model parameters

CDTR(**c**): Charge Discharge Time Ratio. Equal to time required for the compressor to charge the cavern divided by the time required by the expander to drain the cavern

$\boldsymbol{\eta^{comp}}$(**c**): percentage of electric energy consumed by compressor c converted to mechanical energy [%]

$\boldsymbol{\eta^{CAES}}$(**c**): the efficiency of CAES device equal to $\dfrac{P^D}{P^C + (Q_{in} \cdot \eta^{GT})}$

$\boldsymbol{\eta^{GT}}$: $Thermal\ efficiency\ of\ a\ typical\ gas\ turbine$ ($assumed\ to\ be$ 35%)

$\mathbf{Cost^{exp}_{StUp}}$(**c**): Start Up cost for expander c [$]

$\mathbf{Cost_{StUp}^{comp}}(\mathbf{c})$: Start Up cost for compressor c [$]

$\mathbf{Cost_{VOM}^{CAES}}(\mathbf{c})$: VOM costs for CAES c $\left[\frac{\$}{\mathrm{MWh}}\right]$

$\boldsymbol{ER_{CAES}}(\mathbf{c})$: CAES energy ratio of CAES unit c [−]

$\mathbf{HR_{CAES}}(\mathbf{c})$: Heat Rate of CAES expander $\left[\frac{\mathrm{GJ}}{\mathrm{MWh}}\right]$

$\mathbf{ST_{CAES}}(\mathbf{c})$: Storage time. The time needed for the expander to bring the cavern pressure from maximum to minimum operational levels

$\mathbf{P_{max}^{exp}}(\mathbf{c},\mathbf{i})$: Maximum capacity of CAES expander c connected at bus i[MW]

$\mathbf{P_{min}^{exp}}(\mathbf{c},\mathbf{t})$: Minimum output of CAES expander c connected at bus i [MW]

$\mathbf{P_{min}^{comp}}(\mathbf{c},\mathbf{t})$: Minimum power drawn by CAES compressor c connected at bus i [MW]

$\mathbf{P_{max}^{comp}}(\mathbf{c},\mathbf{t})$: Maximum power drawn by CAES compressor c connected at bus i [MW]

$\mathbf{p_{el}^{wh}}(\mathbf{i},\mathbf{t})$: price of wholesale electricity at node i in hour t $\left[\frac{\$}{\mathrm{MWh}}\right]$

$\mathbf{p_{el}^{sp}}(\mathbf{i},\mathbf{t})$: price of spinning reserves at node in hour t $\left[\frac{\$}{\mathrm{MWh}}\right]$

$\mathbf{p_{el}^{ns}}(\mathbf{i},\mathbf{t})$: price of non − spinning reserves at node i in hour t $\left[\frac{\$}{\mathrm{MWh}}\right]$

$\mathbf{p^{ng}}$: price of natural gas $\left[\frac{\$}{\mathrm{GJ}}\right]$

$\mathbf{Q^{in}}(\mathrm{c})$: the thermal input at the expander $\left[\frac{\mathrm{MJ}}{\mathrm{sec}}\right]$

$\mathbf{T_{storage}}(\mathbf{c})$: Hours of storage in CAES cavern [hrs]

Continuous Variables

$\mathbf{E}(\mathbf{c},\mathbf{t})$: Storage level in the cavern at time t [MWh]

$\boldsymbol{E^{in}}(\mathbf{c},\mathbf{t})$: Energy entering the cavern at time t [MWh]

$\boldsymbol{E^{out}}(\mathbf{c},\mathbf{t})$: Energy exiting the cavern at time t [MWh]

$\mathbf{P^{D}}(\mathbf{c},\mathbf{t})$: Power discharged at hour t from CAES unit c [MW]

$\mathbf{P^{C}}(\mathbf{c},\mathbf{t})$: Power needed to charge CAES unit c at time t [MW]

Binary Variables

$\mathbf{u^{exp_{StUp}}}(\mathbf{c},\mathbf{t})$: binary variable indicating if expander c started up – up at time t

$\mathbf{u^{exp_{ShDn}}}(\mathbf{c},\mathbf{t})$: binary variable indicating if expander c shut down – at time t

$\mathbf{u}^{\boldsymbol{comp}_{\mathbf{StUp}}}(\mathbf{c},\mathbf{t})$: binary variable indicating if compressor c started up – up at time t

$\mathbf{u}^{\boldsymbol{comp}_{\mathbf{ShDn}}}(\mathbf{c},\mathbf{t})$: binary variable indicating if compressor c shut down – at time t

$\mathbf{u^{exp}}(\mathbf{c},\mathbf{t})$: binary variable indicating if expander c operates at time t

$\mathbf{u^{comp}}(\mathbf{c},\mathbf{t})$: binary variable indicating if compressor c operates at time t

$\mathbf{u^{idle}}(\mathbf{c},\mathbf{t})$: binary variable indicating if CAES unit c idles at time t

Objective function

The objective function of the problem of profit maximization of a single CAES unit arbitraging energy in a wholesale market is:

$$\boldsymbol{max} \sum_{t=t1}^{NT} \left[\boldsymbol{Revenues_{el}(c,t) - Cost_{Fuel}^{CAES}(c,t) - Cost_{VOM}^{CAES}(c,t) - Cost_{el}^{Comp}(c,t)} \right.$$

$$\left. - \boldsymbol{Cost_{StUp}^{CAES}}\ (\mathbf{c,t}) \right]$$

$$[\boldsymbol{eq.3-39}]$$

Where:

$\mathbf{Revenues_{el}(c,t)}$: Revenues of CAES device c during time period t[$]

$$\boldsymbol{Revenues_{el}(c,t) = P^D(c,t) \cdot SL \cdot p_{el}^{wh}(t)} \qquad [\boldsymbol{eq.\ 3-40}]$$

$\boldsymbol{Cost_{Fuel}^{CAES}(c,t)} = C$ost of natural gas consumed at burners during time period t [$]

$$\boldsymbol{Cost_{Fuel}^{CAES}(c,t) = p^{ng}(t) \cdot HR_{CAES}(c) \cdot P^D(c,t) \cdot SL} \qquad [\boldsymbol{eq.3-\ 41}]$$

$\boldsymbol{Cost_{VOM}^{CAES}(c,t)} = Variable\ cost\ of\ CAES\ operation\ during\ time\ period\ t$ [$]

$$\boldsymbol{Cost_{Fuel}^{CAES}(c,t) = Cost_{VOM}^{CAES}(c) \cdot P^D(c,t) \cdot SL} \qquad [\boldsymbol{eq.3-42}]$$

$\boldsymbol{Cost_{StUp}^{CAES}}\ (\mathbf{c,t}) = \boldsymbol{S}$tart Up Costs cost of CAES during time period t [$]

$$\boldsymbol{Cost_{StUp}^{CAES}}\ (\mathbf{c,t}) = \mathbf{u^{exp_{StUp}}(c,t) \cdot Cost_{StUp}^{exp}(c) - u^{\mathit{comp}_{StUp}}(c,t) \cdot Cost_{StUp}^{comp}(c)}$$

$$[eq.3-43]$$

$\boldsymbol{Cost_{el}^{Comp}(c,t)}$: The cost of electricity consumed by the compressor during time period t

$$\boldsymbol{Cost_{el}^{Comp}(c,t) = P^C(c,t) \cdot SL \cdot p_{el}^{wh}(t)} \qquad \textbf{[eq.3-44]}$$

Profit equals revenues from selling electricity to the wholesale market minus operating costs. Operating costs include: Start-up costs for the turbine and compressor, cost of fuel during expansion, variable O&M costs and the cost of purchasing electricity to run the compressors (see figure 3.7).

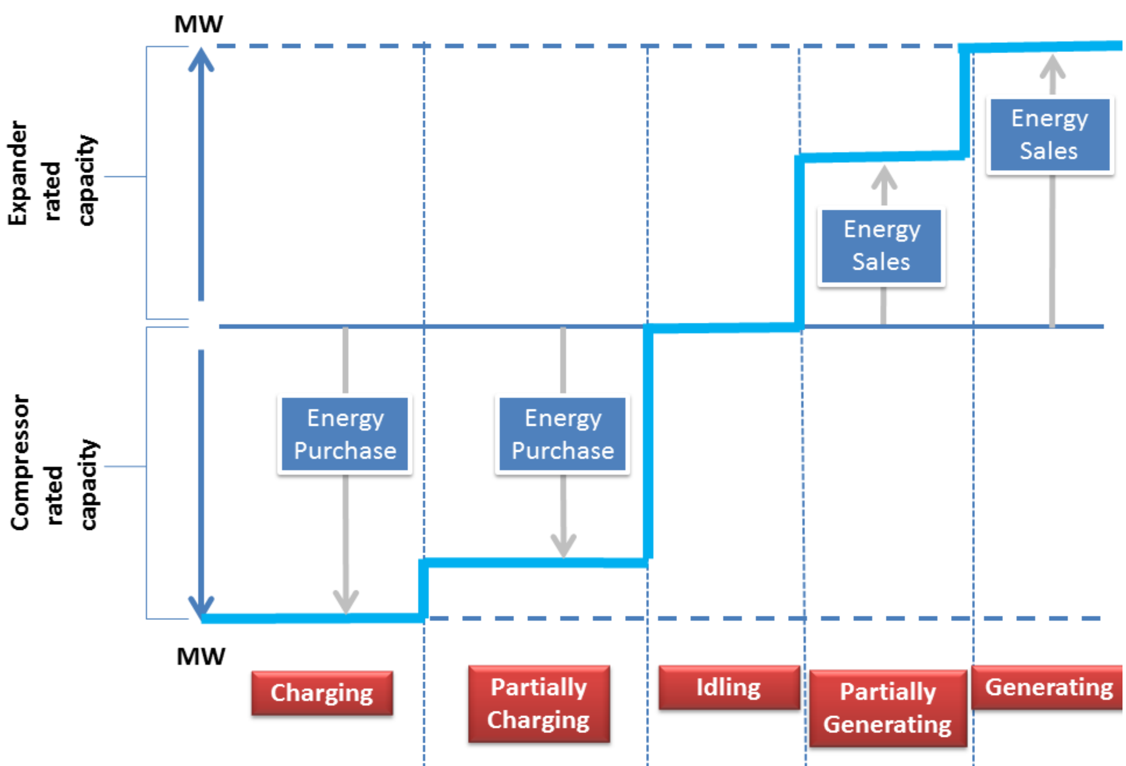

Figure 3-7: Various operation modes of a CAES device performing energy arbitrage

Table 3-1: Revenue sources and costs during operation of CAES device

	Discharging	Charging
Operating Revenues	$\boldsymbol{P^D(c,t) \cdot p_{wh}^{el}(t) \cdot SL}$	
Operating Costs	$\boldsymbol{p^{ng}(t) \cdot HR_{CAES}(c) \cdot P^D(c,t) \cdot SL}$ $\boldsymbol{+Cost_{VOM}^{CAES}(c) \cdot P^D(c,t) \cdot SL}$ $\mathbf{+u^{exp_{StUp}}(c,t) \cdot Cost_{StUp}^{exp}(c)}$	$\boldsymbol{P^C(c,t) \cdot SL \cdot p_{el}^{wh}(t) +}$ $\mathbf{u^{\mathit{comp}_{StUp}}(c,t) \cdot Cost_{StUp}^{comp}(c)}$

CONSTRAINTS

1. Energy Ratio

$$\sum_{t=1}^{NT}(P^c(c,t) \cdot SL) = ER_{CAES}(c) \cdot \sum_{t=1}^{NT}(P^D(c,t) \cdot SL) \qquad [3-46]$$

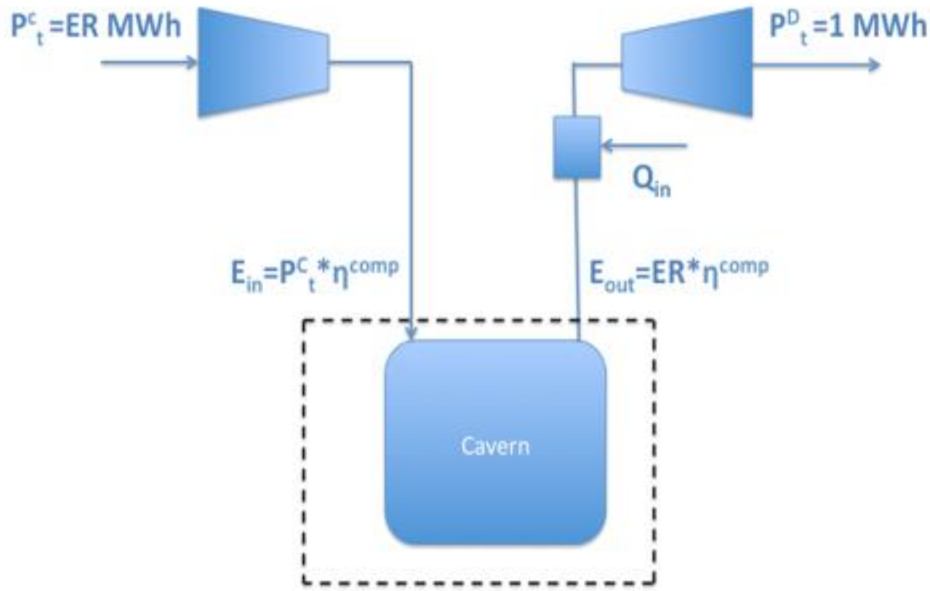

Figure 3-8: Energy balance of CAES cavern. For every 1MWh of energy output, ER[17] MWh are required to charge the compressor. Out of the amount of electricity being drawn only a percentage equal to the efficiency of the compressor will be stored as mechanical energy. Additional thermodynamic losses are experienced in the cavern and during expansion. Thus thermal input equal to Qin is required to account for all losses experienced during different stages of compression and expansion.

2. Energy entering the cavern

$$E^{in}(c,t) = P^c(c,t) \cdot \eta^{comp}(c) \cdot SL \qquad [3-46]$$

3. Energy exiting the cavern

$$E^{in}(t) = \left[P^c(t) - Q^{in}(t)\right] \cdot SL \qquad [3-47]$$

[17] ER in this figure is the energy ratio of a CAES device equal to electrical input versus electrical output. The energy ratio does not measure total but rather only electrical efficiency. Its value is less than 1 because CAES units also require thermal input through combustion of natural gas.

4. Thermal input during expansion

$$Q^{in}(c,t) = \left[P^{D} \cdot HR^{CAES} \cdot \frac{1}{3.6}\right] \cdot SL \qquad [3-48]$$

5. Balance of energy in cavern[18]

$$E(t) = E(t-1) + E^{in}(t) - E^{out}(t) \qquad [3-47]$$

6. Efficiency of CAES device

$$\sum_{t=t1}^{NT} \left(\frac{P^{C}(c,t)}{P^{D}(c,t) + \eta^{GT}(c) \cdot Q^{in}(c)} \right) = \eta^{CAES}(c) \qquad [3-47]$$

7. Setting generator start-up binary

$$u^{expStUp}(c,t) - u^{expShDn}(c,t-1) = u^{exp}(c,t) - u^{exp}(\mathrm{c,t\text{-}1}) \qquad [\mathrm{eq.3\text{-}51}]$$

8. Setting compressor start-up binary

$$u^{compStUp}(c,t) - u^{compShDn}(c,t-1) = u^{comp}(c,t) - u^{comp}(\mathrm{c,t\text{-}1}) \qquad [\mathrm{eq.\,3\text{-}52}]$$

9. CAES unit can either compress or generate or idle at a given time[19]

$$u^{exp}(c,t) + u^{comp}(c,t) + u_{t}^{idle}(c,t) = 1 \qquad [\mathrm{eq.\ 3\text{-}53}]$$

---

[18] We assume energy losses in the cavern through heat exchange with the surroundings or air leakage are negligible

[19] The binary variable u_{t}^{idle} is not a necessary decision variable to develop the energy arbitrage model (without reserves). In that case an inequality is being used instead : $u_{t}^{exp} + u_{t}^{comp}$ £1

10. Define upper and lower operational limits for the expander

$$u^{\exp}(c,t)\cdot P_{\min}^{Exp}(c)\leq P^{D}(c,t)\leq u^{\exp}(c,t)\cdot P_{\max}^{Exp}(\mathrm{c}) \qquad \text{[eq.3-54]}$$

11. Define upper and lower operational limits for the compressor

$$u^{comp}(c,t)\cdot P_{\min}^{comp}(c)\leq P^{C}(c,t)\leq u^{comp}(c,t)\cdot P_{\max}^{comp}(\mathrm{c}) \qquad \text{[eq.3-55]}$$

12. Expander can only start-up or shut-down within a time step

$$u^{\exp StUp}(c,t)+u^{\exp ShDn}(c,t)\leq 1 \qquad \text{[eq. 3-56]}$$

13. Compressor can only start-up or shut-down within a time step

$$u^{compStUp}(c,t)+u^{compShDn}(c,t)\leq 1 \qquad \text{[eq. 3-57]}$$

14. Set upper and lower limits for energy stored

$$0\leq E(c,t)\leq ST(c)\cdot P_{\max}^{\exp}(\mathrm{c}) \qquad \text{[eq. 3-58]}$$

15. Set upper and lower limits for energy stored

$$0\leq E(c,t)\leq ST(c)\cdot P_{\max}^{\exp}(\mathrm{c}) \qquad \text{[eq. 3-59]}$$

16. The cavern needs to return at its initial state by the end of the optimization cycle to be ready for the next cycle[20]

$$E(c,t_1) = E(c,t_{NT}) \qquad [eq.3-60]$$

3.4.3.2 Mathematical Formulation of a MIP Thermo-Economic CAES model performing energy arbitrage

In this section we show the mixed integer linear formulation of a thermodynamic CAES model for energy arbitrage. I used the name "Thermo-Economic" being a combination of words "thermodynamic" and "economic". Unlike the "Fixed Parameter" model, the "Thermo-Economic" model uses power curves of a compressor and expander to simulate the performance of a CAES unit. The power drawn by the compressor is not defined by some constant efficiency number but rather depends on the back pressure the compressor experiences and the speed of charging (Air flow in the cavern). I use a fixed heat rate for the expansion since fuel consumption is weakly connected with the power output (heat rate is relatively flat within the operational range). However, we use technical data from the manufacturer to relate the power output with the speed of cavern discharge. Before formulating the Thermo-Economic CAES model we give the model parameters and variables below:

[20] The initial state of the cavern is an input in the model and it is reasonable to be assumed the average between maximum and minimum energy levels in the cavern.

Sets

AMF: The air mass flow at the compression side $AMF_1 \leq$ AMF $\leq AMF_N$ [21]

Pr: The compressor discharge pressure $Pr_1 \leq$ Pr $\leq Pr_N$ [22]

c: CAES units, $c_1 \leq$ c $\leq c_N$

t: time steps $t_1 \leq$ t $\leq t_N$

Where:

$\boldsymbol{c_N}$: *Total number of CAES units*

$\boldsymbol{t_N}$: Total number of time steps

$\boldsymbol{AMF_N}$: Total number of Air Mass Flow segments

$\boldsymbol{Pr_N}$: Total number of back pressure segments

---

21 In this thesis the number of AMF segments is 21 so that AMF1 represents 270lb/sec, AMF2 represents a value of 280lb/sec, Pr3 a value of 290 lb/sec, ….. , AMF121 represents a value of 470 lb/sec (see figure 3-10).

22 In this thesis the number of pressure segments is 13 so that Pr1 represents 900PSI, Pr2 represents a value of 950PSI, Pr3 a value of 1000 PSI, ….. , Pr13 represents a value of 1500PSI (see figure 3-10).

Model Parameters

$\boldsymbol{AMF_{min}^{in}}(\mathbf{c})$: The minimum CAES compressor air mass flow entering the cavern $\left[\frac{lb}{sec}\right]$ [23]

$\boldsymbol{AMF_{max}^{in}}(\mathbf{c})$: The maximum CAEScompressor air mass flow entering the cavern $\left[\frac{lb}{sec}\right]$

$\boldsymbol{AMF_{min}^{out}}(\mathbf{c})$: The minimumCAES expander air mass flow exiting the cavern $\left[\frac{lb}{sec}\right]$ [24]

$\boldsymbol{AMF_{max}^{out}}(\mathbf{c})$: The maximum CAEScompressor air mass flow exiting the cavern $\left[\frac{lb}{sec}\right]$

$\mathbf{CompPower}(\mathbf{c}, \mathbf{AMF}, \mathbf{Pr})$ **:** Power requirement of CAES compressor c to discharge to specific air mass flow and back pressure levels [MW]

$\mathbf{Cost_{StUp}^{exp}}(\mathbf{c})$: Start Up cost for CAES expander c [$]

$\mathbf{Cost_{StUp}^{comp}}(\mathbf{c})$: Start Up cost for CAES compressor c [$]

$\mathbf{Cost_{VOM}^{CAEgS}}(\mathbf{c})$: VOM costs for CAES c $\left[\frac{\$}{\mathrm{MWh}}\right]$

$\boldsymbol{HR_{Rated}^{CAES}}(\mathbf{c})$: Rated heat rate of CAES expander $\left[\frac{\mathrm{GJ}}{\mathrm{MWh}}\right]$

$\mathbf{P_{max}^{exp}}(\mathbf{c}, \mathbf{t})$: Maximum capacity of CAES expander c connected at bus i[MW]

$\mathbf{P_{min}^{exp}}(\mathbf{c}, \mathbf{t})$: Minimum output of CAES expander c connected at bus i [MW]

$\mathbf{P_{min}^{comp}}(\mathbf{c}, \mathbf{t})$: Minimum power drawn by CAES compressor c connected at bus i [MW]

$\mathbf{P_{max}^{comp}}(\mathbf{c}, \mathbf{t})$: Maximum power drawn by CAES compressor c connected at bus i [MW]

$\mathbf{p^{ng}}$: price of natural gas $\left[\frac{\$}{\mathrm{GJ}}\right]$

[23] The air mass flow range of a compressor depends on manufacturer and model. It can be obtained from power curves becoming available from the manufacturer

[24] The air mass flow range of an expander depends on manufacturer and model. It can be obtained from power curves becoming available from the manufacturer

$\mathbf{p_{el}^{wh}}(\mathbf{t})$: price of wholesale electricity during hour t $\left[\frac{\$}{\mathrm{MWh}}\right]$

$\boldsymbol{PrCavern_{min}}(\boldsymbol{c})$**:** The minimum working pressure in the cavern [PSI]

$\boldsymbol{PrCavern_{max}}$**(c):** The maximum working pressure in the cavern [PSI]

R: Constant of ideal gasses (equal to 0.0000813$\left[\frac{m^3 \cdot \mathrm{Bars}}{K \cdot mole}\right]$)

$\mathbf{Tcavern}(\mathbf{c})$: Temperature in the cavern[^oK][25]

$\mathbf{Vcavern}(\mathbf{c})$: Volume of the cavern[^oK]

Continuous Variables

$\mathbf{AM}(\mathbf{c}, \mathbf{t})$:Total air mass in the cavern at the end of time period t [kgs]

$\mathbf{AMF^{in}}(\mathbf{c}, \mathbf{t})$: Air mass flow entering the cavern of unit c during time period t [$\frac{\mathrm{lb}}{\mathrm{sec}}$]

$\mathbf{AMF^{out}}(\mathbf{c}, \mathbf{t})$: Air mass flow exiting the cavern of unit c during time period t [$\frac{\mathrm{lb}}{\mathrm{sec}}$]

$\boldsymbol{Comp_{Consumption}^{Power}}(\mathbf{c}, \mathbf{t})$: CAES Compressor power consumption during time t [MW]

$\mathbf{P^C}(\mathbf{c}, \mathbf{t})$: Power input to compress air during time period t [MW]

$\mathbf{P^D}(\mathbf{c}, \mathbf{t})$: Power output during time increment t from CAES unit c [MW]

$\boldsymbol{P_{max}^D}(\mathbf{c}, \mathbf{t})$: Maximum allowable power discharged at hour t from CAES unit c [MW]

$\mathbf{PrCavern}(\mathbf{c}, \mathbf{t})$: Pressure level in the cavern of unit c at the end of period t [PSI]

$\boldsymbol{PrCavern^{Average}}(\mathbf{c}, \mathbf{t})$: Average pressure level in the cavern of unit c during period t

[25] We assume isothermal CAES units that charge the cavern at constant temperature

PrComp(c, t): Average compressor discharge pressure during time t[26]

w(c, t): Continuous variable equal to the bilinear term for the McCormick reformulation

Binary Variables

$\mathbf{u}^{\mathbf{exp}_{\mathbf{StUp}}}(\mathbf{c}, \mathbf{t})$: expander c started up at time t (1: YES, 0: NO)

$\mathbf{u}^{\mathbf{exp}_{\mathbf{ShDn}}}(\mathbf{c}, \mathbf{t})$: expander c shut down at time t (1:YES, 0: NO)

$\mathbf{u}^{comp_{\mathbf{StUp}}}(\mathbf{c}, \mathbf{t})$: compressor c started up at time t (1:YES, 0: NO)

$\mathbf{u}^{comp_{\mathbf{ShDn}}}(\mathbf{c}, \mathbf{t})$: compressor c shut down at time t (1: YES, 0: NO)

$\mathbf{u}^{\mathbf{exp}}(\mathbf{c}, \mathbf{t})$: expander c operates at time t (1:YES, 0: NO)

$\mathbf{u}^{\mathbf{comp}}(\mathbf{c}, \mathbf{t})$: compressor c operates at time t (1: YES, 0: NO)

$\mathbf{u}^{\mathbf{comp}}_{\mathbf{power}}(\mathbf{c}, \mathbf{AMF}, \mathbf{Pr}, \mathbf{t})$: compressor c operates at air mass flow levels indicated by AMF and back pressure levels indicated by Pr (1: YES, 0: NO)

The basic differences between the Thermo-Economic and Fixed Parameter models are listed below:

1 Expansion side

In a CAES unit the power output P^D depends on a) the rate of fuel consumption (HR_{CAES}), b) the pressure in the cavern (PrCavern) and c) the air mass flow exiting the

[26] A compressor's discharge pressure follows the cavern's back pressure. However it is necessary to introduce an additional variable that can take value zero. This is because the compressor doesn't operate at all times and in that respect the compressor discharge pressure needs to take value zero when CAES is discharging or idling. On the other side the pressure of the cavern has positive values even when the compressor is not operating. The introduction of this second variable is necessary for building the model.

cavern AMF_{out}. Figure 3-9 is a graphical representation of the above relationships for a 135MW CAES unit proposed by Dresser Rand. Based in figures 3-9 and 3-10 for the same CAES device with: a) rated lower heating value (LHV) heat rate of 3959BTU/kWh b) design minimum inlet pressure of 864PSI and c) design air flow of 400lbs/sec during expansion we get the following mathematical relationships:

- **Actual power output expressed as linear function of air mass flow exiting the cavern**

$$\mathbf{P^D(c,t) = a01 \cdot AMF^{out}(c,t) + b01} \qquad [\mathbf{eq.3-61}]$$

Where:

$a01, b01$ *constants*

$a01 = \quad 0.3953 \frac{MW}{\left(\frac{lb}{sec}\right)}$

$b01 = -23.1\ [MW]$

$$0.1 \cdot AMF_{min}^{out} = 40 \frac{lbs}{sec} \leq AMF^{out}(c,t) \leq AMF_{max}^{out} = 400 \frac{lb}{sec}$$

- **Maximum power output expressed as function of the pressure in the cavern**

$$\boldsymbol{P_{max}^D(c,t) = a02 \cdot PrCavern(c,t) + b02} \qquad [\boldsymbol{eq.3-62}]$$

$$if\ \boldsymbol{PrCavern_{Design}(c) \cdot 0.1 = 0.187[PSI] \leq PrCavern(c,t) \leq PrCavern_{Design}}$$
$$\boldsymbol{= 864[PSI]}$$
$$\boldsymbol{[eq.3-63]}$$

Where:

$\boldsymbol{P^D_{max}(c,t)}$: The maximum power output of the CAES unit c during time period t

$a02, b02\ constants$

$a02 = \quad 0.1841\ \frac{MW}{PSI}$

$b02 = -23.1\ [MW]$

$$\boldsymbol{P^D(c,t) = 135MW}\ \ if\ Pcavern(c,t) > PrCavern_{Design} = 864[PSI]$$
$$\boldsymbol{[eq.3-64]}$$

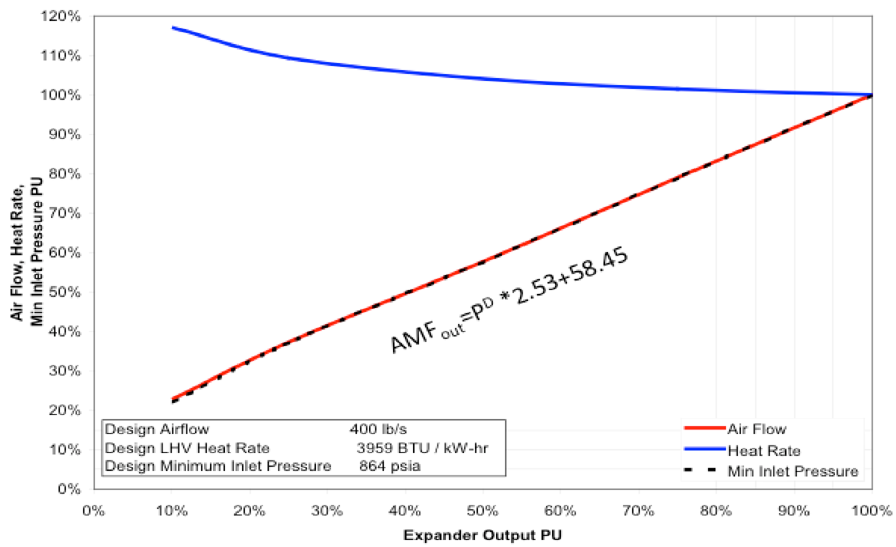

Figure 3-9: CAES expander performance curves. The red line shows percentage of design expander power output (135MW) as a function of percentage of design air mass flow (400lb/sec). The figure also depicts the mathematical relationship of actual air mass flow as a function of actual power output. Equation 3-62 shown above is the inverse function used in the model.

However,

- **CAES heat rate as function of power output**

One of the advantages of a CAES unit is the relatively flat heat rate. Unlike the heat rate of natural gas turbine that can grow 50% more than the rated value at part load conditions the heat rate of a CAES unit doesn't go more than ~15% of rated value even at loading levels equal to 15% of rated capacity. In order to avoid increasing the computational complexity[27] of the problem we have decided to assume the heat rate is independent of power output; such an assumption is not far from reality.

$$\mathbf{HR_{CAES}(c)} = \boldsymbol{HR^{CAES}_{Rated}}\mathbf{(c)} \qquad \textbf{[eq. 3-65]}$$

2 Compression side

The compressor of a CAES unit doesn't operate under constant efficiency in reality. The efficiency of conversion of electrical energy to mechanical energy can vary from around 80% to 85% depending on the discharge pressure and air mass flow from compressor to cavern. Additionally, turbo compressors have inlet guide vanes to regulate the air mass

[27] We could break down the output of the expander into segments based on the heat rate level of each segment and model it similar as the compressor. However, we would need to add also at least one bi-linear equation similar as to equation 3-78. We have decided to assume constant heat rate to avoid increasing the computational complexity of the problem

flow entering the cavern. The highest the flow the more the power requirement to compress air. Additionally, the higher the back pressure in the cavern the higher the power requirement to compress. Figure 3-10 shows the relationship between Brake Power [MW], air mass flow [lb/sec] and discharge pressure [PSI]. The implication on modeling is that the operator of CAES unit can decide to charge the cavern fast for an additional expense on power to acquire an opportunity to discharge at will responding to electricity price differentials. In that respect the model we introduce in this thesis is more detailed compared to a fixed parameter model and can give additional insights on benefits and costs of CAES operation.

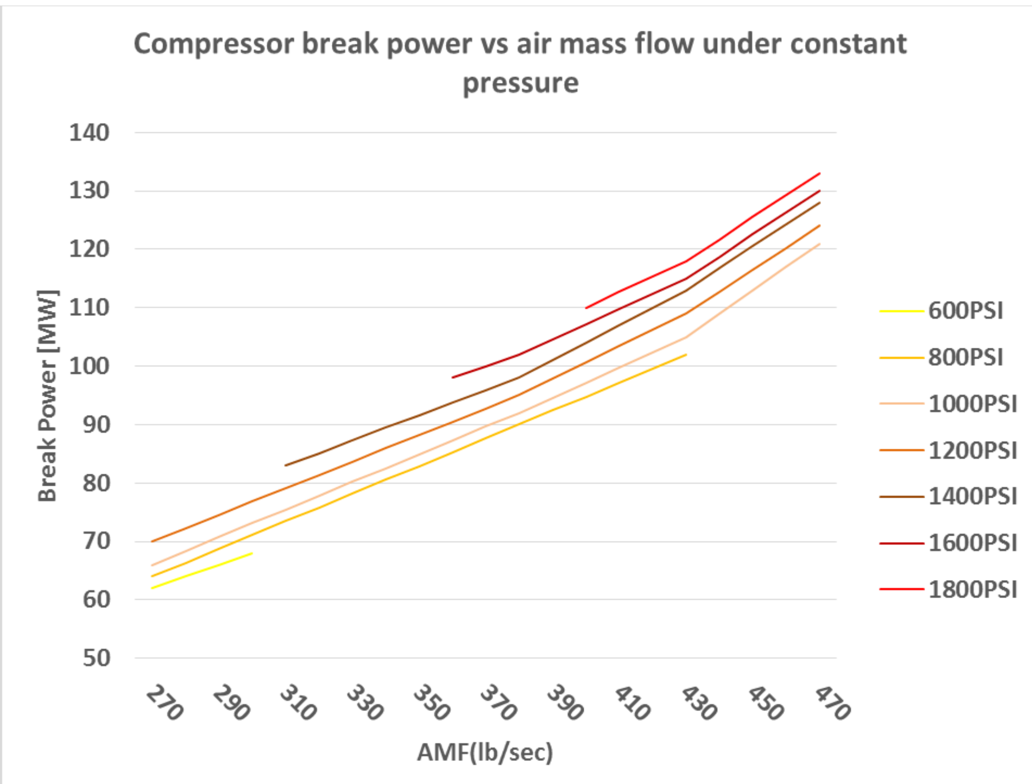

Figure 3-10: CAES compressor performance curves. The curves shown are for a compressor with rated capacity of 128MW. Figure 3-11 has been made using proprietary data from a major CAES manufacturer. Such data were shared with the center of life cycle analysis (CLCA) at Columbia University during a CAES workshop that took place in 2010. We do not have permission to cite the name of manufacturer however, we use data of figure 3-11 to model CAES compressors in this thesis. The red dotted lines show the discharge pressure and air mass flow at the optimum point (operational point at maximum efficiency of 85%). The blue lines represent stalling/surging limits. Above the upper blue line and below the lower blue line the compressor might stall and the region must be avoided.

The mathematical relationship connecting charging power $\mathbf{P^C}$, discharge pressure **PrComp** and air mass flow $\mathbf{AMF^{in}}$ for the compressors of figure 3-10 is not known. However it can be observed from the graph that the mathematical relationship connecting the three variables above is not linear as per the shape of the graph. In this thesis the following approach to simulate compressor performance while maintaining the mixed integer nature of the problem is followed:

- I used data from figure 3-10 to create a matrix with values of break power as a function of air mass flow (AMF) and compressor back pressure (Pr).

AMF/Pr	900	950	1000	1050	1100	1150	1200	1250	1300	1350	1400	1450	1500
270	61.60	62.98	64.37	65.75	67.13	68.52	70.00	71.50					
280	64.00	65.39	66.77	68.15	69.54	70.92	72.30	73.00	74.00				
290	66.41	67.79	69.17	70.56	71.94	73.32	74.71	76.09	75.00	76.00			
300	68.81	70.19	71.58	72.96	74.34	75.73	77.11	78.49	79.88	78.00			
310	71.21	72.60	73.98	75.36	76.75	78.13	79.51	80.90	82.28	80.00	82.00		
320	73.77	75.00	76.38	77.77	79.15	80.53	81.92	83.30	84.68	84.00	84.00	86.00	
330	76.52	77.41	78.79	80.17	81.56	82.94	84.32	85.71	87.09	88.47	88.00	90.00	
340	79.28	79.81	81.19	82.58	83.96	85.34	86.73	88.11	89.49	90.88	92.26	94.26	92.00
350	82.03	82.21	83.60	84.98	86.36	87.75	89.13	90.51	91.90	93.28	94.66	96.66	94.00
360	84.78	84.78	86.00	87.38	88.77	90.15	91.53	92.92	94.30	95.68	97.07	98.45	98.00
370	87.54	87.54	88.40	89.79	91.17	92.55	93.94	95.32	96.70	98.09	99.47	100.85	102.24
380	90.29	90.29	91.03	92.41	93.80	95.18	96.56	97.95	99.33	100.71	102.10	103.48	104.86
390	93.05	93.05	93.88	95.26	96.65	98.03	99.41	100.80	102.18	103.56	104.95	106.33	107.71
400	95.80	95.80	96.73	98.11	99.50	100.88	102.26	103.65	105.03	106.41	107.80	109.18	110.56
410	99.13	99.13	99.58	100.96	102.35	103.73	105.11	106.50	107.88	109.26	110.65	112.03	113.41
420	102.47	102.47	102.47	103.81	105.20	106.58	107.96	109.35	110.73	112.11	113.50	114.88	116.26
430	105.80	105.80	105.80	106.66	108.05	109.43	110.81	112.20	113.58	114.96	116.35	117.73	119.11
440		110.43	110.43	111.22	112.61	113.99	115.37	116.76	118.14	119.52	120.91	122.29	123.67
450			115.06	115.78	117.17	118.55	119.93	121.32	122.70	124.08	125.47	126.85	128.23
460				120.34	121.73	123.11	124.49	125.88	127.26	128.64	130.03	131.41	132.79
470					127.73	129.11	130.49	131.88	133.26	134.64	136.03	137.41	138.79

Figure 3-11: Matrix with values of power requirement by the compressor to discharge at specified air mass flow (lb/sec) and back pressure (Pr) levels. The yellow region is the compressor stall region.

- The above matrix is unique for different types/manufacturers of compressors. We create a parameter with the content of figure 3-10 called **CompPower(c,AMF,Pr).**

- We create a binary variable (named $\boldsymbol{u_{power}^{comp}}(\mathbf{c}, \mathbf{AMF}, \mathbf{Pr}, \mathbf{t})$) to scan across elements of the above matrix. The binary variable takes value zero if the compressor idles or value 1 at the optimum compressor power input.

- ***Objective function***

The objective function of the Thermo-Economic model of a CAES unit performing energy arbitrage is the following:

$$\boldsymbol{max} \sum_{t=t1}^{NT} \left[\boldsymbol{Revenues_{el}(c,t) - Cost_{Fuel}^{CAES}(c,t) - Cost_{VOM}^{CAES}(c,t) - Cost_{el}^{Comp}(c,t)} \right.$$
$$\left. - \boldsymbol{Cost_{StUp}^{CAES}}(\mathbf{c}, \mathbf{t}) \right] \qquad [\boldsymbol{eq.3-66}]$$

Where:

$\mathbf{Revenues_{el}}(\mathbf{c}, \mathbf{t})$: Revenues of CAES device c during time period t [$]

$$\boldsymbol{Revenues_{el}(c,t) = P^D(c,t) \cdot SL \cdot p_{el}^{wh}(t)} \qquad [\boldsymbol{eq.3-67}]$$

$\boldsymbol{Cost_{Fuel}^{CAES}(c,t)} = \boldsymbol{C}$ost of natural gas burned during time period t [$]

$$\boldsymbol{Cost_{Fuel}^{CAES}(c,t) = p^{ng}(t) \cdot HR_{CAES}(c,t) \cdot P^D(c,t) \cdot SL} \qquad [\boldsymbol{eq.3-68}]$$

$$\boldsymbol{Cost_{VOM}^{CAES}(c,t)} = Variable\ cost\ of\ CAES\ operation\ during\ time\ period\ t\ [\$]$$

$$\boldsymbol{Cost_{Fuel}^{CAES}(c,t) = Cost_{VOM}^{CAES}(c) \cdot P^{D}(c,t) \cdot SL} \qquad [\boldsymbol{eq.\ 3-69}]$$

$\boldsymbol{Cost_{StUp}^{CAES}}\ (\mathbf{c},\mathbf{t}) = \boldsymbol{S}$tart Up Costs cost of CAES during time period t [\$]

$$\boldsymbol{Cost_{StUp}^{CAES}}\ (\mathbf{c},\mathbf{t}) = \mathbf{u}^{\mathbf{exp}_{\mathbf{StUp}}}(\mathbf{c},\mathbf{t}) \cdot \mathbf{Cost_{StUp}^{exp}}(\mathbf{c}) - \mathbf{u}^{\boldsymbol{comp}_{\mathbf{StUp}}}(\mathbf{c},\mathbf{t}) \cdot \mathbf{Cost_{StUp}^{comp}}(\mathbf{c})$$

[Eq. 3-70]

$\boldsymbol{Cost_{el}^{Comp}(c,t)}$: The cost of electricity consumed by the compressor during time period t

$$\boldsymbol{Cost_{el}^{Comp}(c,t) = P^{C}(c,t) \cdot SL \cdot p_{el}^{wh}(t)} \qquad [\boldsymbol{eq.3-71}\ ]$$

Plugging equations 3-68 to 3-72 into equation 3-67 gives the following objective function.

$$\begin{aligned} \boldsymbol{max}\ \sum_{\boldsymbol{t=t1}}^{\boldsymbol{NT}} \Big[& \boldsymbol{P^{D}(c,t) \cdot SL \cdot p_{el}^{wh}(t) - p^{ng}(t) \cdot HR_{CAES}(c,t) \cdot P^{D}(c,t) \cdot SL - Cost_{VOM}^{CAES}(c)} \\ & \boldsymbol{\cdot P^{D}(c,t) \cdot SL - \cdot P^{C}(c,t)} \cdot \mathbf{SL} \cdot \boldsymbol{p_{el}^{wh}(t)} - \mathbf{u}^{\mathbf{exp}_{\mathbf{StUp}}}(\mathbf{c},\mathbf{t}) \cdot \mathbf{Cost_{StUp}^{exp}}(\mathbf{c}) \\ & - \mathbf{u}^{\boldsymbol{comp}_{\mathbf{StUp}}}(\mathbf{c},\mathbf{t}) \cdot \mathbf{Cost_{StUp}^{comp}}(\mathbf{c})\ \Big] \end{aligned}$$

$$[\boldsymbol{eq.3-72}\ ]$$

CONSTRAINTS

1. **Power consumption at the compressor**

$$\boldsymbol{P^C}(\mathbf{c},\mathbf{t}) = \sum_{AMF=AMF_1}^{AMF_N} \sum_{Pr=Pr_1}^{Pr_N} \Big(\boldsymbol{CompPower}(\boldsymbol{c},\boldsymbol{AMF},\boldsymbol{Pr}) \cdot \boldsymbol{u}_{\boldsymbol{Power}}^{\boldsymbol{Comp}}(\boldsymbol{c},\boldsymbol{AMF},\boldsymbol{Pr},\boldsymbol{t})\Big)$$

$[\boldsymbol{eq}.\mathbf{3}-\mathbf{73}]$

2. **Air Mass Flow in the cavern (compression side)**

$$\boldsymbol{AMF_{in}}(\boldsymbol{c},\boldsymbol{t}) = \sum_{AMF=AMF_1}^{AMF_N} \sum_{Pr=Pr_1}^{Pr_N} \Big(\big(\mathbf{260}+\mathbf{10}\cdot\mathbf{ord}(\mathbf{AMF})\big)\cdot \boldsymbol{u}_{\boldsymbol{Power}}^{\boldsymbol{Comp}}(\boldsymbol{c},\boldsymbol{AMF},\boldsymbol{Pr},\boldsymbol{t})\Big)$$

$[\mathbf{eq}.\ \mathbf{3}-\mathbf{74}]$

Where:

$\mathbf{ord}(\mathbf{AMF})$: The number of AMF. For example if AMF=AMF_{10}, then ord (AMF)=10.

3. **The compressor can idle or operate at a unique power input at each time increment**

$$\sum_{AMF=AMF_1}^{AMF_N}\sum_{Pr=Pr_1}^{Pr_N}\left(\boldsymbol{u_{Power}^{Comp}(c,AMF,Pr,t)}\right)=\boldsymbol{u^{comp}(c,t)} \qquad [\boldsymbol{eq.3-75}]$$

4. **Relationship connecting the compressor discharge pressure with power input**

$$\mathbf{PrComp(c,t)}=\sum_{AMF=AMF_1}^{AMF_N}\sum_{Pr=Pr_1}^{Pr_N}\left(\boldsymbol{u_{Power}^{Comp}(c,AMF,Pr,t)\cdot(850+ord(Pr)\cdot 50}\right)$$ [28]

[eq. 3-76]

5. **Relationship connecting compressor discharge pressure and the pressure of the cavern**

$$\mathbf{PrComp(c,t)}\leq\boldsymbol{u^{comp}(c,t)\cdot PrCavern^{Average}(c,t)} \qquad [\boldsymbol{eq.3-77}]$$

An upper bound for variable **PrComp(c, t)** is not needed because the power input in the compressor is increasing function of both air mass flow and back pressure. The model will always decide to match the compressor power input with the cavern pressure to minimize the cost of compression. Additionally, equation 3-78 is not linear. It is called bilinear since it contains a term with a binary and a continuous variable being multiplied. However, it

[28] ord(Pr) is the number of set Pr. For example if Pr=Pr_{10} then ord(Pr)=10

can become mixed integer linear with the McCormick linearization method demonstrated on equations 3-79 to 3-84 shown below.

$$\mathbf{PrComp}(\mathbf{c},\mathbf{t}) \leq \boldsymbol{w}(\boldsymbol{c},\boldsymbol{t}) \qquad [\boldsymbol{eq}.\mathbf{3-78}]$$

$$\boldsymbol{w}(\boldsymbol{c},\boldsymbol{t}) \geq \mathbf{0} \qquad [\boldsymbol{eq}.\mathbf{3-79}]$$

$$\boldsymbol{w}(\boldsymbol{c},\boldsymbol{t}) \geq \boldsymbol{u}^{\boldsymbol{comp}}(\boldsymbol{c},\boldsymbol{t}) \cdot \boldsymbol{PrCavern}_{\boldsymbol{min}}(\boldsymbol{c}) \qquad [\boldsymbol{eq}.\mathbf{3-80}]$$

$$\boldsymbol{w}(\boldsymbol{c},\boldsymbol{t}) \leq \boldsymbol{u}^{\boldsymbol{comp}}(\boldsymbol{c},\boldsymbol{t}) \cdot \boldsymbol{PrCavern}_{\boldsymbol{max}}(\boldsymbol{c}) \qquad [\boldsymbol{eq}.\mathbf{3-81}]$$

$$\boldsymbol{w}(\boldsymbol{c},\boldsymbol{t}) \geq \boldsymbol{PrCavern}^{\boldsymbol{Average}}(\boldsymbol{c},\boldsymbol{t}) + \boldsymbol{u}^{\boldsymbol{comp}}(\boldsymbol{c},\boldsymbol{t}) \cdot \boldsymbol{PrCavern}_{\boldsymbol{max}}(\boldsymbol{c}) - \boldsymbol{PrCavern}_{\boldsymbol{max}}(\boldsymbol{c}) \qquad [\boldsymbol{eq}.\mathbf{3-82}]$$

$$\boldsymbol{w}(\boldsymbol{c},\boldsymbol{t}) \leq \boldsymbol{PrCavern}^{\boldsymbol{Average}}(\boldsymbol{c},\boldsymbol{t}) + \boldsymbol{u}^{\boldsymbol{comp}}(\boldsymbol{c},\boldsymbol{t}) \cdot \boldsymbol{PrCavern}_{\boldsymbol{min}}(\boldsymbol{c}) - \boldsymbol{PrCavern}_{\boldsymbol{min}}(\boldsymbol{c}) \qquad [\boldsymbol{eq}.\mathbf{3-83}]$$

6. **Relationship connecting CAES output with air mass flow exiting the cavern**

$$\boldsymbol{P^{D}(c,t) = \mathrm{a01} \cdot AMF^{out}(c,t) + b01 \cdot u^{Exp}(c,t)}$$ **[eq. 3-84]**

7. **Relationship connecting CAES maximum allowable output with pressure in the cavern**

$$\boldsymbol{P^{D}_{max} = \mathrm{a02} \cdot AMF^{out}(c,t) + b02}$$ **[eq. 3-85]**

$$\boldsymbol{P^{D}(c,t) \le P^{D}_{max}}$$ **[eq.3-86]**

8. **Balance of air mass in cavern**[29]

$$\boldsymbol{\mathrm{AM}(c,t) = \mathrm{AM}(\mathrm{c},\mathrm{t}-1) + \left(AMF^{in}(c,t) - AMF^{out}(c,t)\right) \cdot 3600 \cdot 0.45359}$$

[eq 3-87]

9. **Balance of air mass flow in cavern**[30]**.**

$$\sum_{t=t1}^{t_N} AMF^{in}(c,t) = \sum_{t=t1}^{t_N} AMF^{out}(c,t) \qquad [eq.\ 3-88]$$

[29] We assume energy losses in the cavern through heat exchange with the surroundings or air leakage are negligible

[30] Equation 3-89 ensures the cavern returns in its initial energy level at the end of each optimization cycle to be ready for the next one. If the specific constraint is not entered the program will tend to deplete the cavern by the end of each cycle. As a result when the new cycle begins the cavern will have no stored energy and will need to charge before being able to make profit again. The initial energy level can be established through fixing the pressure in the cavern at time t1 equal to the average working pressure for example.

10. Relationship determining the operational status of CAES

$$u^{Exp_{StUp}}(c,t) - u^{Exp_{ShDn}}(c,t) = u^{Exp}(c,t) - u^{Exp}(c,t-1) \qquad [eq.\ 3-89]$$

11. Relationship determining the operational status of the compressor

$$u^{Comp_{StUp}}(c,t) - u^{Comp_{ShDn}}(c,t) = u^{Comp}(c,t) - u^{Comp}(c,t-1) \qquad [eq.\ 3-90]$$

12. Relationship connecting air mass and pressure in the cavern (law of ideal gases)

$$\frac{AM(c,t) \cdot R \cdot Tcavern(c)}{0.001 \cdot Vcavern(c) \cdot MW_{air}} = \frac{PrCavern(c,t)}{14.95} \qquad [eq.3-91]$$

13. Relationship determining average pressure in the cavern[31]

$$PrCavern^{Average}(c,t) = \frac{PrCavern(c,t) + PrCavern(c,t-1)}{2} \qquad [eq.3-92]$$

14. Compressor cannot start-up and shut-down during the same time period

$$u^{Comp_{StUp}}(c,t) + u^{Comp_{ShDn}}(c,t) \leq 1 \qquad [eq.\ 3-93]$$

15. CAES unit can either compress or generate or idle at a given time

[31] The variable PrCavern is the pressure in the cavern at the end of each time period t. However it is important to know the average pressure in the cavern at each time period otherwise we will overestimate the costs of compression because the power input increases with pressure in the cavern

$$\boldsymbol{u^{Exp}(c,t) + u^{Comp}(c,t) \leq 1} \qquad [\boldsymbol{eq.\ 3-94}]$$

16. Expander cannot start up and shut down during the same time period

$$\boldsymbol{u^{Exp_{StUp}}(c,t) + u^{Exp_{ShDn}}(c,t) \leq 1} \qquad [\boldsymbol{eq.\ 3-95}]$$

17. Operational limits for expander

$$\boldsymbol{P^{D}(c,t) \geq P^{Exp}_{min}(c) \cdot u^{Exp}(c,t)} \qquad [\boldsymbol{eq.\ 3-96}]$$

$$\boldsymbol{P^{D}(c,t) \leq P^{Exp}_{max}(c) \cdot u^{Exp}(c,t)} \qquad [\boldsymbol{eq.\ 3-97}]$$

$$\boldsymbol{AMF^{out}(c,t) \geq AMF^{out}_{min}(c) \cdot u^{Exp}(c,t)} \qquad [\boldsymbol{eq.\ 3-98}]$$

$$\boldsymbol{AMF^{out}(c,t) \leq AMF^{out}_{max}(c) \cdot u^{Exp}(c,t)} \qquad [\boldsymbol{eq.3-99}]$$

18. Operational limits for compressor

$$\boldsymbol{P^{C}(c,t) \geq P^{Comp}_{min}(c) \cdot u^{Comp}(c,t)} \qquad [\boldsymbol{eq.3-100}]$$

$$\boldsymbol{P^{C}(c,t) \leq P^{Comp}_{max}(c) \cdot u^{Comp}(c,t)} \qquad [\boldsymbol{eq.3-101}]$$

$$\boldsymbol{AMF^{in}(c,t) \geq AMF^{in}_{min}(c) \cdot u^{Comp}(c,t)} \qquad [\boldsymbol{eq.3-102}]$$

$$\boldsymbol{AMF^{in}(c,t) \leq AMF^{in}_{max}(c) \cdot u^{Comp}(c,t)} \qquad [\boldsymbol{eq.3-103}]$$

3.4.3.3 Mathematical Formulation of a deterministic Unit Commitment Model for a power system with thermal generators, wind and solar generators, hydro generators and energy storage (CAES)

In this section a unit commitment model that simulates a power system with CAES being part of the generation fleet is formulated. The model includes the Thermo-Economic CAES model and it is a combination of the models introduced in sections 3.4.2 and 3.4.3.2. It is a least-cost optimization algorithm. This model will be applied on the power system of Ireland in chapter 5.

Sets

g: Generators $g_1 \leq g \leq g_{NG}$

t: Time steps $t_1 \leq t \leq t_{NT}$

f: Fuel $f_1 \leq f \leq t_{NF}$

i: Buses $i_1 \leq i \leq i_{NI}$

l: Power segments of fuel cost function $l_1 \leq l \leq l_{NL}$

AMF: The air mass flow at the compression side $AMF_1 \leq$ AMF $\leq AMF_N$ [32]

Pr: The compressor discharge pressure $Pr_1 \leq$ Pr $\leq Pr_N$ [33]

c: CAES units, $c_1 \leq \mathrm{c} \leq c_N$

---

[32] In this thesis the number of AMF segments is 21 so that AMF1 represents 270lb/sec, AMF2 represents a value of 280lb/sec, Pr3 a value of 290 lb/sec, ….. , AMF121 represents a value of 470 lb/sec (see figure 3-10).

[33] In this thesis the number of pressure segments is 13 so that Pr1 represents 900PSI, Pr2 represents a value of 950PSI, Pr3 a value of 1000 PSI, ….. , Pr13 represents a value of 1500PSI (see figure 3-10).

G(i): The subset of generators g being connected to bus i

G' : The subset of generators that are must-run

C(i): The subset of CAES units c being connected to bus i

where:

NG: Total number of generators

NT: Total number of time steps comprising one optimization cycle

NF: Total number of fuels

NI: Total number of buses

NL: Total number of power segments to break down the power curves of generators

NC: $Total\ number\ of\ CAES\ units$

NT: Total number of time steps

NAMF: Total number of Air Mass Flow segments

NPr: Total number of back pressure segments

Binary variables

$\boldsymbol{u}(\boldsymbol{g},\boldsymbol{y})$: Unit g operates at time t (1: YES, 0: NO)

$\boldsymbol{uStUp}(\boldsymbol{g},\boldsymbol{y})$: Unit g started up at time t (1:YES, 0: NO)

$\boldsymbol{uShDn}(\boldsymbol{g},\boldsymbol{y})$: Unit g shut down at time t (1:YES, 0: NO)

$\mathbf{u}^{\mathbf{exp}_{\mathbf{StUp}}}(\mathbf{c},\mathbf{t})$: CAES expander c started up at time t (1: YES, 0: NO)

$\mathbf{u}^{\mathbf{exp}_{\mathbf{ShDn}}}(\mathbf{c},\mathbf{t})$: CAES expander c shut down at time t (1:YES, 0: NO)

$\mathbf{u}^{comp_{\mathbf{StUp}}}(\mathbf{c},\mathbf{t})$: CAES compressor c started up at time t (1: YES, 0: NO)

$\mathbf{u}^{comp_{\mathbf{ShDn}}}(\mathbf{c},\mathbf{t})$: CAES compressor c shut down at time t (1: YES, 0: NO)

$\mathbf{u}^{\mathbf{exp}}(\mathbf{c},\mathbf{t})$: CAES expander c operates at time t (1: YES, 0: NO)

$\mathbf{u}^{\mathbf{comp}}(\mathbf{c},\mathbf{t})$: CAES compressor c operates at time t (1: YES, 0: NO)

$\mathbf{u}^{\mathbf{comp}}_{\mathbf{power}}(\mathbf{c},\mathbf{AMF},\mathbf{Pr},\mathbf{t})$: CAES compressor c operates at air mass flow levels indicated by AMF and back pressure levels indicated by Pr (1: YES, 0: NO)

Continuous variables

$\mathbf{AM}(\mathbf{c},\mathbf{t})$: Total air mass in the CAES cavern at the end of time period t [kgs]

$\mathbf{AMF}^{\mathbf{in}}(\mathbf{c},\mathbf{t})$: Air mass flow entering the cavern of CAES unit c during time period t $[\frac{\mathrm{lb}}{\mathrm{sec}}]$

$\mathbf{AMF}^{\mathbf{out}}(\mathbf{c},\mathbf{t})$: Air mass flow exiting the cavern of CAES unit c during time period t $[\frac{\mathrm{lb}}{\mathrm{sec}}]$

$\boldsymbol{Comp}^{\boldsymbol{Power}}_{\boldsymbol{Consumption}}(\mathbf{c},\mathbf{t})$: CAES compressor power input during time t [MW]

$\mathbf{FC}\ (\mathbf{g},\mathbf{f},\mathbf{t})$: Fuel cost by generator g, during time increment t, due to burning fuel f $[\frac{\$}{\mathrm{time\ increment}}]$

$\mathbf{P}\ (\mathbf{g},\mathbf{f},\mathbf{t})$: Power produced by generator g, during time increment t, due to burning fuel f [MW]

$\mathbf{P\ l}(\mathbf{l},\mathbf{g},\mathbf{t})$: Power per piece wise linear segment of the I/O curve by generator g, during time increment t, due to burning fuel f [MW]

$\mathbf{Pmax}\,(\mathbf{g},\mathbf{t})$: Maximum power output of generator g, during time increment t [MW]

(depends on ramp rates and future state of unit g, (see eq. 13)

$\boldsymbol{P_{W\_curt}}(\mathbf{i},\mathbf{t})$: Curtailed wind power at bus i and time t [MW]

$\boldsymbol{P_{PV\_curt}}(\mathbf{i},\mathbf{t})$: Curtailed PV power at bus i and time t [MW]

$\mathbf{P^C}(\mathbf{c},\mathbf{t})$: Power needed to charge CAES unit c at time t [MW]

$\mathbf{P^D}(\mathbf{c},\mathbf{t})$: Power discharged at hour t from CAES unit c [MW]

$\boldsymbol{P^D_{max}}\,(\mathbf{c},\mathbf{t})$: Maximum allowable power discharged at hour t from CAES unit c [MW]

$\mathbf{PrCavern}(\mathbf{c},\mathbf{t})$: Pressure level in the cavern of unit c at the end of period t [PSI]

$\boldsymbol{PrCavern^{Average}}(\mathbf{c},\mathbf{t})$: Average pressure level in the cavern of unit c during period t

$\mathbf{PrComp}(\mathbf{c},\mathbf{t})$**:** Average compressor discharge pressure during time t[34]

$\mathbf{UNMET}(\mathbf{i},\mathbf{t})$: Unmet demand during time increment t [MW]

$\mathbf{w}(\mathbf{c},\mathbf{t})$**:** Continuous variable equal to the bilinear term for the McCormick reformulation

Model parameters (inputs)

$\boldsymbol{AMF^{in}_{min}}(\mathbf{c})$: The minimum compressor air mass flow entering the cavern $\left[\frac{lb}{sec}\right]$

$\boldsymbol{AMF^{in}_{max}}(\mathbf{c})$: The maximum compressor air mass flow entering the cavern $\left[\frac{lb}{sec}\right]$

[34] A compressor's discharge pressure follows the cavern's back pressure. However it is necessary to introduce an additional variable that can take value zero. This is because the compressor doesn't operate at all times and in that respect the compressor discharge pressure needs to take value zero when CAES is discharging or idling. On the other side the pressure of the cavern has positive values even when the compressor is not operating. The introduction of this second variable is necessary for building the model.

$\boldsymbol{AMF_{min}^{out}}(\mathbf{c})$: The minimum expander air mass flow exiting the cavern $\left[\frac{lb}{sec}\right]$

$\boldsymbol{AMF_{max}^{out}}(\mathbf{c})$: The maximum compressor air mass flow exiting the cavern $\left[\frac{lb}{sec}\right]$

$\mathbf{Cap}\ (\mathbf{g})$: Rated capacity of thermal generator g [MW]

$\boldsymbol{CarbonPrice}$: Cost of CO2 emissions $\left[\frac{\$}{\mathrm{kg}}\right]$

$\boldsymbol{CarbonCap}$: Maximum number of tonnes of CO2 alowed during the optimization cycle[35] $\left[\frac{\$}{\mathrm{kg}}\right]$

$\boldsymbol{CoUE}$: Cost of Unserved Energy $\left[\frac{\$}{\mathrm{MWhr}}\right]$

$\boldsymbol{Cost_W}$: Cost of curtailed wind energy $\left[\frac{\$}{\mathrm{MWhr}}\right]$

$\boldsymbol{Cost_{PV}}$: Cost of curtailed PV energy $\left[\frac{\$}{\mathrm{MWhr}}\right]$

$\mathbf{CompPower}(\mathbf{c},\mathbf{AMF},\mathbf{Pr})$ **:** Power requirement of CAES compressor c to discharge to specific air mass flow and back pressure levels [MW]

$\mathbf{Cost_{StUp}^{exp}}(\mathbf{c})$: Start Up cost for CAES expander c [$]

$\mathbf{Cost_{StUp}^{comp}}(\mathbf{c})$: Start Up cost for CAES compressor c [$]

$\mathbf{Cost_{VOM}^{CAES}}(\mathbf{c})$: VOM costs for CAES c $\left[\frac{\$}{\mathrm{MWh}}\right]$

$\mathbf{Dn}\boldsymbol{T}^{\mathbf{0}}(\mathbf{g})$: Number of hours the unit was down since last shut down [hr]

$\boldsymbol{ER}(\boldsymbol{f})$: Emissions rate of fuel f $\left[\frac{kg\ CO2}{GJ}\right]$

$\boldsymbol{FuelCost(f)}$: Cost of fuel f $[\frac{\$}{\mathrm{GJ}}]$

$\boldsymbol{FuelLim(f)}$: Maximum daily fuel reserve of fuel f during year y $\left[\frac{MMBTU}{day}\right]$

$\boldsymbol{HR_{Rated}^{CAES}}(\mathbf{c})$: Rated heat rate of CAES expander $\left[\frac{\mathrm{GJ}}{\mathrm{MWh}}\right]$

$\boldsymbol{HRNL(g)}$: No Load Heat Requirement of generator g $[\frac{\mathrm{GJ}}{\mathrm{hr}}]$

$\boldsymbol{HRINC0(g)}$: Incremental heat requirement of generator g from no load to LP1 $[\frac{\mathrm{GJ}}{\mathrm{hr}}]$

$\boldsymbol{HRINCl(g)}$: Incremental heat requirement of generator g from LPl to LPl $+ 1 \left[\frac{\mathrm{GJ}}{\mathrm{hr}}\right]$

$1 \leq \mathrm{l} \leq 4$

$\mathbf{LoadPart(i)}$: Load participation at bus i.It is the percentage of total load allocated at each bus [%]

$\boldsymbol{LPx(g)}$: Load point x of generator g [MW], $1 \leq \mathrm{x} \leq 5$

$\mathbf{MinDnT\ (g)}$: Minimum down time of generator g [hr]

$\mathbf{MinUpT\ (g)}$: Minimum up time of generator g [hr]

$\mathbf{PF\ (i, j, t)}$: Power flow from bus i to bus j at time t [MW]

$\mathbf{Pmin\ (g)}$: Minimum power output of generator g [MW]

$\mathbf{P_{max}^{exp}(c, t)}$: Maximum capacity of CAES expander c connected at bus i[MW]

$\mathbf{P_{min}^{exp}(c, t)}$: Minimum output of CAES expander c connected at bus i [MW]

$\mathbf{P_{min}^{comp}(c, t)}$: Minimum power drawn by CAES compressor c connected at bus i [MW]

$\mathbf{P_{max}^{comp}(c, t)}$: Maximum power drawn by CAES compressor c connected at bus i [MW]

$\mathbf{p^{ng}}$: price of natural gas $\left[\frac{\$}{\mathrm{GJ}}\right]$

$\boldsymbol{PrCavern_{min}(c)}$**:** The minimum working pressure in the cavern [PSI]

$\boldsymbol{PrCavern_{max}}$**(c):** The maximum working pressure in the cavern [PSI]

R: Constant of ideal gasses (equal to 0.0000813$\left[\frac{m^3 \cdot \mathrm{Bars}}{K \cdot mole}\right]$)

RunDn (g): The ramp down rate of generator g during shut down $[\frac{\mathrm{MW}}{\mathrm{hr}}]$

RunUp(g): The ramp up rate of generator g during start up $[\frac{\mathrm{MW}}{\mathrm{hr}}]$

RampDn (g): The ramp down rate of generator g during normal operation $[\frac{\mathrm{MW}}{\mathrm{hr}}]$

RampUp (g): The ramp up rate of generator g during normal operation $[\frac{\mathrm{MW}}{\mathrm{hr}}]$

$\boldsymbol{S(g,l)}$: Maximum power of piece wise linear segment l of generator g [MW]

$\boldsymbol{SL}$: Time length of one time step [hr]

$\boldsymbol{S(g,l)}$: Maximum power of piece wise linear segment l of generator g [MW]

$\boldsymbol{StUpCost(g)}$: Start up cost of generator g$\left[\frac{\$}{MWh}\right]$

Tcavern(c): Temperature in the cavern[^oK][36]

$\boldsymbol{TL(i,j)}$: Transmission losses from bus i to bus j [%]

$\mathbf{Up}\boldsymbol{T^0}\mathbf{(g)}$: Number of hours the unit was up since last start up [hr]

Vcavern(c): Volume of the cavern[^oK]

[36] We assume isothermal CAES units that charge the cavern at constant temperature

$\boldsymbol{VOM(g)}$: Variable O&M cost of generator g $\left[\frac{\$}{MWh}\right]$

Objective function

The objective function of the UC problem with CAES is:

$$\boldsymbol{Minimize} \sum_{g=g1}^{g_{NG}} \sum_{t=t1}^{t_{NT}} \sum_{f=f1}^{f_{NF}} \sum_{i=i1}^{i_{NI}} \Big(\boldsymbol{Cost_{Fuel}}\,(\boldsymbol{g},\boldsymbol{f},\boldsymbol{t}) + \boldsymbol{Cost_{VOM}}(\boldsymbol{g},\boldsymbol{f},\boldsymbol{t})$$

$$+ \boldsymbol{Cost_{CO2}}(\boldsymbol{g},\boldsymbol{f},\boldsymbol{t}) + \ \boldsymbol{Cost_{Start\ Up}}\,(\boldsymbol{g},\boldsymbol{t}) + \boldsymbol{Cost_{UNMET}}(\boldsymbol{i},\boldsymbol{t})$$

$$+ \boldsymbol{Cost_{VRE_{Curtailment}}}(\boldsymbol{i},\boldsymbol{t}) \Big)$$

$$+ \sum_{t=t1}^{t_{NT}} \sum_{c=c1}^{c_{NC}} \Big(\boldsymbol{Cost_{Fuel}^{CAES}}(\boldsymbol{c},\boldsymbol{t}) + \boldsymbol{Cost_{VOM}^{CAES}}(\boldsymbol{c},\boldsymbol{t}) + \boldsymbol{Cost_{StUp}^{CAES}}\,(\mathbf{c},\mathbf{t}) \Big)$$

$$[\boldsymbol{eq}.\mathbf{3-104}]$$

where:

$\boldsymbol{Cost_{Fuel}}$: Operational cost of fuel for each generator [$] (see figure 3-7)

$$\boldsymbol{Cost_{Fuel}\,(g,f,t)} = \left[\mathbf{HRNL\ (g) \cdot u(g,t) + LP1(g) \cdot HRINC0(g) \cdot u(g,t)} + \sum_{l=1}^{NL} (\boldsymbol{S(g,l)} \cdot \mathbf{HRINC(g,l)})\right] \cdot \left(\mathbf{FuelCost(f)}\right) \cdot \boldsymbol{SL}$$

$$[\boldsymbol{eq}.\mathbf{3-105}]$$

$\boldsymbol{Cost_{VOM}}$: Variable O&M cost for each generator [$]

$$\boldsymbol{Cost_{VOM}\,(g,t)} \ = \left(\mathbf{P(g,f,t)}\right) \cdot \mathbf{VOM(g)}) \times \mathbf{SL} \qquad [\mathbf{eq.3-106}]$$

$\boldsymbol{Cost_{StartUp}}$: Start Up cost for each generator at time t [$]

$$\boldsymbol{Cost_{StartUp}\,(g,t)} \ = \ \mathbf{uStUp(g,t) \cdot StUpCost(g)} \qquad [\boldsymbol{eq}.\ \mathbf{3-107}]$$

$\boldsymbol{Cost_{C02}}$: Cost of carbon [$]

$$\boldsymbol{Cost_{C02}\,(g,f,t)} = \left[\mathbf{HRNL\ (g) \cdot u(g,t) + LP1(g) \cdot HRINC0(g) \cdot u(g,t)} + \sum_{l=1}^{NL} (\boldsymbol{S(g,l)} \cdot \mathbf{HRINC(g,l)})\right] \times (\mathbf{ER(f)} \cdot \boldsymbol{Carbon\ Price}) \times \boldsymbol{SL}\,, \quad \boldsymbol{f \in F(g)}$$

$$[\boldsymbol{eq}.\ \mathbf{3-108}]$$

$\boldsymbol{Cost_{USE}}$: Cost of unused energy [$]

$$\boldsymbol{Cost_{USE}\ (i,t)}\ =\ \mathbf{UNMET(i,t) \times CoUE \times \boldsymbol{SL}} \qquad [\boldsymbol{eq.3-109}]$$

$\boldsymbol{Cost_{VRE\_Curt}}$: Cost of curtailed VRE energy [$]

$$\boldsymbol{Cost_{VRE_{Curt}}\ (i,t)} = \left[\boldsymbol{P_{W_{Curt}}}(\mathbf{i,t}) \times \mathbf{CostW} + \boldsymbol{P_{PV_{Curt}}}(\mathbf{i,t}) \times \mathbf{CostPV}\right] \cdot \boldsymbol{SL}$$

$$[\boldsymbol{eq.3-110}]$$

$\boldsymbol{Cost^{CAES}_{Fuel}(c,t)} = \boldsymbol{C}$ost of natural gas burners during time period t [$]

$$\boldsymbol{Cost^{CAES}_{Fuel}(c,t) = p^{ng}(t) \cdot HR_{CAES}(c,t) \cdot P^{D}(c,t) \cdot SL} \qquad [\boldsymbol{eq.3-111}]$$

$\boldsymbol{Cost^{CAES}_{VOM}(c,t)} = Variable\ cost\ of\ CAES\ operation\ during\ time\ period\ t$ [$]

$$\boldsymbol{Cost^{CAES}_{Fuel}(c,t) = Cost^{CAES}_{VOM}(c) \cdot P^{D}(c,t) \cdot SL} \qquad [\boldsymbol{eq.3-112}]$$

$\boldsymbol{Cost^{CAES}_{StUp}}\ (\mathbf{c,t}) = \boldsymbol{S}$tart Up Costs cost of CAES during time period t [$]

$$\boldsymbol{Cost^{CAES}_{StUp}}\ (\mathbf{c,t}) = \ \mathbf{u^{exp_{StUp}}(c,t) \cdot Cost^{exp}_{StUp}(c) - u^{\boldsymbol{comp}_{StUp}}(c,t) \cdot Cost^{comp}_{StUp}(c)}$$

$$[\boldsymbol{eq.3-113}]$$

SYSTEM CONSTRAINTS

1. **Fuel reserve constraint** (the amount of fuel that can be consumed for each optimization period is constraint by some value FL(f) [

$$\sum_{g=g1}^{gNG}\sum_{t=t1}^{tNT}[\mathbf{HRNL}\,(\mathbf{g})\times\mathbf{u}(\mathbf{g},\mathbf{t})+\mathbf{LP1}(\mathbf{g})\times\mathbf{HRINC0}(\mathbf{g})\times\mathbf{u}(\mathbf{g},\mathbf{t})+\sum_{l=1}^{NL}(\boldsymbol{S}(\boldsymbol{l})\cdot\mathbf{HRINC}(\mathbf{g},\mathbf{l}))]\cdot\left(\frac{\boldsymbol{NT}}{\mathbf{24}}\right)\leq\boldsymbol{FL}(\boldsymbol{f})\cdot\left(\frac{\mathbf{1}}{\mathbf{0.97}}\right)$$

[eq. 3-114]

2. **Power flow across transmission lines** (transport model)

$$\sum_{g=g1}^{g_{NG}}\sum_{f=f1}^{f_{NF}}[\mathbf{P}(\mathbf{g},\mathbf{f},\mathbf{t})]+\mathbf{UNMET}(\mathbf{i},\mathbf{t})+\mathbf{P_w}(\mathbf{i},\mathbf{t})+\mathbf{P_{PV}}(\mathbf{i},\mathbf{t})+\mathbf{P_H}(\mathbf{i},\mathbf{t})$$
$$+\sum_{j=j1}^{j_{NJ}}[\mathbf{PF}(\mathbf{j},\mathbf{i},\mathbf{t})\cdot(\mathbf{1}-\mathbf{TL}(\mathbf{j},\mathbf{i}))]-\sum_{j=j1}^{j_{NJ}}[\mathbf{PF}(\mathbf{i},\mathbf{j},\mathbf{t})]$$
$$=\mathbf{Demand}(\mathbf{i},\mathbf{t})\cdot\mathbf{LoadPart}(\mathbf{i})$$
$$+\sum_{c=c1}^{c_{NC}}\mathbf{Pc}(\mathbf{c},\mathbf{t})\qquad\forall\ \mathbf{c}\in\mathbf{C}(\mathbf{i}),\ \forall\ \mathbf{g}\in\mathbf{G}(\mathbf{i})$$

$[\mathbf{eq.3-115}]$

3. **Reserve margin constraint**

$$\sum_{g=g1}^{g_{NG}}\left[\boldsymbol{u(g,t)\cdot Gmax(g)-\sum_{f}P(g,f,t)}\right]\leq \boldsymbol{ResMarg\cdot Demand(t)}\quad \boldsymbol{f}\in \boldsymbol{F(g)}$$

$$[\boldsymbol{eq.3-116}]$$

UNIT CONSTRAINTS

4. **The power output of each unit is the sum of power output from each power segment of the I/O curve**

$$\sum_{\mathbf{f}}\mathbf{P(g,f,t)}\leq\sum_{\mathbf{l=l1}}^{\mathbf{lNL}}\mathbf{(Pl(l,g,t))+LP1\cdot u(g,t)}\qquad\forall\ \ \mathbf{f}\in\mathbf{F(g)}\qquad[\mathbf{eq.3-117}]$$

5. **Power output per power segment**

$$\mathbf{0}\leq \boldsymbol{Pl(l,g,t)}\leq \boldsymbol{LP_{l+1}(g)-LP_{l}(g)}\qquad[\mathbf{eq.3-118}]$$

6. **Defining operation range of thermal generators**

$$\boldsymbol{Pmin(g) \leq \sum_{f} P(g,f,t) \leq Pmax(g,t) \qquad \forall\ f \in F(g)} \qquad [\boldsymbol{eq.\ 3-119}]$$

7. **Capping maximum power output based on ramping limits of generators**

$$\mathbf{Pmax(g,t) \leq Cap(g) \cdot \big(u(g,t) - uShDn(g,t+1)\big) + RunDn(g) \cdot uShDn(g,t+1)}$$

$$[\mathbf{eq.\ 3-120}]$$

8. **Relationship connecting on/off , start-up and shut-down binary variables for thermal generators**

$$\boldsymbol{uStUp(g,t) - uShDn(g,t) = u(g,t) - u(g,t-1)} \qquad [\boldsymbol{eq.3-121}]$$

9. **Thermal units can-not start-up and shut-down within the same time step**

$$\mathbf{uStUp(g,t) + uShDn(g,t) \leq 1} \qquad [\mathbf{eq.\ 3-122}]$$

10. **Minimum up time (MUT) constraints**

$$\mathbf{\sum_{t=1}^{Lg} (1 - u(g,t)) = 0 \qquad \forall\ g \in G, \qquad \forall\ t \in 1, \ldots L_g} \qquad [\mathbf{eq.\ 3-123}]$$

$$\boldsymbol{\sum_{\tau=t}^{T1} u(g,\tau) \geq MinUpT(g) * uStUp(g,t),}$$

$$\forall \;\; \boldsymbol{t} \in \boldsymbol{L_g} + \mathbf{1} \ldots . \mathrm{NT} - \boldsymbol{MinUpT(g)} + \mathbf{1} \qquad [\boldsymbol{eq} \;\; \mathbf{3-124}]$$

$$\sum_{\tau=t}^{NT} (\boldsymbol{u(g,\tau)} - \boldsymbol{uStUp(g,t)}) \geq \mathbf{0} \qquad \forall \quad \boldsymbol{t} \in \;\; \mathrm{NT} - \boldsymbol{MinUpT(g)} + \mathbf{2} \ldots \boldsymbol{NT}$$

[eq. 3- 125]

Where:

L_g:Number of time steps the unit has to stay on at the beginning of an optimization cycle. L_g depends on how many hours before the optimization the unit started up

$$\boldsymbol{Lg} = \mathbf{min}\{\boldsymbol{\Theta}, (\boldsymbol{MinUpT(g)} - \boldsymbol{UpT^0}) \times \boldsymbol{u(g,0)}\} \qquad \textbf{[eq. 3-126]}$$

11. Minimum down time (MDT) constraints

$$\sum_{\mathbf{t=1}}^{\mathbf{Kg}} \mathbf{u(g,t)} = \mathbf{0} \qquad \forall \quad \mathbf{g} \in \mathbf{G}, \quad \forall \;\; \mathbf{t} \in \mathbf{1}, \ldots \mathbf{K_g} \qquad [\mathbf{eq.} \;\; \mathbf{3-127}]$$

$$\sum_{\tau=t}^{T2} \left(\mathbf{1} - \boldsymbol{u(g,\tau)}\right) \geq \boldsymbol{MinDnT(g)} * \boldsymbol{uShDn(g,t)},$$

$$\forall \;\; \boldsymbol{t} \in \boldsymbol{K_g} + \mathbf{1} \ldots . \mathrm{NT} - \boldsymbol{MinDnT(g)} + \mathbf{1} \qquad [\mathbf{eq.3-128}]$$

$$\sum_{\tau=t}^{NT}(\mathbf{1}-u(g,\tau)-uShDn(g,t)) \geq \mathbf{0}\ ,$$

$$\forall\ t \in NT - MinUpT(g) + \mathbf{2} \ldots NT \qquad [eq\ \mathbf{3}-\mathbf{129}]$$

Where:

$\boldsymbol{Kg}$: Number of time steps the unit has to stay off when the optimization cycle begins

Kg depends on how many hours before the optimization cycle the unit shut down

$$\boldsymbol{Kg} = \min\{NT, (MinDnT(g) - DnT^{0}) \times (\mathbf{1}-u(g,\mathbf{0}))\} \qquad [eq.\mathbf{3}-\mathbf{130}]$$

12. Unit ramping up and ramp down constraints

$$\mathbf{Pmax(g,f,t)} \leq \sum_{\mathbf{f}} \mathbf{P(g,f,t-1)} + \mathbf{RampUp(g)} \times \mathbf{u(g,t-1)} + \mathbf{RunUp(g)} \times \mathbf{uStUp(g,t)}$$

$$[\mathbf{eq.}\ \mathbf{3}-\mathbf{131}\ ]$$

$$\sum_{\mathbf{f}}(\mathbf{P(g,f,t-1)} - \mathbf{P(g,f,t-1)}) \leq \mathbf{RampDn(g)} \times \mathbf{u(g,t)} + \mathbf{RunDn(g)} \times \mathbf{uShDn(g,t)}\ , \forall\ \ \mathbf{f} \in\ \mathbf{F(g)}$$

$$[\mathbf{eq.3}-\mathbf{132}\ ]$$

13. Must-run operation

$$\sum_{g} \boldsymbol{u}(\boldsymbol{g},\boldsymbol{t}) = \boldsymbol{NT} \quad \boldsymbol{g} \in \boldsymbol{G}' \qquad [\boldsymbol{eq}.3 - 133]$$

CAES CONSTRAINTS

14. Power consumption at the compressor

$$\boldsymbol{P^C}(\mathbf{c},\mathbf{t}) = \sum_{AMF=AMF_1}^{AMF_N} \sum_{Pr=Pr_1}^{Pr_N} \Big(\boldsymbol{CompPower}(\boldsymbol{c},\boldsymbol{AMF},\boldsymbol{Pr}) \cdot \boldsymbol{u}_{Power}^{Comp}(\boldsymbol{c},\boldsymbol{AMF},\boldsymbol{Pr},\boldsymbol{t})\Big)$$

$$[\boldsymbol{eq}.3 - 134]$$

15. Air Mass Flow in the cavern (compression side)

$$\boldsymbol{AMF}_{in}(\boldsymbol{c},\boldsymbol{t}) = \sum_{AMF=AMF_1}^{AMF_N} \sum_{Pr=Pr_1}^{Pr_N} \Big(\big(\mathbf{260} + \mathbf{10} \cdot \mathbf{ord}(\mathrm{AMF})\big) \cdot \boldsymbol{u}_{Power}^{Comp}(\boldsymbol{c},\boldsymbol{AMF},\boldsymbol{Pr},\boldsymbol{t})\Big)$$

$$[\mathbf{eq.}\ 3 - 135]$$

Where:

ord(AMF): The number of AMF. For example if AMF=AMF_{10}, then ord (AMF)=10.

16. The compressor can idle or operate at a unique power input at each time increment

$$\sum_{AMF=AMF_1}^{AMF_N}\sum_{Pr=Pr_1}^{Pr_N}\left(u_{Power}^{Comp}(c,AMF,Pr,t)\right)=u^{comp}(c,t) \qquad [eq.3-136]$$

17. Relationship connecting the compressor discharge pressure with power input

$$\mathbf{PrComp}(\mathbf{c},\mathbf{t})=\sum_{AMF=AMF_1}^{AMF_N}\sum_{Pr=Pr_1}^{Pr_N}\left(u_{Power}^{Comp}(c,AMF,Pr,t)\cdot(850+ord(Pr)\cdot 50\right)$$ [37]

[eq. 3-137]

18. Relationship connecting compressor discharge pressure and the pressure of the cavern

$$\mathbf{PrComp}(\mathbf{c},\mathbf{t})\leq u^{comp}(c,t)\cdot PrCavern^{Average}(c,t) \qquad [eq.3-138]$$

$$\mathbf{PrComp}(\mathbf{c},\mathbf{t})\leq w(c,t) \qquad [eq.3-139]$$

[37] ord(Pr) is the number of set Pr. For example if Pr=Pr_{10} then ord(Pr)=10

$$w(c,t) \geq 0 \qquad [eq.3-140]$$

$$w(c,t) \geq u^{comp}(c,t) \cdot PrCavern_{min}(c) \qquad [eq.3-141]$$

$$w(c,t) \leq u^{comp}(c,t) \cdot PrCavern_{max}(c) \qquad [eq.3-142]$$

$$w(c,t) \geq PrCavern^{Average}(c,t) + u^{comp}(c,t) \cdot PrCavern_{max}(c) - PrCavern_{max}(c) \qquad [eq.3-143]$$

$$w(c,t) \leq PrCavern^{Average}(c,t) + u^{comp}(c,t) \cdot PrCavern_{min}(c) - PrCavern_{min}(c) \qquad [eq.3-144]$$

19. Relate CAES output with air mass flow exiting the cavern

$$P^{D}(c,t) = \mathrm{a01} \cdot AMF^{out}(c,t) + b01 \cdot u^{Exp}(c,t) \qquad \text{[eq. 3-145]}$$

20. Balance of air mass in cavern[38]

$$\mathrm{AM}(c,t) = \mathrm{AM}(\mathrm{c},\mathrm{t}-1) + \left(AMF^{in}(c,t) - AMF^{out}(c,t)\right) \cdot 3600 \cdot 0.45359 \qquad \text{[eq 3-146]}$$

[38] We assume energy losses in the cavern through heat exchange with the surroundings or air leakage are negligible

21. Balance of air mass flow in cavern[39].

$$\sum_{t=t1}^{t_N} \boldsymbol{AMF^{in}(c,t)} = \sum_{t=t1}^{t_N} \boldsymbol{AMF^{out}(c,t)} \qquad [\boldsymbol{eq.\ 3-147}]$$

22. Relationship determining the operational status of the generator

$$\boldsymbol{u^{Exp_{StUp}}(c,t) - u^{Exp_{ShDn}}(c,t) = u^{Exp}(c,t) - u^{Exp}(c,t-1)} \qquad [\boldsymbol{eq.\ 3-148}]$$

23. Relationship determining the operational status of the compressor

$$\boldsymbol{u^{Comp_{StUp}}(c,t) - u^{Comp_{ShDn}}(c,t) = u^{Comp}(c,t) - u^{Comp}(c,t-1)} \qquad [\boldsymbol{eq.\ 3-149}]$$

24. Relationship connecting air mass and pressure in the cavern (law of ideal gases)

$$\boldsymbol{\frac{AM(c,t) \cdot R \cdot Tcavern(c)}{0.001 \cdot Vcavern(c) \cdot MW_{air}} = \frac{PrCavern(c,t)}{14.95}} \qquad [\boldsymbol{eq.3-150}]$$

[39] Equation 3-149 ensures the cavern returnes in its initial energy level at the end of each optimization cycle to be ready for the next one. If the specific constraint is not entered the program will tend to deplete the cavern by the end of each cycle. As a result when the new cycle begins the cavern will have no stored energy and will need to charge before being able to make profit again. The initial energy level can be established through fixing the pressure in the cavern at time t1 equal to the average working pressure for example.

25. Relationship determining average pressure in the cavern[40]

$$PrCavern^{Average}(c,t) = \frac{PrCavern(c,t) + PrCavern(c,t-1)}{2} \quad [eq. 3-151]$$

26. Compressor cannot start-up and shut-down during the same time period

$$u^{Comp_{StUp}}(c,t) + u^{Comp_{ShDn}}(c,t) \leq 1 \quad [eq.\ 3-152]$$

27. CAES unit can either compress or generate or idle at a given time

$$u^{Exp}(c,t) + u^{Comp}(c,t) \leq 1 \quad [eq.\ 3-153]$$

28. Expander cannot start up and shut down during the same time period

$$u^{Exp_{StUp}}(c,t) + u^{Exp_{ShDn}}(c,t) \leq 1 \quad [eq.\ 3-154]$$

29. Operational limits for expander

$$P^{D}(c,t) \geq P^{Exp}_{min}(c) \cdot u^{Exp}(c,t) \quad [eq.\ 3-155]$$

$$P^{D}(c,t) \leq P^{Exp}_{max}(c) \cdot u^{Exp}(c,t) \quad [eq.\ 3-156]$$

$$AMF^{out}(c,t) \geq AMF^{out}_{min}(c) \cdot u^{Exp}(c,t) \quad [eq.\ 3-157]$$

$$AMF^{out}(c,t) \leq AMF^{out}_{max}(c) \cdot u^{Exp}(c,t) \quad [eq. 3-158]$$

[40] The variable PrCavern is the pressure in the cavern at the end of each time period t. However it is important to know the average pressure in the cavern at each time period otherwise we will overestimate the costs of compression because the power input increases with pressure in the cavern

30. Operational limits for compressor

$$P^{C}(c,t) \geq P_{min}^{Comp}(c) \cdot u^{Comp}(c,t) \qquad [eq.3-159]$$

$$P^{C}(c,t) \leq P_{max}^{Comp}(c) \cdot u^{Comp}(c,t) \qquad [eq.3-160]$$

$$AMF^{in}(c,t) \geq AMF_{min}^{in}(c) \cdot u^{Comp}(c,t) \qquad [eq.3-161]$$

$$AMF^{in}(c,t) \leq AMF_{max}^{in}(c) \cdot u^{Comp}(c,t) \qquad [eq.3-162]$$

POLICY CONSTRAINTS

31. Carbon cap constraint

$$\sum_{g=g1}^{gNG} \sum_{t=t1}^{tNT} (\mathbf{HRNL}(\mathbf{g}) \times \mathbf{u}(\mathbf{g},\mathbf{t}) + \mathbf{LP1}(\mathbf{g}) \times \mathbf{HRINC0}(\mathbf{g}) \times \mathbf{u}(\mathbf{g},\mathbf{t}) + \sum_{l=1}^{NL} (S(l) \times \mathbf{HRINC}(\mathbf{g},\mathbf{l}))) \cdot ER \cdot SL \cdot NT \cdot 0.001 \leq CarbonCap$$

[eq. 3-163]

Chapter 4 : Irish Power Sector Overview

4.1 Context

This chapter presents information and analysis of the Irish power sector that is pertinent to the application of the developed UCED and CAES models in the Irish grid. More specifically, I present information about:

1. The Irish Electricity market structure.
2. Current supply-demand balance.
3. Related issues of utilization and availability of existing generators as well as plans for adding generating capacity up to year 2020.
4. A basic analysis of past demand trends and presentation of latest demand projections for the country.
5. Dependence of the country on imported fuels.
6. Existing high level transmission network.
7. Regional interconnections.
8. A range of policy issues such as: renewable energy targets, carbon reduction goals, diversification of the fuel mix, and energy efficiency.

The above information will be used for the construction, validation and application of a mixed integer programming (MIP) unit commitment and economic dispatch (UCED) model of the Irish grid. The validation of the model will be presented on chapter 5. In chapter 7 the model is being applied to simulate the 2020 Irish grid when RE penetration is expected to reach 40%.

4.2 Irish electricity market structure

The Republic of Ireland has a partially decentralized system with a fully liberalized wholesale market, comprising a centrally regulated Transmission System Operator (TSO) also called EIRGRID and an open competitive retail market. Also, North Ireland (NI) which is part of the UK has its own transmission operator (SONI). The island of Ireland - also called All-Island in this thesis- is composed of the Republic of Ireland and Norther Ireland.

The electricity sector in All-Island Ireland previously operated as two separate markets, but on November 1st, 2007 the EIRGRID and SONI established the Single Electricity Market (SEM). The SEM has created a gross mandatory pool market that sets prices for trade of wholesale electricity. EIRGRID and SONI are both owned by EirGrid plc which acts as the Single Energy Market Operator (SEMO). All electricity is centrally traded through a pool system where licensed generators sell their electricity to a licensed supplier who sells it onto the pool, and receives a single market price (SMP). The Trading and Settlement Code (TSC) outlines the rules for remuneration for payment for availability to increase generation should the grid operator instruct them to [19].

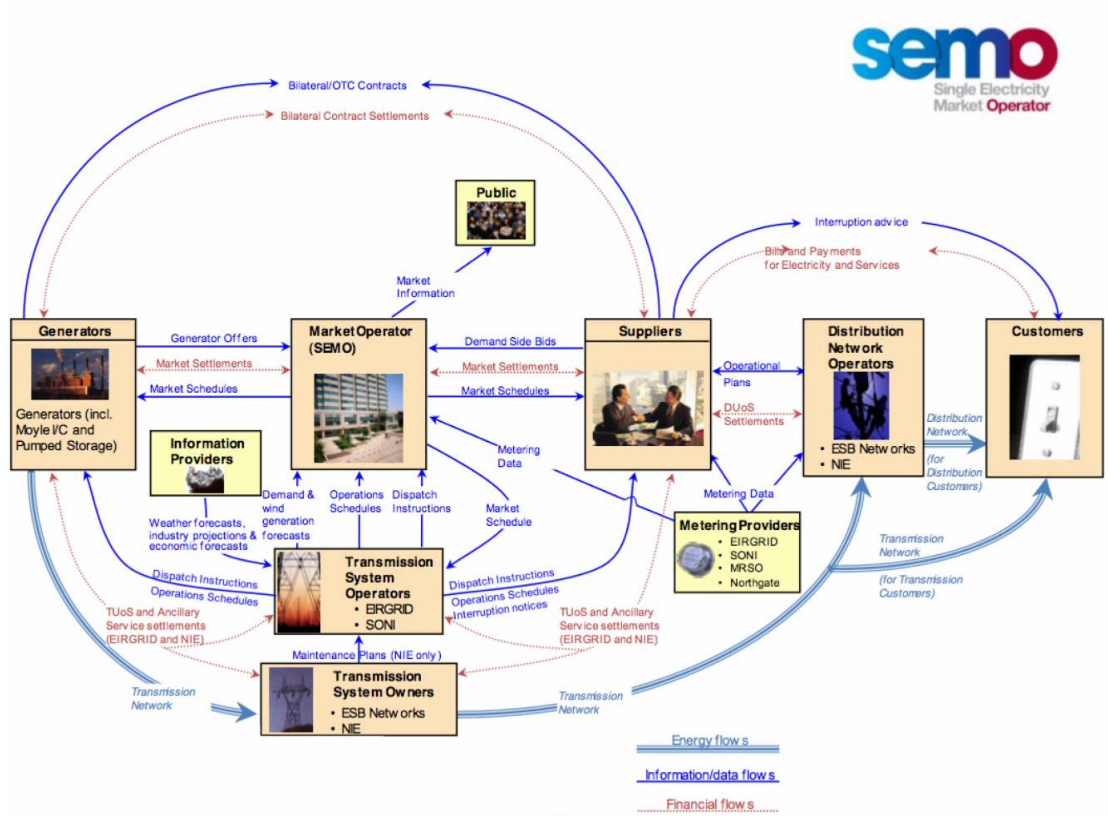

Figure 4-1: The SEMO structure (Source: Wattics website: http://www.wattics.com/the-electricity-market-in-ireland/).

Within SEM, electricity generators with capacity higher than 10MW are obliged by law to sell electricity into this single pool for the island of Ireland. This mandatory centralized pool market in SEM is different than in most European and American markets in which most of trade takes place through bilateral contracts. In that respect, Ireland is a transparent market that can be well approximated with a least-cost UCED model. This is one of the main reasons the Irish grid was chosen as a in this PhD work to be used for the UCED model validation presented in chapter 5. Since deterministic models cannot predict non-deterministic decisions exercised on a market environment the validation process becomes easier if it is applied in a transparent market that operates as closely towards least-cost market balance.

The individual generators in Ireland must submit bids that reflect their Short Run Marginal Costs (SRMC) (€/MWh). The bidding process is regulated by a Bidding Code of Practice[41]. The SRMCs are defined as the cost of generating electricity minus costs of not generating. Therefore, in addition to their fuel costs, generators must also provide technical data related to their start-up costs, carbon emissions costs and minimal ramping costs. The Bidding Code of Practice connects the cost of fuel commodities to the prevailing spot prices on the appropriate accessible market.

A generator selling electricity to the wholesale pool market may receive the following payments that are presented here but not used in this thesis:

- **Energy payment**: It is the System Marginal Price to be discussed in detail later on this section.
- **Capacity payments**: It is compensation for providing available capacity. Capacity payments are calculated based on the relatively low fixed costs of a peaking plant and generally cover only a portion of overnight capital costs for building most plants.
- **Constraint Payments:** Compensation for being constraint from exporting the already scheduled amount of energy onto the system due to grid stability issues [20].

[41] . The Bidding Code of Practice is available at https://www.allislandproject.org

Generators must submit that represent their short-term marginal costs (SRMC[42] s) bids to SEMO the day before generation, known as D-1. SRMCs represent the opportunity cost of producing electricity. Separate cost components submitted through bids reflect generator start-up and generator no-load costs.

The system marginal price is determined by SEMO, considering offers from generators and suppliers. The dispatch calculation is performed using a stack of the cheapest all-island generator cost bids necessary to meet all-island demand. Most efficient generators participate in the half hourly "Market Schedule" while more expensive or inefficient generators are "out of merit". The most expensive bid that makes it into the Market Schedule sets the System Marginal Price (SMP). All generators that bid below the SMP make profit known as "infra-marginal rent" or the difference between SRMC bid offer and the SMP. The SMP itself is composed of two elements a) the shadow price and b) the uplift component. The shadow price is composed of the SRMC bids of generators. The uplift component is paid if generator start-up and no-load costs are not covered through infra-marginal rent payments. This can happen for example if a generator only runs for a short time to meet demand [21].

[42] For example if a gas generator wouldn't be generating it could make profit through selling its gas to the spot market.

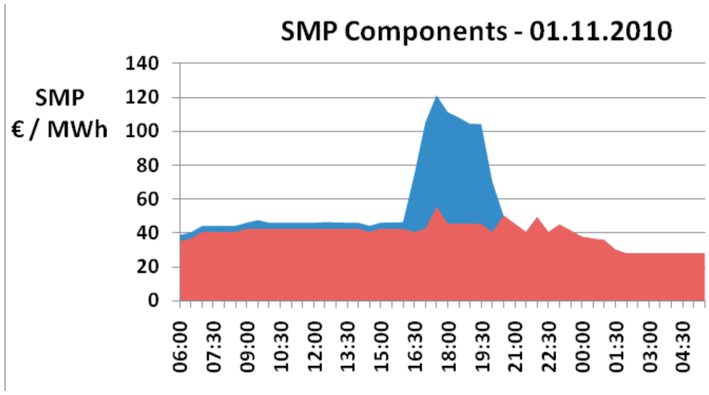

Figure 4-2: Shadow (red) and Uplift (red) components of the SMP during 1 day in SEM (Source: **[21]**).

As it will be discussed later in this chapter, most of thermal generation in All-Island is natural gas-fired. Therefore, the wholesale gas price is a key driver of electricity prices in the SEM. This is also shown on graph 4-3, and it has been the case historically. A more detailed discussion about natural gas and how it affects prices on SEM can be found on section 4.3.2.1. The same trend exists in GB as well. In chapter 5, I discuss the method applied to approximate the GB as a gas generator and estimate the electricity production cost that determines the electricity exchange between the SEM and GB. The electricity trading principles are discussed in detail in section 4.2.2.

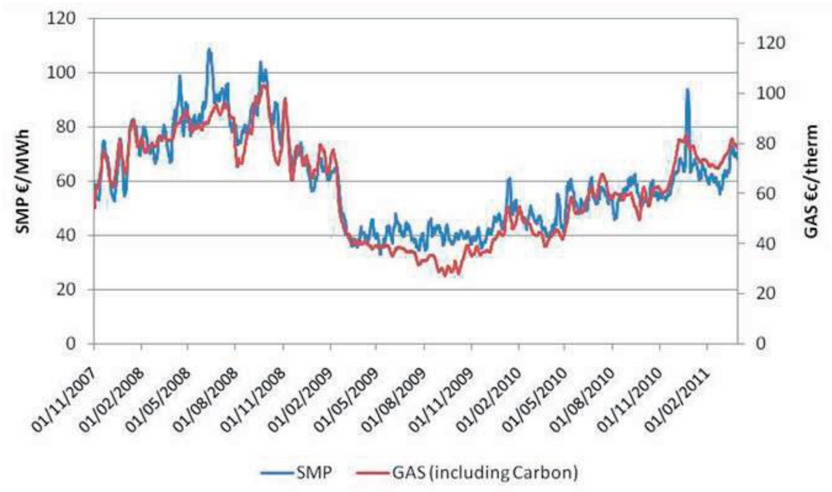

Figure 4-3: SMPs and Natural Gas spot prices from late 2007 to early 2011 (Source: **[21]**)

The system operators produce the Indicative Operations Schedule the day before the trading day (D-1). However, because of uncertainty on demand forecast, on wind production and system constraints the indicative plan diverts from the actual plan. For that reason additional software runs take place the day after (D+1) and 4th day after trading day (D+4) to finalize the SMP paid to generators. Generators that had to produce more than what was in the Indicative Plan due to technical constraints receive constraint payments. Generators that were initially scheduled to run but ended up not generating are getting the SMP minus their bid [21]. In the SEMO website one can find important historical information regarding the bids generators submitted, technical information of generators and the output of each of the clearing machine runs described above. As will be discussed more thoroughly in chapter 5, such data are important for the validation of a new UC model and are used extensively in this thesis. More specifically, I use D-1 runs also called ex-ante or unconstrained because transmission constraints are not taken into account at this point.

4.2.1 Regional Interconnectors and the SEM

As will explained in detail on section 4.5, the island of Ireland is connected with Great Britain by two high voltage DC (HVDC) submarine interconnectors. The East West interconnector (EWIC) and Moyle. In this section, the operational scheme of the interconnectors is being discussed to introduce the logic of energy trading between countries. The information presented in this section is used in chapter 5 to describe mathematically the rules of energy trade and explain deviations during the UC model's calibration process.

The construction of an interconnector can potentially increase economic welfare based on the discussion below that adopted from Ralph Turvey [22] by Aaoife Wilson [23]. In the example depicted in figure 4-4, the price of electricity in country A is P_A based on the demand supply curves in the specific example. Similarly, the price of electricity on country B is P_B. The quantities of energy traded at market equilibrium on countries A and B are Q_A and Q_B respectively. Energy production on country A is more efficient than country B so that $P_A < P_B$. After the interconnector is being built country A exports energy quantity K so that the cost of energy per unit is increased to P_A^* and country B imports the equivalent amount so that the cost of energy per unit is increased to P_B^*(see figure 4-4). At the same time, the domestic consumption in country A will decrease by an amount from Q_A^* to Q_A^{*cons} but the total quantity produced will increase from Q_A^* to Q_A^{*prod}. Similarly, domestic consumption in country B will increase from Q_A^* to Q_A^{*cons} but the total quantity produced will decrease from Q_A^* to Q_A^{*prod} so that Q_A^{*cons} $-Q_A^{*prod}$ $=K$. After the construction of the interconnector, country A experiences a total loss of consumer surplus of area (a+b), however producers on country A have access to a wider market and they experience gains of (a+b+c) so that the net welfare benefit is equal to c (see figure 4-5). Similarly, in country B there has been a loss of produces surplus of (d), but a gain in consumer surplus of area (d+e+f) so that the net welfare benefit is equal to (e+f) [22].

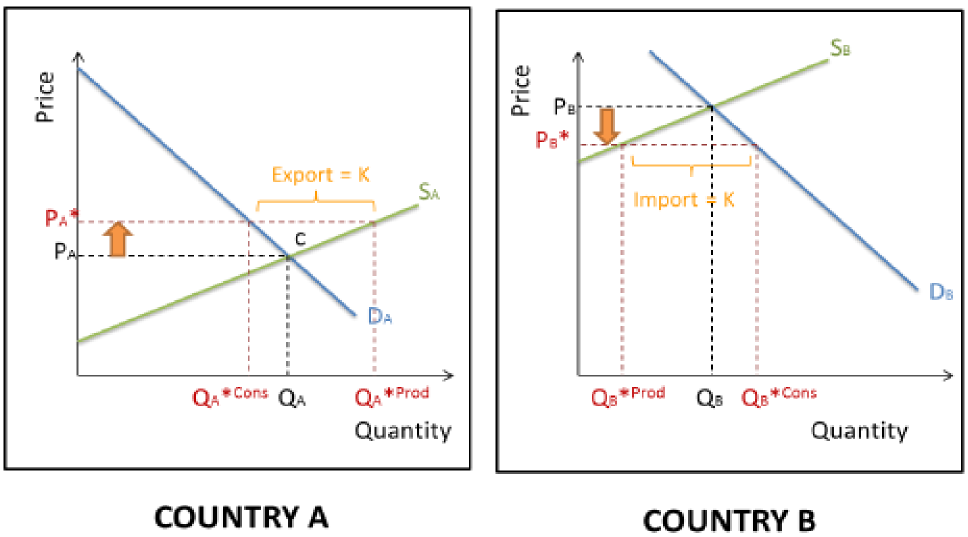

Figure 4-4: Demand and supply curves and energy prices and energy quantities at equilibrium for two hypothetical countries before and after interconnection (Source **[23]**).

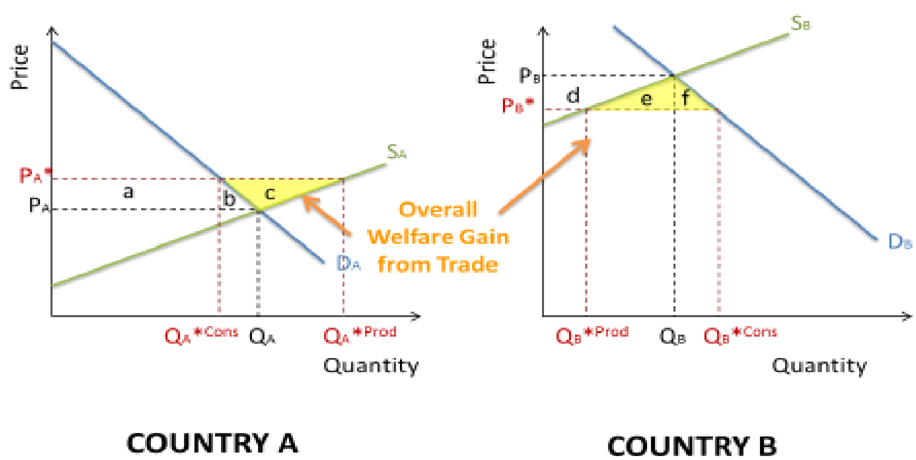

Figure 4-5: Figure 4-4 with the overall welfare gains added (Source: **[23]**).

The interconnector provider in this example gains rents for use of the interconnector of $(P_B^* - P_A^*) \times K$. The above example is a simplified representation of what would happen in an ideal market without distortions and was an introduction to the economics of interconnecting national grids. For the case of Ireland advantages of interconnection with GB are:

- Support the integration of European energy markets
- Greater security of supply
- Opens cross border access to all market participants and increases competitiveness
- Offers diverse product portfolio including capacity via implicit and explicit auctions for market participants as will be explained later in this section
- Allows provision of ancillary services such as frequency response, reactive power and black start capability

The Trading and Settlement Code (TSC) describes trading rules across the interconnectors within the SEM. There are three main parties with respect to regional trading: a) The Interconnector Administrator (IA), The Market Operator (MO) and the Interconnector Units (IUs). Their roles are briefly described below:

1. The IA is responsible for the administration of trading between Northern Ireland and the Republic of Ireland and Great Britain. The designated IA for EWIC and Moyle is the System Operator for Northern Ireland (SONi). SONi facilitates capacity allocaton and energy trading through the interconnections via the

Auction Management Platform (AMP). The AMP is a computerized system that provides the necessary mechanisms and outupts to facilitate trading across Moyle and EWIC.

2. The SEM is the designated MO for the All Island.
3. Interconnector Units (IUs) or interconnector users represent any party that trades on the interconnectors via the SEM. Each interconnector user needs to register an IU, which is the entity against which the user trades capacity and energy [23].

Figure 4-6: Graphic of EWIC and Moyle interconnector stakeholders, Source: **[23]**) .

In general, the trading capacity of the interconnectors is made available to allow trading of electricity between SEM and British Electricity Trading and Transmission Arrangements BETTA (the British market). Available capacity is offered to the market via auctions over a number of timescales including annual, seasonal, quarterly, monthly, daily and intraday. There are two types of auctions, explicit and implicit.

- Explicit auctions allow market participants to purchase the right to use capacity (for each direction West-East or East-West) on the interconnector from between one day and one year through the AMP. Successful bidders pay the clearing price. An annual auction time table is published in advance of each year [24].
- Implicit auctions take place within the intraday time scale. Any capacity that is unused after the first SEM run ("Ex-Ante 1") is made available to the market via the intraday market runs ("SEM Ex-Ante 2") and "Within-Day 1"). Interconnector users may submit half hourly bids to trade electricity across Moyle in these runs to the SEM operator [25].

As discussed in this section, optimally energy trade takes place based on energy arbitrage principles where power flows from an area with low electricity prices to an area with high prices. However, a portion of the interconnector's capacity is allocated months before through explicit auctions, and in this respect there might be deviations from optimal least-cost operation of the interconnectors. This can possibly cause deviations during the validation of a deterministic least-cost UCED model. More discussion on this issue is given in chapter 5.

4.3 Generation capacity status in Ireland

4.3.1 Current thermal capacity

Generation adequacy studies for All Island are performed annually by SONI. The latest reports [26], [27] present the current generating capacity in RoI and the NI as well as planned capacity and decommissioning schedules up to 2025. Additionally, a detailed data set, with technical characteristics of all generating units within SEM, was published for the years of 2010, 2011 and 2012 by the Regulatory Authorities (RAs), the Commission for Energy Regulation (CER) and the Northern Ireland Authority for Utility Regulation (NIAUR)[43]. The data sets are used for the validation of a model used to forecast system marginal prices in SEM and are also used as inputs in the UCED model presented in this thesis. A more detailed discussion about the data sets is given in chapter 5. Such published data suggest a total installed capacity of 8,689MW of thermal capacity. Out of those 6,364MW are in RoI and 2,325 in NI.

---

[43] All-Island generator info can be found at: http://www.allislandproject.org/en/market_decision_documents.aspx?article=cb4ee33b-a83a-47ce-956a-6cff30900495

Table 4-1: Current 2015 installed thermal capacity by fuel and region for All-Ireland.

		Installed Capacity by Fuel and Region (MW)	% of Installed Capacity by Fuel and Region
ROI	Natural Gas	4,234	67%
	Coal	855	13%
	Distillate	324	5%
	Oil	588	9%
	Peat	346	5%
	Waste	17	0%
	Total ROI	**6,364**	**100%**
NI	Natural Gas	1,692	73%
	Coal	476	20%
	Distillate	142	6%
	Oil	0	0%
	Peat	0	0%
	Waste	15	1%
	Total NI	**2,325**	**100%**
All-Island	Natural Gas	5,927	68%
	Coal	1,331	15%
	Distillate	466	5%
	Oil	588	7%
	Peat	346	4%
	Waste	32	0%
	Total All-Island	**8,689**	**100%**

Half of all thermal installed capacity in 2015 is Combined Cycle Gas Turbines (CCGTs) while conventional steam cycle units comprise around one third of total installed capacity (see figure 3-3). Natural gas fired plants comprise around 67% of total installed capacity in RoI and 73% in NI. A list of all current thermal power stations is given in table 4-6. The Aghada and Whitegate located in the South of Ireland and Poolbeg located in NI are the largest CCGT power plants with capacities of 440MW or more. There are only two large coal-fired power plants in All-Island. One is the Kilroot power plant located in Northern Ireland with total capacity ~480MW; the second is the Moneypoint power plant with total capacity of ~855MW located in West ROI. Moneypoint was refurbished in 2008-2009 to comply with environmental standards and it is planned to operate up to 2025. Oil and distillate together comprise 19% of total installed capacity

Table 4-2: Current 2015 installed capacity by technology and region for All-Ireland.

		Installed Capacity by Technology and Region (MW)	% of Installed Capacity by Technology and Region
ROI	CCGT	3,341	53%
	OCGT	199	3%
	OCCT	442	7%
	CHP	166	3%
	Conventional Steam	2,216	35%
	Total ROI	6,364	100%
NI	CCGT	999	43%
	OCGT	684	29%
	OCCT	142	6%
	CHP	9	0%
	Conventional Steam	491	21%
	Total NI	2,325	100%
ALL-Island	CCGT	4,340	50%
	OCGT	883	10%
	OCCT	584	7%
	CHP	175	2%
	Conventional Steam	2,707	31%
	Total All-Island	8,689	100%

Table 4-3: List with thermal units in All-Island in year 2015.

Unit	Technology	Fuel	Max Capacity (MW)	Location
Kilroot Unit 1 FGD	Conventional Steam	Coal	238.0	NI
Kilroot Unit 2 FGD	Conventional Steam	Coal	238.0	NI
Moneypoint Unit 1 FGD SCR	Conventional Steam	Coal	285.0	ROI
Moneypoint Unit 2 FGD SCR	Conventional Steam	Coal	285.0	ROI
Moneypoint Unit 3 FGD SCR	Conventional Steam	Coal	285.0	ROI
Kilroot GT1	OCCT	Distillate	29.0	NI
Kilroot GT2	OCCT	Distillate	29.0	NI

Kilroot GT3	**OCCT**	**Distillate**	**42.0**	**NI**
Kilroot GT4	**OCCT**	**Distillate**	**42.0**	**NI**
Rhode 1	**OCCT**	**Distillate**	**52.0**	**ROI**
Rhode 2	**OCCT**	**Distillate**	**52.0**	**ROI**
Tawnaghmore 1	**OCCT**	**Distillate**	**52.0**	**ROI**
Tawnaghmore 3	**OCCT**	**Distillate**	**52.0**	**ROI**
Cushaling	**OCCT**	**Distillate**	**58.0**	**ROI**
Cushaling	**OCCT**	**Distillate**	**58.0**	**ROI**
Tarbert Unit 1	**Conventional Steam**	**HFO**	**54.0**	**ROI**
Tarbert Unit 2	**Conventional Steam**	**HFO**	**54.0**	**ROI**
Tarbert Unit 3	**Conventional Steam**	**HFO**	**240.0**	**ROI**
Tarbert Unit 4	**Conventional Steam**	**HFO**	**240.0**	**ROI**
Ballylumford Unit 10	**CCGT**	**Natural Gas**	**101.0**	**NI**
Ballylumford CCGT Unit 31	**CCGT**	**Natural Gas**	**247.0**	**NI**
Ballylumford Unit 32	**CCGT**	**Natural Gas**	**247.0**	**NI**
Huntstown	**CCGT**	**Natural Gas**	**343.0**	**ROI**
Tynagh	**CCGT**	**Natural Gas**	**388.5**	**ROI**
Coolkeeragh CCGT	**CCGT**	**Natural Gas**	**404.0**	**NI**
Huntstown Phase II	**CCGT**	**Natural Gas**	**404.0**	**ROI**
Dublin Bay Power	**CCGT**	**Natural Gas**	**415.0**	**ROI**
Great Island CCGT	**CCGT**	**Natural Gas**	**431.0**	**ROI**
Aghada CCGT	**CCGT**	**Natural Gas**	**435.0**	**ROI**
Whitegate	**CCGT**	**Natural Gas**	**445.0**	**ROI**
Poolbeg Combined Cycle	**CCGT**	**Natural Gas**	**480.0**	**ROI**
Contour Global unit 1	**CHP**	**Natural Gas**	**3.0**	**NI**
Contour Global unit 2	**CHP**	**Natural Gas**	**3.0**	**NI**
Contour Global unit 3	**CHP**	**Natural Gas**	**3.0**	**NI**
Sealrock 3 (Aughinish CHP)	**CHP**	**Natural Gas**	**83.0**	**ROI**
Sealrock 4 (Aughinish CHP)	**CHP**	**Natural Gas**	**83.0**	**ROI**
Aghada CT Unit 1	**Conventional Steam**	**Natural Gas**	**90.0**	**ROI**
Aghada CT Unit 2	**Conventional Steam**	**Natural Gas**	**90.0**	**ROI**
Aghada CT Unit 4	**Conventional Steam**	**Natural Gas**	**90.0**	**ROI**
Aghada Unit 1	**Conventional Steam**	**Natural Gas**	**258.0**	**ROI**
Ballylumford GT1	**OCGT**	**Natural Gas**	**58.0**	**NI**

Ballylumford GT2	**OCGT**	**Natural Gas**	**58.0**	**NI**
Coolkeeragh GT8	**OCGT**	**Natural Gas**	**58.0**	**NI**
Marina No ST	**OCGT**	**Natural Gas**	**95.0**	**ROI**
Northwall Unit 5	**OCGT**	**Natural Gas**	**104.0**	**ROI**
Ballylumford Unit 4	**OCGT**	**Natural Gas**	**170.0**	**NI**
Ballylumford Unit 5	**OCGT**	**Natural Gas**	**170.0**	**NI**
Ballylumford Unit 6	**OCGT**	**Natural Gas**	**170.0**	**NI**
Lough Rea	**Conventional Steam**	**Peat**	**91.0**	**ROI**
West Offaly Power	**Conventional Steam**	**Peat**	**137.0**	**ROI**
Edenderry	**OCCT**	**Peat/Biomass**	**117.6**	**ROI**
Lisahally Waste	**Conventional Steam**	**Waste**	**15.0**	**NI**

4.3.2 Current renewable generators

Currently there is around 237MW of hydro installed capacity in ROI. The largest stations have a total capacity of 216MW and are:

- Ardnacrusha (86MW)
- Erne (65MW)
- Lee (27MW)
- Liffey (38MW)

Additionally, there is the pumped hydro station in Turlough hill with total capacity of 292MW. Hydro generation in Northern Ireland accounts only for 4MW. As per the Irish Wind Energy Association, there are currently 3,083MW of installed wind capacity in All-Ireland. 2,441MW are installed in RoI while 624MW in NI.

4.3.3 Future power mix

EIRGRID and SONI publish annual generation capacity reports with data on current generation mix and planned changes for the following decade. Their projections of future capacity are used for the 2020 scenario presented on chapter 7.

Future changes in thermal generation by 2025 include [28]:

- Commissioning of a 58MW Waste to Energy in Dublin built by Covanta[44] in late 2017.
- Commissioning of a Biomass CHP plant (Mayo) sometime by 2025.
- Decommissioning of the four Tarbert HFO fired units TB1 to TB4 of total capacity 592MW in 2023.
- Increase of capacity of the Contour Global CHP power plant in Northern Ireland from 12MW to 18MW in 2017.
- Decommissioning of the Aghada AD1 (258 MW) and AT1 (90MW), Marina CC (95MW), North Wall 5 (104MW).

[44] The Covanta press release for the project can be found at: http://www.covanta.com/news/press-releases/2014/Sept-19.aspx

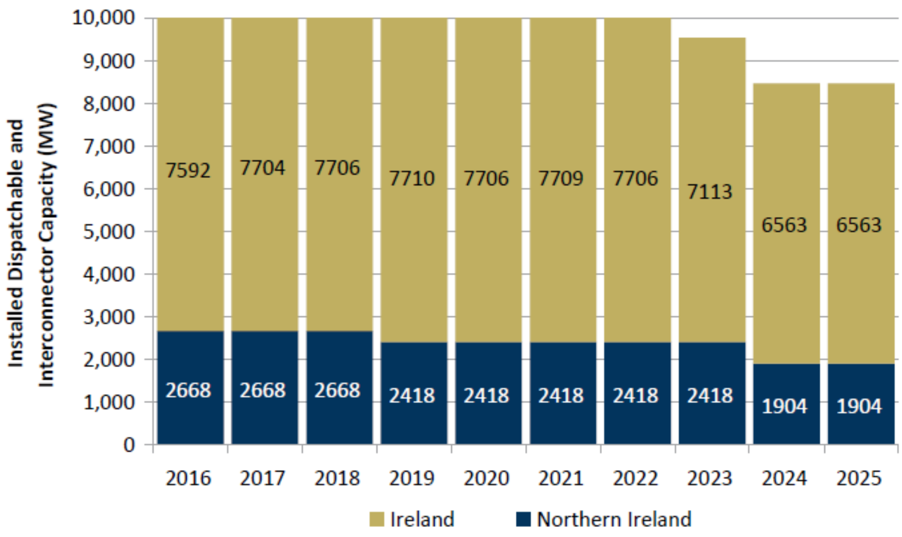

Figure 4-7: Future changes on dispatchable capacity in All-Island including transmission (Source: **[29]**)

Under the 2009 Renewable Energy Directive, Ireland is committed to produce from renewable sources at least 16% of all energy consumed by 2020. This will be met by 40% penetration of from renewable energy in the electricity sector, 12% in heating, and 10% in the transportation sector. The main bulk renewable electricity is expected to be generated by wind. Wind power is currently the most abundant renewable energy source on the island of Ireland due to the onshore wind resources representing some of the most effective renewable resources in Europe and offshore benefiting from Ireland's extensive area of offshore territory in the Atlantic and the Irish Sea. As a consequence, it is expected that the RES share of installed generation capacity will more than double in the ROI and will more than triple in NI by 2020 [30].

Table 4-4: Past and projected installed capacity of various renewable energy sources for ROI (Source: EIRGRID and SONI All-Island Capacity Statement (2010,2011, 2012b, 2014)).

	2010	2011	2012	2013	2014	2015	2016	2017	2018	2019	2020	2021	2022	2023	2024
Hydro	237	237	237	237	237	237	237	237	237	237	237	237	237	237	237
Wave	0	0	0	0	0	0	0	0	0	0	0	N/A	N/A	N/A	N/A
Wind	1,538	1,629	1,642	1,938	2,165	2,386	2,709	3,219	3,385	3,520	3,600	3,727	3,854	3,982	4,109
Biomass /LFG	48	56	59	76	76	82	112	142	172	202	232	232	232	232	232

Table 4-5: Past and projected installed capacity of various renewable energy sources for NI (Source: EIRGRID and SONI All-Island Capacity Statement (2010,2011, 2012b, 2014).

	2010	2011	2012	2013	2014	2015	2016	2017	2018	2019	2020	2021	2022	2023	2024
Hydro	3	4	4	4	4	4	4	4	4	4	4	4	4	4	4
Wave	1	1	1	1	1	1	1	11	11	11	201	201	201	201	201
Wind	308	405	467	550	658	870	975	1,036	1,094	1,145	1,205	1,256	1,297	1,345	1,389
Biomass/ Biogass/ Landfill Gas	19	19	23	26	28	50	70	88	92	95	99	102	105	108	110

Table 4-6: Past and projected installed capacity of various renewable energy sources for All Island (Source: EIRGRID and SONI All-Island Capacity Statement (2010, 2011, 2012b, 2014).

	2010	2011	2012	2013	2014	2015	2016	2017	2018	2019	2020	2021	2022	2023	2024
Hydro	240	241	241	241	241	241	241	241	241	241	241	241	241	241	241
Wave	1	1	1	1	1	1	1	11	11	11	201	201	201	201	201
Wind	1,846	2,034	2,109	2,488	2,823	3,256	3,684	4,255	4,479	4,665	4,805	4,983	5,151	5,327	5,498
Biomass/ Biogass/ Landfill Gas/LFG	67	75	82	102	104	132	182	230	264	297	331	334	337	340	342

4.4 Transmission Network

4.4.1 Internal Interconnections

ROI and NI used to be electrically separate. Both networks were designed and constructed independently in the first half of the 1900s. However, they are currently connected. The Northern Ireland transmission system is operated at 275 kV and 110 kV while the transmission system of Ireland is operated at 400 kV, 220 kV and 110 kV. The internal interconnection is composed of one 275 kV double circuit connection from Louth station in Co. Louth (Irl) to Tandragee station in Co. Armagh (NI) and two 110 kV connections:

- Letterkenny station in Co. Donegal (ROI) to Stabane station in Co. Tyrone (NI); and
- Corraclassy station in Co. Carraclassy (ROI) to Enniskillen station in Co. Fermanagh (NI) [31].

These two 110 kV circuits were designed to provide limited support to the local electricity networks in those areas rather than the wider transmission system. Neither of these connections on their own or combined have sufficient capacity to securely maintain the connection between the Irish and Northern Irish transmission systems [32]. The interconnection is secured through the two 275/220kV circuits.

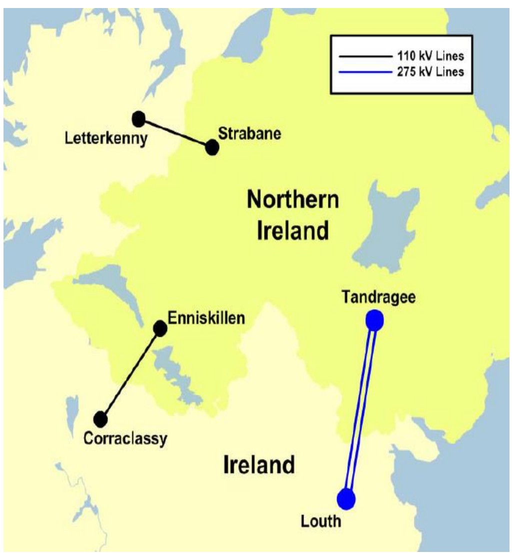

Figure 4-8: Existing cross border circuits between ROI and NI . (Source: [31]).

While the design capacity of each of the 275/220 kV cross-border circuits is 750 MVA in both sides, the actual capacity of the circuits to accommodate transfers between the two systems at any time is much lower because of system reliability issues. In case the interconnector fails, the system will experience “separation”. The one system will experience over generation while the other shortage of power. Either of these situations can lead to system failure and a possible blackout. To mitigate such a risk, the North/South interconnector is currently operated at maximum transfer capacity of 450MVA either direction [32]. EIRGRID and SONI state that “in practice during normal operation of the transmission system, a limit of 300 MW applies in either direction as 150 MW of transfer capacity should be kept free to allow one transmission system provide the other with reserve power in the event of the unexpected loss of a generator in either jurisdiction. During regular and unscheduled maintenance, it is normal for these limits to be further reduced. The 450 MW limit is known as the ‘Total Transfer Capacity’ (TTC) of the current North South Interconnector” [32].

The danger of separation will always be present for as long as there is only one interconnection for the two systems. For that reason, an additional 400kV interlink namely Tyrone Cavan Interconnector is planned to commission by 2019 to increase current internal capacity during normal operations to ~1100MVA and to ensure there are no transmission bottlenecks prohibiting the most economic dispatch of generators.

As SONI states, “the key benefits of the interconnector are:

- It will improve security of supply by providing a reliable high capacity link the two parts of the all-island transmission system;

- It will allow the all-island wholesale electricity market to work more efficiently, enabling wider competition between power generators and electricity suppliers throughout the island, and therefore ensuring that future electricity prices will be as competitive as possible;

- It will enable more renewable generator capacity (mostly wind generation) to be connected to the electricity network [9, 10]". The Governments in both jurisdictions have set challenging targets for the amount of electricity to be generated from renewable sources, 40% by 2020, and these targets cannot be met without additional interconnection.

The proposal of the project was undertaken by both SONI and EIRGRID and more detailed information can be found on footnotes 9 and 10 at the bottom of this page [45],[46]. In the 2020 scenario we assume the 1,100 has been commissioned and it has been added into the model (see chapter 7).

[45] Source: EIRGRID (http://www.eirgridgroup.com/site-files/library/EirGrid/North-South-Project-Summary-Report-20-October-2015_Final.pdf

[46] Source: SONI (http://www.soni.ltd.uk/TransmissionProjects/Tyrone-CavanInterconnector/)

Figure 4-9: Current and proposed North-South interconnectors in Ireland. The new Tyrone Cavan interconnector will increase the transfer capability from around 700MW to 1500MW.

4.4.2 International Interconnections

Until recently, there was only one interconnector from the island of Ireland to the GB system, the Moyle Interconnector. It links Northern Ireland to Scotland with a capacity of 500 MW in both directions. As stated in the '2013 All-Island Transmission Forecast, 2013', "… at present a cable fault on Pole 1 of the Moyle Interconnector means that 250 MW of the capacity is unavailable. Moyle Interconnector Limited (MIL) has indicated a prudent base case assumption would be to assume the interconnector is restored to full capacity in autumn 2017. Therefore, in that thesis we assume assumed the import capacity of the Moyle Interconnector is restored to 450 MW in 2017. The Moyle Interconnector export capacity is limited to 80 MW from 2016 onwards due to the commissioning of a large wind farm in Scotland which will use up capacity on the single circuit from Auchencrosh to Coylton" [31].

In December 2012 operation of the new East-West interconnector commenced; it is an HVDV transmission line that connects the ROI and GB directly with a capacity of 500 MW [30]. The East-West Interconnector is an HVDC link which runs between Woodland, County Meath in Ireland and Deeside in North Wales. The link comprises approximately 186 km of sub-sea cable and 70 km of land underground cable. The East-West Interconnector is built using Voltage Source Converter (VSC) technology and is the largest capacity VSC interconnector in operation worldwide.

EIRGRID is currently undertaking a feasibility study for a new 700MW interconnector – called the Celtic interconnector, to link Ireland and France. The Celtic interconnector is expected to a) to link SEM with mainland European markets, b) facilitate further development of renewables as well as increased market competition and c) make Ireland less dependent on its electricity interconnection with GB. The decision is expected to be made within 2016.

4.5 Past and current supply and demand balance

4.5.1 Historical demand and future demand projection

SONI with EIRGRID publish annually an All-Island Capacity Statement, where they provide the latest demand projections for both ROI and NI. EIRGRID and SONI use econometric models based on historical trends, economic forecasts and energy policies at regional, national and European level to predict future electricity demand. Forecasts are initially built separate for ROI and NI and then combined to produce an All-Island energy and peak demand forecast [29]. Three scenarios are modeled, low, medium (or base) and high[47]. Historical demand data have been used in this thesis to simulate past operation of the Irish grid and more specifically on the validation exercise of the UCED model presented on chapter 5. Future medium demand and peak demand projections shown in figures 4-7 to 4-12 are being used to simulate operation of the Irish grid in the 2020 scenario. As seen in table 4-1, historically the load participation is 74%-26% for RoI and NI respectively. We assume the same demand participation for the UCED model validation and application presented on chapters 5 and 7 respectively.

[47] Weather conditions as well economic growth are the main factors that affect future projections. The Base scenario is based on average temperature year with most likely economic projections being applied. The median demand forecast is based on an average temperature year, with the central economic factor being applied and this is our best estimate of what might happen in the future. The low demand forecast is based on a relatively high temperature year, with the pessimistic economic factor being applied. Conversely, the high demand forecast is based on a relatively low temperature year, with the more optimistic economic factor being applied. The medium demand scenario shows an All-Island demand recovery to 2008 levels by 2019. A more detailed description of the type of analysis used for demand projections can be found on [29]

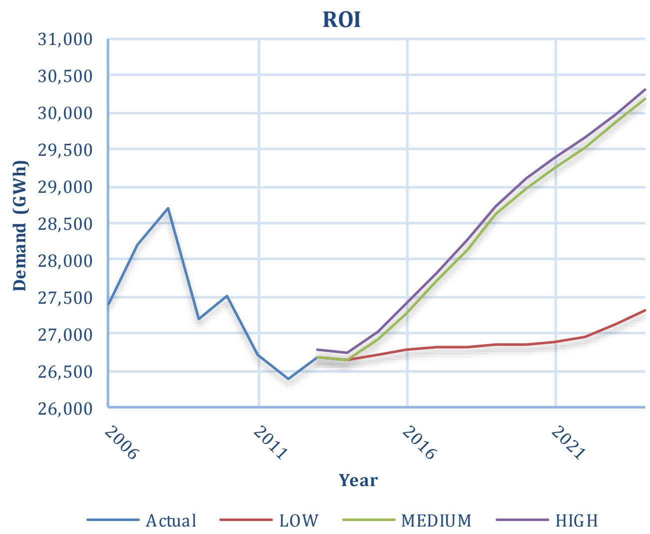

Figure 4-10: Past demand and demand projections for Ireland (created using data from **[29]**).

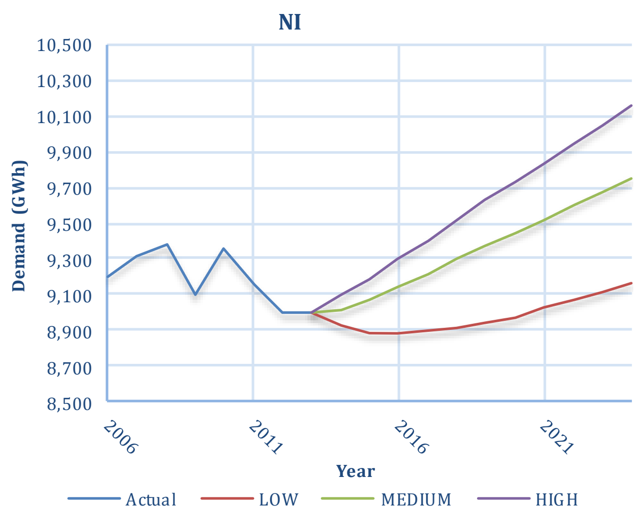

Figure 4-11: Past demand and demand projections for North Ireland (created using data from **[29]**).

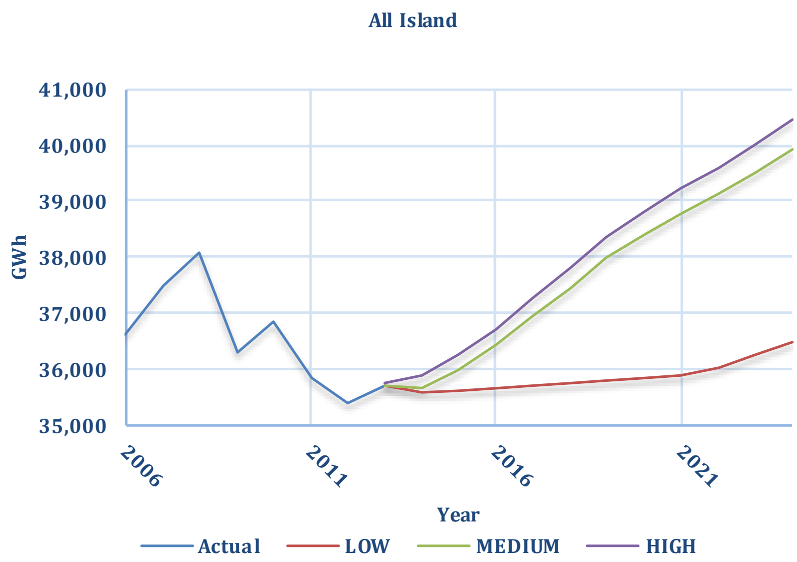

Figure 4-12: Past demand and demand projections for All Island (created using data from **[29]**).

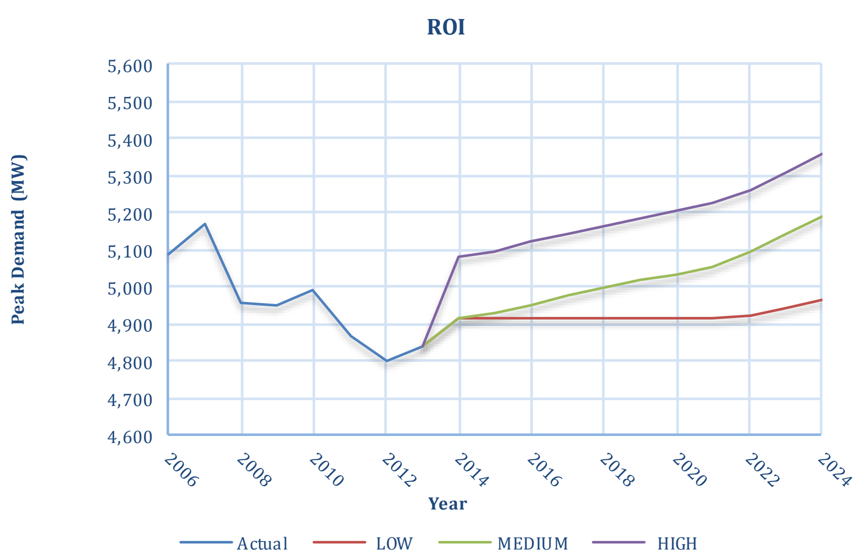

Figure 4-13: Actual peak demand and peak demand projections for ROI. Peak demand in the ROI takes place in winter (created using data from **[29]**).

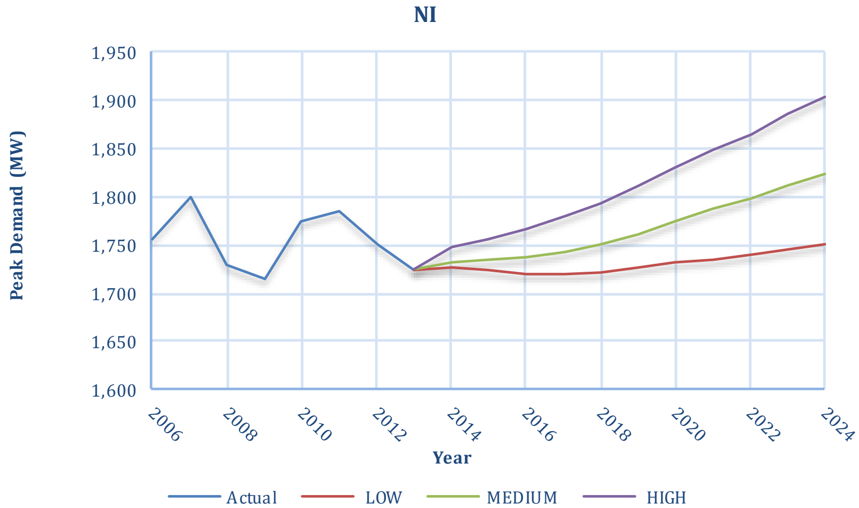

Figure 4-14: Actual peak demand and demand projections for NI. Peak demand in NI takes place in winter (created using data from **[29]**

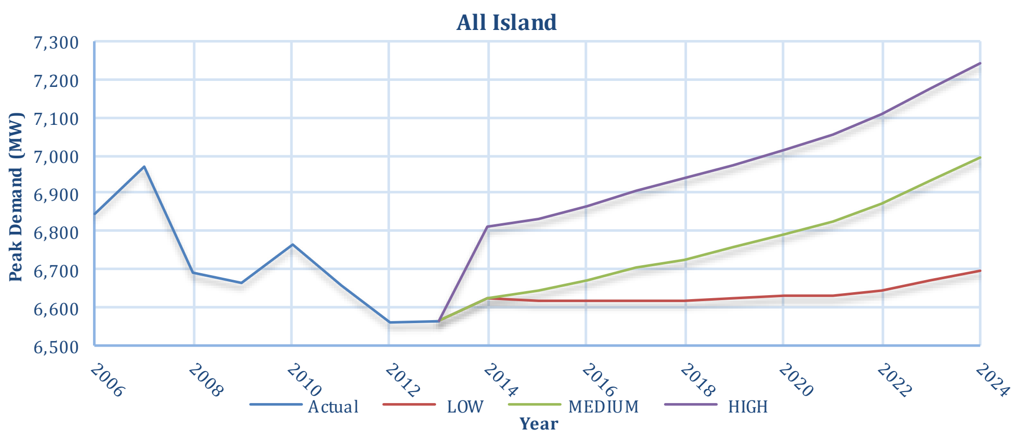

Figure 4-15: All-Island actual TER peak demand and TER peak demand projections. Peak demand takes place in winter (created using data from **[29]**).

Table 4-7: Historical demand and peak demand data, demand projections and the load participation of Roil and NI*

	Demand (GWh)		% Participation on total All-Island		Peak Demand (MW)		% Participation on total All-Island Peak	
Year	ROI	NI	ROI	NI	ROI	NI	ROI	NI
2006	27,400	9,200	75%	25%	5,090	1,755	74%	26%
2007	28,200	9,310	75%	25%	5,170	1,800	74%	26%
2008	28,700	9,380	75%	25%	4,960	1,730	74%	26%
2009	27,200	9,100	75%	25%	4,950	1,715	74%	26%
2010	27,500	9,350	75%	25%	4,990	1,775	74%	26%
2011	26,700	9,150	74%	26%	4,870	1,785	73%	27%
2012	26,390	9,000	75%	25%	4,800	1,750	73%	27%
2013	26,699	9,000	75%	25%	4,840	1,725	74%	26%
2014	26,648	9,011	75%	25%	4,915	1,732	74%	26%
2015	26,915	9,074	75%	25%	4,929	1,734	74%	26%
2016	27,286	9,146	75%	25%	4,953	1,738	74%	26%
2017	27,715	9,219	75%	25%	4,978	1,744	74%	26%
2018	28,152	9,293	75%	25%	4,995	1,752	74%	26%
2019	28,613	9,368	75%	25%	5,016	1,762	74%	26%
2020	28,973	9,443	75%	25%	5,036	1,774	74%	26%
2021	29,250	9,518	75%	25%	5,056	1,787	74%	26%
2022	29,532	9,594	75%	25%	5,096	1,799	74%	26%
2023	29,852	9,671	76%	24%	5,143	1,811	74%	26%
2024	30,179	9,748	76%	24%	5,190	1,824	74%	26%

***Hourly peak demand doesn't necessarily coincide in ROI and NI. For that reason the total peak demand in All-Island is less than the sum of peak demands for ROI and NI.**

4.5.2 Past and current supply options

Coal and natural gas are the two primary fuel sources for producing electricity within the SEM. Over the last decade, the share of coal in All-Island has been fluctuating between 14% and 18%. Coal fired production in 2014 was around 5,600GWh or ~16%. Gas fired production had been declining since 2010 from ~23,500 to 14,800 in 2014 (~44% share). The requirement for oil in the power sector has been declining since 2005 and it currently accounts for less than 1%. The decline of fossil fuels happens in expense of an increase on generation from renewable sources the share of which has grown from 11% in 2008 to 32% in 2014 (see figure 4-13).

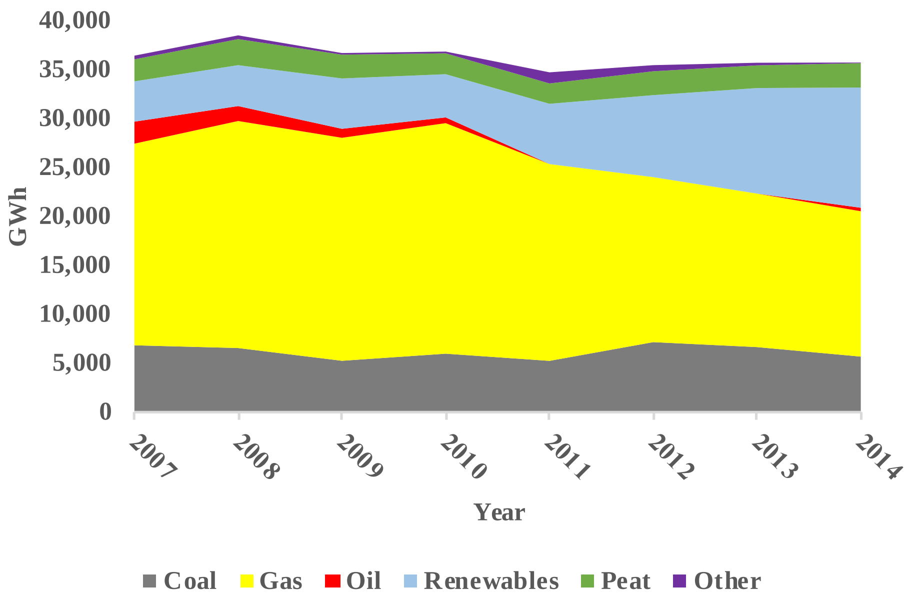

Figure 4-16: Historic electricity production from various fuels sources in All-Island (Data source: **[28]**).

Figures 4-17 and 4-18 show the share of each fuel on electricity demand in RoI and NI in 2014. In the RoI around 1% of electricity demand is satisfied by the pumped hydro unit which of course is charged from the grid. Also, net imports from the Moyle and EWIC accounted for around 8% of total demand in the RoI and 15% in NI.

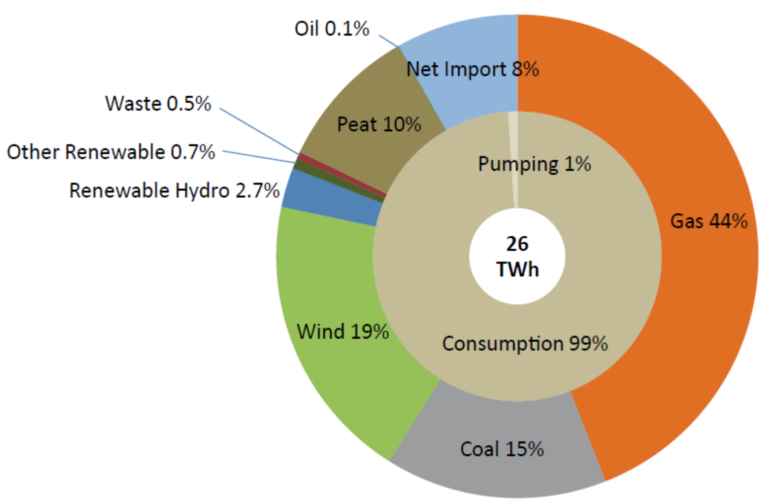

Figure 4-17: Share of demand supplied by various sources in the RoI in 2014 (Source: **[28]**).

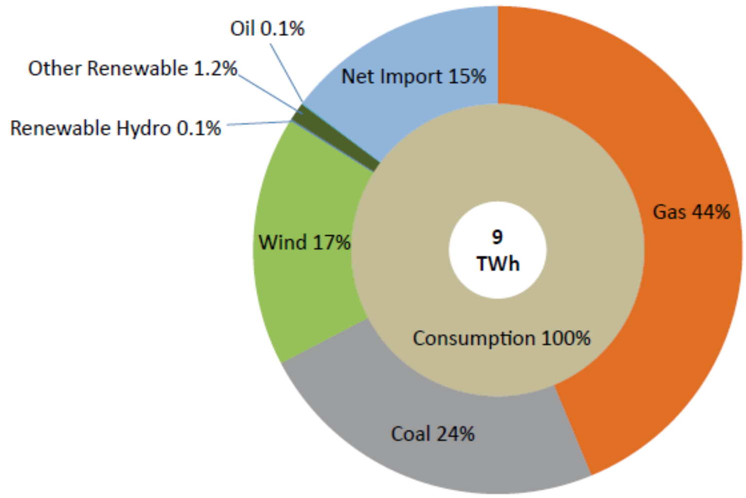

Figure 4-18: Share of demand supplied by various sources in Northern Ireland in 2014 (Source: **[28]**).

4.5.2.1 Natural Gas in All-Ireland

Natural gas industry for both Northern Ireland and the Republic of Ireland is part of a single price zone for gas that extends to North Germany. Gas is traded within that zone between a series of hubs, and prices differ between these hubs generally only to reflect transport costs [33]. In Roil, the CER is responsible for the economic regulation of the gas network and the supply of gas to end customers. The relevant entity in NI is the Utility Regulator.

Republic of Ireland’s natural gas comes from both indigenous production and imports. There are a number of operational gas fields off the coast of Ireland. Kinsale Head, Ballycotton and the Seven Heads fields are located off the coast of County Cork. There is also a new gas field located at Corrib off the west coast of Ireland which came on line in 2015 to enhance RoI's security of supply. Due to the finite nature of gas, imports from abroad are very important to the market in Ireland as mentioned earlier. Approximately 96% of Ireland's natural gas demand is bought on the international gas markets and imported to the RoI through the natural gas network, or specifically through interconnection with Britain (figure 4-17). As a result, Irish customers are exposed to fluctuations in international gas price and neither the CER nor the gas suppliers have direct control of this part of the value chain [34]. Since the marginal power plant is natural gas fired most of the time, the price of gas affects greatly prices on SEM. RoI currently sources most of its gas from Great Britain. Great Britain provided 91% of RoI's gas demand in 2012/13 and 96% in 2014. Natural gas is traded at Great Britain's National Balancing Point (NBP) which is characterized by high levels of liquidity. The link between prices in natural gas and oil has been weakened in Northwest Europe (i.e. Belgium, Denmark, France, Germany, Ireland, Netherlands and UK) the Gas-on-Gas [48] competition pricing mechanism for gas has been prevailing. Figure 4-16 below shows the average gas price from 2009 to 2015 in the UK [35]. For the model validation exercise presented in chapter 5 we use historical indexpriced data for natural gas traded in balancing point.

[48] Traditionally gas prices have been linked to oil prices with varying time lags and linkages. This type of pricing mechanism is referred to as Oil Price Escalation (OPE), where gas price is linked, usually through a base price and an escalation clause, to a competing fuel, typically crude oil or another oil product. There are a number of alternative pricing mechanisms, the most important of which is Gas-on-Gas Competition (GOG). In this case gas price is determined by the interplay of supply and demand [35].

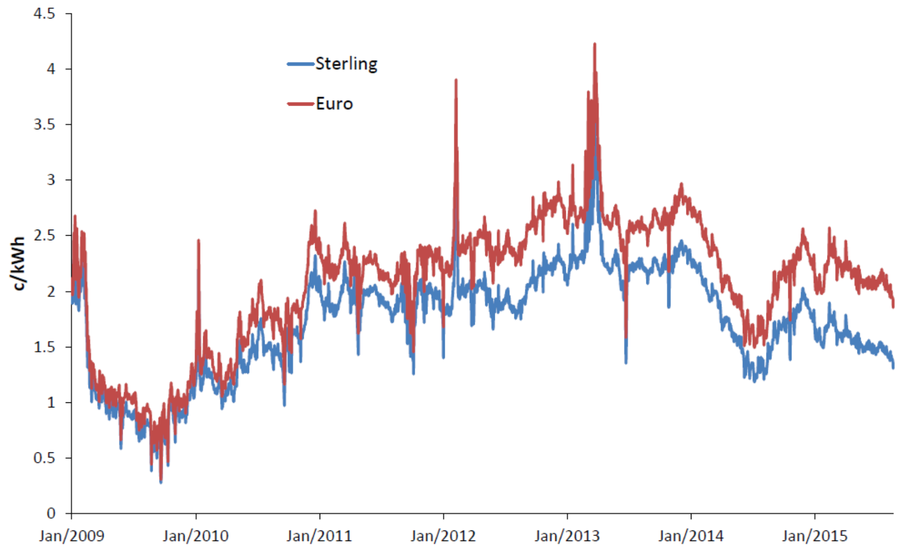

Figure 4-19: UK national balancing point gas price 2009-2015 (Data source: UK National Gas Transmission Grid. Figure Source: **[35]**).

Since 2008, the two regulators on the island (CER and NIAUR) have been working together to develop Common Arrangements for Gas (CAG). This would allow the gas transmission systems in Ireland and Northern Ireland to operate on an all-island basis. However, there have been challenging issues raised including physical capacity limitations to the operation of a single physical balancing regime, so implementation has been delayed.

Figure 4-20: Ireland's natural gas network.

4.5.2.2 Coal and Peat

Coal is important fuel in the Irish electricity production arguably because of security of supply. The majority of coal supply in the RoI is being imported from Colombia since 1995. In 2014, (78%) of imported coal was Colombian, 8% Polish and 3% from the UK. Coal in All Island is mostly traded against the API 2[49] Index based upon the price of coal delivered into the Amsterdam, Rotterdam, and Antwerp (ARA) region. In this thesis I use historical coal data from the same markets for the UCED model validation. All of coal imported for power production is consumed at the Moneypoint stations located in the RoI and the Kilroot station located in NI. As figures 4-22 and 4-23 show, coal prices rose over the last decade globally peaking at more than $200 per metric tonne in 2008 at the ARA trading point. The 2008 peak was in line with the super-cycle of coal related to increase in demand. More recently, overcapacity has driven prices down and as of early 2016 the CIF ARA prices of coal futures contracts were priced at around $40/tonne.

Peat is the largest indigenous energy source in the RoI. Ireland has three peat-fired power plants with total capacity of 370MW. These plants are Lough Ree, West Offaly and Bord na Monda (Edenberry) [36]. Peat power plants receive fixed price support for their output through government policies and tend to run for long periods at high outputs. In the models presented in this thesis, peat generation is modeled as must-run generation having priority among other thermal sources. Renewable energy is only allowed to displace peat output if the system is highly constrained [37]. The peat support measures were established to

[49] The API 2 index is the benchmark price reference for coal imported into northwest Europe. It is calculated as an average of the Argus cif ARA assessment and the IHS McCloskey NW Europe Steam Coal marker

support the security of supply and economy of Ireland since peat is indigenously available as mentioned before.

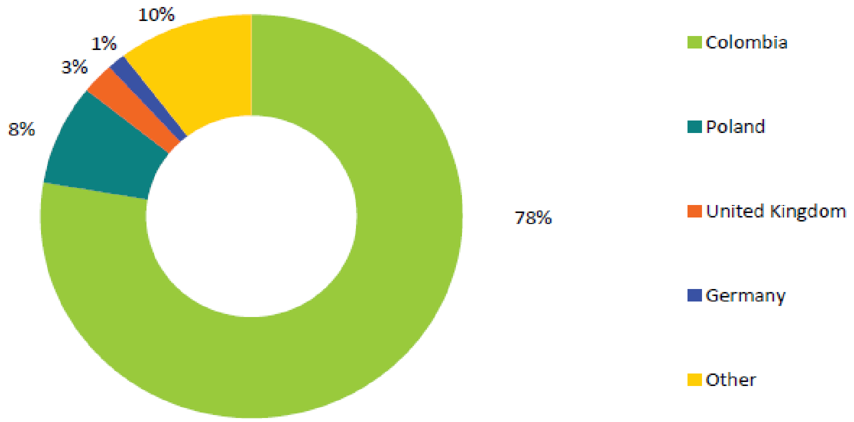

Figure 4-21: Coal imports by country of origin in the RoI in 2014 **[26]**.

Figure 4-22: Historical coal prices based on various trading points around the world (Source: **[38]**).

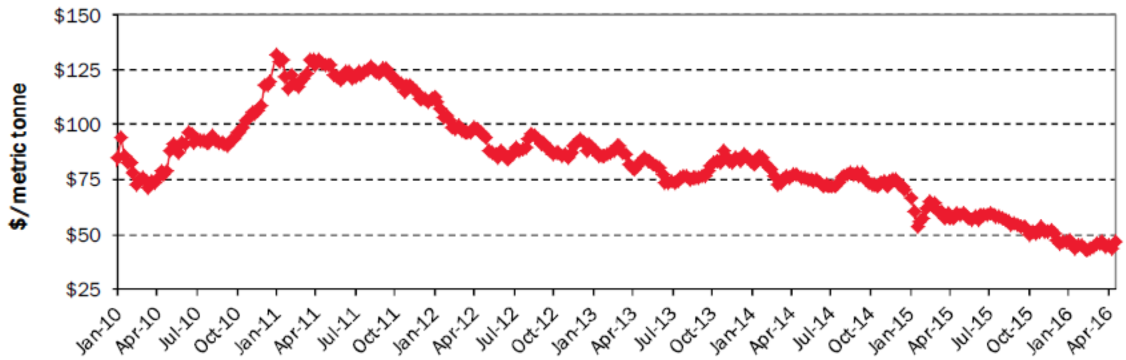

Figure 4-23: Historical coal spot prices (API2) CIF (Cost, Insurance, Freight) ARA (ARGUS-McCloskey) (Source: **[39]**, data source: Bloomberg).

Table 4-8: Quarterly coal spot prices ($US/tonne) (API2) CIF ARA (Source: **[39]**, data source: Bloomberg).

	2011	2012	2013	2014	2015	2016
Q1	$122.97	$100.57	$86.39	$79.00	$60.39	$44.94
Q2	$124.70	$89.47	$79.87	$74.51	$58.30	$45.02
Q3	$123.90	$90.93	$76.27	$75.51	$55.85	
Q4	$114.51	$88.77	$84.28	$72.96	$49.77	
Year	**$121.52**	**$92.43**	**$81.70**	**$75.50**	**$56.08**	

Table 4-9: Coal quality and market operation specifications for coal trading at ARA (Source: **[40]**).

ARA (Rotterdam area)		
Characteristics	**Typical**	**Rejection limits**
Delivery basis	Cif ARA (Amsterdam-Rotterdam-Antwerp)	
Delivery timing	in two calendar months	
Assessment timing	daily	
Inclusion guidelines	Deals must be conducted no earlier than 8.00am and no later than 5.30pm London time. Physical bids and offers and price submissions from market participants will be accepted until 5.45pm London time	
Basis	NAR (net as received)	
NCV	6,000 kcal/kg	less than 5,850 kcal/kg
Sulphur	less than 1%	more than 1%
Ash	11-15%	more than 15%
Total moisture	12-15%	more than 15%
Volatile matter	22-37%	less than 22% or more than 37%
Hardgrove grindability	45-70	less than 44
Size range	50mm	-
Cargo size	50,000-150,000t	

4.5.2.2.1 Biomass

Biomass generation in All Island comprises of landfill gas generation (LFG), some biomass CHP and biomass co-firing with peat. All existing biomass fired power plants in All Ireland are below the 10MW threshold and thus cannot participate in the SEM, but rather are dispatched outside the compulsory pool. Such generators also called de-minimis generators can enter into a PPA with a supplier and are treaded by the Meter Registration Service Operator (MRSO) [41].

4.6 Key policies in the Irish power sector

4.6.1 Renewables

The European Renewable Energy Directive 2009/28/EC sets a mandatory target of 16% of gross final energy consumption to come from renewable energy sources by 2020. In response, Ireland's National Renewable Energy Action Plan (NREAP) further sets out targets of 40% 12% and 10% for the contributions renewable energy to electricity generation, heating and transport respectively. The vast majority of RE electricity in the power sector is expected to come from wind. The 40% VRE scenario is of foremost importance in this thesis and will be modeled extensively in chapter 7.

Chapter 5 : Validation of the UCED model

5.1 Chapter introduction

In chapter 3 the mathematical formulation of a) a deterministic mixed integer programming MIP UC model and b) a MIP Thermo-Economic model for CAES performance simulations was unfolded. In chapter 4 we introduced the structure of the energy markets and the power sector –in general- of Ireland. In this chapter actual historical 2010-2011 demand, generation and transmission data from the Irish grid are being used as inputs to the UC model described in chapter 3 to develop a "Reference UC" model. Thus, the Reference 2010-2011 model is a representation of the state of the Irish grid during year 2010-2011. This chapter presents the validation process that was followed to prove the Reference UC model can represent accurately the Irish power system. The same reference model is used as a basis to develop a 2020 version of the model to simulate future states of the Irish system with higher wind penetration and CAES (presented in chapter 7). The rationale for this thesis' focus on the Irish power system is listed below:

1. **Data availability**: The commission for energy regulation (CER) has supported the development of modelling tools for simulating the performance of the Single Electricity Market (SEM) as well as publication of relevant data.
2. **Structure of the SEM**: unlike other energy markets, the SEM is a mandatory centralized pool where almost all energy in the Irish power

sector is traded through the SEM (there is minor bilateral trade). Such a market structure can better be validated through a least-cost UC model like the one presented in this thesis.

3. **The existence of an aggressive VRE portfolio.**
4. **The active interest for constructing a 330MW CAES unit in Northern Ireland.**

The above conditions 3 and 4 are aligned with the objective of this thesis to develop sophisticated modelling tools to quantify the impacts of VRE integration and simulate the performance of CAES as a method to minimize such impacts. Conditions 1 and 2 provide a suitable environment for validating a new model like the Reference model. The reason 2010-2011 data have been used is the extensive documentation produced from previous efforts to validate a PLEXOS model of the Irish power system [42], [43]. Such documentation is useful for the validation of a new model.

5.2 Context of validation process and data availability

As described earlier, the Reference model is validated in this chapter against actual historical half hourly ex-post SEM data on dispatch schedules. Such data are released annually by the Irish grid operators to update a PLEXOS[50] model used to simulate SMPs

[50] PLEXOS is a commercial software used to simulate steady-state operation of power systems

in the SEM[51] and were obtained from the All-Island website[52] and SEM-O. The basic inputs to the model also obtained from the same sources are listed below:

- **Technical characteristics of the thermal generation fleet**. Those are technical parameters needed for the formulation of the UC problem already mentioned in Chapter 3. The following technical parameters were obtained for Ireland:
  - Operational range of generators (minimum and maximum output)
  - ramp rates
  - minimum up and down times
  - hot, warm and cold start-up energy requirements; time to transit from one state to another
  - efficiency curves (No load heat requirement, incremental heat rates and power output bands for various operational regimes (see figure 3.6)
- **Availability of generators**: Such data represent historical actual available capacity for each generator. Throughout a year, capacity availability data also represent the actual maximum capacity factor of each generator. Such information is useful for the validation exercise because the UC calculation might overestimate annual generation if downtime periods were not accounted for.

[51] The key use of the model that is being updated annually is to support the Regulatory Authorities' (RAs) [Commission for Energy Regulation (CER) and the Northern Ireland Authority for Utility Regulation (NIAUR)] market power mitigation strategy. One of the mitigation measures is creation of Direct Contracts (DCs)[51] on the large market participants, ESB Power Generation and NIE Power Procurement Business [42].

[52] The All-Island Project is a joint initiative run by the Commission for Energy Regulation (CER) & the Northern Ireland Authority for Utility Regulation (NIAUR)The aim of the project is to create a single market for natural gas and electricity on the island of Ireland. The project was started following a joint policy decision by the Minister for Enterprise, Trade and Investment in Northern Ireland and the Minister for Communications, Marine and Natural Resources to create the all-island energy market. On 1st November 2007 the Single Electricity Market (SEM) went live, commencing the trading of wholesale electricity in Ireland and Northern Ireland on an All-Island basis.

- **Power flows through the EWIC and the Moyle interconnector**: Those are actual historical half-hour power flow data between Great Britain and the island of Ireland.
- **Wind data.** The SEM-O website lists actual historical wind generation data and projected on-shore wind data for All-Island. Projected future wind data have been modelled through splitting the All-Ireland into 13 regions and allocating specific hourly wind profiles representative to each region. Future wind generation is calculated through multiplying the predicted future installed capacity for each region with the specific capacity factor profile and estimating the aggregated output. More information with regards to the methodology can be found in the reports cited as [44], [45].

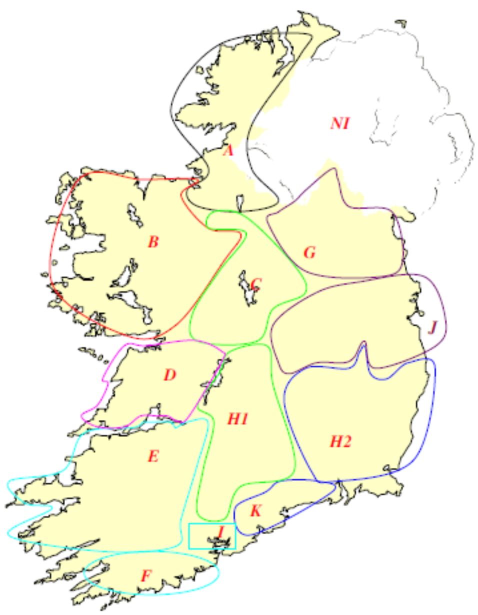

Figure 5-1: All-Island split in 13 wind regions (Source: **[42]**).

- **Hydrological data**: Two types of hydrological data are available in the SEM-O website: 1) actual historical hydro generation and 2) actual historical hydro generation limits (daily values). The latter is daily information generators submit on SEM on the maximum amount of energy that can be supplied based on hydrological availability and other technical constraints. The final amount of energy to be supplied is decided through the UC "clearing" process.

5.3 Description of the Reference UCED model

Below we present a list of the basic assumptions made for the basic 2010-2011 validation model.

1. **Moyle Interconnection**: The validation exercise for the reference model does not include the EWIC interconnector because it didn't exist during the optimization period (November 2010-October 2011). The existence of a regional interconnector introduces opportunity for electricity exchange with Great Britain (GB). Imported electricity can set the price within SEM if representing the marginal price. Additionally, opportunity for electricity exports creates additional demand for All-Island generators. In this thesis GB is approximated as a set of gas turbines each of them with different heat rates, VOM costs and operational time spans but zero no-load costs. When multiplied with the cost of natural gas, the incremental heat rate of each turbine represents the cost of electricity production in British Electricity Trading and Transmission Arrangements (BETTA). Such approximation is based on the fact that the marginal generator in BETTA is a gas turbine for most of the time and a high correlation between the cost of gas generation and the GB electricity price has been determined [43]. The CER also adopts this simplified GB representation to simulate SEM operations [42]. The technical data for

the gas turbines approximating GB have been obtained from source [43]. For the validation exercise I calibrate the model having fixed Moyle flows to its actual historical levels. The reason for that decision is that – in reality- power flows across Moyle are not determined purely on a price differential between GB and the SEM because:

a) A large portion of Moyle capacity is allocated through explicit annual and monthly auctions with no liquid secondary market for capacity. As a result the access for market players in the implicit market is limited.

b) There are differences in market arrangements between SEM and the British Electricity Trading and Transmission Arrangements (BETA) [42].

The objective of the validation exercise is to prove that the mathematical formulation of a generic MIP UC model I have developed is correct and I need to exclude any deviations on results due regional power flow exchange miscalculations attributed to a) and b) mentioned above. However, in chapter 7 where I model future scenarios I let the power flows be purely based on price differentials since there are no actual data to fix the flows.

2. **Thermal generation**: The 2010 data suggest a total thermal installed capacity of ~8,600MW over the whole island. Around two thirds of this capacity exist in the Republic of Ireland (ROI) (5,652MW); total installed capacity in Northern Ireland (NI) was 2,962MW in 2010. The above numbers don't include the old oil and gas fired units Poolbeg 1, 2 and 3 of total capacity of 486MW which got decommissioned in 2010.

The current generation fleet is given in table 4-4. Below are the additions and decommissioning that took place since 2010.

- Decommissioning of the old Great Island GI1, GI2 and GI3 HFO fired units of total capacity of 212MW in year 2015[53].
- Conversion of the North wall CCGT unit to OCGT in 2012. The whole power plant has a total capacity of 104MW[54].
- Doubling of capacity of the Contour Global gas fired CHP power plant in Northern Ireland from 6MW to 12MW[6].
- Commissioning of the Great Island CCGT with capacity of 431MW[6] in 2015.
- Commissioning of the Meath Waste-to-Energy power plant with capacity of 17MW in 2011[55].
- Commissioning of the Lisahally Waste to Energy power plant in Northern Ireland in 2015[6].

A detailed list with all technical specifications of each generator is given on ANNEX I.1.

[53] Source: [29]
[54] Source Electricity Supply Board (ESB): https://www.esb.ie/main/about-esb/power-stations-pdfs/ESB_NORTH_WALL_POWER_STATION.pdf?v=20141010
[55] Source: http://www.mercuryeng.com/ie/project/indaver-waste-to-energy/

3. **Demand data**

We use actual half hourly historical demand data for All-Island obtained from the SEM-O website. We assume a participation factor of 75% of total demand being allocated to the RoI and 25% to the NI as discussed in chapter 4 (see table 4-7).

4. **Wind generation**

Actual historic wind data obtained from the SEM-O website were used. Wind generation has priority over other types of generation due to low operational costs. The Reference model can curtail wind generation if needed in order to avoid violating system constraints.

5. Hydro generation

Actual historic daily energy limits were used for hydro generation. The UCED model dispatches hydro generation in priority due to very low operational costs and only curtails hydro power if needed to avoid violating system constraints.

6. Peat generators and waste generators

Peat and waste generators are registered as predictable price taker generators (PPTG) units meaning that they operate whenever being available. For that reason peat and waste generators are treated as must-run generators operating at their declared available capacity.

7. Fuel Costs

Assumptions for 2010-2011 fuel prices were based on a) index fuel prices at relevant markets b) transport costs for delivering the fuel to the power station and c) the cost of carbon being applied on fuel costs in Ireland. Transport costs are calculated using a fuel delivery calculator developed by the CER and NIAUR. Carbon costs have been added based on historical ETS data obtained from [46]. Fuel cost calculation as well other conversions have been made based on exchange rates shown in table 5-3.**Error! Not a valid link.**a: Coal contracts are financially settled based upon the price of coal delivered into the Amsterdam, Rotterdam, and Antwerp (ARA) region in the Netherlands Bloomberg (Source: Coal prices used were approximated using information from [47], [48])

b: We use historical data from Great Britain's National Balancing Point (NBP) UK National Transmission Grid (Gas prices were approximated using source [47])

c: : Costs of heavy fuel oil and distillate have been approximated based on historical brent prices obtained from Bloomberg that have been adjusted to account for distillate products based on data comparison from source [49]

Table 5-1: Cost per tonne of CO2 based on the ETS scheme and the associated cost of carbon applied to each fuel.

Year	Quarter	Carbon (€/t)	Coal (€/GJ)	Gas (€/GJ)	Distillate (€/GJ)	Oil (€/GJ)
2010	Q4	16	1.50	0.89	1.18	1.23
2011	Q1	17	1.59	0.95	1.25	1.31
2011	Q2	15	1.40	0.84	1.11	1.16
2011	Q3	13	1.22	0.73	0.96	1.00
2011	Q4	9	0.84	0.50	0.66	0.69

8. **Planned and unscheduled maintenance schedules**: In the absence of any maintenance schedules we used capacity availability data to represent the availability of generators.

9. **Start costs**: We have implemented the step model (see section 3.3.1) with regards to start-up costs and we use three start-up costs (hot, warm, cold) for each thermal generator based on heating requirement data to pass from one state to the next one available at ANNEX I.1.

10. **VOM costs**: In the absence of VOM data per generator, specific assumptions have been made and presented in table 5-4.

Table 5-2 :Assumptions for variable operation and maintenance (VOM) costs for various types of generators (Source: **[50]**).

Technology	USD/MWh	Euro/MWh	Reference country
OCGT	7.7	5.5	ESAA
CCGT	5.7	4.1	Belgium
Brown Pulverized Coal Combustion	14.0	10.1	Germany
Brown Coal Fluidized Bed with biomass	9.2	6.6	Czech Republic
Steam cycle run on Gas*	10.0	7.2	
CHP Gas Fired	8.7	6.3	Germany
Heavy Fuel Oil	20.0	14.4	Mexico
Large Hydro	6.4	4.6	Czech Republic
Onshore Wind	36.6	15[1]	Germany
Waste incinerator	49.4	35.5	Czech Republic

*: Assumption by the author
1: Source: [51]

11. **Optimization period**: The optimization cycle of the UC problem consists of 336 half hourly time steps (1 week). The state of the system at the end of each optimization cycle (final conditions) is considered to be the starting state at the beginning of the next

optimization cycle (initial conditions). The total optimization period is 52 weeks comprising a period from the beginning of November 2010 to end of October 2011.

12. **Optimization software**: In this thesis, the General Algebraic Modeling System (GAMS)[56] has been used as the platform for formulating the MIP UCED model. GAMS is a modeling system for mathematical programming and optimization. It consists of a language compiler and high-performance solvers. It is tailored for complex, large scale modeling applications, and allows someone to build large maintainable models that can be adapted quickly to new situations. GAMS model types include Linear Programming (LP), Mixed Integer Programming (MIP), Mixed Integer Non-Linear Programming (MINLP), and different forms of Non-Linear Programs (NLPs). Within GAMS the user can choose among a number of solvers capable of handling MIP programs[57]. CPLEX is the solver that has been used in this thesis. The IBM ILOG CPLEX Optimizer solves integer programming problems, very large linear programming problems using either primal or dual variants of the simplex method or the barrier interior point method, convex and non-convex quadratic programming problems, and convex quadraticaly constrained problems (solved via second-order cone programming, or SOCP) [18].

13. **System representation**: A simple three node transmission representation for modelling SEM and GB has been adopted. SEM alone is comprised of RoI and NI. NI

[56] General information about GAMS presented on this section have been obtained mainly from GAMS website : https://www.gams.com/docs/intro.htm

[57] A complete list of embedded commercial GAMS is using can be found on: https://www.gams.com/help/index.jsp?topic=%2Fgams.doc%2Fsolvers%2Findex.html&anchor=SOLVERS_MODEL_TYPES

is connected to GB through the Moyle interconnector. All types of generators are allocated to the respective node. GB is modelled as an elastic demand.

14. **Model focus/objective**: The output of the Reference UCED model is half hourly however, for the validation exercise –and also for the model application exercise described in chapter 7- a decision has been made to compare against historical generation. Unlike the CER supported models, the motivation of this thesis is not to specialize the model for SMP forecasting. Emphasis has been given on quantification of actual operational costs and environmental impact experienced in the Irish grid overall due to VRE penetration. The Reference model focuses primarily on generation because approximating the commitment of units can lead to estimation of all types of costs and emissions mentioned above.

5.4 Validation Results

5.4.1 Generation: A comparison between the Reference model and actual historical output

For the model validation exercise we simulated the unit commitment and economic dispatch of the Irish grid using the Reference 2010-2011 model. Moyle flows were not fixed but rather optimized based on least-cost principles as discussed earlier. However, Moyle's available capacity was restricted on a weekly basis based on historical capacity availability data to avoid overutilization of the interconnection. Figure 5-2 compares aggregated daily generation between actual historic data and the Reference model's output. Specific periods of disagreement between the model and actual data can be observed throughout the year. More specifically there are small periods where swapping of gas-fired generation with coal–fired generation can be observed[58]. Some discussion about potential sources of such disagreements will follow in the next section. Figure 5-3 presents aggregated monthly output of the Reference model and actual data where previously observed differences are smoothened out.

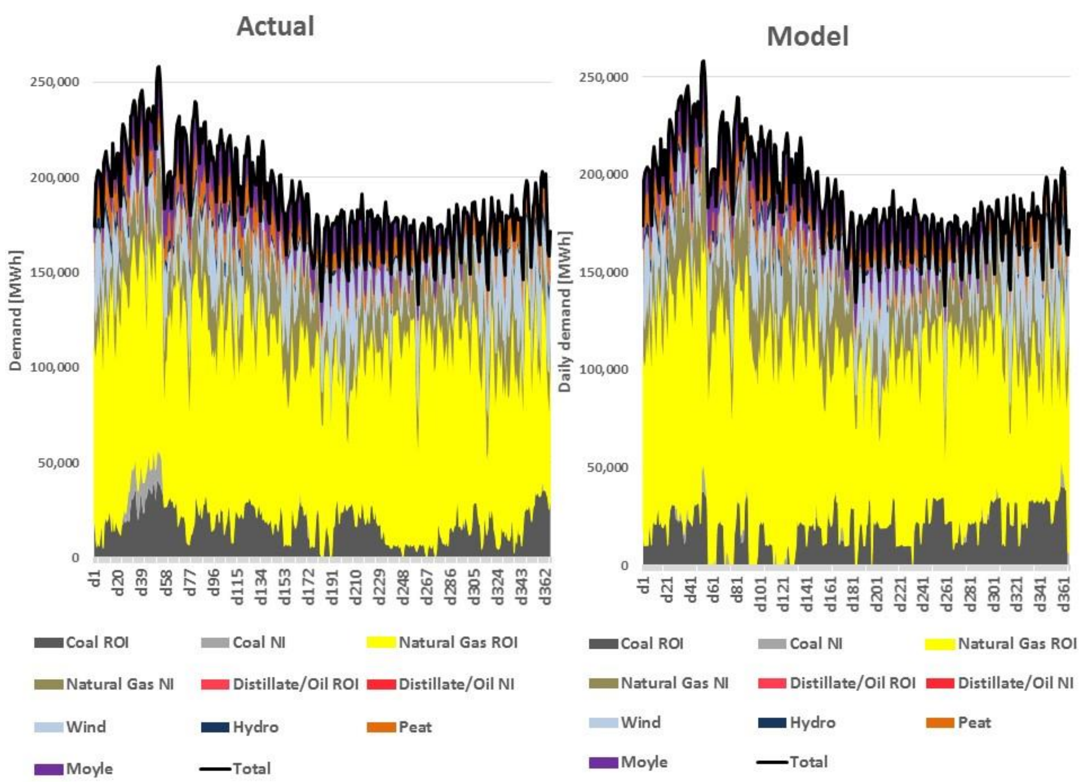

Figure 5-2: Daily generation (Reference model versus actual data, period Nov 2011-Oct 2011).

[58] One might observe that coal units under-operate in AI. The reason for coal-fired units in All-Ireland running at a capacity factor of only around 30% is due to compliance with the Large Combustion Plant Directive (LCPD, 2001/80/EC) [84] [85].

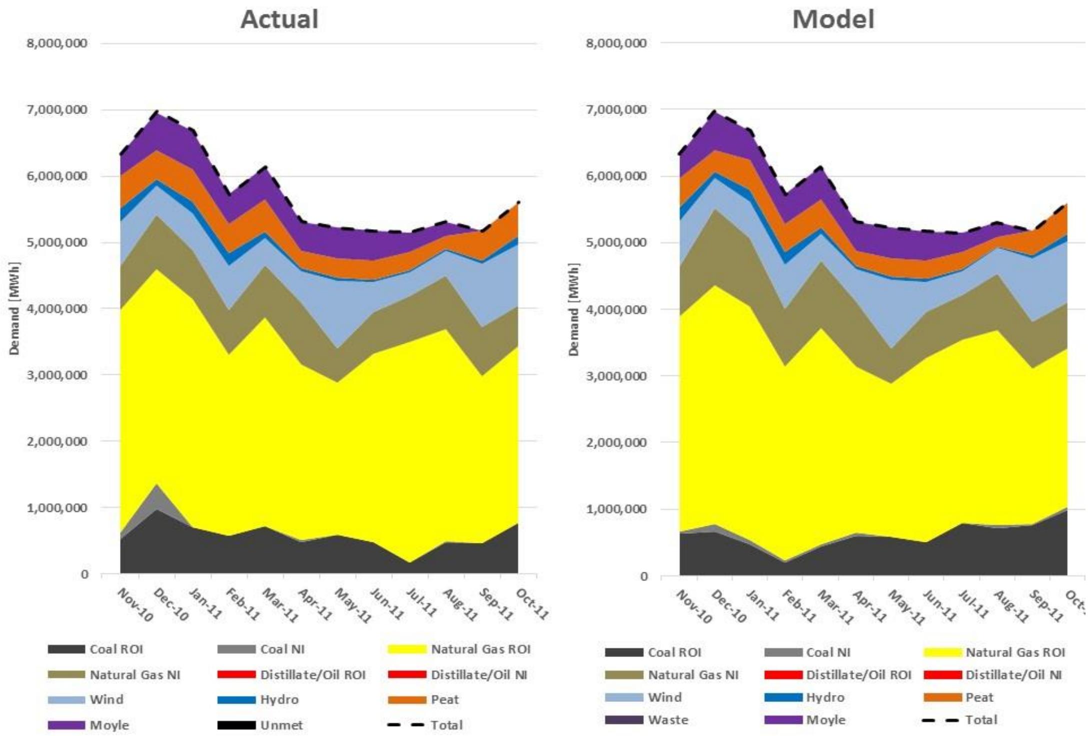

Figure 5-3: Monthly generation (Reference model versus actual data, period Nov 2011-Oct 2011).

One way to quantify the Reference model's output accuracy over the optimization period is by comparing the annual utilization factors of thermal generators with actual utilization factors. Such a method has been used before by CER to validate a PLEXOS model that was made to simulate dispatch in the Irish grid [42], [43]. Tables 5-5 to 5-10 list utilization factors of all thermal generators in AI. The tables present the deltas of utilization factors from actual historical data and the Reference model's output. A negative delta denotes underutilization of a generator by the model while a positive delta an overutilization. The results show that:

- Deltas are less than 5% for all coal fired generators.
- Deltas are less than 10% for 12 out of 16 gas fired generators in the RoI. However there are significant differences on utilization factors of the large PBC (510MW)

and TY (410MW) generators. The Reference model underutilizes the PBC by 14% while over utilizes the TY by 15%.

- Agreement is better (compared to RoI gas-fired generators) for the gas-fired generators in the NI. There is less than 5% agreement for 9 out of 10 generators including the large B31 (247MW), B32 (247MW) and CPS (404MW) generators.
- Deltas are less than 1% for all distillate and oil generators.
- Deltas are relatively large (~12%) for the two [ED (118MW and WO4 (137MW)] out the three peat generators operating in AI. The model underutilized both of them with deltas of around 12%.
- High level figures comparing aggregated generation per fuel show less than 5% disagreement for all fuel types (see tables 5-11 and 5-12).

Table 5-3: Comparison of utilization factors of coal-fired generators (Reference model vs Actual historical dispatch, Nov 2010, Oct 2011).

Fuel	COAL NI		COAL ROI		
Generator code name	K1	K2	MP1	MP2	MP3
Capacity [MW]	238	238	285	285	285
Actual annual utilization factor (%)	6.6%	6.4%	45.8%	47.3%	45.5%
Model annual utilization factor (%)	4.8%	5.0%	48.8%	48.1%	50.4%
Deltas	-1.9%	-1.4%	3.0%	0.8%	4.8%

Table 5-4: Comparison of utilization factors of gas-fired generators in the RoI (Reference model vs Actual historical dispatch, Nov 2010, Oct 2011).

Fuel	GAS ROI															
Generator code name	AD1	ADC	AT1	AT2	AT4	DB1	HN2	HNC	MRC	NW4	NW5	PBC	SK3	SK4	TY	WG
Capacity [MW]	258	435	90	90	90	415	412	352	88	161.8	104	510	83	83	404	460
Actual annual utilization factor (%)	0.4%	83.1%	0.2%	0.1%	0.0%	87.7%	74.9%	59.9%	0.2%	0.0%	1.5%	30.5%	82.4%	91.7%	49.7%	57.5%
Model annual utilization factor (%)	0.6%	88.8%	0.3%	0.2%	0.1%	85.8%	64.8%	65.2%	0.0%	0.0%	4.1%	16.5%	66.7%	74.2%	64.8%	54.6%
Deltas	0.2%	5.7%	0.1%	0.1%	0.1%	-1.9%	-10.1%	5.3%	-0.2%	0.0%	2.5%	-13.9%	-15.7%	-17.5%	15.1%	-2.9%

Table 5-5: Comparison of utilization factors of gas-fired generators in the NI (Reference model vs Actual historical dispatch, Nov 2010, Oct 2011).

Fuel	GAS NI									
Generator code name	B10	B31	B32	B4	B5	B6	Contour_1	Contour_2	Contour_3	CPS_CCGT
Capacity [MW]	101	247	247	170	170	170	3	3	3	404
Actual annual utilization factor (%)	10.0%	25.2%	28.0%	1.7%	0.5%	1.0%	1.8%	1.8%	1.6%	85.5%
Model annual utilization factor (%)	33.8%	31.4%	32.9%	1.8%	1.3%	4.1%	0.0%	0.0%	0.0%	89.4%
Deltas	23.8%	6.2%	4.9%	0.1%	0.8%	3.2%	-1.8%	-1.8%	-1.6%	3.9%

Table 5-6: Comparison of utilization factors of distillate-fired generators in both the RoI and NI (Reference model vs Actual historical dispatch, Nov 2010, Oct 2011).

Fuel	DISTILLATE NI							DISTILLATE ROI					
Generator code name	BGT1	BGT2	CGT8	KGT1	KGT2	KGT3	KGT4	ED3	ED5	RH1	RH2	TP1	TP3
Capacity [MW]	58	58	58	29	29	42	42	58	58	52	52	52	52
Actual annual utilization factor (%)	0.0%	0.0%	0.0%	0.1%	0.0%	0.1%	0.1%	0.0%	0.0%	0.0%	0.0%	0.0%	0.0%
Model annual utilization factor (%)	0.0%	0.0%	0.1%	0.1%	0.1%	0.3%	0.2%	0.0%	0.0%	0.6%	0.6%	0.0%	0.0%
Deltas	0.0%	0.0%	0.1%	0.1%	0.1%	0.2%	0.1%	0.0%	0.0%	0.6%	0.6%	0.0%	0.0%

Table 5-7: Comparison of utilization factors of oil-fired generators in the RoI (Reference model vs Actual historical dispatch, Nov 2010, Oct 2011).

Fuel	OIL ROI						
Generator code name	GI1	GI2	GI3	TB1	TB2	TB3	TB4
Capacity [MW]	54	49	113	54	54	240	240
Actual annual utilization factor (%)	0.0%	0.0%	0.0%	0.0%	0.1%	0.4%	0.0%
Model annual utilization factor (%)	0.0%	0.0%	0.0%	0.0%	0.2%	0.5%	0.0%
Deltas	0.0%	0.0%	0.0%	0.0%	0.2%	0.1%	0.0%

Table 5-8: Comparison of utilization factors of peat generators (Reference model vs Actual historical dispatch, Nov 2010, Oct 2011).

Fuel	PEAT		
Generator code name	ED1	LR4	WO4
Capacity [MW]	118	91	137
Actual annual utilization factor (%)	84.7%	97.2%	53.0%
Model annual utilization factor (%)	72.9%	96.8%	40.7%
Deltas	-11.8%	-0.4%	-12.3%

Table 5-9: Comparison of utilization factors of generators aggregated based on type of fuel and geography (Reference model vs Actual historical dispatch, Nov 2010, Oct 2011).

	Coal		Natural gas		Distillate/Oil			
Fuel	Coal RoI	Coal NI	Gas RoI	Gas NI	Distillate RoI	Distillate NI	Oil RoI	Peat
Capacity [MW]	855	476	4,036	1,518	324	274	804	850
Actual annual utilization factor (%)	46.2%	6.5%	49.9%	32.4%	0.0%	0.0%	0.1%	30.7%
Model annual utilization factor (%)	49.1%	4.9%	48.5%	37.3%	0.2%	0.1%	0.2%	27.0%
Deltas	2.9%	-1.6%	-1.3%	4.9%	0.2%	0.1%	0.1%	-3.7%

Table 5-10: Comparison of utilization factors of generators aggregated based on type of fuel (Reference model vs Actual historical dispatch, Nov 2010, Oct 2011).

Fuel	Coal	Natural Gas	Distillate/Oil	Peat
Capacity [MW]	1,331	5,554	1,443	346
Actual annual utilization factor (%)	32.0%	45.1%	0.1%	30.7%
Model annual utilization factor (%)	33.3%	45.5%	0.2%	27.0%
Deltas	1.3%	0.4%	0.1%	-3.7%

Previous efforts of the CER to validate a backcast PLEXOS model of the Irish system reported similar findings[59] [42], [43] .

[59] The backcast PLEXOS model uses actual historical quantity-price pairs as while the UCED model developed in this thesis uses fixed technical characteristics of generators and historical fuel price data to approximate the SRMCs of generators during the UCED calculation. Thus the validation of the backast PLEXOS model has better chances of success since the effect of gaming of generator was not present (see section 5.4.2)

Previous efforts of the CER to validate a backcast PLEXOS model of the Irish system are documented on sources[60] [42] and [43]. The PLEXOS model reported absolute deltas between 10% and 15% for the following units: PBC (510MW), K1 Coal (238MW), K2 Coal (238MW), B31(247MW) and B32(247MW) totaling capacity of 1,480MW. The great majority of rest of units reported absolute deltas of 5% or less. The UCED model reported relatively high delta's for units B10 (110MW) and SK4 (83MW)- 23% and 17.5% respectively. In addition the following 6 units had deltas between 10% and 15.7%: PBC(510MW), SK3(83M2), TY (404MW), HN2(412MW), ED1(118MW) and WO4 (137MW). All before mentioned units totaled a capacity 1,857MW. The great majority of rest of units had a delta less than 2%. The results of the UCED model can be observed in Tables 10 to 15. Comparing the results of the backcast PLEXOS model and the UCED model we conclude that the former reports relatively better results. However, it should be noted that the PLEXOS backcast model optimized historical generation using as inputs the actual bids that the Irish market experienced (price/quantity pairs) during the optimization period and as a result it can better represent the outcome since gaming doesn't factor in the calculation. On the other hand -as noted before- the UCED model presented in this paper is a least-cost dispatch model that doesn't consider gaming. Considering the above facts, the performance of the UCED model presented in this paper has been regarded sufficient. The following section discusses possible sources of disagreements in the results that were discussed earlier.

[60] The backcast PLEXOS model uses actual historical quantity -price pairs as while the UCED model developed in this thesis uses fixed technical characteristics of generators and historical fuel price data to approximate the SRMCs of generators during the UCED calculation. Thus the validation of the backast PLEXOS model has better chances of success since the effect of gaming of generator was not present

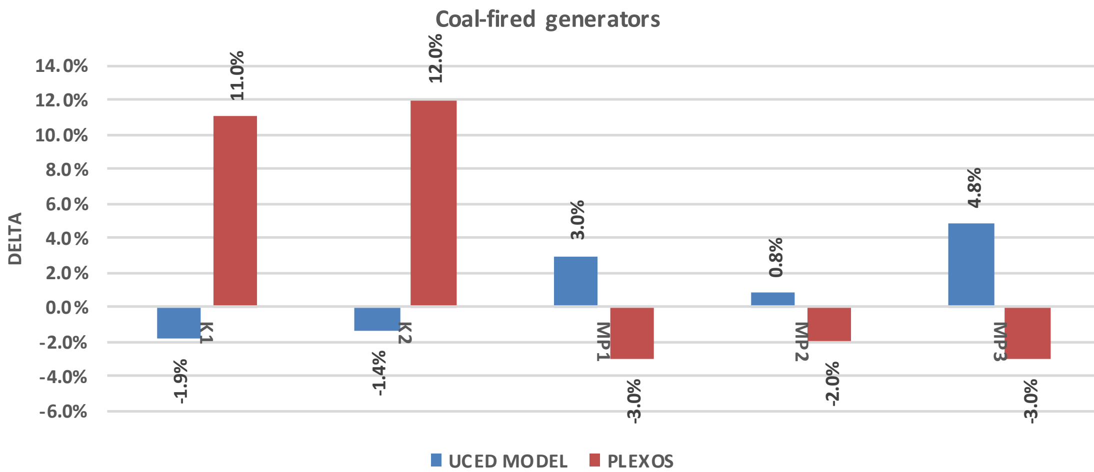

Figure 5-4: Deltas for coal-fired generator utilization factors; comparison of estimates from the UCED model and PLEXOS used to model the Irish power system

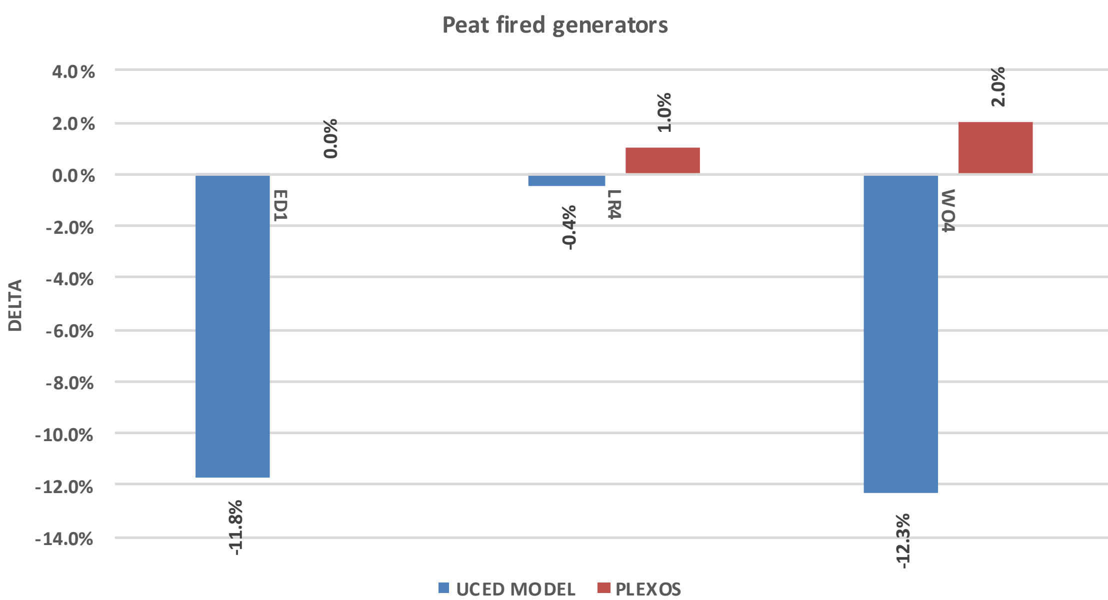

Figure 5-5: Deltas for peat-fired generator utilization factors; comparison of estimates from the UCED model and PLEXOS used to model the Irish power system

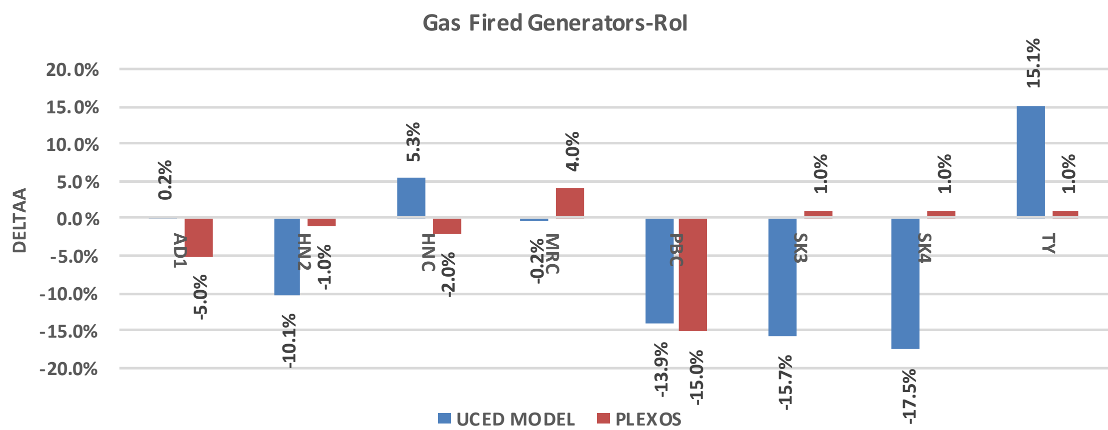

Figure 5-6: Deltas for gas-fired generator utilization factors: Comparison between the UCED model and PLEXOS used to model the RoI segment of the Irish power system. Generators with Delta ≤3% are excluded from the graph.

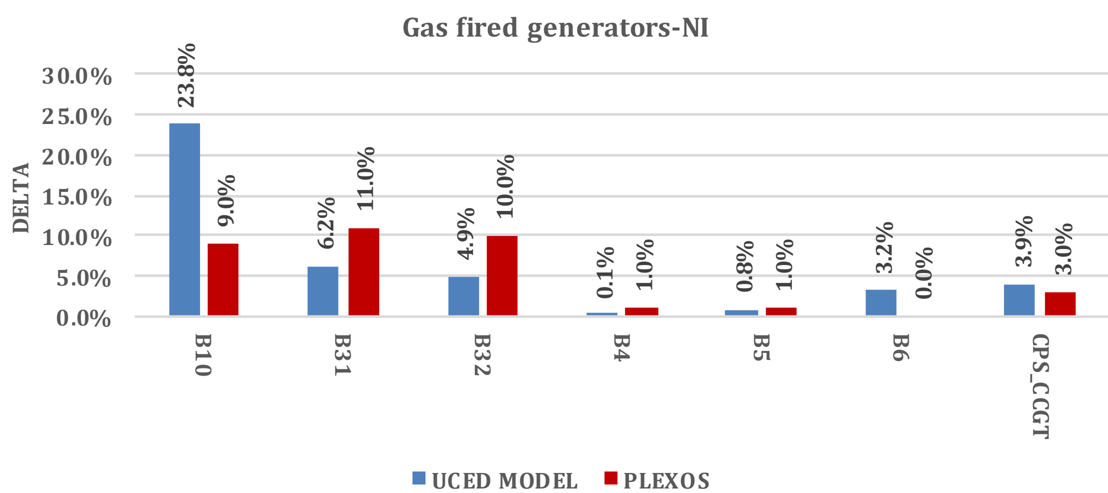

Figure 5-7: Deltas for gas-fired generator utilization factors: Comparison between the UCED model and PLEXOS used to model the NI segment of the Irish power system.

5.4.2 Possible sources of disagreement between modeled and actual dispatch

Possible sources of differences between actual historical data and the model's output are listed below:

- Actual market environment versus deterministic least-cost optimization

The UCED model represents the ideal operation of a system that if it dispatched its units according to the model's outcome would experience the minimum cost possible overall. In reality though, no matter how transparent SEM claims to be in a market environment there are inefficiencies resulting from the bidding process. Even though generators should ideally bid their short marginal cost (SRMC) of operation, in reality the bidding pattern of some generators doesn't correspond to the SRMCs that would be expected based on their technical characteristics. A short discussion of the bidding process in the SEM an illustrative example will follow.

The SEM uses the so called "3-part offers" which allows the market participants to enter information with regards to start-costs, no-load costs and price-quantity pairs. The terms "offer price" and "offer quantity" relate to the price quantity pairs and represent the average cost of production within specific generation bands. Each generator submits such information into up to 10 bands. For example, according to some hypothetical price-quantity data in table 5.5 for an output up to 200MW the incremental cost of electricity production of the hypothetical unit is €50/MWh; for an output 201-300MW the incremental cost is €55/MWh while for an output of 301MW to 400MW the incremental cost is €80/MWh.

Table 5-11: Hypothetical price quantity pair

Band	Offer Price	Offer Quantity
1	50 €/MWh	200 MW
2	55 €/MWh	300 MW
3	80 €/MWh	400 MW

Let us illustrate the actual bidding strategy of two coal-fired generators – Kilroot (476MW) and Moneypoint (855) during the 1st day of 2011. The Kilroot units K1 and K2 submitted identical commercial offer data (COD). Kilroot runs at much higher no-load costs compared to Moneypoint units (MP1, MP2, and MP3). The high fixed costs of Kilroot are related to burning oil to start-up and at very low outputs; the generators need to recover such costs through the no-load component [43]. The Kilroot units submit comparable production costs as the Moneypoint ones over the 1st band of operation (€52 /MWh up to 175MW). However, the Kilroot bids 7 times as much marginal price over the second band (176MW - 238MW). Possible reasons for generating unit to bid far from their SRMCs are:

- Attempt to maximize profits through gaming
- A unit is trying to recover some investment or other type of costs
- SRMCs are very high due to inefficiencies related to aging of generating assets
- A power plant is a located in a transmission constrained area and there is high chance of coming on line even at high bids.

Table 5-12: No load and price quantity pairs submitted to the SEM operator on the 1st of January 2011 by the Moneypoint and Kilroot generators.

		Band 1		Band 2	
	No-Load Cost	Quantity	Price	Quantity	Price
	€	MW	€/MWh	MW	€//MWh
K1	2,233	175	52	238	357
K2	2,244	175	52	238	357
MP1	895	195	51	280	52
MP2	895	195	51	280	52
MP3	895	195	51	280	52

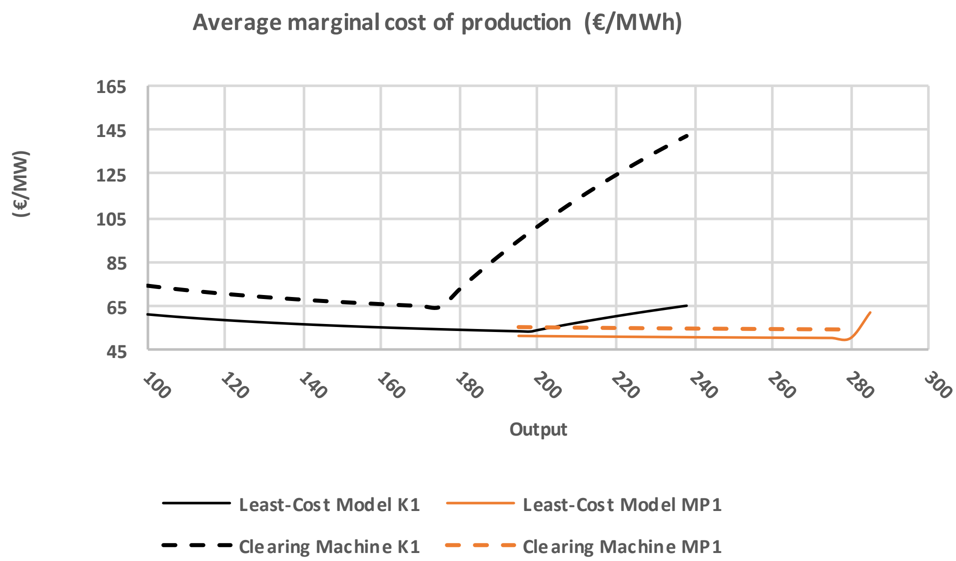

Figure 5-8: The cost of production for K1 and MP1 units based on a) data submitted to the operator and b) technical information used in the Least-Cost model of this thesis.

It is noted that there are some differences in the inputs of the UCED least-cost model developed in this thesis and the inputs of the clearing engine as submitted by the generators. The possible reason for this is that the claimed by generator's operational costs can vary on a daily basis depending on a generator's strategy to enter the dispatch, whereas the

UCED model uses fixed technical parameters to calculate the dispatch based on demand data and fuel prices.

Chapter 6 : Application of the "Thermo-Economic" CAES Model. Participation on Energy and Ancillary Services Markets in Ireland

6.1 Introduction

In this chapter the MIP "Thermo-Economic" CAES model presented on chapter 3 is compared with a simpler MIP CAES model where the CAES unit is modeled having fixed thermodynamic properties, also introduced on chapter 3 as the "Fixed Parameter (FP)" model.

The "Thermo-Economic (TE)" CAES model introduced in this chapter does simulate the following, not represented by fixed parameter models:

- **The effect of cavern pressure on power requirement during compression:** The compressor can-not discharge air at pressure lower of the cavern back pressure. The higher the cavern back pressure the higher the power requirement to compress at constant air mass flow.
- **The effect of speed of charging on power requirement for compression**: The higher the air mass flow entering the cavern, the higher the power requirement to compress at constant back pressure.
- **Variable compression efficiency depending on the operational regime**: The efficiency of compression is inherently represented in the data of figure 3-11. The efficiency of the compressor represented varies from 81% to 85% depending on cavern pressure and speed of charging[61].

---

[61] according to proprietary data a major CAES manufacturer has shared with the center of life cycle analysis at Columbia university

- **The effect of cavern pressure on CAES output**: As shown in figure 3-10 the maximum output of CAES depends on the cavern pressure levels. Rated output (135MW) can only be achieved if pressure levels are above 864PSI (design pressure). The maximum output decreases linearly to reach 10% of rated output when the cavern operates at 20% of design pressure.
- **The effect of discharge speed on CAES output**: Rated CAES output can only be achieved when the expander is run at rated expander air mass flow rate (400lb/sec). CAES output decreases linearly as air mass flow rate decreases to reach a minimum of 10% of rated output when air mass flow rate is at 20% of rated levels (see figure 3-10).

As mentioned earlier, the "Thermo-Economic" model is compared with a "Fixed Parameter" model similar to CAES models often used in literature to study CAES performance. More specifically both models are applied in the Irish power sector. We use 2015 SMP and ancillary services pricing data to simulate CAES performance when participating in the Irish energy and ancillary services markets. A number of scenarios has been defined to perform sensitivity analysis on key issues like discharge time, price of natural gas and SMPs and we compare metrics like net present value (NPV), profit, fuel costs, cost of compression, start-up costs and CO2 emissions. As there are currently only a few CAES units operating around the world it was not possible to obtain any detailed actual data to validate my model. However, in this thesis I prove I have built a model that represents the thermodynamic behavior of figures 3-9 and 3-10. Thus, my model is as valid as the thermodynamic information released by major CAES manufacturers. At the same time the TE CAES model is more detailed and complex compared to widely used FP models and as we show in the following chapters it gives insights that FP models can't capture.

6.2 Overview of existing CAES models

The need of integration of large scale energy storage has become eminent during the last decade as the share of variable renewable energy increases globally. As discussed on chapter 2 energy storage technologies can provide various services/benefits including energy time shift, ancillary services (like regulation and contingency reserves) and firm capacity. The increasingly complex economics of energy storage is key for realizing such benefits. Quantifying the value of storage technologies is a mathematically intensive problem that requires use of sophisticated software.

In regulated markets utilities try to minimize risks and adoption of new technologies has been slow [52]. The introduction of energy and ancillary services markets has introduced new opportunities of investment on energy storage technologies (this topic is being discussed on section 6.3.1.7). Planning in competitive markets is complicated by independent investment decisions, market rules and bid strategies that increase the variability of unit commitment and ancillary service providers and network flows [53]. Introduction of new technologies like variable renewables create additional changes on the state of the system and thus modelling power systems performance is a continuous need. The economic performance of new storage technologies can be assessed from such models. The economic performance of a storage technology depends on factors like capital costs and operating costs and as well as on the structure of electricity markets and the resulting SMPs. SMPs are very important because peak/off peak prices for electricity together with the efficiency of the storage device are essential for the economic viability of a storage device.

The value of energy storage has been assessed in various US energy markets. Drury et al. used historical market data to co-optimize CAES participating on energy and ancillary services markets to maximize profits [54] . The authors used a MIP model similar to the FP model we introduced on chapter 3 to assess the economics of CAES on CAISO, MISO, NYISO and PJM. Yang Du et al. developed an FP MIP model to evaluate the economic value of CAES in systems with large-scale wind power generation. Co-optimization of energy and ancillary markets was implemented to analyze the impacts of CAES on energy supply and operating reserves [55]. The economics of CAES when coupled with wind power has also been studied by Lund and Salgi [56] through a FP model for the Danish case. Wolf et al. developed a FP MIP model to co-optimize the performance of an adiabatic CAES unit that participates on energy and ancillary markets in Germany [57]. The fore-mentioned models simulate CAES performance as an individual unit responding to historical SMPs and reserve price data. It is however advantageous to include CAES into a UC model because such a representation gives additional insights. A UC model doesn't assume any historical price data but rather predicts SMPs with CAES contributing to their values. Thus a UC model captures the impact of CAES on total system economics rather focusing on the economics of CAES as a standalone unit. Additionally UC models account for complex generator parameters like ramp rates, minimum up and down times and thus account for a better representation of the actual system. PLEXOS is a well-known commercial MIP UC software that includes CAES representation. CAES in PLEXOS is modelled as a combination of a pumped hydro unit and a gas turbine. The CAES model in PLEXOS is in reality a FP parameter model where the performance of the device is described through a fixed pumping efficiency, a fixed heat rate for the gas-turbine and some storage capacity (expressed as a black box that stores energy rather than air). Foley and Lobera [58] and Brendan et al. [59] have used PLEXOS to assess the benefits of CAES on SEM in 2020 when the renewable energy penetration is expected to reach levels of 40%.

In this thesis the first "Thermo-Economic" CAES model that simulates the effect of cavern pressure on CAES performance is developed. Since the model adds technical insights technical and economic insights on CAES modelling, the "Thermo-Economic" model is compared with a built in-the-house "Fixed-Parameter" model to directly compare the two types of models and identify key differences.

6.3 Comparison of two CAES models participating on the energy and ancillary services markets in Ireland

6.3.1 Development of scenarios

For comparing the TE and FP model a set of scenarios has been developed. All scenarios were developed to test some sensitivities around the Base scenario and compare the economic and technical performance and also operational costs of a CAES unit among different environments and between the two models. In the Base scenario CAES performs energy arbitrage using latest SMPs and natural gas prices. Sensitivities are applied on main key performance parameters like cavern volume, gas prices and SMPs. Additionally, the CAES unit participates on the ancillary services market while also performing energy arbitrage and I co-optimize its operation having an objective to maximize its profit. Finally, all scenarios are compared based on key metrics like Net Present Value (NPV), operational revenues and costs, technical performance and emissions rates. A summary of all scenarios is shown in table 6-1. A more detailed description is given right below:

Table 6-1: Description of scenarios.

Scenarios	CAES technical specifications	Objective	SMPs	Natural gas price
Base	See figure 6-2	Profit maximization through energy arbitrage	SMPs for period Jan-Dec 2015	€4/GJ
High Discharge Time	Same as Base but cavern is increased to 140,000m3 (2,269MWh for FP model)	Same as Base	Same as BASE	€4/GJ
Low Discharge Time	Same as Base but cavern is decreased to 37,000m4 (589 MWh for FP model)	Same as Base	Same as BASE	€4/GJ
High Natural Gas Price	Same as Base	Same as Base	Same as BASE	**€8**/GJ
High SMPs	Same as Base	Same as Base	SMPs for the period Nov 2010 to Oct 2011	€4/GJ
Base+Ancillary Services	Same as Base	Profit maximization through energy arbitrage+providing spinning and non-spinning reserves	Same as BASE	€4/GJ

6.3.1.1 Base scenario

The assumptions for the "Base" scenario is shown in table 6-1. The technical details of both models at each scenario are similar for fair comparison. For the Base scenario I make use of the technical details for the expander and compressor of figures 3-10 and 3-11. The Thermo-Economic model makes use of the full information presented on the specified figures while the Fixed Parameter model only uses specific values (for example the energy ratio) or ranges (for example power operational range of compressor and expander). To give an example both models allow the same operational range for the compressor (65MW to 134MW). However, the compressor power requirement in the Thermo-Economic follows the pressure in the cavern. The compressor cannot be operated at its lowest power requirement levels if the pressure in the cavern is approaching maximum levels. It will always withdraw power according to information in figure 3-11. On the other hand, in the Fixed Parameter model the compressor can be operated within its full operational range at any time step. Similar constraints apply on the expansion side. As per figure 3-10 the heat rate of CAES is nearly constant for the greatest range of its operations. However, the output is capped by the cavern pressure and air mass flow levels. If the pressure drops below expander design levels the output can never reach rated levels.

The optimization time for the Base scenario is 52 weeks. The optimization step is half an hour. The SMP data used are for year 2016 obtained from the SEM-O website. The storage capacity is set at 13 hours. The discharge time the FP model is constrained through a maximum energy cap in the cavern (1,755 MWh). In the TE model discharged time is constrained through the volume of the cavern (120,000m3).

Table 6-2: Assumptions for " Base" scenario

	Fixed Parameter	Themo-Economic
CAES OPERATION METRICS[1]		
Design Heat Rate(BTU/kWh)1	3,959	3,959
Compressor/Turbine Power Ratio	1	1
Energy ratio (MWh-in/MWh-out)	0.75	Unconstrained; it Varies
CAES COMPRESSOR CHARACTERISTICS[2]		
Compressor Rated Power (MW)	128	128
Compressor Power Range (MW)	62-134	62-134
Compressor Air Mas Flow Range (kg/sec)	Not Applicable	122-211
Compressor Air Mass Flow Range (lb/sec)	Not Applicable	270-465
Turndown Ratio %	49%	49%
Compressor Discharge Pressure Range (PSIA)	Not Applicable	864-1500
Compressor Efficiency (%)[3]	83%	Not Applicable
Operational Pressure Range (PSI)	Not Applicable	900-1,800
CAES EXPANDER CHARACTERISTICS[4]		
Expander Rated Power (MW)	135	135
Expander Power Range (MW)	27-135	27-135
Expander Air Mass Flow Range (kg/sec)	Not Applicable	58-181
Expander Air Mass Flow Range (lb/sec/sec)	Not Applicable	127-400
Turndown Ratio%	80%	80%
Expander Design Back Pressure [PSI]	Not Applicable	864
Expander Pressure Range (PSI)	Not Applicable	173-864
STORAGE CHARACTERISTICS		
Cavern Volume (million m3)[5]	Not Applicable	70,000
Storage Capacity (MWhs)	1,092	1,092
Discharge Time (Hrs)[5]	13	13
Energy Level in the Cavern (MWh)[6]	0-1,092	Not Applicable
Total energy output from highest to lowest storage level including contribution of natural gas (MWh)	1,755	1,755
Operational Pressure Range (PSI)	Not Applicable	174-1,800
CAES COSTS		
Expander Start Up Cost (€)[7]	3,500	3,500
Compressor Start Up Cost (€)[7]	0	0
Expander VOM Cost (€/MWh)[7]	1.5	1.5
Compressor VOM costs (€/MWh)[7]	1.5	1.5
Natural Gas Cost (€/ GJ)[7]	4.0	4.0
EMISSIONS FACTORS		
Natural Gas [kg/GJ][8]	57	57
Grid Emissions Factor (ton CO2 per MWh)[8]	0.732	0.732
OPTIMIZATION OBJECTIVE	Energy Arbitrage (Profit Maximization)	Energy Arbitrage (Profit Maximization)
YEAR OF DATA	SEM SMPs for year 2016	SEM SMPs for year 2016
OPTIMIZATION PARAMETERS		
Optimization resolution (length of 1 time step) [hours]	0.5	0.5
Length of one optimization cycle [time steps]	1 week (336 time steps)	1 week (336 time steps)
Initial cavern Pressure at the beginning of each optimization cycle (PSI)[9]	Not Applicable	fixed at 1050 PSI
Initial energy Level in the Cavern at the beginning of each optimization cycle(MWh)[9]	fixed at half the maximum storage (546 MWh)	Not Applicable

1: Metrics are calculated based in figures 3-10 and 3-11
2: CAES compressor characteristics were obtained from figure 3-11

3: Compressor efficiency for the compressor of figure 3-11 varies within the range 81% to 85%. However, the relevant figure is confidential. For the Fixed Parameter model we assumed for the compressor a fixed efficiency of 83% that is the average of the range mentioned before

4: CAES expander characteristics were obtained from figure 3-10

5: CAES discharge time varies with application. For this work I have assumed a discharge time of 13 hours. In the Thermo-Economic model discharge time is represented through pressure volume. It would take 13 hours of continuous expansion at rated capacity to bring the cavern down to 174PSI. However, the maximum output will gradually decrease after the cavern reached design pressure (864PSI) and for that reason the actual discharge time is longer.

6: In the Fixed Parameter model discharge time is represented by the maximum energy level in the cavern which is 13hrs times rated capacity (135MW) equal to 1,755MWh

7: Source of data is [59]

8: The emissions in all scenarios are calculated at both the expansion and compression side. The emissions factor for natural gas was obtained from the fuel price calculator being public at the SEM committee website where the validated generator data requirements for the PLEXOS SMP forecast models are located[62]. The emissions for the compression side are based on the grid emissions factor for Ireland obtained from Covenant of Mayors[63]

9: The pressure in the cavern for the TE model and the energy level in the cavern for the FP model are set to some fixed levels at the beginning of each optimization cycle. If such a constraint was not implemented the models would deplete the cavern by the end of each optimization cycle to maximize profit. However, at the beginning of the next cycle the cavern would be empty

6.3.1.2 Low discharge time scenario

Discharge time varies with CAES application. A CAES unit designed to provide intermediate/peak energy and also provide ancillary services would need to have a higher discharge time compared to a CAES unit providing only frequency regulation. The implication of discharge time on CAES economics is obvious. A unit that has the ability to discharge for a longer period has higher opportunity to make revenues. However, we selected to perform sensitivity on discharge time because we expect to see higher impact on the Thermo-Economic model compared to the Fixed Parameter. The reason is that in the Thermo-Economic model discharge time is regulated through cavern volume; at the same time cavern volume affects pressure in the cavern and as explained before cavern pressure affects compressor and expander performance. It takes longer time to build pressure in a larger cavern and the opposite is true for a small cavern. For the low discharge time scenario we have chosen discharge time of 7 hours (almost half the time of the Base

[62] Source of price fuel price calculator (https://www.semcommittee.com/news-centre/2011-plexos-validation-reports-and-models)

[63] The grid emissions factor for Ireland was obtained at (http://www.eumayors.eu/IMG/pdf/technical_annex_en.pdf)

scenario). The cavern volume for 7 hours of discharge is 40,000m^3. For the Fixed Parameter model the upper cap of energy level in the cavern is 945MWh.

6.3.1.3 High discharge time scenario

The high discharge time scenario was developed for similar reasons as the low discharge time scenario. In this scenario we double the discharge time to 26hrs. The cavern volume for the high discharge time scenario is 160,000m^3 (Thermo-Economic model). The upper energy level for the Fixed Parameter model is 3,510MWh.

6.3.1.4 100% higher natural gas prices scenario

Natural gas prices have been very volatile historically. As of summer of 2016 where this thesis is being written natural gas futures at balancing point are traded at around €4/GJ. However, natural gas prices were 50% higher two years ago while almost 3 times as high in 2008. It is likely that natural gas prices will raise in the future. We also run a scenario with 100% higher natural gas prices to test the sensitivity of both models on gas prices as well as CAES profitability.

The sensitivity of CAES on gas prices is shown in figure 6-1. Considering a roundtrip efficiency of 52% the required range between peak-off peak prices so that the CAES unit recovers its operational costs widens if gas prices increase. For example, if a CAES unit charges with average off-peak electricity prices of €30/MWh will require average peak prices €70/MWh to recover its operational costs at natural gas prices of €4/GJ. If gas prices however were €8/GJ the average required peak SMPs would need to be €100/GJ. This is the reason the CAES unit discharges considerably less hours during the high natural gas prices scenario (see table 6-5).

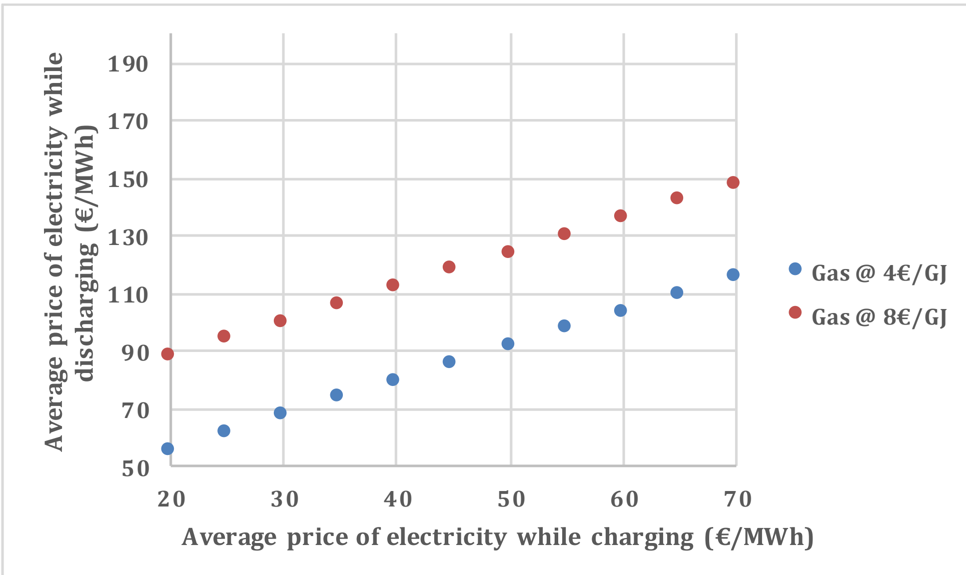

Figure 6-1: Relationship between average price of electricity while charging and while discharging in order for the CAES unit to recover fuel costs and cost of compression (start-up costs not included).

6.3.1.5 23% higher SMPs scenario

Profitability of a CAES unit participating on energy markets depends greatly on the prices of energy. For the high SMP scenario we use actual SMP data for the period November 2010-October 2011 (52 weeks). Since the data for the Base scenario correspond for 52 weeks for the period January 2015-December 2015 the weeks are not chronologically aligned. However, chronological order doesn't' affect the analysis as the scenario was developed to identify differences on two models when prices are just different. Average SMP price for the period 2010-2011 is 62.5 (€/MWh) while for year 2015 is 50.7 (€/MWh). Thus, SMPs for period 2010-2011 are 23% more expensive compared to data for year 2015. Average weekly SMPs and the (%) is shown in figure 6-1. Additionally the 2010 data have an average daily range[64] of €119/MWh compared a range of €88/MWh for year 2015. This means on 2010 data there are higher peak-off peak differences. Wider price range together with higher prices are the two main drivers for higher profitability.

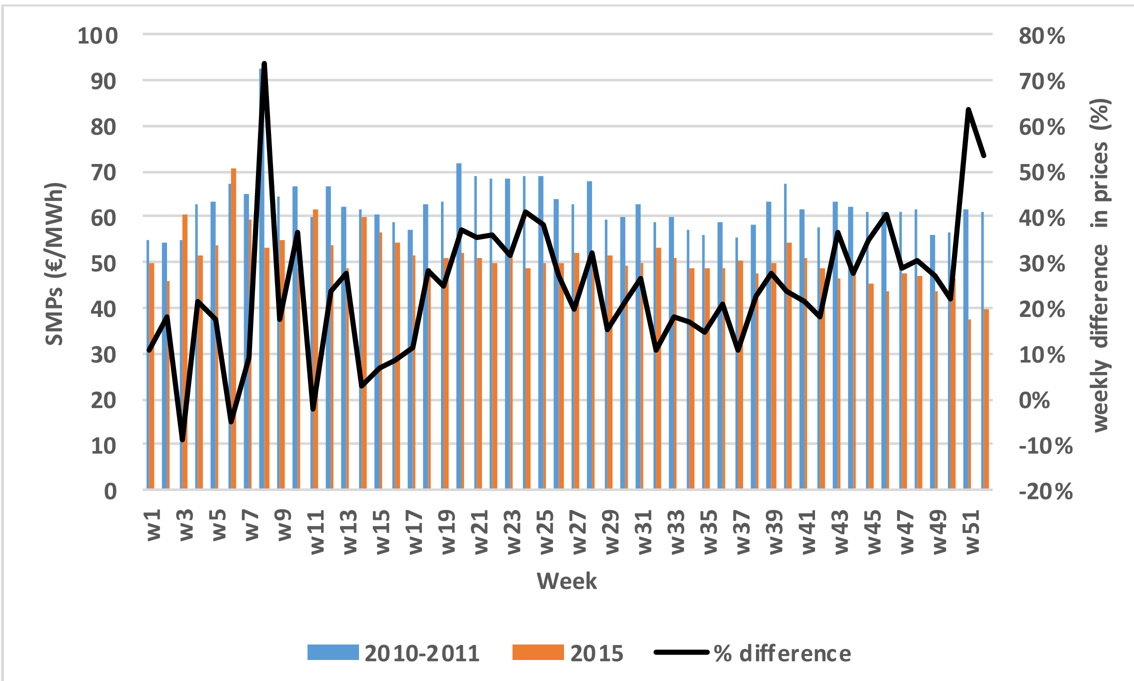

Figure 6-2: Differences on SMPs between " Base" and High "SMPs scenario" for the 52 weeks modeled. The average weekly values range from 38(€/MWh) to 71 (€/MWh) for 2015 data. The same range for the 2010-2011 data is 54(€/MWh) to 92 (€/MWh). The average difference from weekly 2016 SMPs ranges from -9% to 74% as shown in the figure (positive difference means 2010-2011 are higher values).

64 Maximum minus minimum half hourly SMPs over each of 365 days

6.3.1.6 Energy arbitrage + ancillary services co-optimization scenario

The scenarios we presented so far assume CAES will be making profit only through energy arbitrage. In reality CAES systems can provide a long range of services due to its almost flat heat rate, fast ramp rates [65] and long discharge time. Thus, the full economic potential of CAES –and energy storage technologies in general- cannot be fully utilized from only providing energy arbitrage. From a technical view point CAES is a good fit for providing an additional wide range of services including:

- Ancillary services (frequency regulation, spinning and non-spinning reserves, voltage control and black start support)
- Demand response
- Peak capacity
- Transmission congestion relief
- Firming output of renewables
- Ramping control

From an economic view point however the potential for revenue for a storage unit depends on the existence of appropriate markets/revenue sources. The reader of this thesis can refer to source [60] for an update on current state of energy markets for energy storage units.

With regards to Ireland, there are four areas of potential compensation within the reserves services. There are five main types of reserves in Ireland [66] namely: a) operating, b)

[65] Dresser-Rand reports ramp rates of 26MW/min at the expansion side and 38MW/min on the compression side. Time to reach full load from cold start up is a bit less than 10 minutes. The time to change from compression to generation mode is less than 15 minutes

[66] Operating reserves are subject to many different naming conventions around the world. In this thesis I adopt NREL's broader description of operating reserves as :

replacement, c) substitute and d) contingency reserves operating over different time scales. A CAES unit is more suitable for participating on operating reserves since are better paid compared to rest of services and additionally the response times required are fast an ability a CAES unit does have. A detailed explanation of all types of reserves in Ireland can be found on sources [61], [62].

Operating reserve requirements in Ireland can be split into a few categories namely a) primary, b) secondary and c) tertiary reserves. Primary reserves provide frequency support up to 15seconds from a major event through inertia response or governor control. Secondary reserves in Ireland need to respond from 15sec to 75sec after an incident. CAES can provide secondary reserves (also called spinning reserves) through 1) ramping-up the expander and 2) reducing the output of (or turning-off) the compressor. Tertiary reserves (also called non-spinning reserves) are offered through unloaded generators that need to come on-line within 5 minutes (tertiary reserves 1) of an event or 15 minutes of an event (tertiary reserves 2). A CAES unit can offer tertiary reserves 2 through a) starting up the expander from an idling state and b) changing from compression to operational state while charging. Compensatiin figures for participating into ancillary services operations are available by EIRGRID and SONI. In the scenario we assume the CAES unit is compensated with €2.2/MWh for secondary (spinning) reserves and with €0.92/MWh for tertiary 2 (non-spinning reserves) [63].

6.3.2 Results and discussion around the sensitivity scenarios

The results of our analysis are summarized in tables 6-3 to 6-5:

Table 6-3: Summary table with results on operating profit, revenues and costs and (%) differences between a) the two models and b) each scenario with the Base scenario for the same model.

Scenarios	Models	Average SMPs	Total operating profit	Total operating revenues[1]	Total operating costs	Change on operating profits compared to Base scenario	Change on operating revenues compared to Base scenario	Chane on total operating costs compared to Base scenario	Difference on operating profit between models (TE-FP)/FP	Difference on operating revenues between models (TE-FP)/FP	Difference on operating costs between models (TE-FP)/FP
		[€/MWh]	[€m]	[€m]	[€m]	(%)	(%)	(%)	(%)	(%)	(%)
BASE Scenario	FP	50.8	9.5	27.2	17.7	[-]	[-]	[-]	-14.5%	-12.4%	-11.3%
	TE	50.8	8.2	23.9	15.7	[-]	[-]	[-]			
High discharge time	FP	50.8	10.2	29.2	19.0	6.4%	7.2%	7.6%	-12.9%	-10.9%	-9.8%
	TE	50.8	8.8	26.0	17.2	8.4%	9.0%	9.4%			
Low discharge time	FP	50.8	9.2	26.0	16.8	-3.7%	-4.4%	-4.8%	-30.4%	-30.4%	-30.4%
	TE	50.8	6.4	18.1	11.7	-21.6%	-24.1%	-25.3%			
100% higher natural gas price	FP	50.8	5.1	17.8	12.7	-46.3%	-34.6%	-28.4%	-15.6%	-20.1%	-21.9%
	TE	50.8	4.3	14.2	9.9	-47.0%	-40.4%	-37.0%			
23% higher SMPs	FP	62.4	13.4	34.2	20.8	40.3%	25.5%	17.6%	-14.0%	-15.8%	-16.9%
	TE	62.4	11.5	28.8	17.3	41.0%	20.7%	10.2%			
Base+Ancillary Services	FP	50.8	11.1	29.5	18.4	16.2%	8.3%	4.0%	-6.4%	-10.4%	-12.8%
	TE	50.8	10.4	26.4	16.0	27.1%	10.7%	2.2%			

1: For the Base+Ancillary Services scenario total operating revenues account for both arbitrage and operating reserves. For rest of scenarios operating revenues account for energy arbitrage only.

Table 6-4: Summary table with results on operating profit, revenues and costs per unit of energy produced.

Scenarios	Models	Average profit	Average revenues from selling electricity	Average cost of natural gas	Average cost of running the compressor (electricity + VOM)	Average cost of running the compressor (electricity + VOM)	Average expander VOM cost	Average start up cost
		[€/MWh]	[€/MWh]	[€/MWh]	[€/MWh-out]	[€/MWh-in]	[€/MWh]	[€/MWh]
BASE Scenario	FP	26.3	74.0	16.7	26.5	35.5	1.5	3.0
	TE	26.2	76.9	16.7	27.1	36.2	1.5	4.8
High discharge time	FP	25.4	72.5	16.7	26.5	35.4	1.5	2.5
	TE	25.8	75.0	16.7	26.9	36.2	1.5	4.1
Low discharge time	FP	26.7	74.9	16.7	26.7	35.7	1.5	3.3
	TE	29.5	82.5	16.7	27.6	36.6	1.5	7.3
100% higher natural gas price	FP	23.8	87.0	33.4	24.3	32.6	1.5	4.0
	TE	27.3	93.9	33.4	24.8	33.5	1.5	6.8
23% higher SMPs	FP	36.2	90.7	16.7	33.4	44.6	1.5	2.9
	TE	39.8	97.0	16.7	34.3	44.6	1.5	4.7
Base+Ancillary Services	FP	29.2	77.3	16.7	26.9	36.0	1.5	3.0
	TE	33.2	83.1	16.7	26.9	36.2	1.5	4.7

Table 6-5: Summary table with results on technical performance of the CAES unit.

Scenarios	Models	Energy Ratio	Roundtrip efficiency	Average pressure in the cavern[1]	Total energy being sold	Total electrical energy being consumed by compressor	Total mechanical energy being stored [2]	Total hours of charging	Total hours of discharging	Average hours of discharging per day	Average hours of charging per day	Total number of compressor Start-Ups	Total number of expander Start-Ups	Average CO2 emissions
		[Electric energy-in / Electric energy-out]	(%)	[PSI]	[MWh]	[MWh]	[MWh]	[Hrs]	[Hrs]	[Hrs]	[Hrs]			[ton CO2/ MWh]
BASE Scenario	FP	0.75	52%	[-]	369,126	275,987	229,069	2,261	4,255	12	6	687	313	0.79
	TE	0.75	52%	929.00	311,914	234,118	[-]	2,638	2,792	8	7	998	427	0.79
High discharge time	FP	0.75	52%	[-]	401,689	300,152	249,126	2,434	4,430	12	7	644	283	0.78
	TE	0.74	53%	930.34	347,366	258,516	[-]	2,880	3,067	8	8	907	406	0.78
Low discharge time	FP	0.75	52%	[-]	348,423	260,791	216,457	2,277	4,012	11	6	725	323	0.79
	TE	0.75	52%	913.29	220,170	166,047	[-]	1,791	2,108	6	5	1,078	456	0.79
100% higher natural gas price	FP	0.75	53%	[-]	200,845	149,897	124,414	1,203	2,453	7	3	487	216	0.78
	TE	0.74	53%	957.48	148,662	110,620	[-]	1,298	1,300	4	4	688	284	0.78
23% higher SMPs	FP	0.75	52%	[-]	382,854	286,834	238,073	2,269	4,410	12	6	477	307	0.79
	TE	0.77	52%	997.68	302,742	233,738	[-]	2,263	2,692	7	6	843	391	0.80
Base+Ancillary Services	FP	0.75	52%	[-]	381,944	285,867	237,270	2,594	5,783	16	7	526	323	0.79
	TE	0.74	53%	1004.32	320,556	238,372	[-]	2,567	3,067	8	7	986	428	0.79

1: Results about average pressure in the cavern don't exist for the FP model since it doesn't account for cavern pressure

2: Results about energy being stored in the cavern don't exist for the TE model since it doesn't directly calculate for the percentage electrical energy being consumed at the compression side transformed into mechanical energy

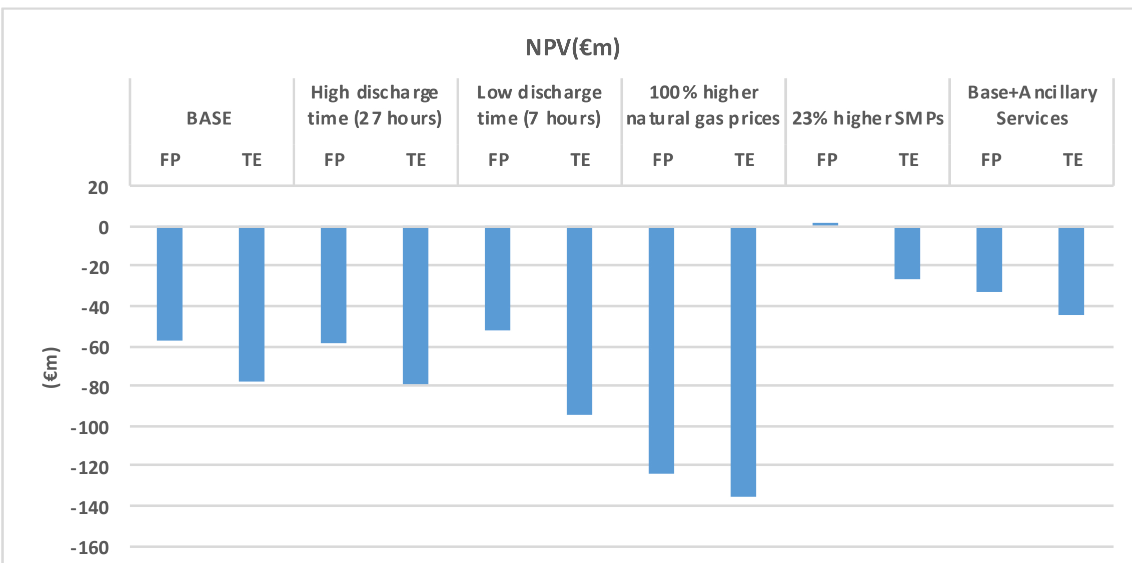

Figure 6-3: NPV of various scenarios based on the results of the TE and FP models. The NPV calculation was based on cost data shown in table 6-6. Additionally an interest rate of 6% and 40 years of operation have been assumed

Table 6-6: Fixed cost assumptions for the NPV calculation were based on EPRI **[64]**. The annual operational profit of the unit was based on the output of the FP and TE models across all modeling scenarios

Cost component	**Units***	**Value**
Plant cost without accounting for the cavern	($/MW)	1,079,000
	(€/MW)	954,867
Cavern cost (7 hours discharge time)	($/MWh)	18,450
	(€/MWh)	16,327
Cavern cost (20-26 hours discharge time)	($/MWh)	11,275
	(€/MW)	9,978
Fixed O&M	($/MW-yr)	3,075
	(€/MW-yr)	2,721
Periodic major maintenance	($/MW-yr)	23,000
	(€/MW-yr)	20,354

*Euro to US dollar conversion rate 0.73/1 has been assumed

The most important messages summarized are discussed below:

- The TE model returns around 15% less profits than the FP model across most of scenarios (table 6-3).
- The difference grows dramatically (almost doubles) for the low discharge time scenario (table 6-3). The reason is the effect of cavern pressure on the profitability of CAES which is magnified when the cavern volume is being reduced. The TE model can capture such effect while the FP model cannot. As we will show on sections 6.3.2.1 to 6.3.2.3 in detail, the TE model has less freedom compared to the FP model on minimizing its compression costs because of back pressure effects. That freedom is related to compressing the maximum amount of air at minimum energy expense while SMPs are at their lowest levels. As a result the TE model decides to charge less amounts of energy compared to the FP model (table 6-5).

Thus, the available energy for discharging will also be reduced and so will the opportunity for revenues.

- An immediate result of the above is that the CAES unit in the TE model will discharge for less hours compared to the FP model (see table 6-5) but during high SMP spikes. This is the reason the TE model has higher revenues per unit of energy produces, because it discharges for less time but during higher SMPs.
- Additionally, the increased on/off cycling of CAES on the TE model results to higher start-up costs compared to the FP model.
- Increasing the discharge time has a more positive effect on profits on the TE scenario compared to the FP one because the effect of pressure is being reduced
- In general, operational cost components per unit of energy produced are very comparable between the two models (figure 6-4) with except of start-up costs. Compression costs is the largest cost component except for the high gas price scenario.
- If the SMPs are increased or the price of gas is increased the % increase (or decrease respectively) of profits is comparable in both models (table 6-3).
- The energy ratio is very comparable between models and scenarios. Same is true for calculated roundtrip efficiencies (the energy ratio is fixed for the FP model).
- Emissions per unit of energy produced are very comparable across both models and scenarios.
- The TE model operates CAES at an average pressure close to 950PSI across all scenarios.

- At current Irish SMPs and compensation for operational reserves and at current natural gas prices all scenarios return a negative NPV for the CAES unit. This means a CAES unit in Ireland can't be deemed profitable without realizing additional revenue sources besides performing energy arbitrage and operational reserves (or unless operational reserves payments increase significantly) (see figure 6-3 and table 6-6). Such a calculation though doesn't include significant benefits a CAES unit can bring into the power system that we discuss in detail in chapter 7.
- The CAES unit would be close to breaking even if the Irish SMPs were at 2010 levels and current gas prices remained in the future according to the FP model. The TE model shows a negative NPV of €25m for the same scenario.
- CAES NPV is very sensitive to fluctuations of gas prices. Doubling natural gas prices will make a CAES investment far from profitable unless significant system wide benefits are being considered.

6.3.2.1 Results-Base Scenario

- Fixed Parameter model

The total operational profit for the FP model over 52 weeks is €9.5m (table 6-3). Total operating costs over the 52 week period account for €17.7m while total operating revenues for €27.2m. As expected, operating revenues and profit are strongly and positively correlated with average SMPs. As shown in table 6-4 a 54% on average SMPs (from €46/MWh-e for week 2 to €71/MWh-e for week 6) can result to a 115% increase on operating profit (from €28/MWh-e to €60/MWh-e accordingly). Additionally, there is a positive correlation between average weekly SMPs and the cost of compression. This is because the more the time the CAES expander operates to make revenues, the larger the time for compression will be needed to charge the cavern. The cost of running the compressor (electricity + VOM) is the largest cost component averaging €26/MWh (ranging between 38% and 62% of total costs) (figure 6-5). The cost of natural gas is fairly constant at €17/MWh. Start-up costs account for around 3% to 8% of total costs for the most of the time (€2/MWh to €3/MWh).

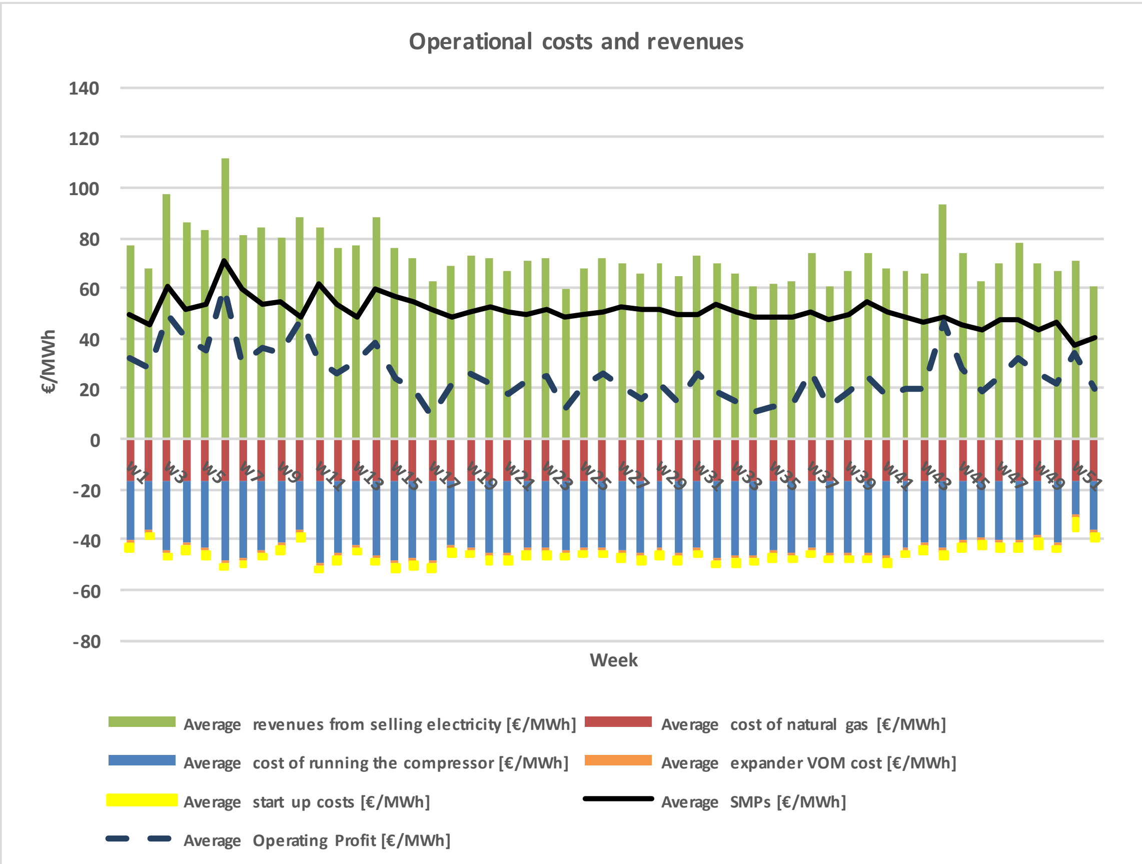

Figure 6-4: Operating profit, main operating costs and revenues expressed as €/MWh-e on a weekly basis (Model: FP, Scenario: Base).

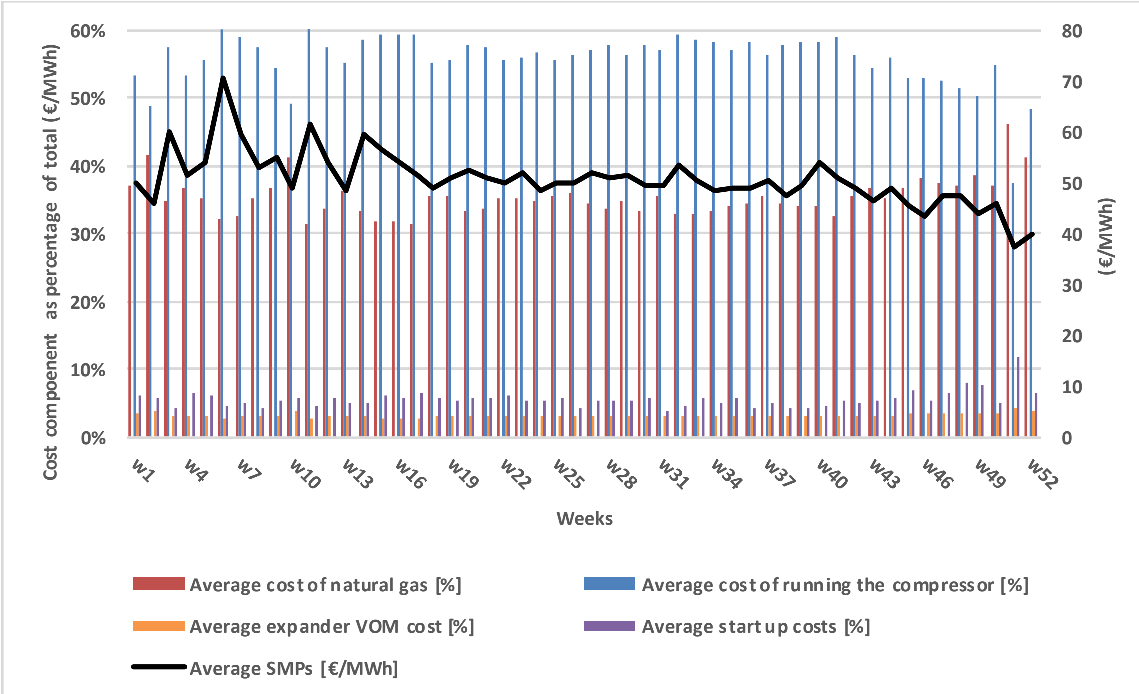

Figure 6-5: Break-down of operating costs expressed in (€/MWh-e) as percentage of total operating cost on a weekly basis (Model: FP, Scenario: Base).

When participating on the energy markets the CAES unit responds to half hourly SMPs to maximize its profit. During peak hours the CAES unit expands decreasing the stored energy in the cavern. During valley hours the compressors charge the storage device (figure 6-6). The FP model shows that on average the expander starts up once a day while the compressor can start-up more than 1 times (figure 6-7). The increased number of compressor start-ups is likely related to our assumption for zero cost for starting up the compressor. Data from figure 6-6 indicate there is no correlation among hours of operation (of either the expander or compressor), number of start-ups (of either the expansion or compression) and average weekly SMPs. The hours of operation and number of start-ups rather depend on the half hourly values of SMPs and the frequency of existence of price spikes up and down.

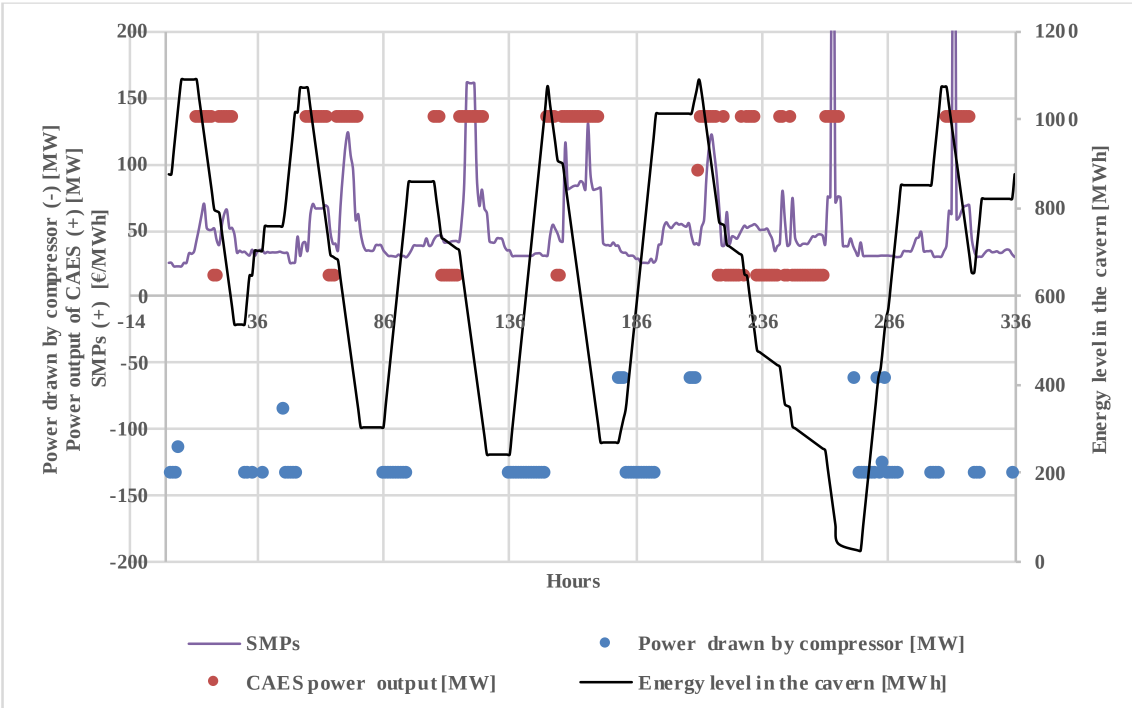

Figure 6-6: One week of CAES simulation (Model: FP, Scenario: Base).

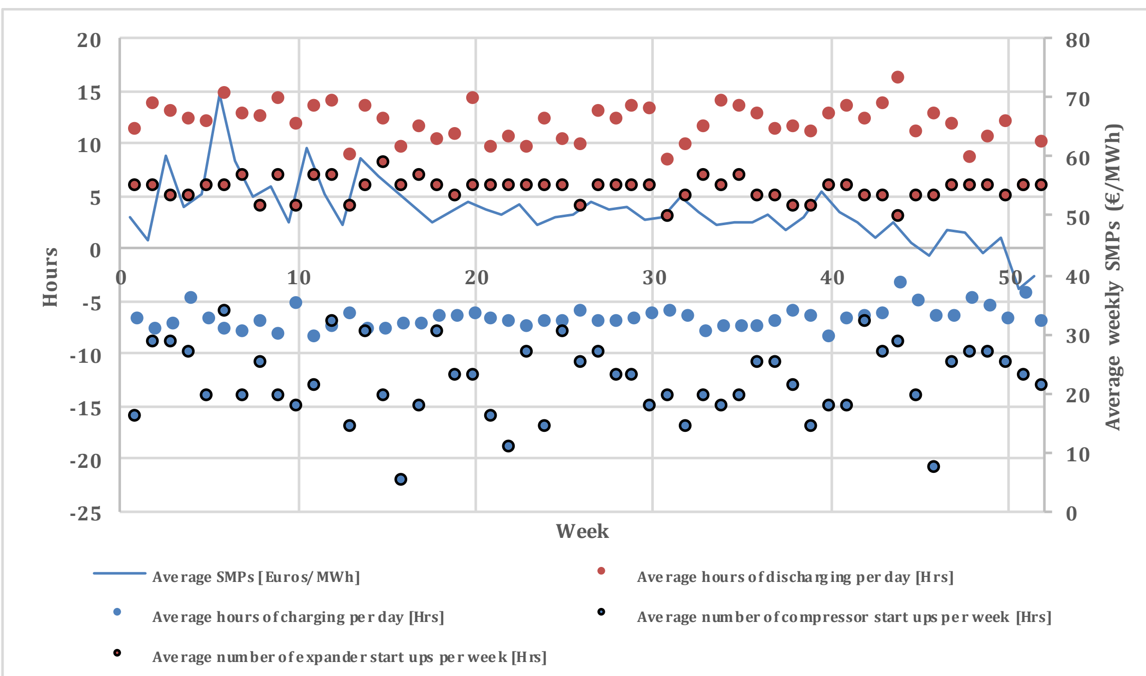

Figure 6-7: Average hours for charging/discharging per day, average number of start-ups per week and average SMPs per week (Model FP, scenario: Base).

Results for the FP model show that the compressor operates for most of the time at full capacity to charge the cavern fast; for a shorter percentage of time operates at its lowest operational point and there are some scattered moments where the compressor operates in between its maximum and minimum operational range (see figure 6-8).

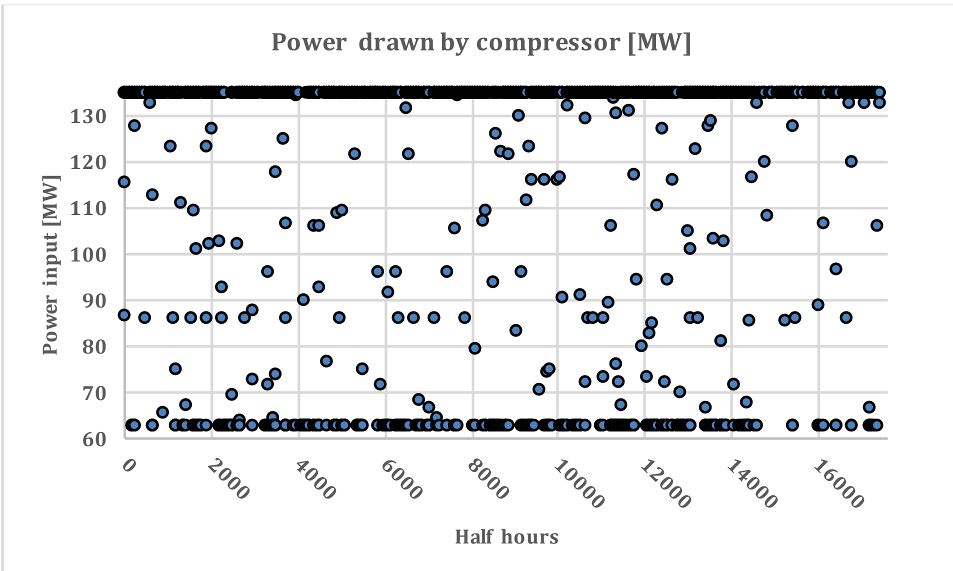

Figure 6-8: Power used for compression at each time increment (half hours) over a period of 52 weeks (Model: FP, Scenario: Base)

Similar is the case for the expander. The FP model operates the expander at the edges of its operational range for the great majority of time. There are also some scattered moments of operation within its operational range (figure 6-7). The model decides to discharge CAES at full capacity during very high SMPs to maximize revenues while when SMPs are not that high it discharges at low levels to make profit but at the same time be conservative to save energy or reduce the compression requirement of the next cycle (see figure 6-9).

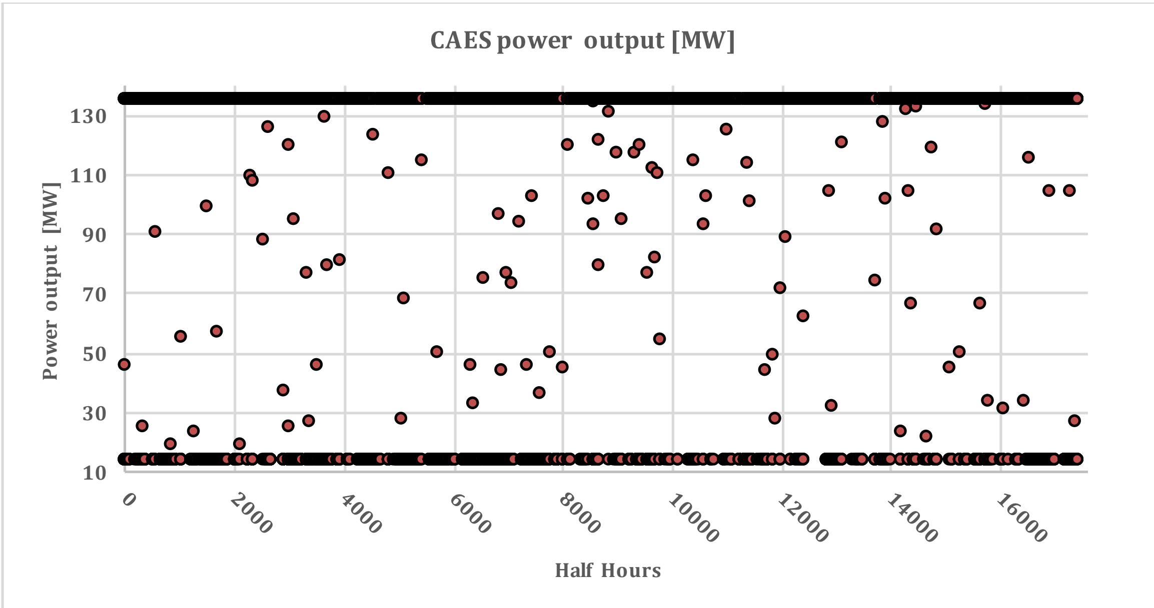

Figure 6-9: CAES power output at each time step (half hours) over a period of 52 weeks (Model: FP, Scenario: Base)

With regards to emissions we have calculated emissions from both the compression and expansion sides of the device. The emissions of compression are related to the power input and are calculated using the emissions factor of the Irish grid. The average emissions factor of the Irish grid is 0.732 tonnes of CO2 per MWh. The average emissions factor from CAES is around 0.785 tonnes of CO2 per MWh (see figure 6-11). It should be noted that emissions from the expansion side is only 0.23 tonnes of CO2 per MWh-e. The reason a CAES unit delivers 1MWh of energy at higher emissions rate than the grid emissions factor is because it burns natural gas in addition to any conversion losses from electrical energy to mechanical and then back to electrical again.

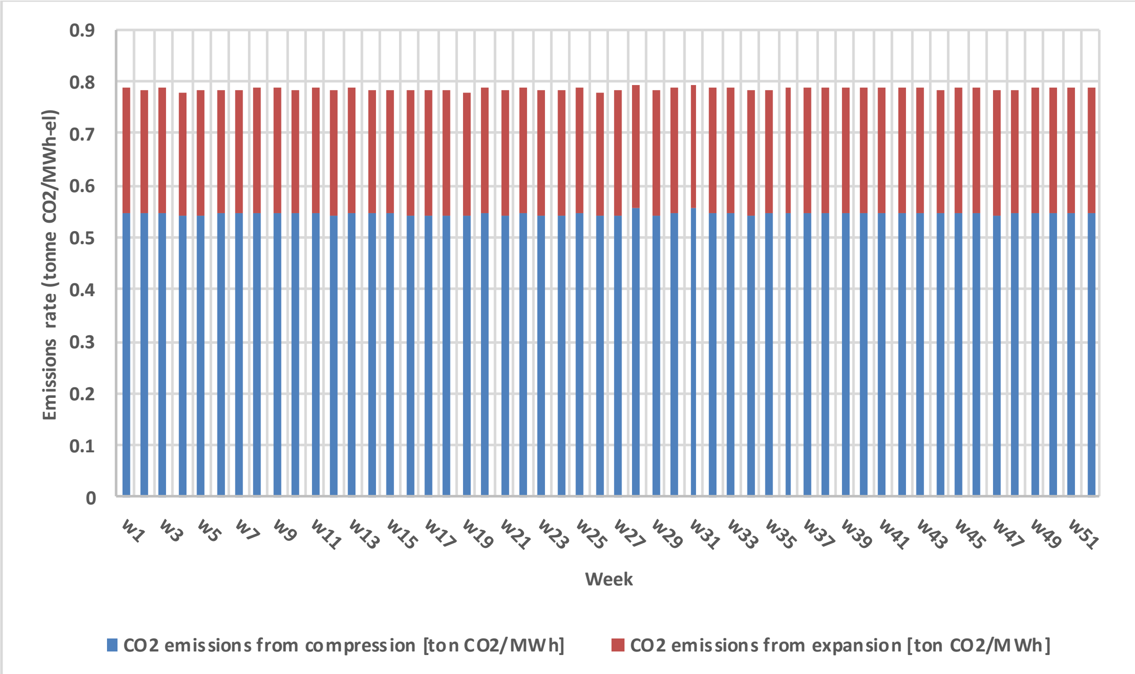

Figure 6-10: Emissions rate for the compression and expansion sides (Model:FP, Scenario:Base).

Total additional emissions from CAES device alone into the environment from producing a total of 370GWh over the period of 52 weeks would be a bit less than 100,000 tonnes

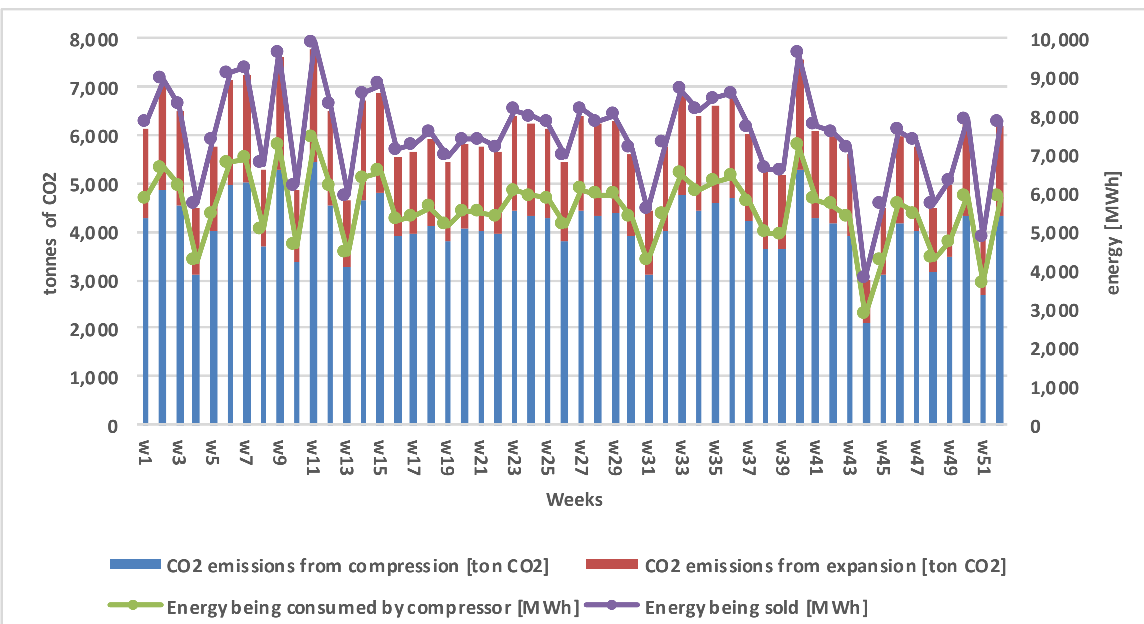

Figure 6-11: Emissions from compression and expansion (Model: FP, Scenario: Base).

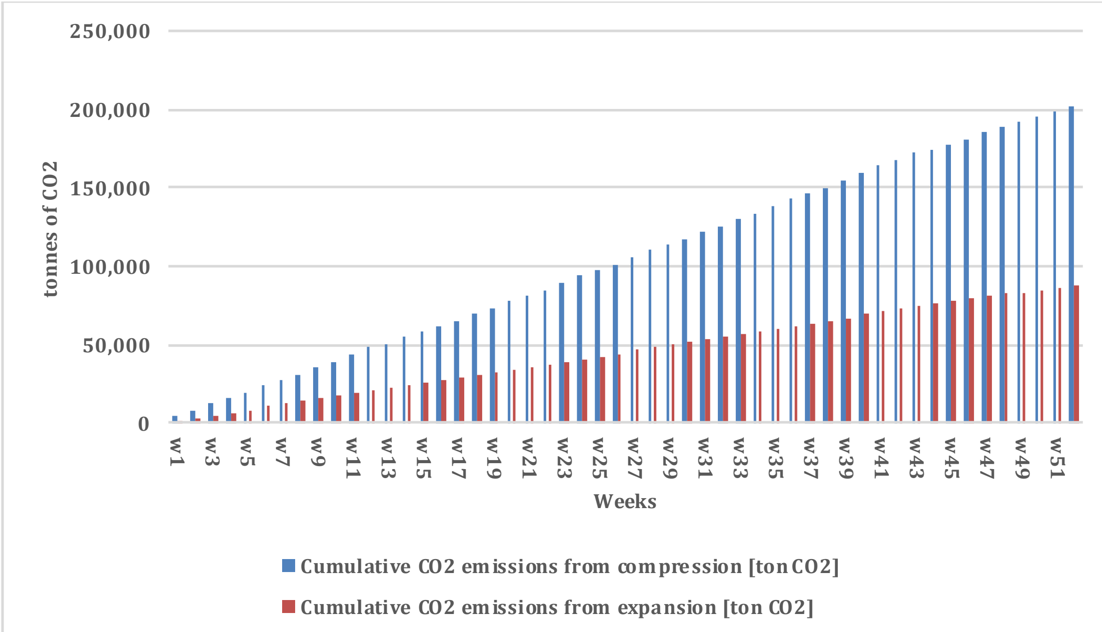

Figure 6-12: Cumulative emissions over the 52 week optimization period (Model: FP, Scenario: Base).

- Thermo-Economic model

The total operational profit for the TE model over 52 weeks is €8.2m, a 14.5% reduction compared to the FP model (€9.5m). Total operating revenues account for €23.9m, or ~12.4% less compared to FP model (€27.2m). Total operating costs over the 52 week period account for €15.7m or ~11% reduction compared to the FP model. Profit margin for the TE model is ~35% over the whole optimization period, same as in the FP model. If we express revenues and costs per unit of output we figure out the TE model returns average operating revenues of €77/MWh (compared to €73/MWh for the FP model) that is a 5% decrease compared to FP model. The cost of running the compressor (electricity + VOM) is similar to the FP model averaging at €28/MWh (ranging between 38% and 60% of total costs). The cost of natural gas is the same as in the FP model at €17/MWh. However, start-up costs per output unit are double than the FP model ranging between

€4/MWh and €6/MWh. As data in table 6-5 show there are 34% more expander and 45% more compressor start-ups in the TE model compared to the FP model. We will return on the start-ups issue later on this section.

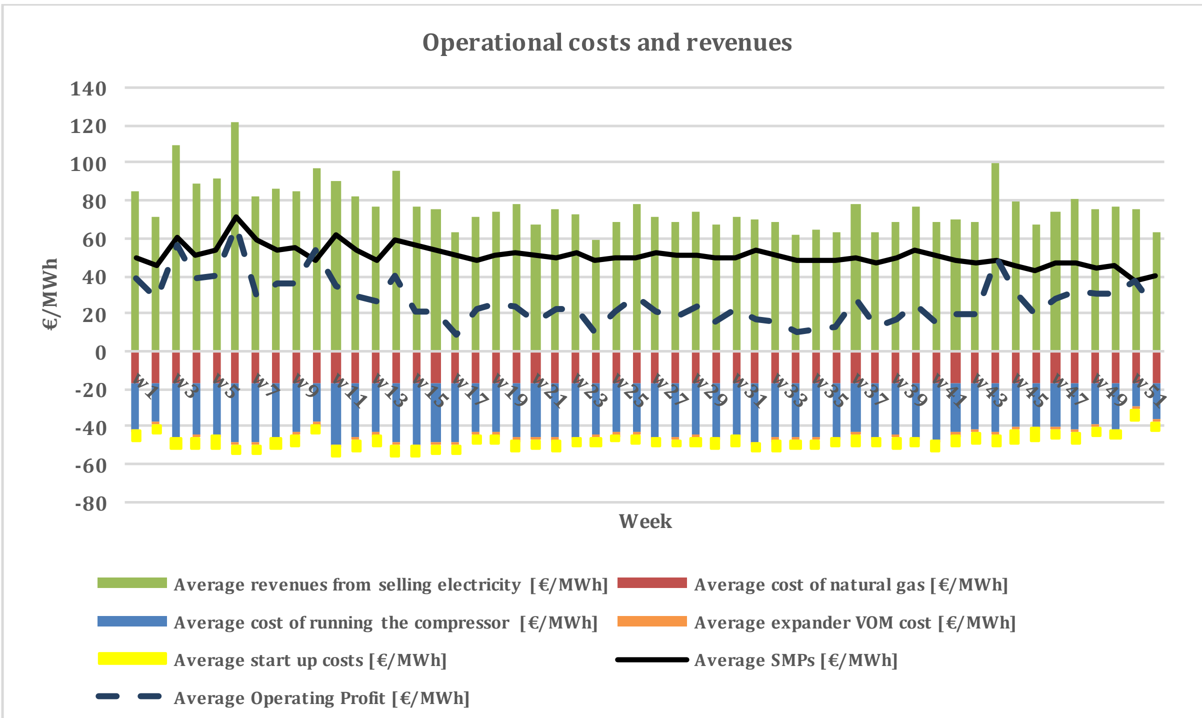

Figure 6-13: Operating profit, main operating costs and revenues expressed as (€/MWh) on a weekly basis (Model: TE, Scenario: Base).

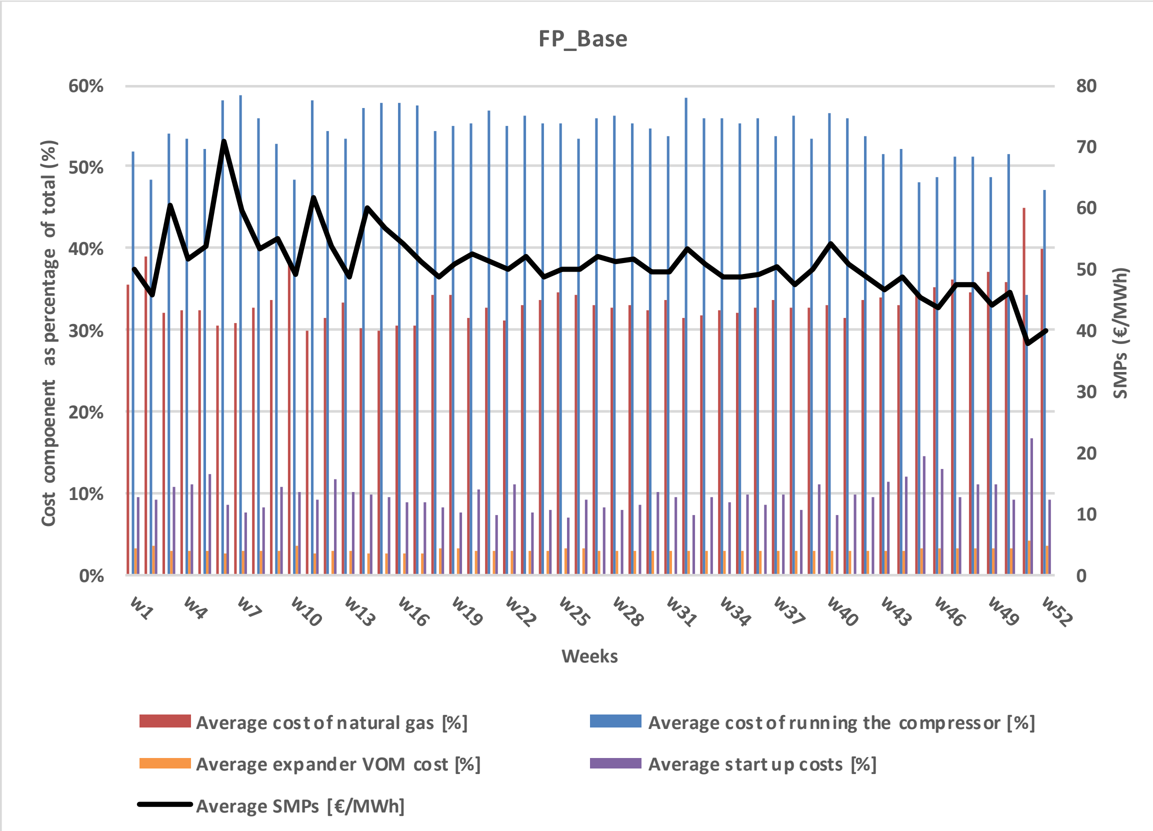

Figure 6-14: Break-down of operating costs as percentage of total operating cost (€/MWh) on a weekly basis (Model: TE, Scenario: Base).

Both models have very comparable compressor and expander costs expressed per unit of output. However, the TE model discharges on average for 8 hours per day to make revenues while the FP model for 12 hours. This is a 33% less hours for the TE model. The same figures for the compression side is 6 and 7 hours for the compression side respectively. There are obviously some differences on the technical and economic performance of the two models and those can be explained by zooming into the differences on the technical performance of the two models.

Figure 6-15 shows the TE model results for the same week as figure 6-6. In figure 6-15 we observe CAES operation relative to SMPs. The storage level in the TE model is represented through the cavern pressure rather than energy. Additionally, we can observe the air mass flow that corresponds to each moment when either compressing or expanding. Observing the data carefully we see that the expander output doesn't only respond to SMPs but also to the cavern pressure. If the cavern pressure drops below the design level of 864 PSI the maximum output is reduced according to figure 3-10. The same is true for the compression side; we observe that compressor operation (speed of charging and power input) depends on both SMP's and cavern pressure.

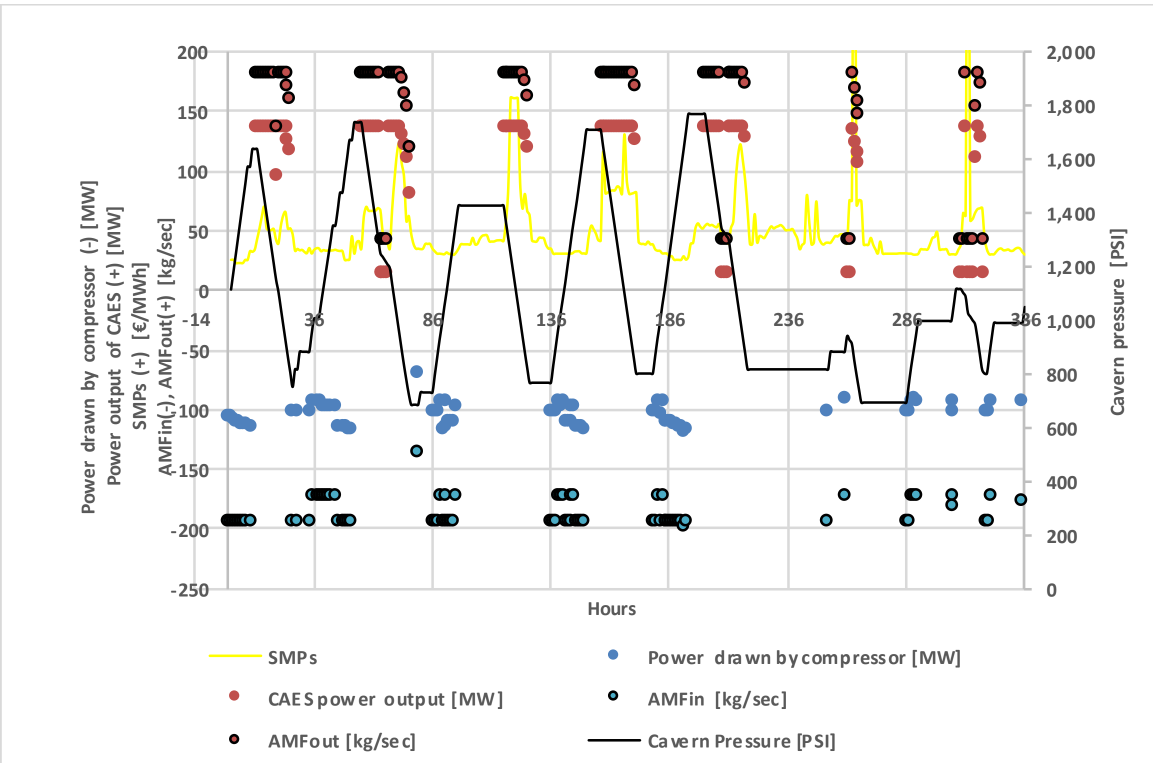

Figure 6-15: One week of CAES simulation (Model: TE, Scenario: Base).

Based on those observations I will explain below why the TE model discharges less time than the FP model:

1. **The TE model has less freedom to optimize its compression economics compared to the FP model.** This because in the TE model the compressor responds to 1) SMPs and 2) to the cavern pressure unlike the FP model which responds only to SMPs. The FP model has the ability to reduce the energy requirement at any level within the compressor operational range (62MW-134MW). However the TE model will operate the compressor according to graph 3-11. The compressor won't discharge air at a pressure above the cavern's back pressure levels. It can increase the air mass flow at its maximum levels but there will be a cap on maximum energy that can be stored at each moment. Higher amounts of energy can be stored when there is high pressure being built up. Similarly there is always a low cap of energy storage at each moment. Even though, there is always some flexibility for the CAES operator to control the compressor power requirement through regulating the air mass flow the operational range depends on the back pressure. For example, if the back pressure is 1600PSI then the possible operational range is from 370 lb/sec to 475 lb/sec (or 112MW to 134MW). The operator cannot decrease the compressor's energy requirement (and subsequently the amount of energy stored[67] within a specific time step) below that level. My point can be shown more clearly through figure 6-16. All three depictions on the graph correspond to the same time period. The top figure shows the compressor's performance for a 12 hour time period (24 half hour time steps) as well as the cavern pressure based on the TE model. The middle figure shows again the compressor's performance versus the SMPs over the same period, again based

[67] The amount of energy stored is equal the compressor energy requirement times the compressor's efficiency which in the TE model can be anything from 81% to 85%.

on the TE model. The bottom figure shows the compressor's performance based on the FP model. As we see based on the top 2 depictions the compressor adjusts its output based on both the SMPs and the cavern pressure. When the compressor begins during time step 184 the pressure in the cavern is very low (~500PSI). At that moment, there is no possibility to compress at high energy levels based in figure 3-11 since the compressor needs to discharge to at least 600PSI and there is little flexibility to adjust the air mass flow at this pressure level. Additionally. SMPs are relatively high at this time and it is not optimum to run the compressor at high levels anyway according to the results of the FP model. As time progresses and SMPs reduce the TE model increases the compressor's power requirement following the cavern pressure. During time period 188 when the SMPs are at the lowest point the FP model charges the compressor at the highest possible level (134MW) to take advantage of low SMPs not being able to "feel" the effect of pressure. However, in the TE model the compressor can't take full advantage of low SMPs and it will only compress using 102MW of power. During time period 192 the cavern reaches pressure of ~1700PSI at the TE model. Even though there is an upwards spike on SMPs the compressor's operator can't do much to reduce the compression energy requirement according to graph 3-11. However, the FP model will adjust its output to reduce the cost of compression. The TE model has reduced flexibility to optimize its economic performance compared to the FP model. However, such a restriction is more realistic in comparison to the FP model that gives a more optimistic output. Because of the fact that the compressor responds to cavern pressure all the time operates uniformly across its whole operational range (see figures 6-19 and 6-20).

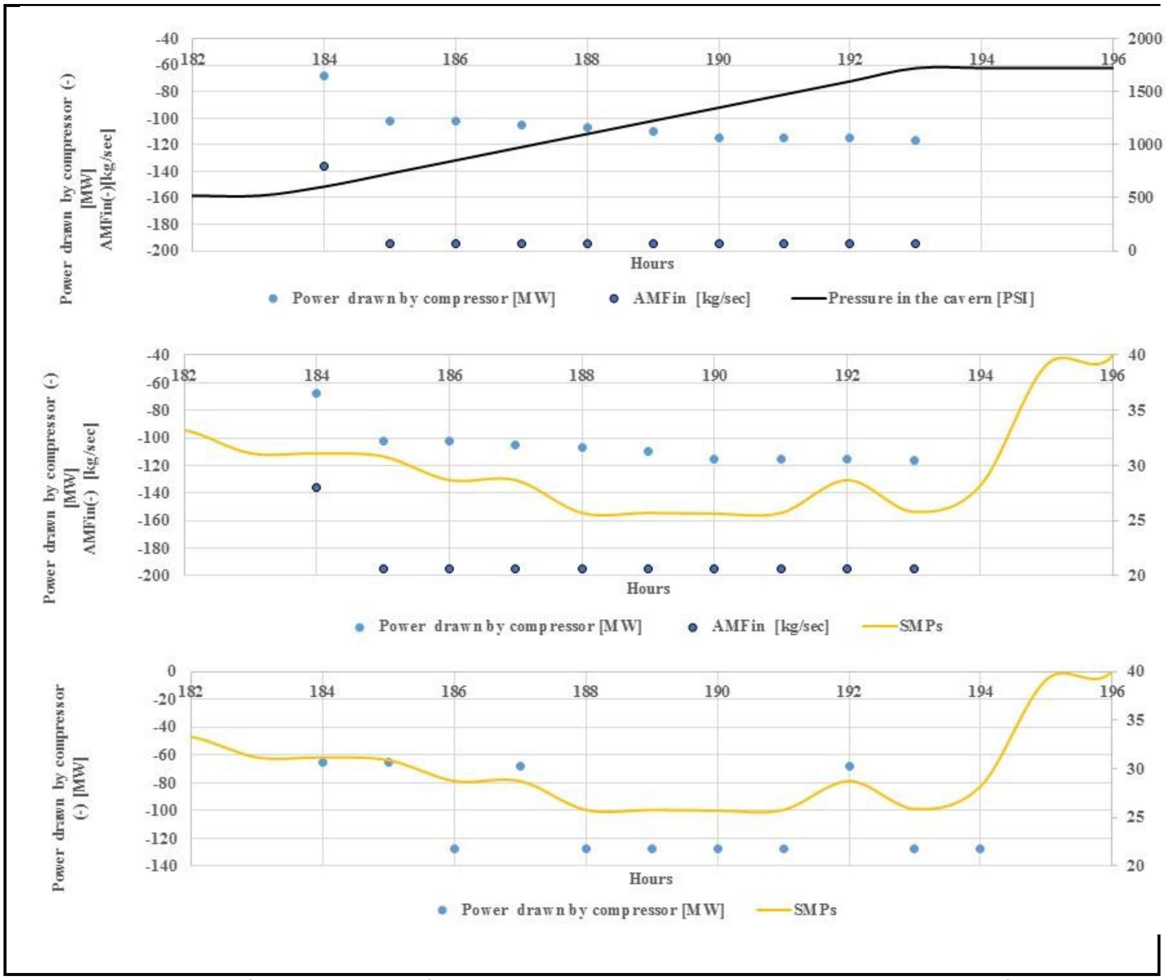

Figure 6-16: 15 hours of CAES operation focusing on the compression part. Upper part: Power input for compression, air mass flow in the cavern and cavern pressure for the TE model. Middle part: power input for compression, air mass flow entering the cavern and SMPs for TE model. Lower part: power input for compression, air mass flow entering the cavern and SMPs for FP model. All depictions are related to the same time period of 24 half hourly time steps (12 hours).

2. **In the TE model the maximum CAES output is restricted based on cavern pressure levels.** Figure 6-17 zooms into another 10 hour long section of the same week as figure 6-16 with higher SMPs. The top part shows CAES performance vs cavern pressure based on the TE model results. The middle part shows CAES performance versus SMPs again for the TE model. The lower part is the result of

the FP model for the same period. The cavern is nearly fully charged at the beginning of the period shown in figure 6-17. During the first high SMP period (time steps 58-64) the CAES unit discharges at full output to make revenues. During lower SMPs (time steps 65-68), CAES air mass flow is being reduced to conserve energy for the second upcoming high SMP period (time steps 69-75). However, after the cavern pressure has dropped below the design pressure [864PSI] level the maximum output is being constrained according to figure 3-10. The effect of pressure is not being captured by the FP model as we see on the lower part of figure 6-17. The cycling pattern of the expander can be seen in figures 6-21 and 6-22.

The discussion above has made clear that there are specific restrictions that cause the TE model to both charge and discharge -on average- less energy during each storage cycle compared to the FP model. The same restrictions cause the TE model have a lower profitability. The effect of pressure is higher as we will show later on the "low discharge time" scenario.

Unlike the FP model, the discharge time on the expansion side seem not to vary considerable among weeks in the TE model (see figure 6-18). Same is true for compression time. However the average number of compressor start-ups per week vary because of our assumption for zero compressor start-up costs.

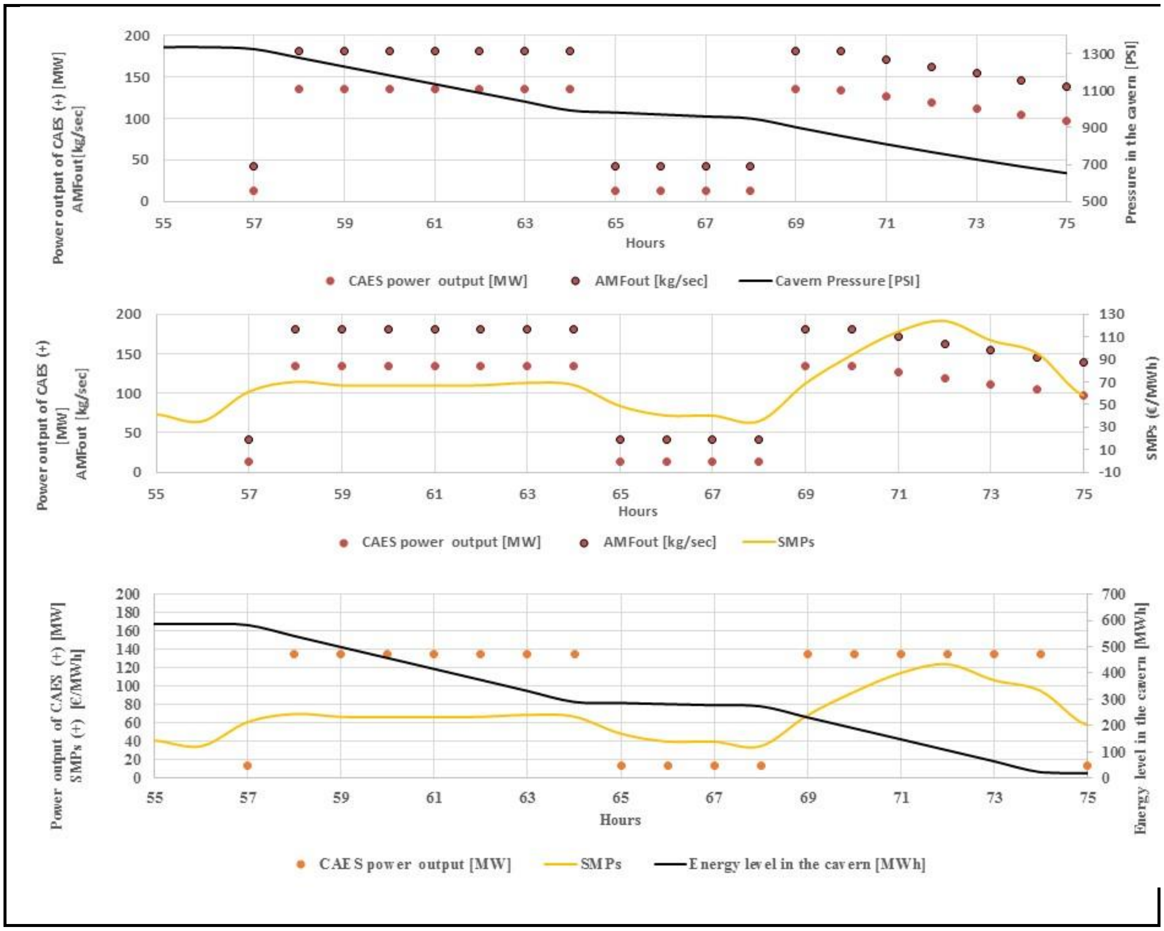

Figure 6-17: 15 hours of CAES operation focusing on the expansion part. Upper part - Power output during expansion, air mass flow exiting the cavern and cavern pressure (TE model). Middle part: power output during expansion, air mass flow exiting the cavern and SMPs (TE model). Lower part:

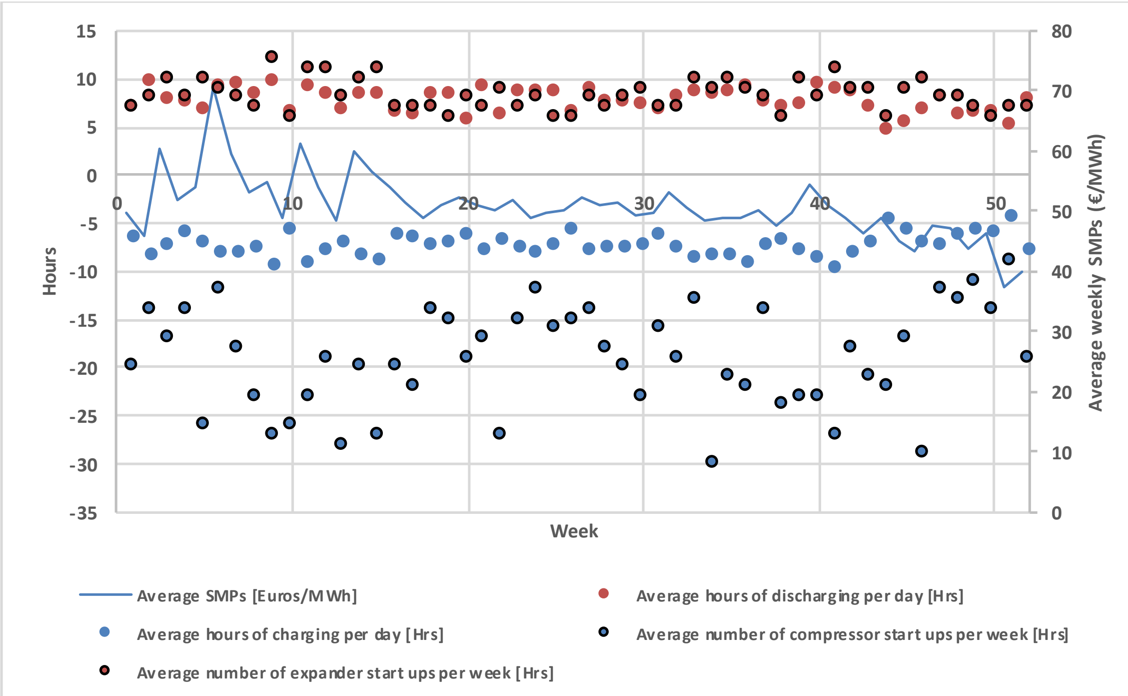

Figure 6-18: Average hours for charging/discharging per day, average number of start-ups per week and average SMPs per week (Model TE, Scenario:Base).

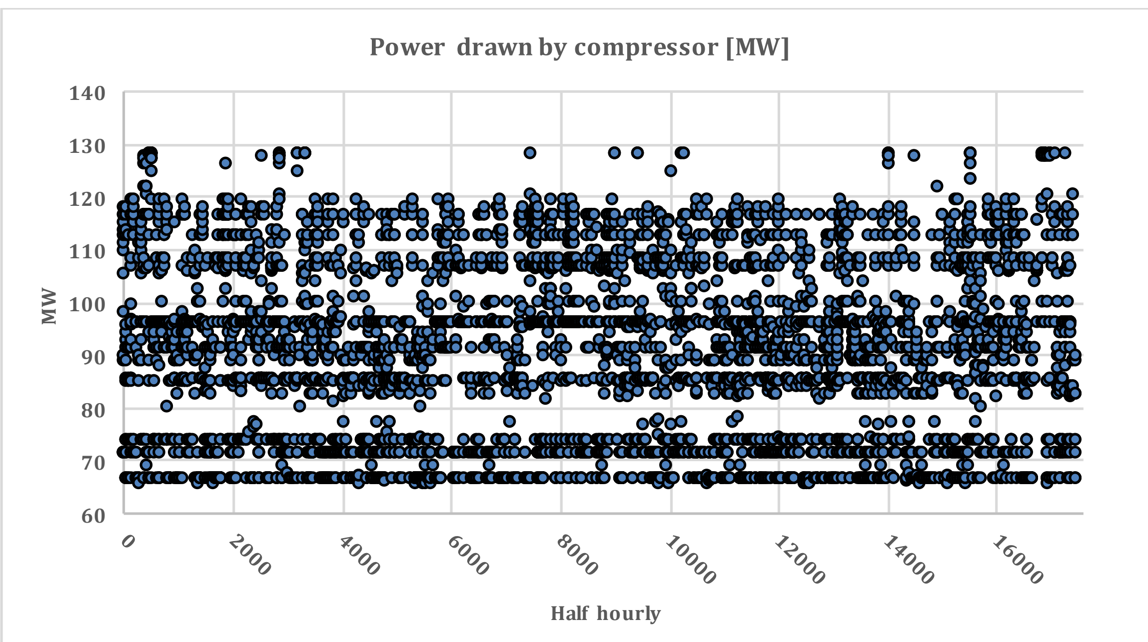

Figure 6-19: Power used for compression at each time increment (half hours) over a period of 52 weeks (Model:TE, Scenario:Base).

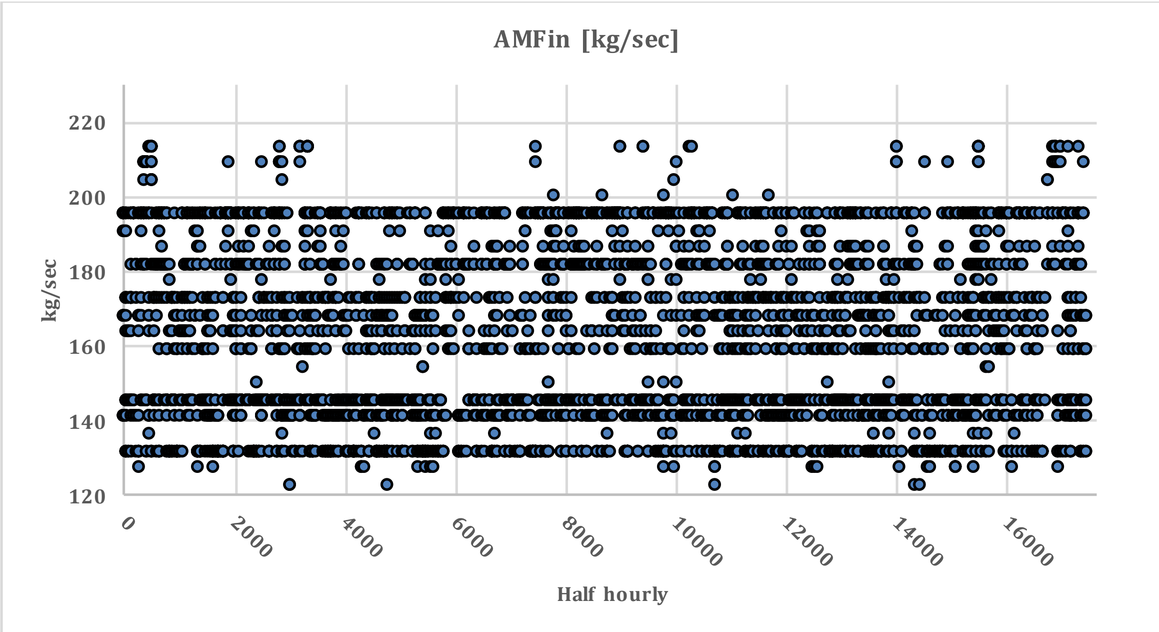

Figure 6-20: Air mass flow for compression during each time increment (half hours) over a period of 52 weeks (Model: TE, Scenario: Base).

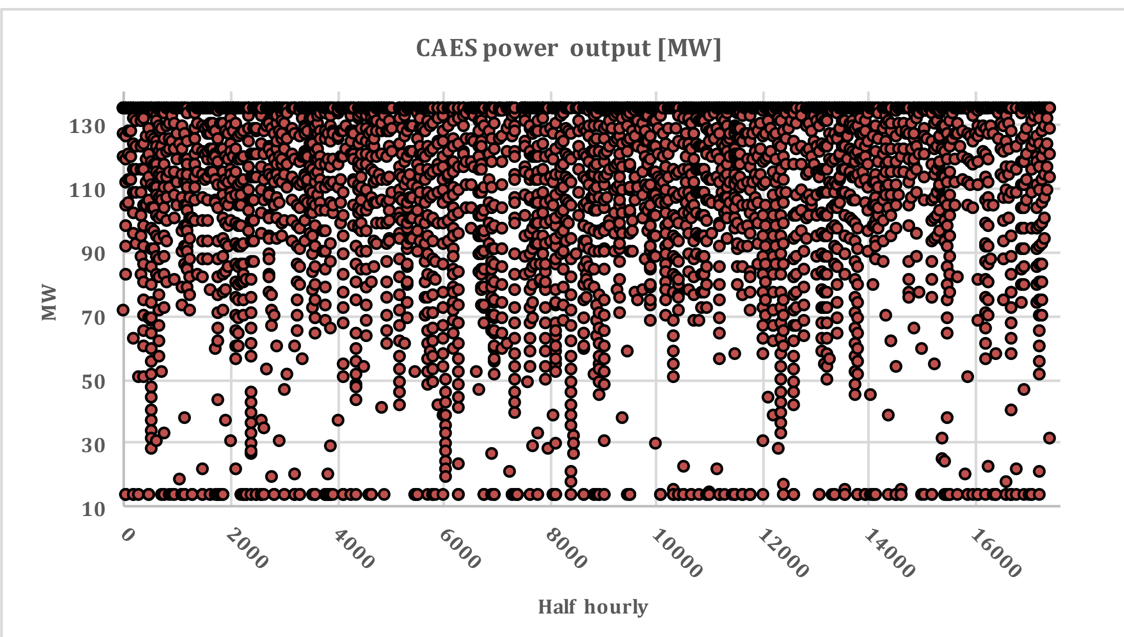

Figure 6-21: CAES power output at each time step (half hours) over a period of 52 weeks (Model: TE, Scenario: Base).

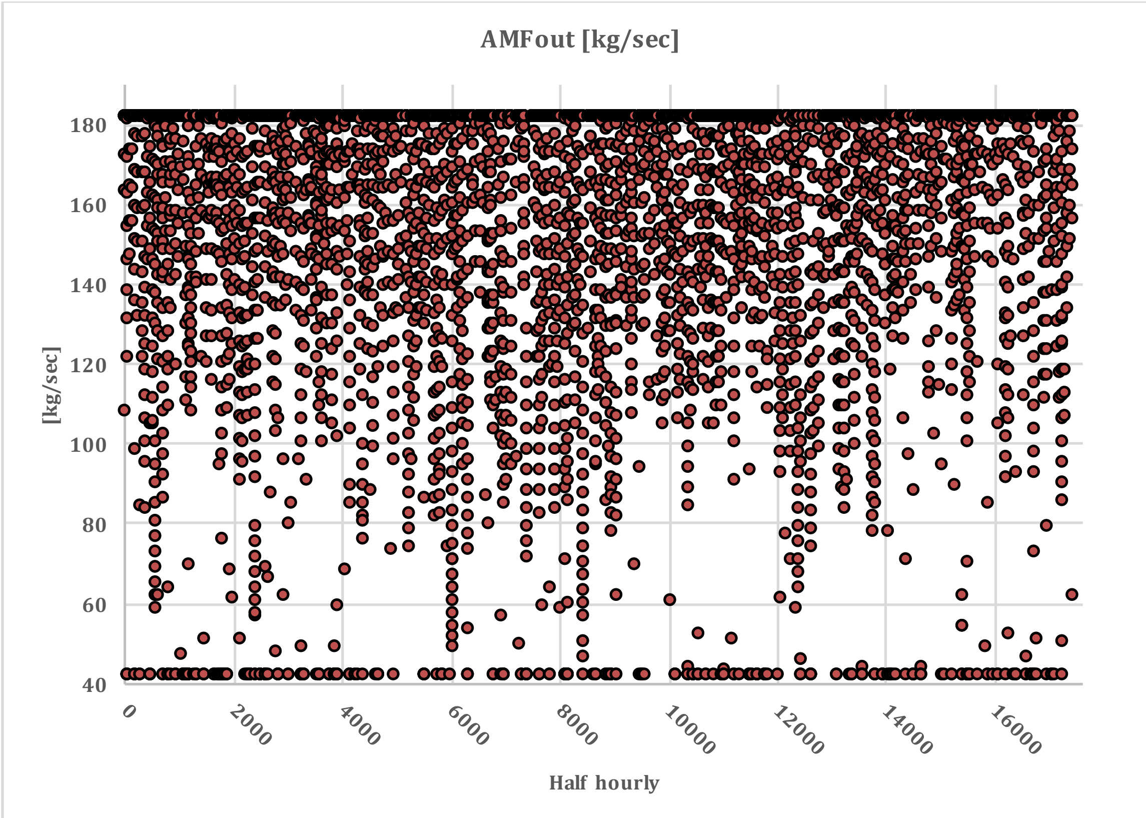

Figure 6-22: Air mass flow for expansion during each time increment (half hours) over a period of 52 weeks (Model: TE, Scenario: Base).

With regards to emissions the TE model exerts very similar behavior as the FP model. The emissions per unit of energy produced are very similar. In absolute numbers the TE model produces less emissions because it stores and discharges less energy. The cumulative emissions for the 52 week period for the FP model is shown in figure 6-25. Emissions patterns per unit of energy produced do not change across all scenarios. For that reason we won't repeat any graphics on the emissions part from now and on.

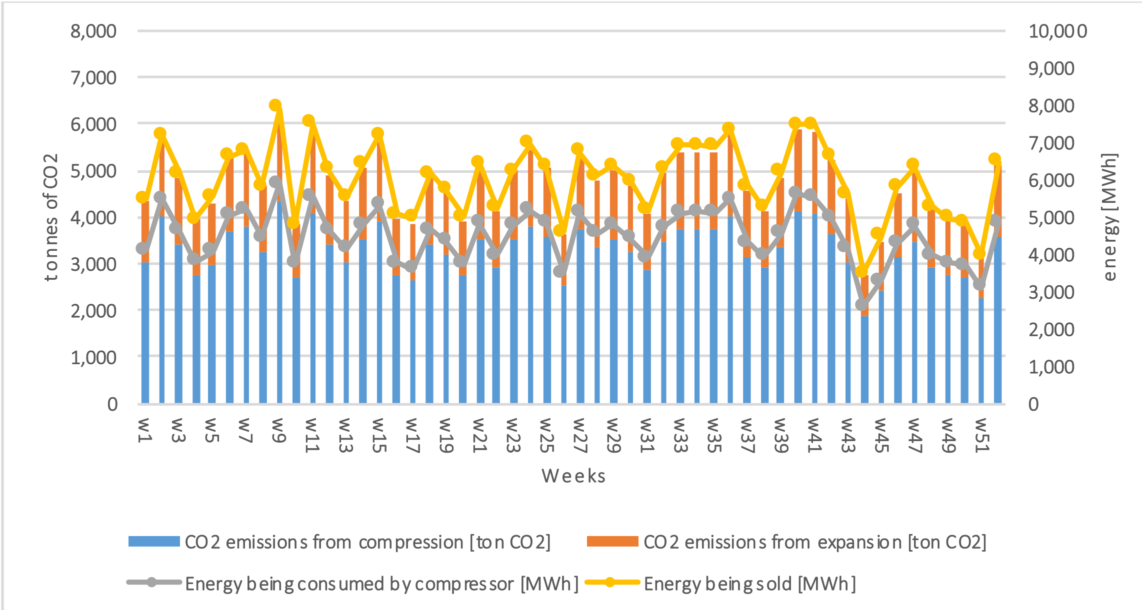

Figure 6-23: Emissions rate for the compression and expansion sides (Model: TE, Scenario: Base).

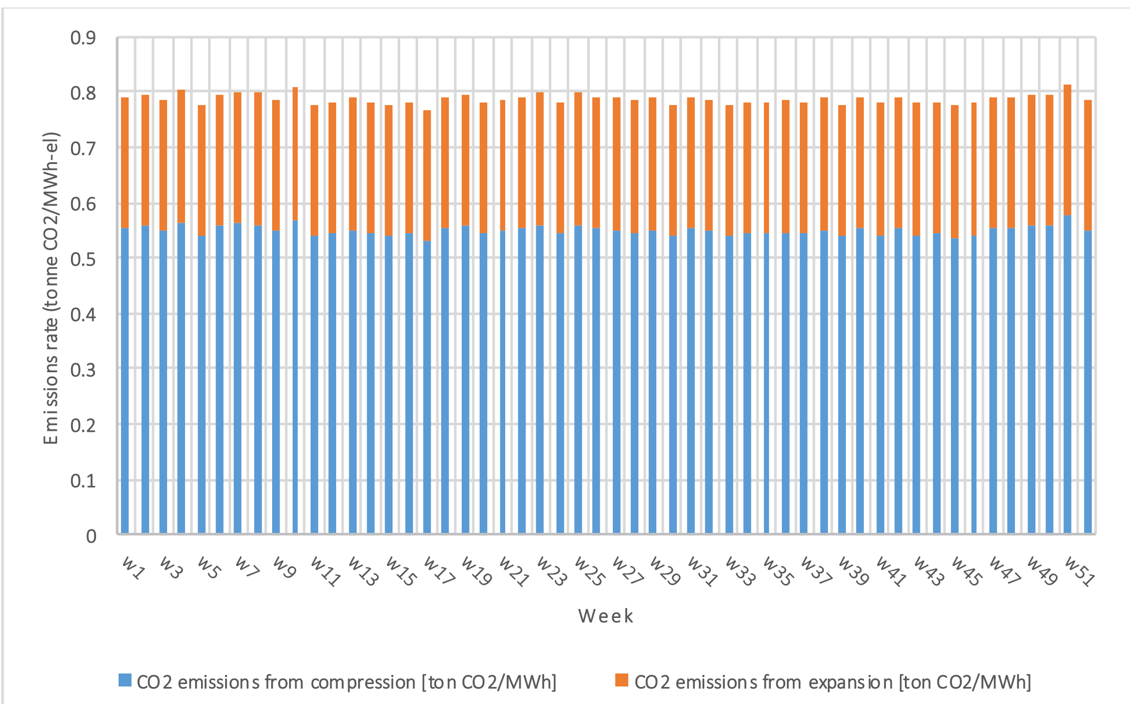

Figure 6-24: Emissions from compression and expansion (Model: TE, Scenario: Base).

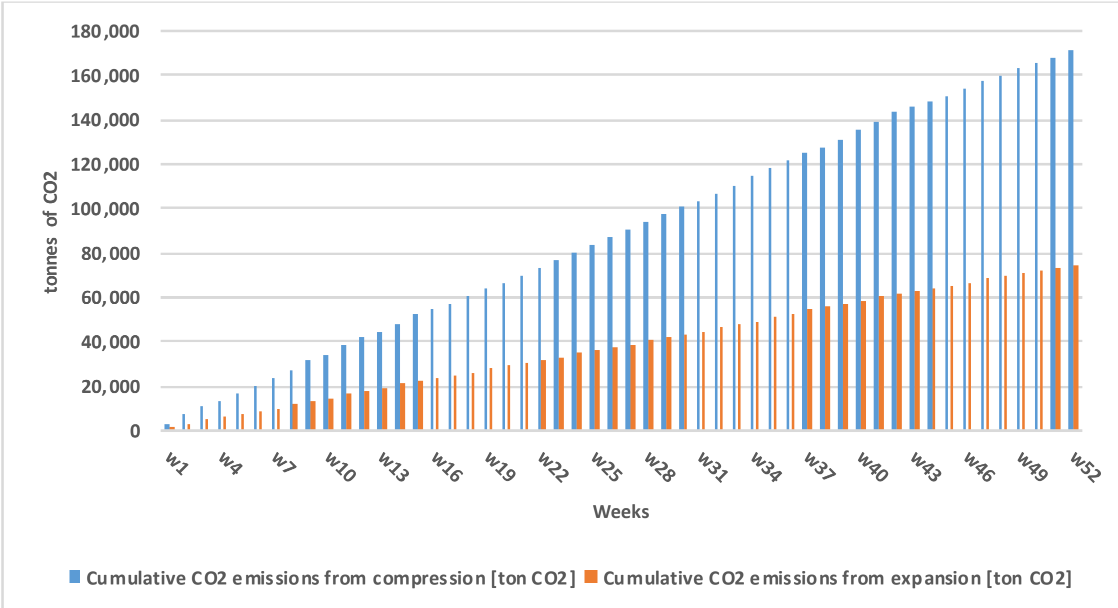

Figure 6-25: Cumulative emissions over the 52 week optimization period (Model: TE, Scenario: Base).

6.3.2.2 Results-Low discharge time scenario

- FP model

The total operational profit for the FP model over 52 weeks is €9.2m (table 6-2). Total operating costs over the 52 week period account for €16.8m while total operating revenues for €26m. The absolute reduction compared to the Base scenario for profits, revenues and costs are -€0.4m, - €1.2m and -€0.9m respectively. The reductions are related to the reduced storage space. Total mechanical energy being stored is reduced by 6% over the 52 week period compared to the Base scenario. The same reduction occurs for the energy being sold. If we observe the cost figures per unit of energy being sold we see there is no difference compared to the Base scenario (see figures 6-26 and 6-27).

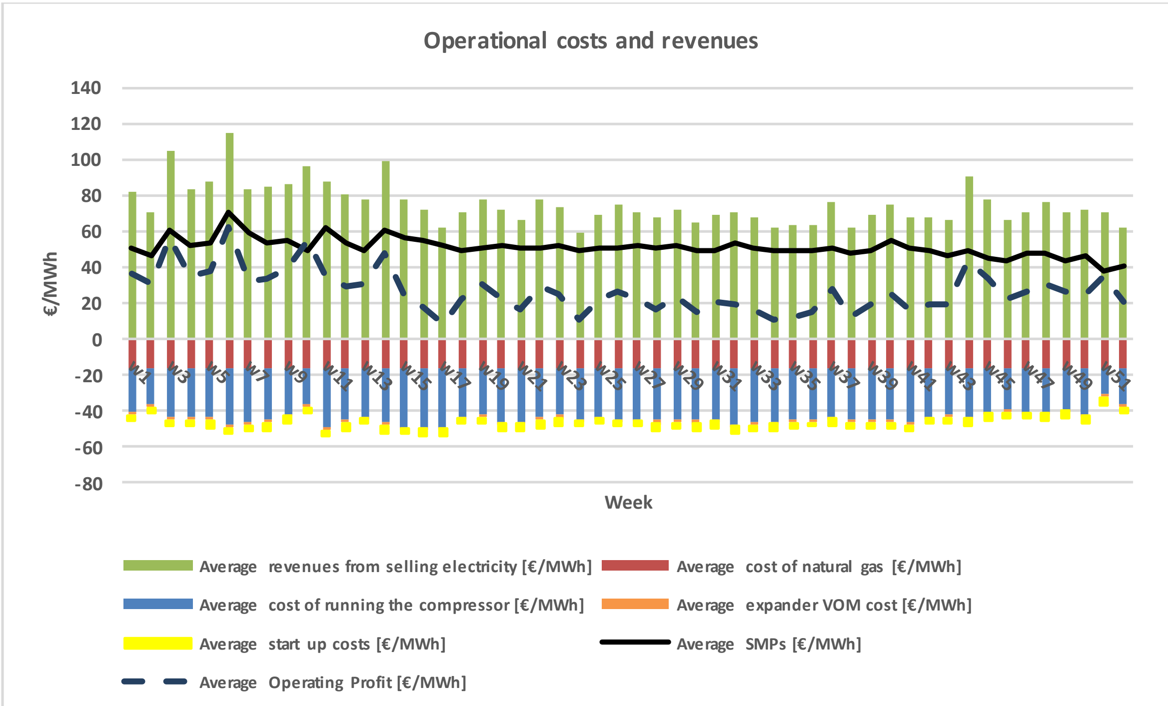

Figure 6-26: Operating profit, main operating costs and revenues expressed as €/MWh-e on a weekly basis (Model: FP, Scenario: Low Discharge time).

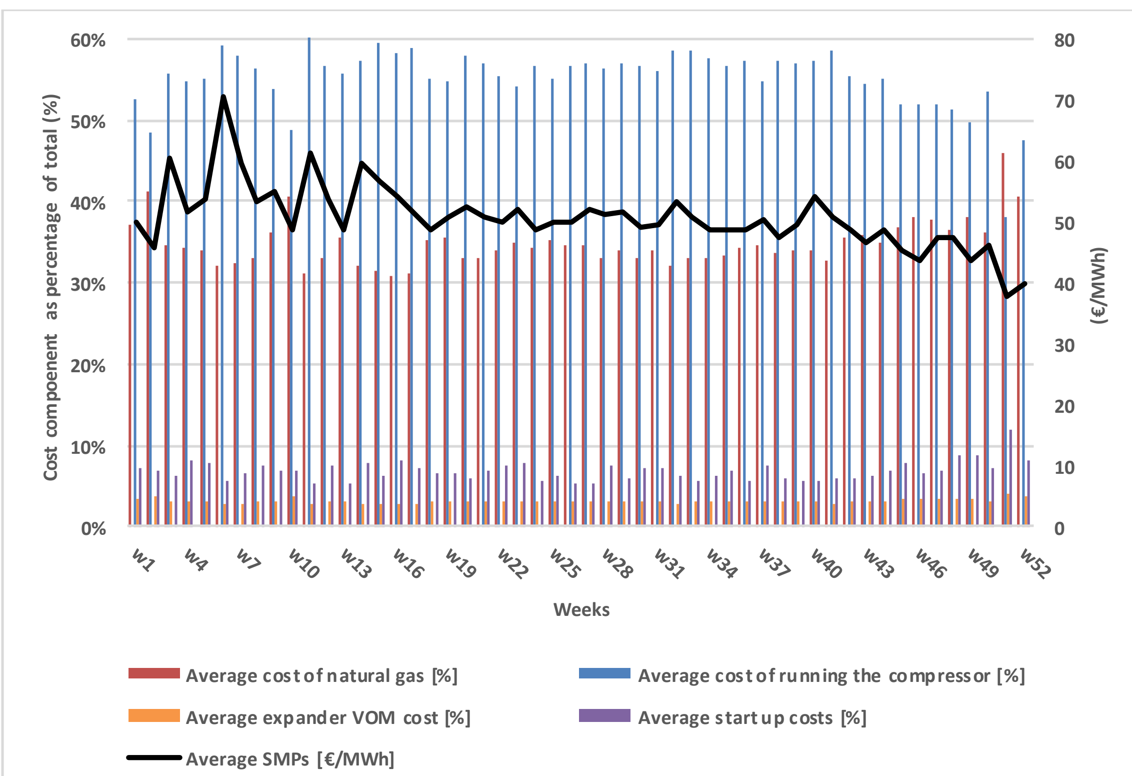

Figure 6-27: Break-down of operating costs expressed in (€/MWh-e) as percentage of total operating cost on a weekly basis (Model: FP, Scenario: Low discharge time).

As graphs 6-28 and 6-29 show, there is no difference on operational pattern between the expander and the compressor compared to the Base scenario.

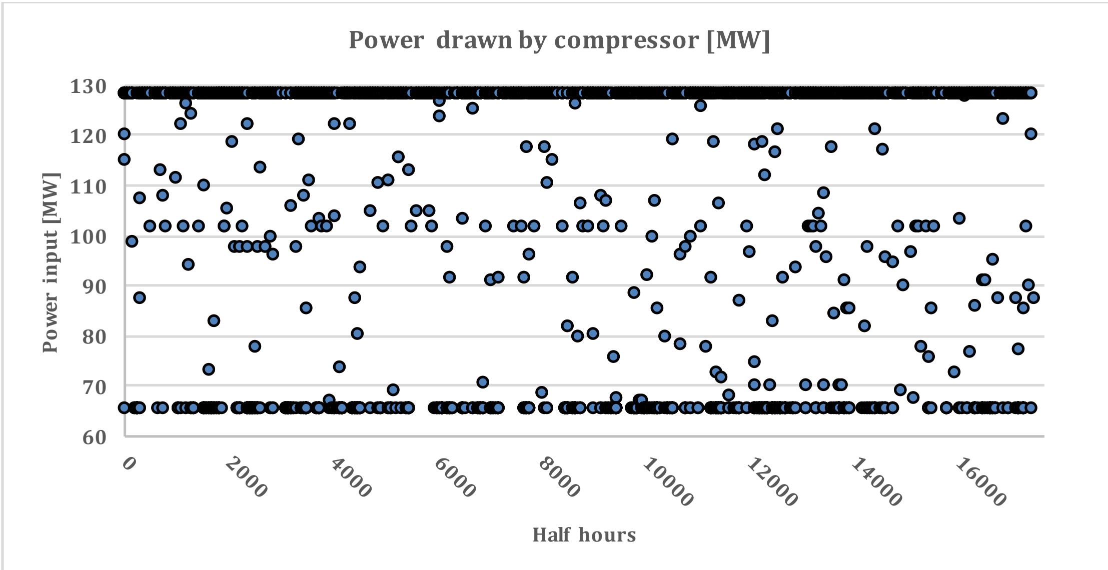

Figure 6-28: Power used for compression at each time increment (half hours) over a period of 52 weeks (Model: FP, Scenario: Low discharge time).

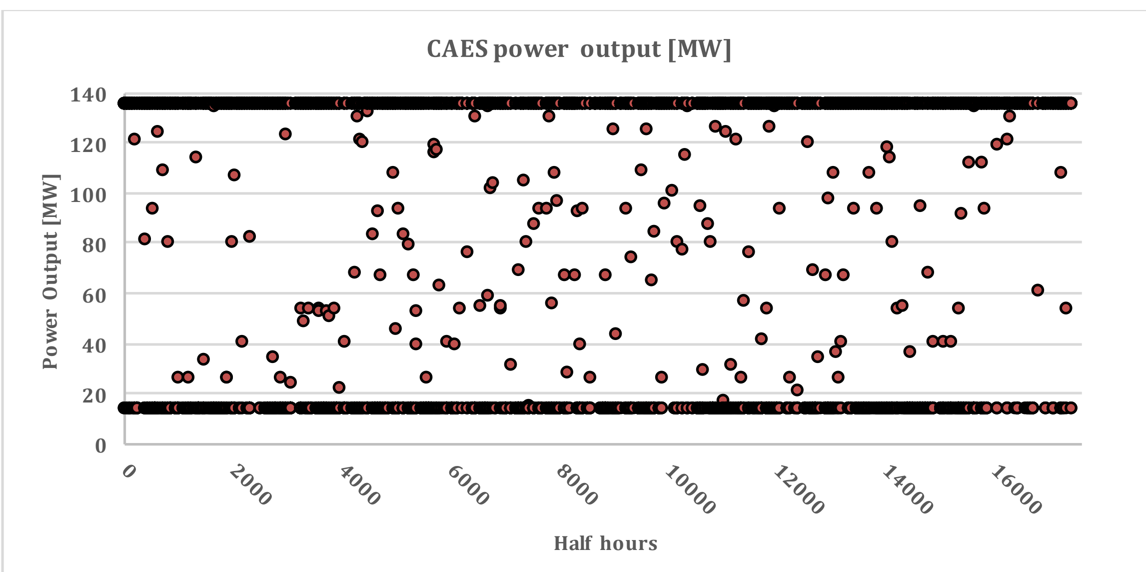

Figure 6- 6-29: CAES power output at each time step (half hours) over a period of 52 weeks (Model: FP, Scenario: Low discharge time).

- Thermo-Economic model

The total operational profit for the TE model over 52 weeks is €6.4m. Total operating revenues are equal to €18.1m and operating costs are equal to €11.7m. The reduction for operating profit, revenues and costs compared to the Base scenario is 22%, 24% and 25% respectively. The TE model exerts 30% less profit, 30% less revenues and 30% less costs compared to the FP scenario. It is obvious that the impact of lowering the discharge time (or cavern volume) is more dramatic in the TE scenario compared to the FP scenario. The results of two models diverge if the cavern volume becomes smaller. However, the revenue and cost figures per unit of energy produced are very similar to the Base scenario.

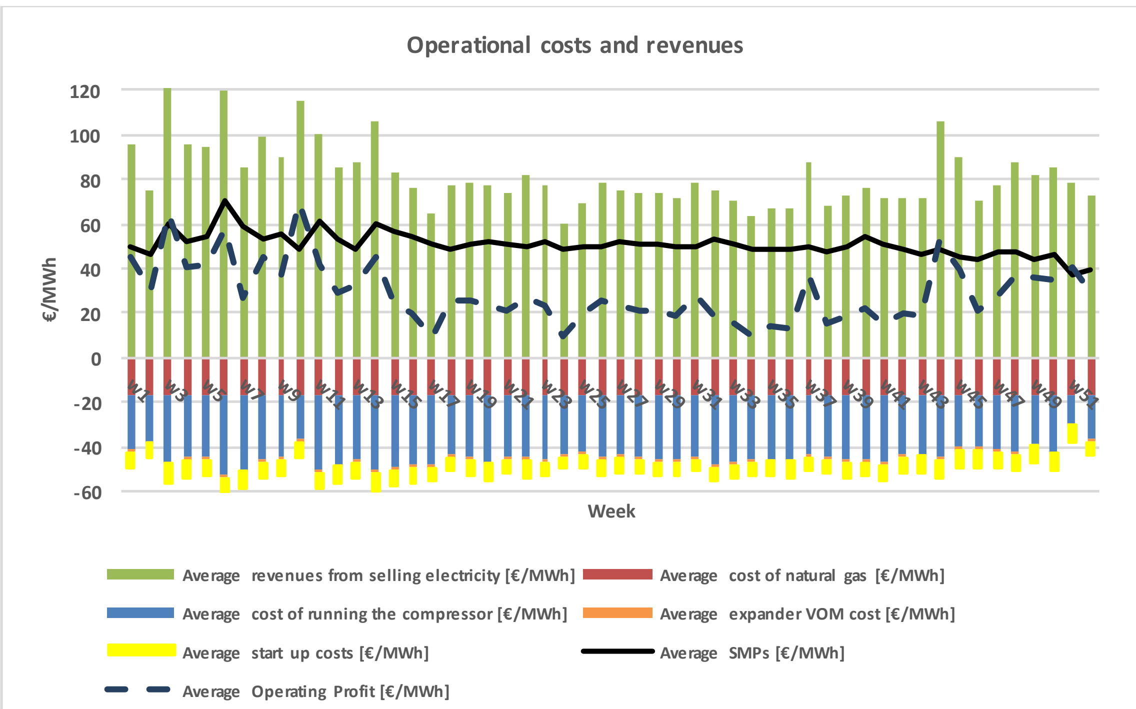

Figure 6-30: Operating profit, main operating costs and revenues expressed as (€/MWh) on a weekly basis (Model: TE, Scenario: Low discharge time).

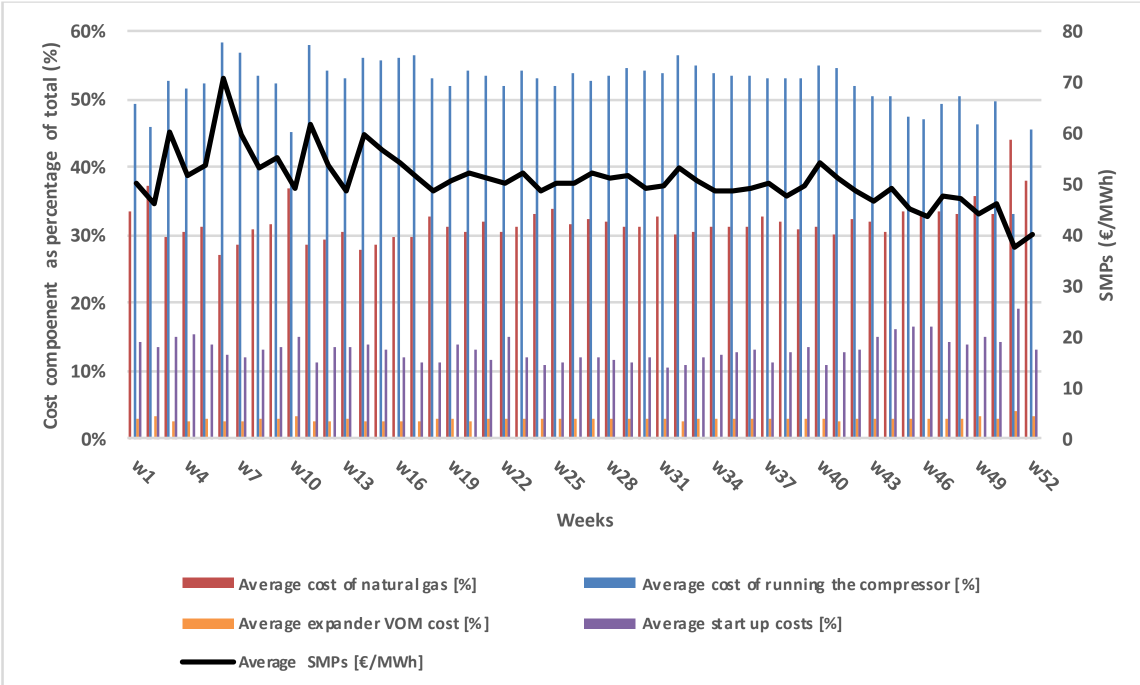

Figure 6-31: Break-down of operating costs as percentage of total operating cost (€/MWh) on a weekly basis (Model: TE, Scenario: Low discharge time).

The dramatic decline on revenues and costs for the TE model at lower cavern volumes is based on the technical restrictions of the compression and expansion parts imposed by the pressure in the cavern. We described in detail such effects in section 6.3.2.1. Cavern pressure effects are mode dramatic when the cavern volume is decreased because pressure increases and drops are more rapid.

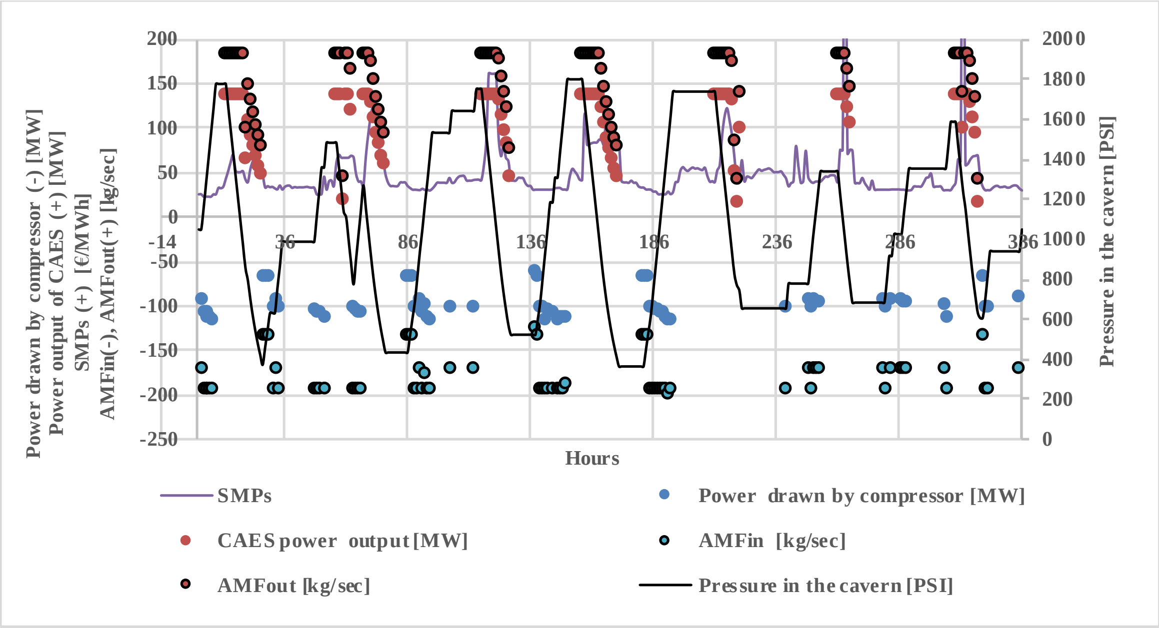

Figure 6-32: One week of CAES simulation (Model: TE, Scenario: Low discharge time).

The impact of low cavern volume on the compressor can be seen in figure 6-33 and 6-34. We see that the compressor is responding to pressure up and downs operating within its whole operational range.

Focusing on the expansion side (figures 6-35 and 6-36) we observe that the expander operates towards more partial outputs compared to Base scenario. Again, this is due to pressure dropping frequently below the design point of 864 PSI resulting to constrained output and low revenues compared to the Base scenario.

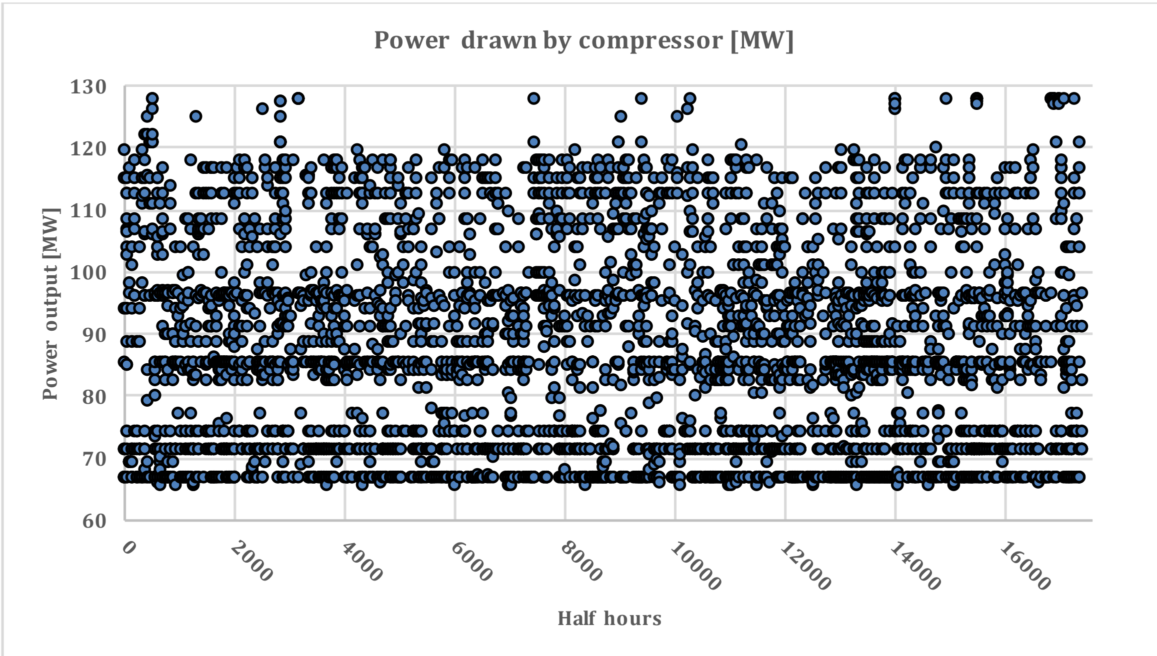

Figure 6-33: Power used for compression at each time increment (half hours) over a period of 52 weeks (Model: TE, Scenario: Low discharge time).

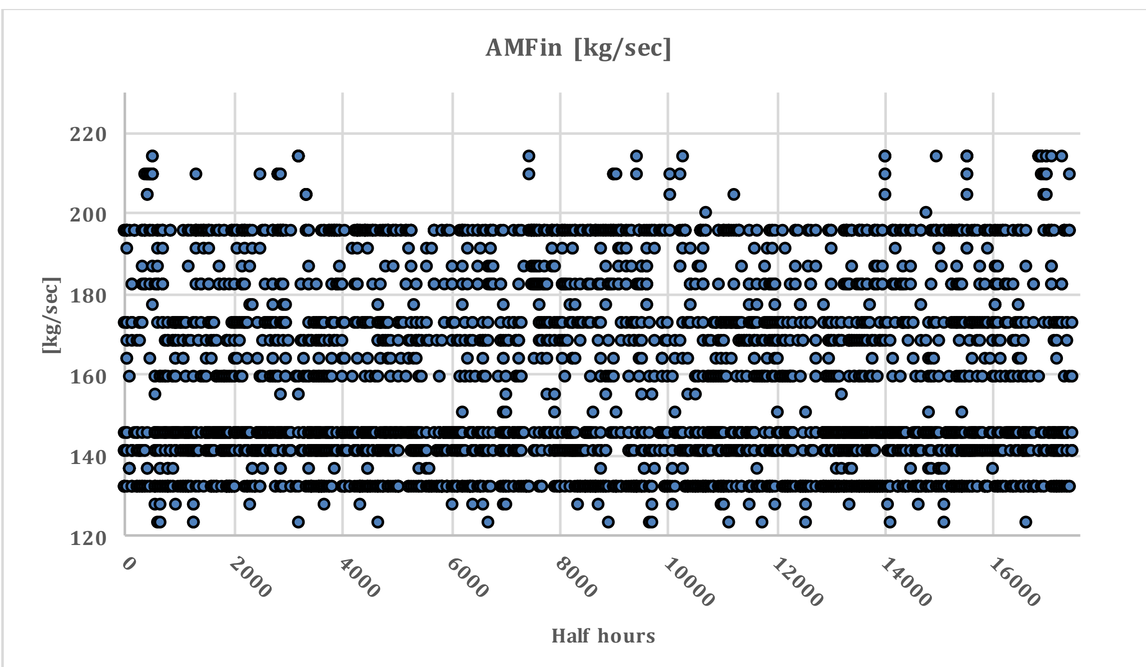

Figure 6-34: Air mass flow for compression during each time increment (half hours) over a period of 52 weeks (Model: TE, Scenario: Low discharge time).

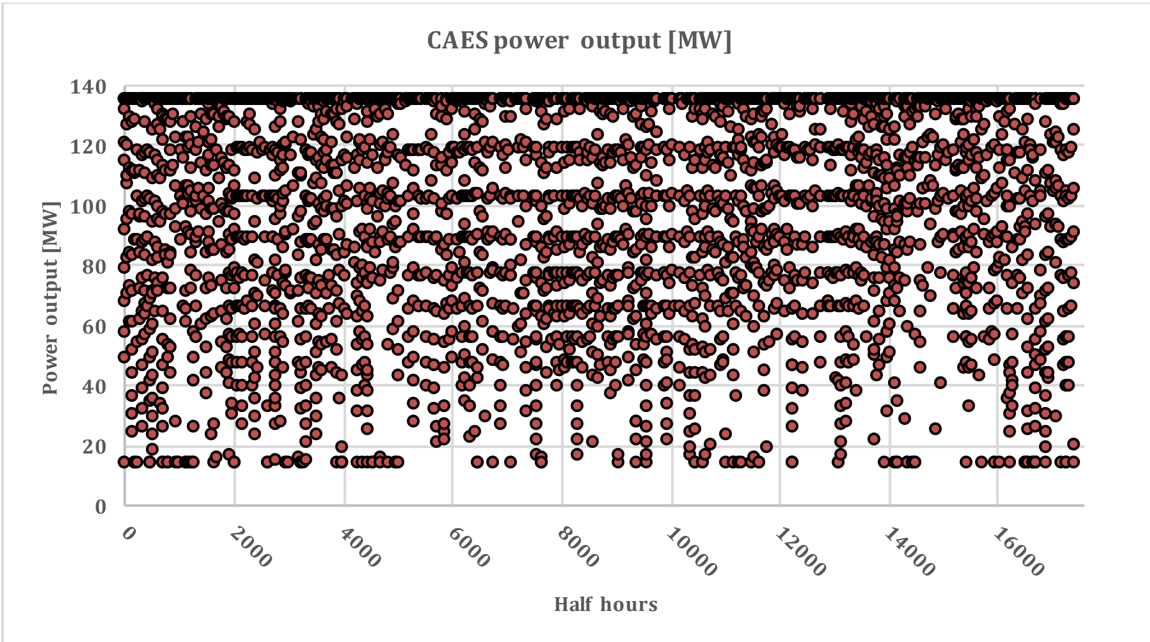

Figure 6-35: CAES power output at each time step (half hours) over a period of 52 weeks (Model: TE, Scenario: Low discharge time).

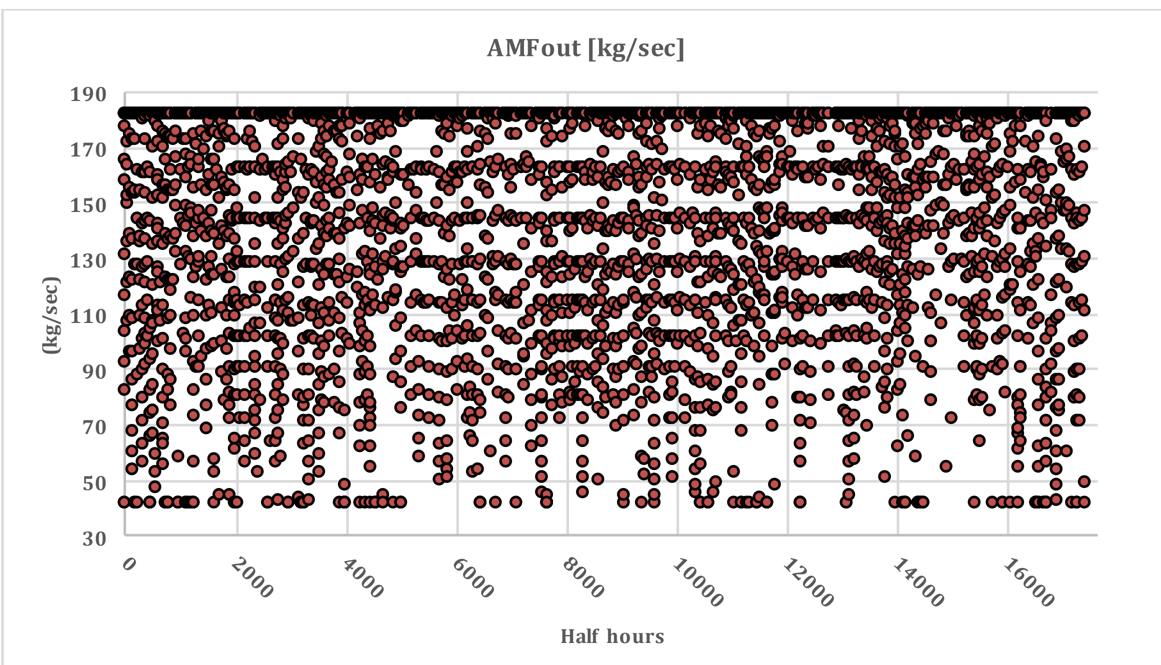

Figure 6-36: Air mass flow for expansion during each time increment (half hours) over a period of 52 weeks (Model: TE, Scenario: Low discharge time).

6.3.2.3 Results-High discharge time scenario

- FP model

If we increase the discharge time, total operational profit for the FP model over 52 weeks becomes €10.2m (table 6-3). Total operating costs over the 52 week period account for €19m while total operating revenues for €29.2m. The absolute increase compared to the Base scenario for profits, revenues and costs is €0.6m, €2m and €1.3m respectively. The same increase expressed as percentages is 6%, 78%, and 7.5% respectively. The increases are related to increased storage space. Total mechanical energy being stored is increased by ~9% over the 52 week period compared to the Base scenario. The same increase occurs for the energy being sold. If we observe the cost figures per unit being sold we see there are no significant differences compared to the Base scenario (figure 6-39 and 6-40).

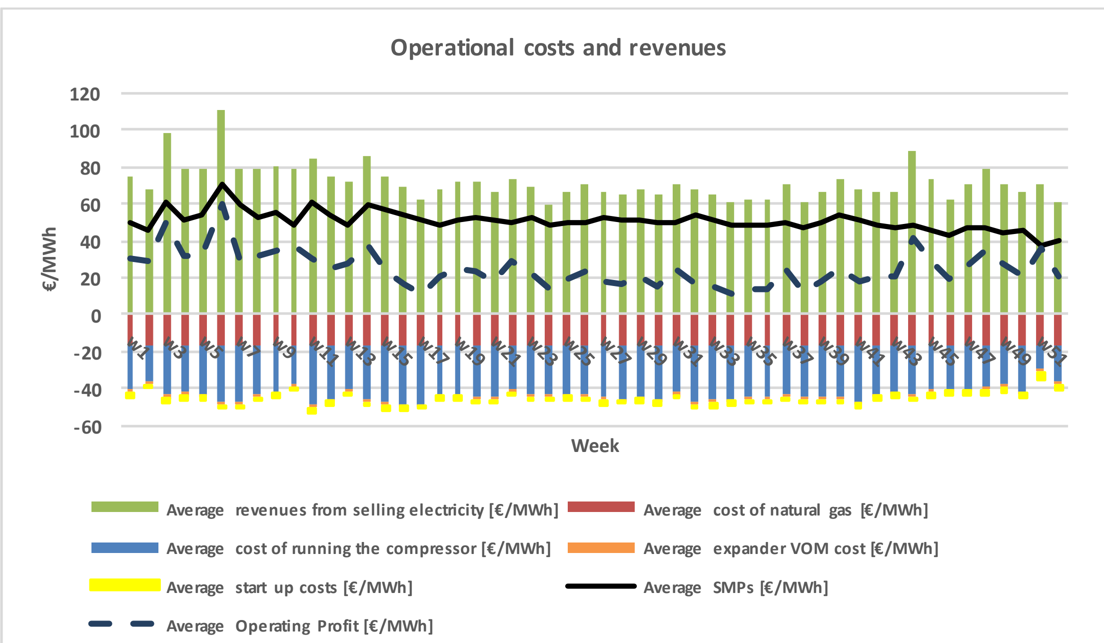

Figure 6-37: Operating profit, main operating costs and revenues expressed as €/MWh-e on a weekly basis (Model: FP, Scenario: High Discharge time).

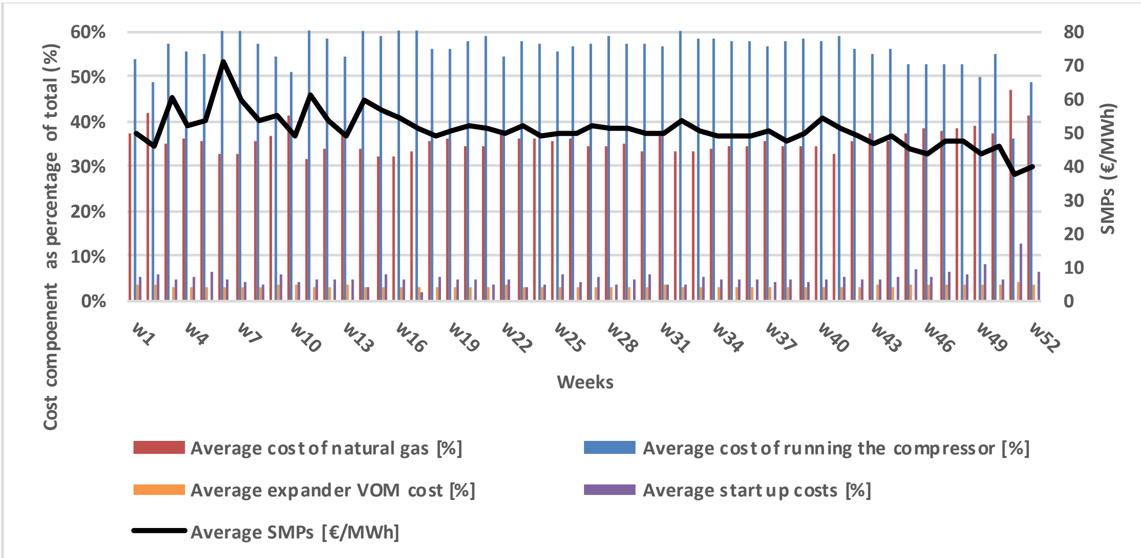

Figure 6-38: Break-down of operating costs expressed in (€/MWh-e) as percentage of total operating cost on a weekly basis (Model: FP, Scenario: High discharge time).

As graphs 6-41 and 6-41 show, by increasing the storage space the compressor and expander operate for the great majority of time at their rated capacity points to maximize opportunity for profit.

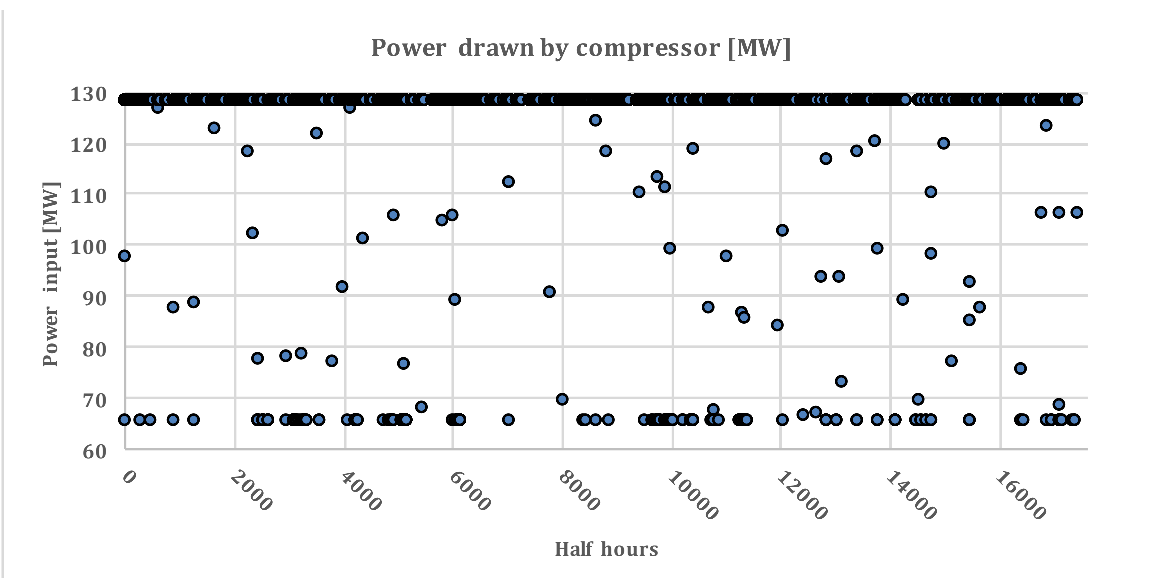

Figure 6-39: Power used for compression at each time increment (half hours) over a period of 52 weeks (Model: FP, Scenario: High discharge time).

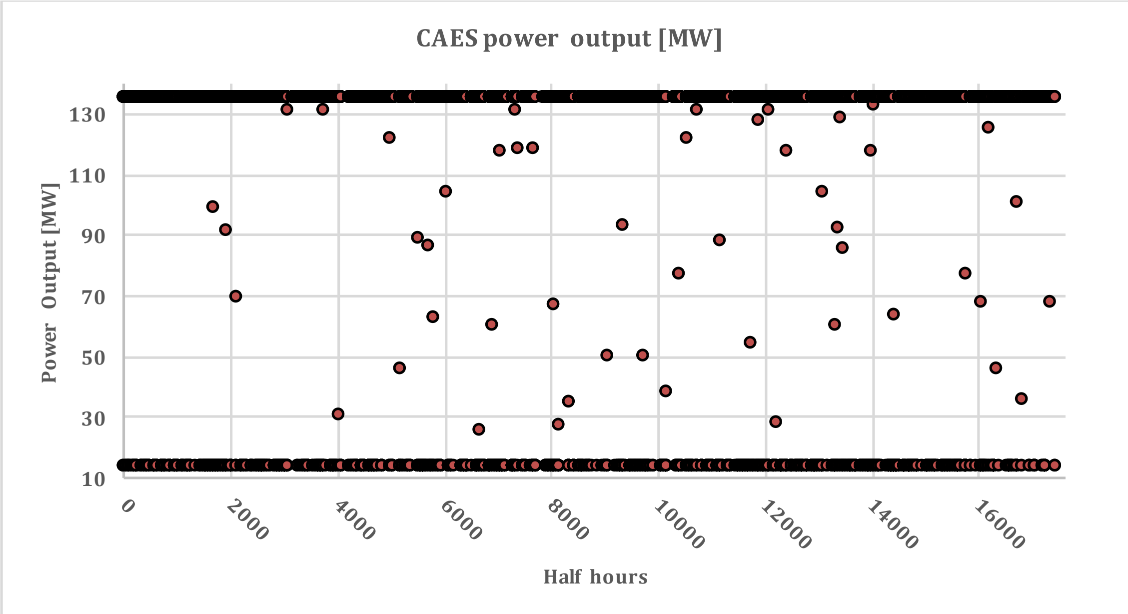

Figure 6-40: CAES power output at each time step (half hours) over a period of 52 weeks (Model: FP, Scenario: High discharge time).

- Thermo-Economic model

The total operational profit for the TE model over 52 weeks is €8.8m. Total operating revenues are equal to €26m and operating costs are equal to €17.2m. The increase for operating profit, revenues and costs compared to the Base scenario is 8.4%, 9% and 9.4% respectively. The TE model exerts 13% less profit, 11% less revenues and 10% less costs compared to the FP scenario. It is now obvious that if the discharge time (or the cavern volume) is increased the results of the two models converge. The impact of increasing the discharge time (or cavern volume) in the TE model is more positive than the FP as the % increase on profit is 8.4% compared to 6.4% for the FP model. This is because the effect of cavern pressure is greatly reduced. Again, the cost figures per unit of energy produced and as a percentage of total cost are very similar to the Base scenario.

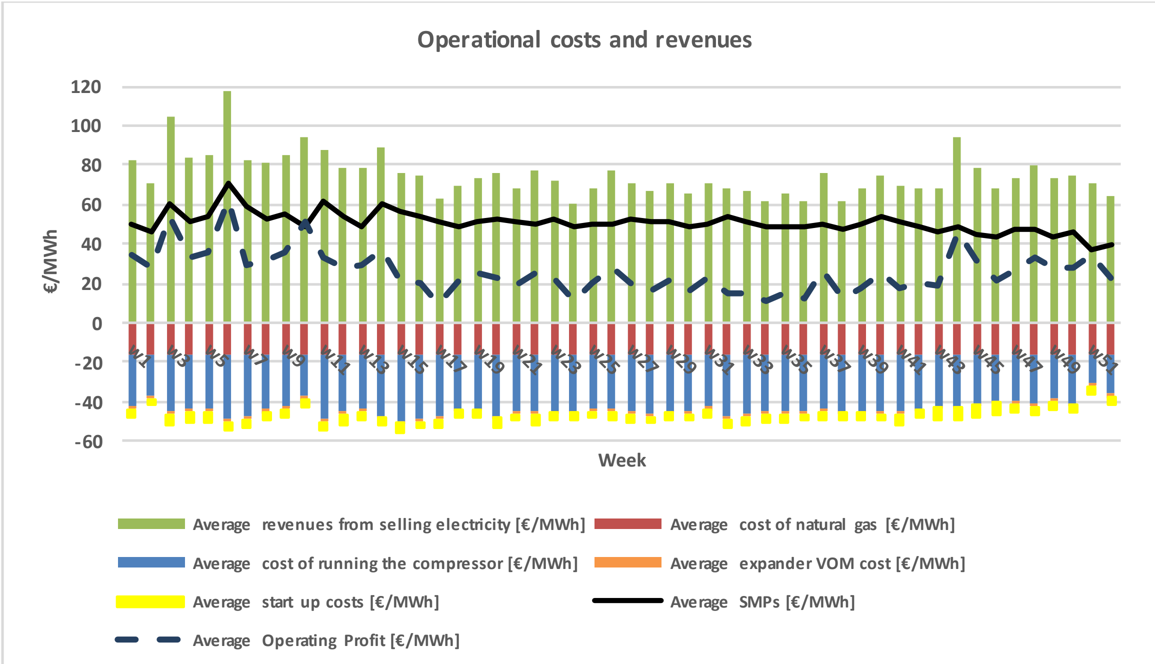

Figure 6-41: Operating profit, main operating costs and revenues expressed as (€/MWh) on a weekly basis (Model: TE, Scenario: High discharge time).

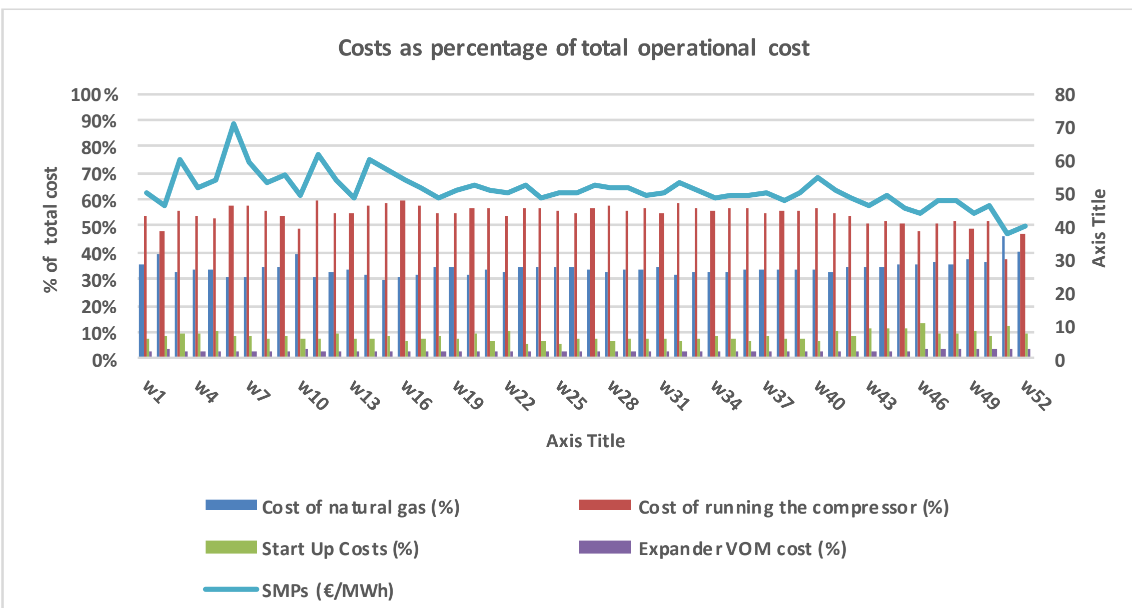

Figure 6-42: Break-down of operating costs as percentage of total operating cost (€/MWh) on a weekly basis (Model: TE, Scenario: High discharge time).

Comparing figure 6-45 with 6-32 we see that the effect of pressure on the compressor and expander operation is greatly reduced if the cavern volume is being increased.

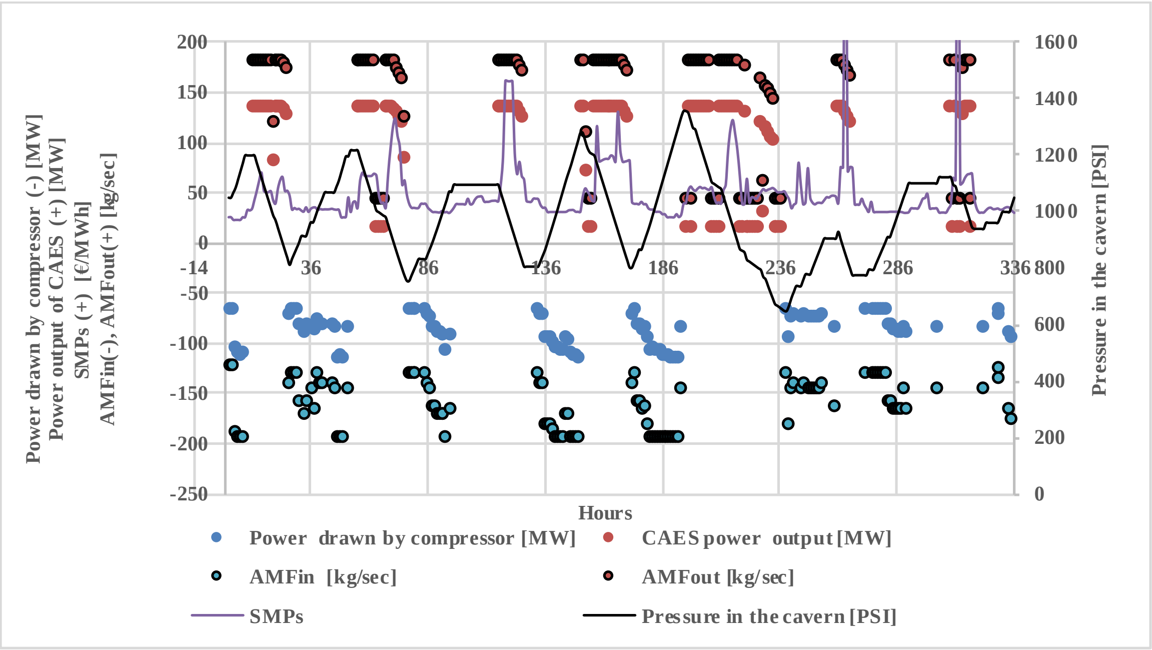

Figure 6-43: One week of CAES simulation (Model: TE, Scenario: Low discharge time).

Observing figures 6-48 to 6-49 we can see that the expander operates most of the time at the high end of its operational range to benefit from high SMPs since pressure effects are reduced compared to Base and Low Discharge time scenarios. The compressor operation is similar to the Base case.

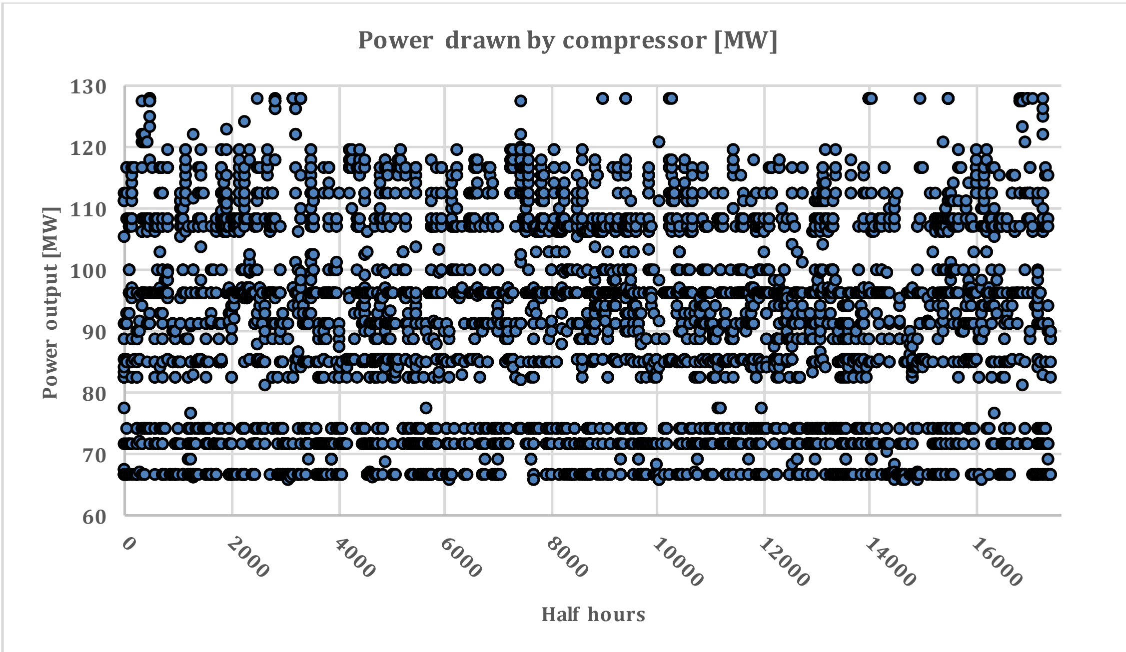

Figure 6-44: Power used for compression at each time increment (half hours) over a period of 52 weeks (Model: TE, Scenario: High discharge time).

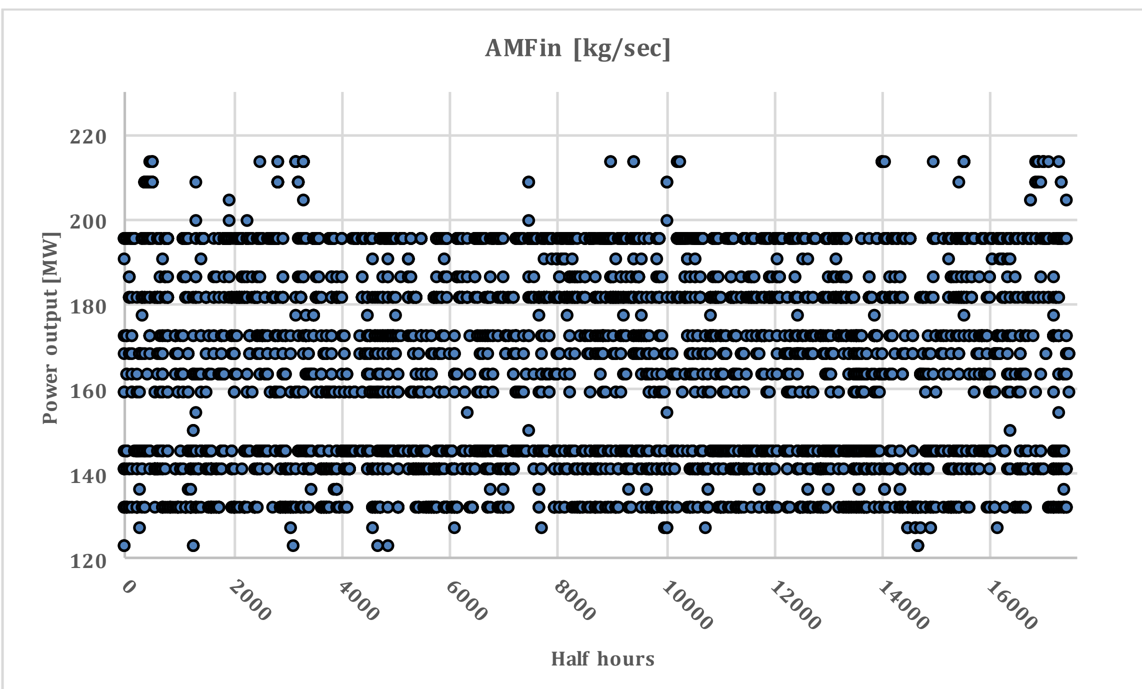

Figure 6-45: Air mass flow for compression during each time increment (half hours) over a period of 52 weeks (Model: TE, Scenario: High discharge time).

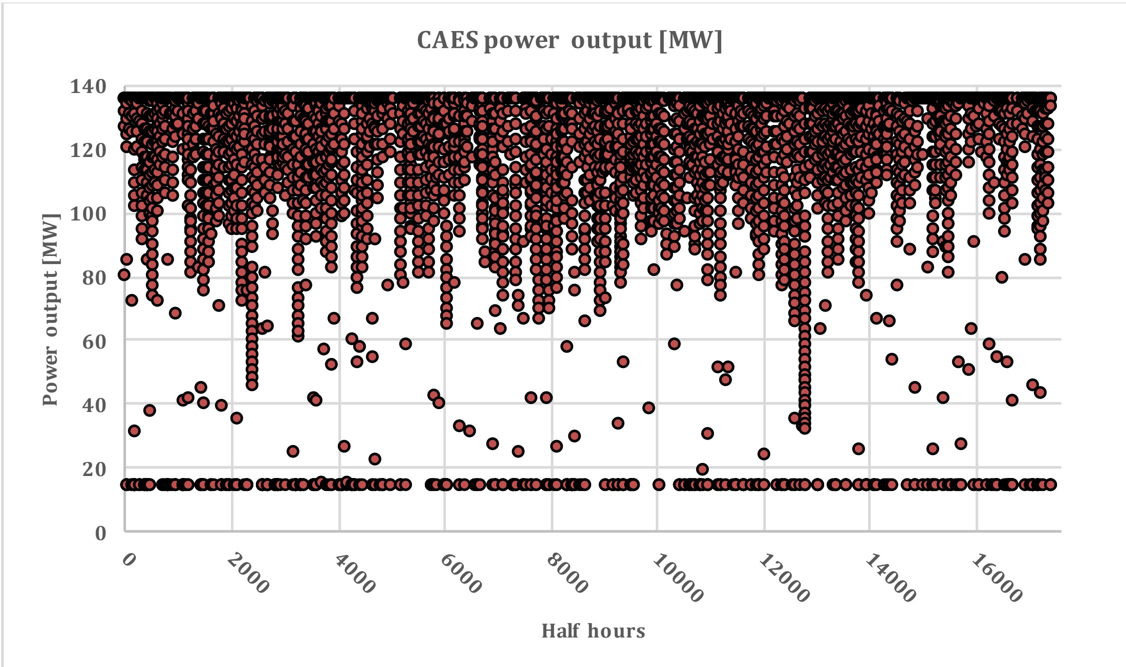

Figure 6-46: CAES power output at each time step (halfhours) over a period of52 weeks (Model: TE, Scenario: High discharge time).

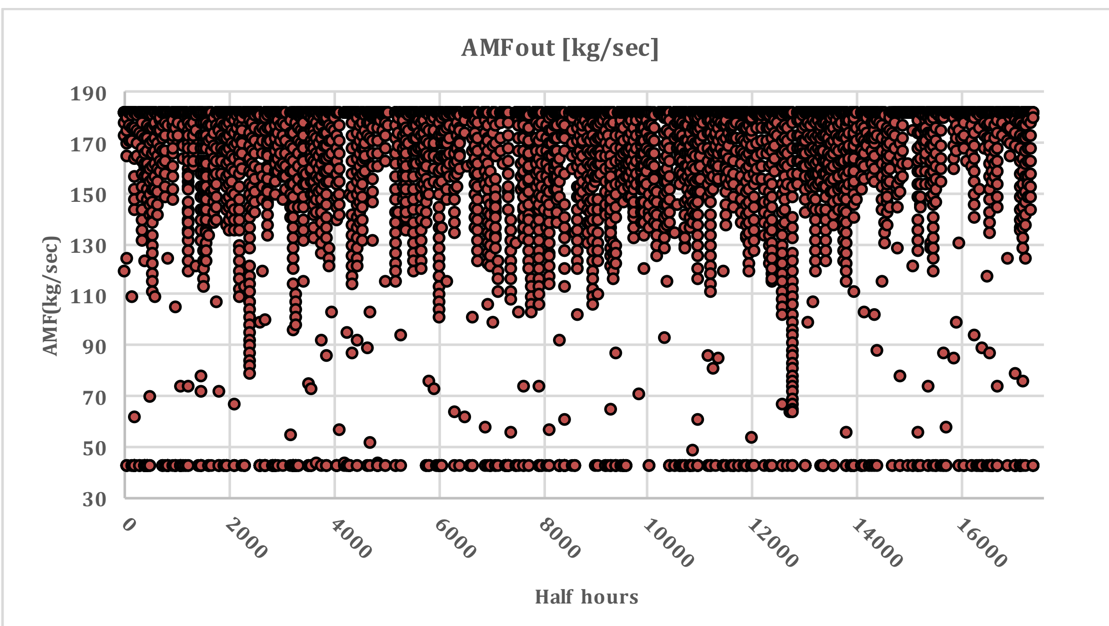

Figure 6-47: Air mass flow for expansion during each time increment (half hours) over a period of 52 weeks (Model: TE, Scenario: High discharge time).

6.3.2.4 Results-100% increase on natural gas price scenario

- FP model

If gas prices double, total operational profit for the FP model over 52 weeks becomes €5.1m (table 6-2). Total operating costs over the 52 week period account for €12.7m while total operating revenues for €17.8m. The absolute decrease compared to the Base scenario for profits, revenues and costs is €4.8m, €10.7m and €5.9m respectively. The same decrease expressed as percentages is 46%, 35%, 28%. Total mechanical energy being stored is decreased by ~45% over the 52 week period compared to the Base scenario. The same decrease occurs for the energy being sold. The decreases this time are not due to decreased storage space but rather due to increased cost of electricity production. CAES needs to discharge during higher SMPs compared to the Base scenario to be profitable and thus operates for less time.

As expected, in the “High gas price” scenario the cost revenues and cost figures as percentages of total energy produced change significantly. The cost of natural gas is now the major cost component averaging €33/MWh or around 53% of total costs. Profits vary significantly among weeks and at weeks where off peak/peak differences on SMPs levels are low profitability approaches zero levels (see figures 6-50 and 6-51).

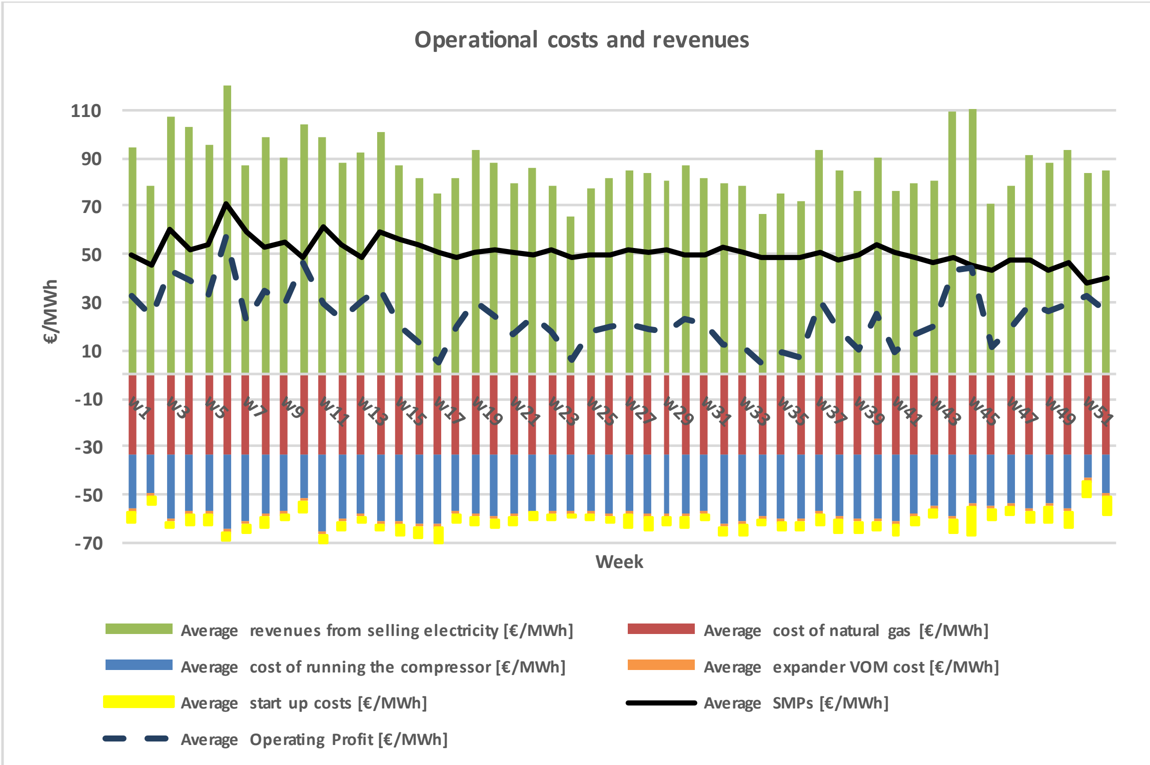

Figure 6-48: Operating profit, main operating costs and revenues expressed as €/MWh-e on a weekly basis (Model: FP, Scenario: High gas price).

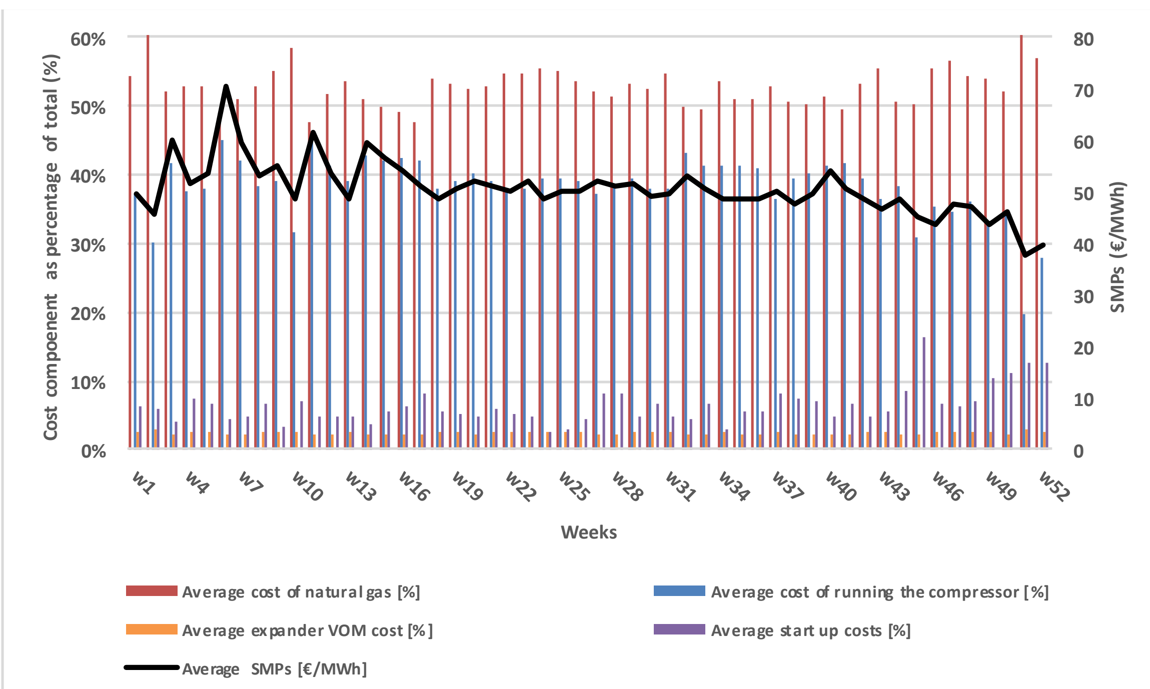

Figure 6-49: Break-down of operating costs expressed in (€/MWh-e) as percentage of total operating cost on a weekly basis (Model: FP, Scenario: High gas price).

As graphs 6-52 and 6-53 show, the compressor and expander operation pattern doesn't change considerably.

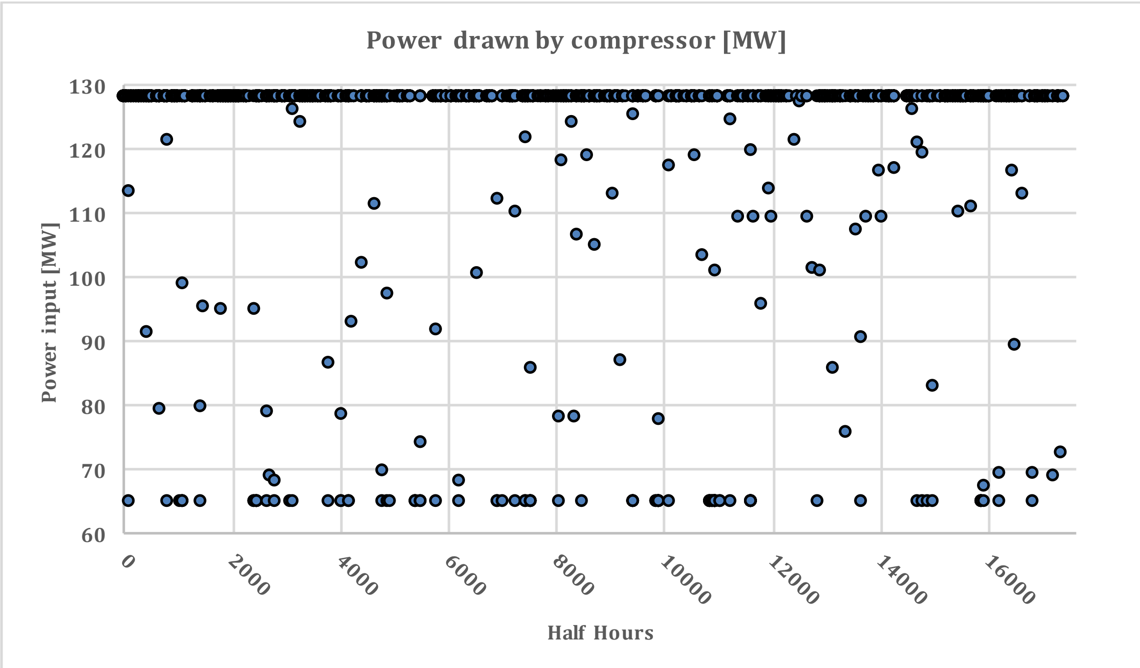

Figure 6-50: Power used for compression at each time increment (half hours) over a period of 52 weeks (Model: FP, Scenario: High gas price).

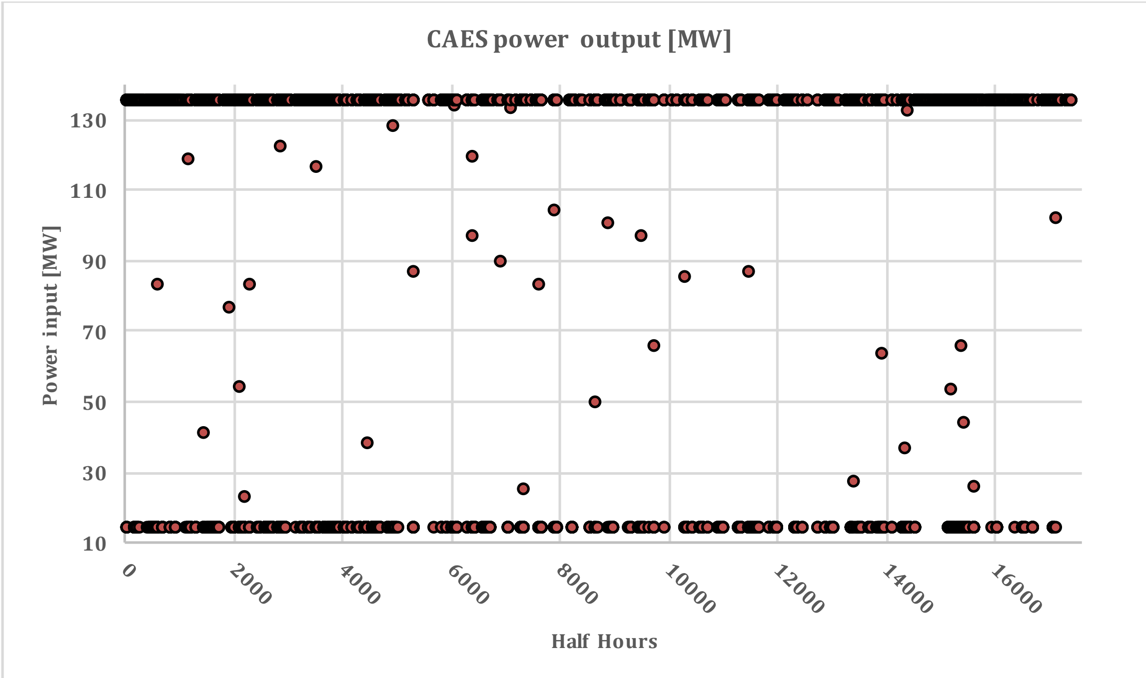

Figure 6-51: CAES power output at each time step (half hours) over a period of 52 weeks (Model: FP, Scenario: High Gas Price).

- Thermo-Economic model

The total operational profit for the TE model over 52 weeks is €4.3m. Total operating revenues are equal to €14.2m and operating costs are equal to €9.9m. The decrease for operating profit, revenues and costs compared to the Base scenario is 47%, 40% and 38% respectively.

The cost figures per unit of energy produced have changed significantly compared to the Base scenario. Cost of natural gas is the highest cost component averaging €33/MWh or 50% of total costs. The cost of compression averages €27/MWh or 37% of total costs. In general cost structure is very similar to the FP scenario, with the exception of start-up costs that are 10% of total costs (compared to 6% for FP scenario) (figures 6-54 and 6-55).

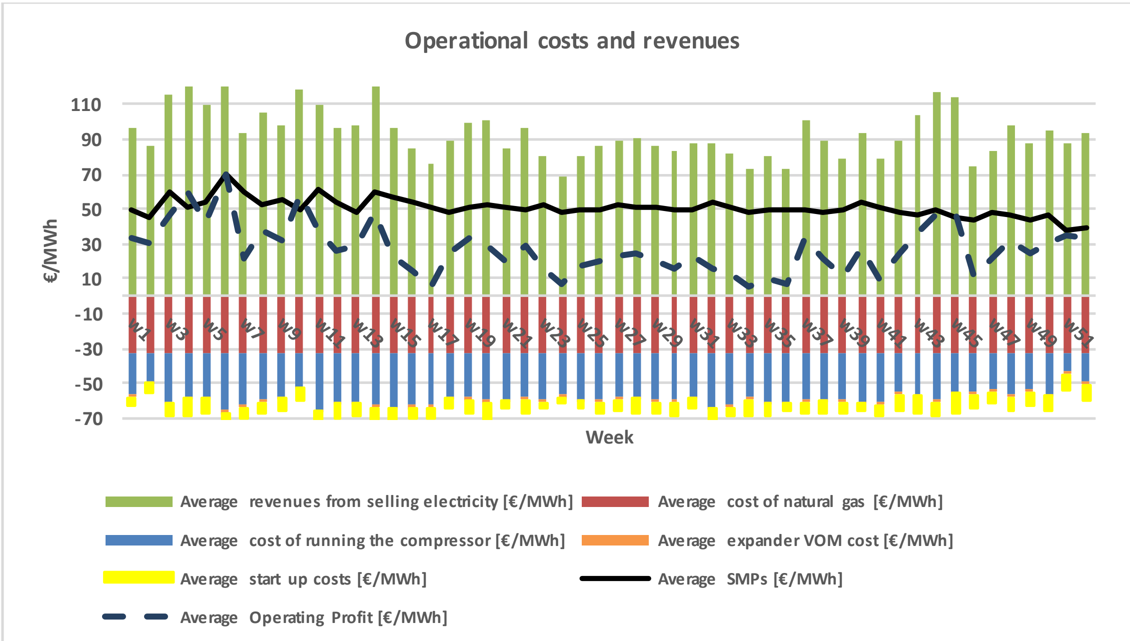

Figure 6-52: Operating profit, main operating costs and revenues expressed as (€/MWh) on a weekly basis (Model: TE, Scenario: High gas price).

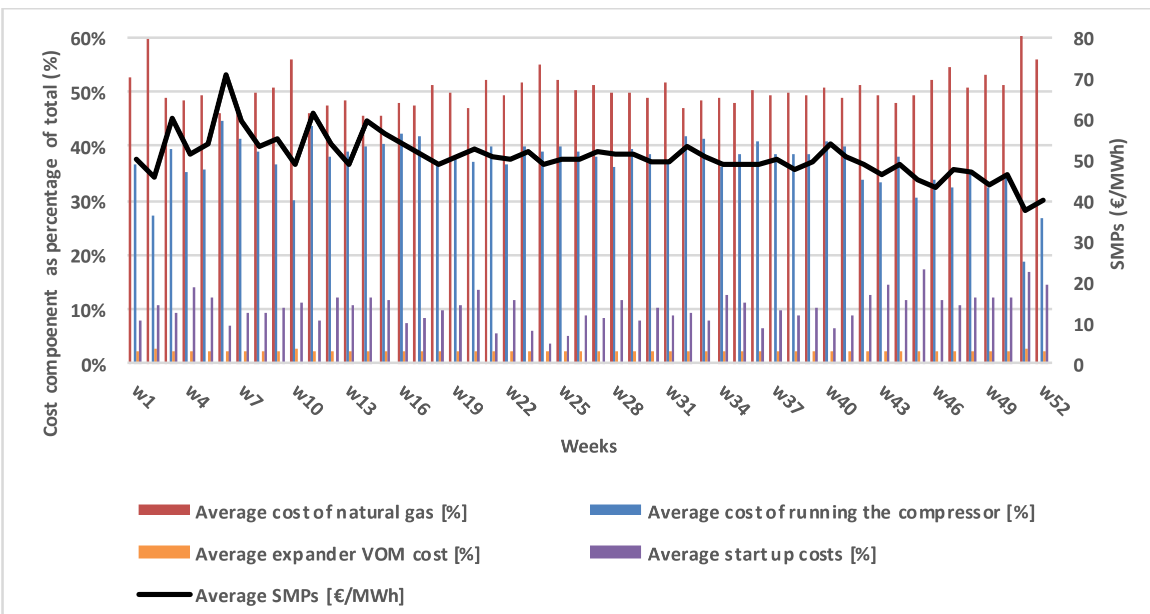

Figure 6-53: Break-down of operating costs as percentage of total operating cost (€/MWh) on a weekly basis (Modeled, Scenario: High gas price).

Observing figures 6-56 to 6-59 we can tell that see that the expander operates most of the time at high end of its operational range to benefit from high SMPs. This is because if the price of gas is high both the TE and FP models for less hours but at the highest SMPs due to high cost of expansion. The compressor operation doesn't depict any considerable differences compared to the Base scenario.

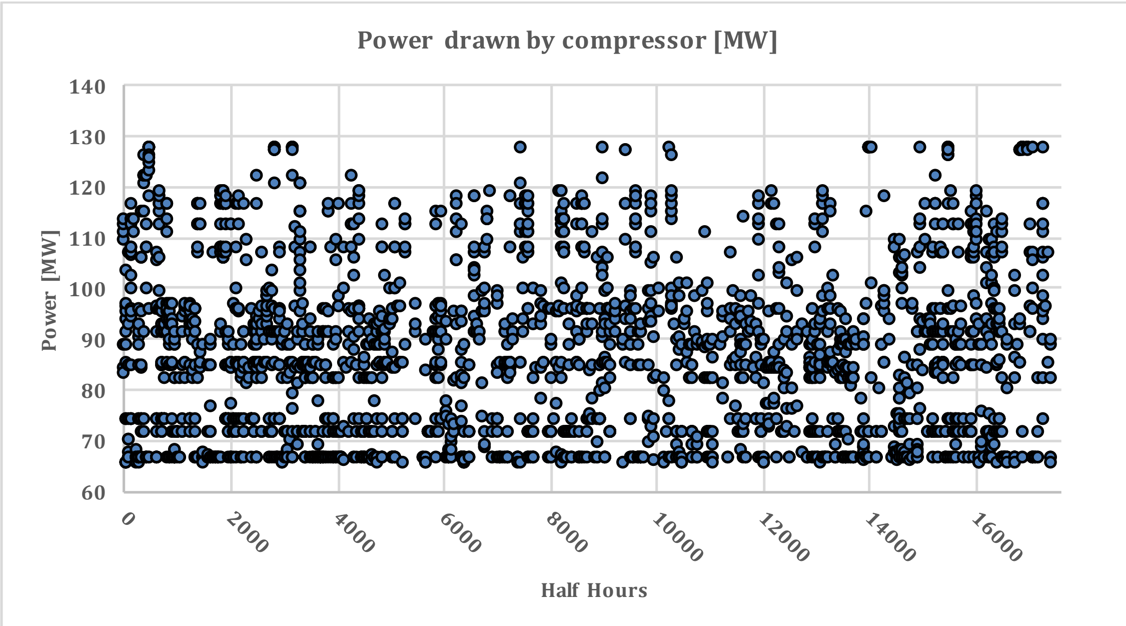

Figure 6-54: Power used for compression at each time increment (half hours) over a period of 52 weeks (Modeled, Scenario: High gas price).

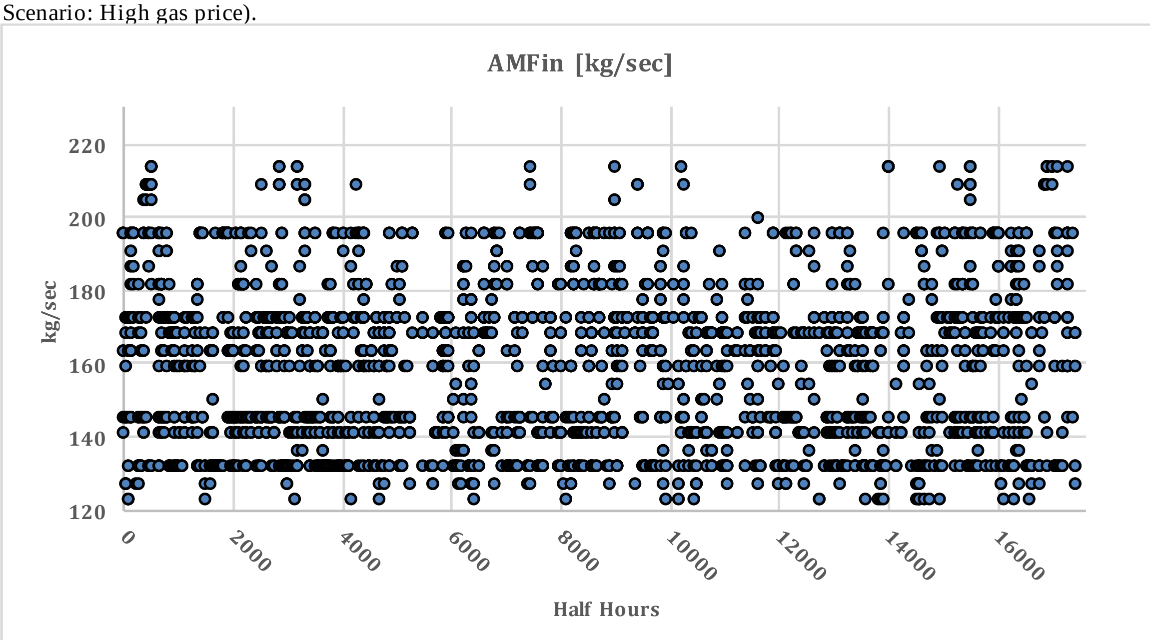

Figure 6-55: Air mass flow for compression during each time increment (half hours) over a period of 52 weeks (Model: TE, Scenario: High gas price).

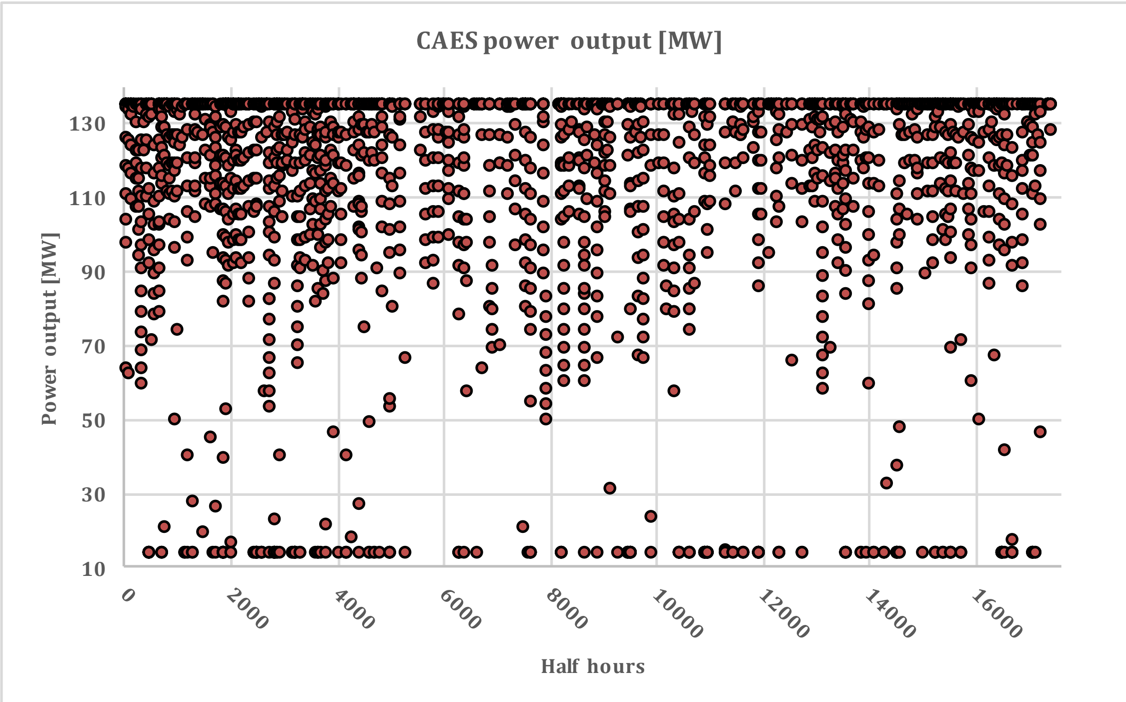

Figure 6-56: CAES power output at each time step (half hours) over a period of 52 weeks (Model: TE, Scenario: High gas price).

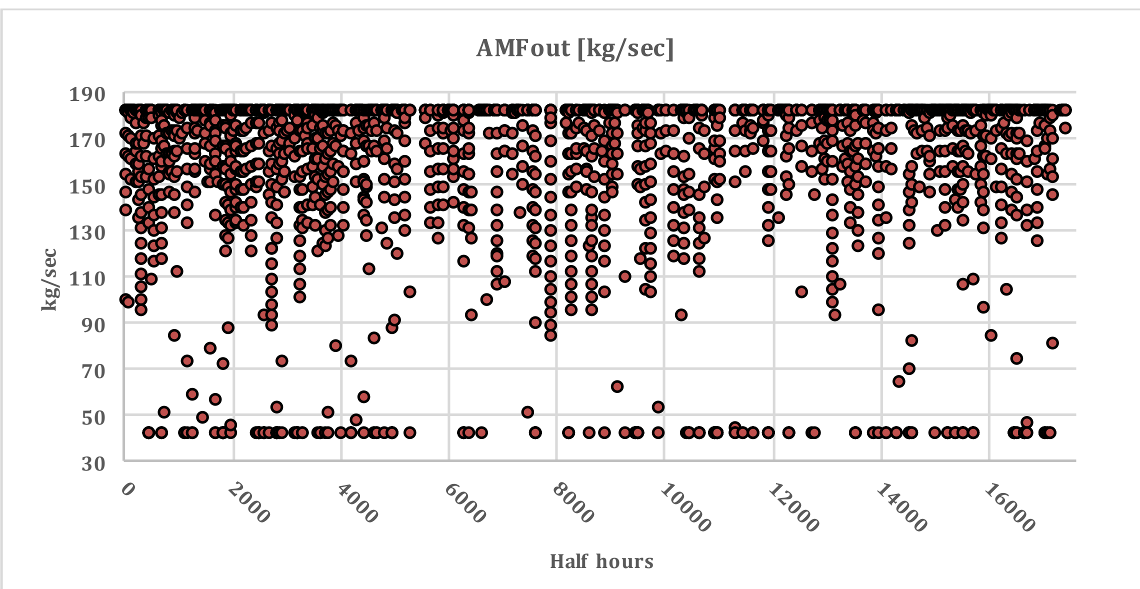

Figure 6-57: Air mass flow for expansion during each time increment (half hours) over a period of 52 weeks (Modeled, Scenario: High Gas price).

6.3.2.5 23% higher SMPs scenario

- FP model

If we use SMP data from year 2010 (23% higher values on average compared to 2015 data) the operational profit for the FP model over 52 weeks becomes €13.4m (table 6-3). Total operating costs over the 52 week period account for €20.8m while total operating revenues for €34.2m. The absolute increase compared to the Base scenario for profits, revenues and costs is €3.9m, €7m and €3.1m respectively. The same increase expressed as percentages is 40%, 26%, 18% respectively. The higher increase on revenues compared to costs is related to higher SMPs and wider peak/off-peak range of the 2010 SMP data I used in this scenario.

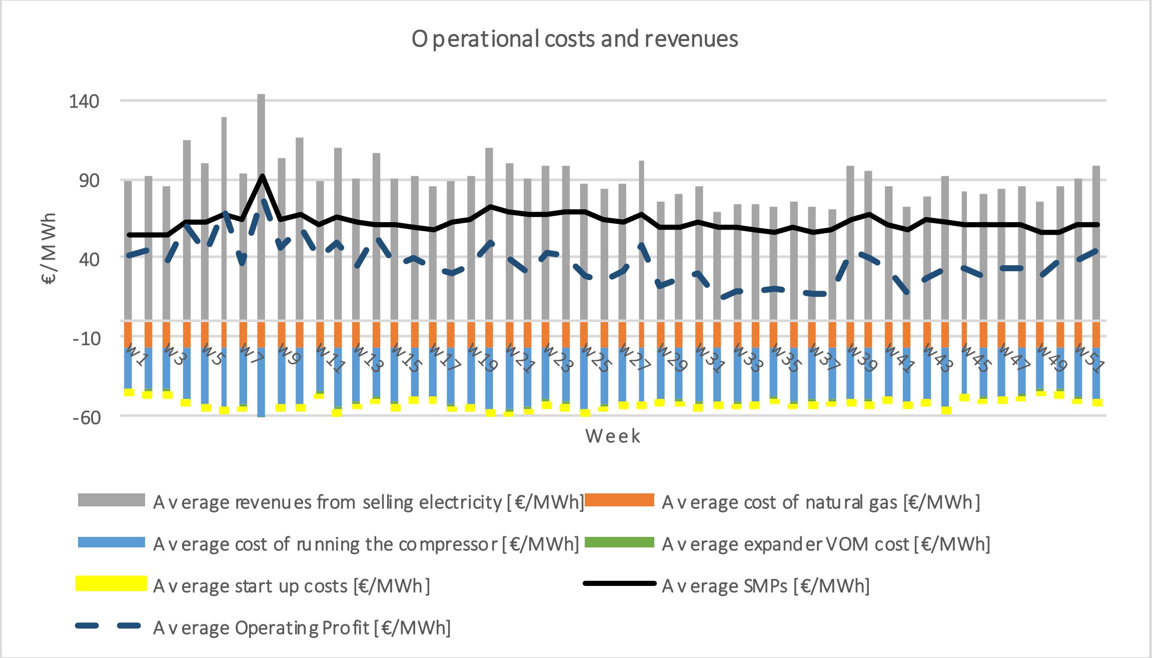

Figure 6-58: Operating profit, main operating costs and revenues expressed as €/MWh-e on a weekly basis (Model: FP, Scenario: High SMPs).

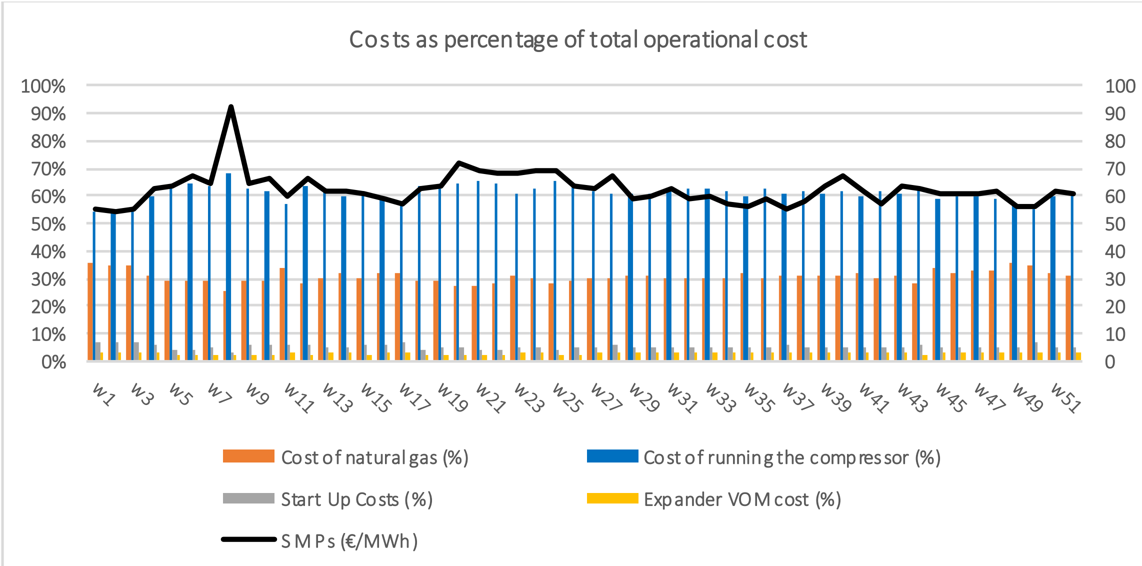

Figure 6-59: Break-down of operating costs expressed in (€/MWh-e) as percentage of total operating cost on a weekly basis (Model: FP, Scenario: High SMPs).

Higher SMPs results on 23% higher compression costs per unit of energy produced compared to the Base scenario. This is due to higher off-peak SMPs on average compared to Base[68]. The operational pattern of the high SMPs scenario is very similar to the Base scenario (see figures 6-62 to 6-64).

[68] 2010 data have an average minimum daily SMP of €38/MWh. The same value for 2015 data is €31/MWh

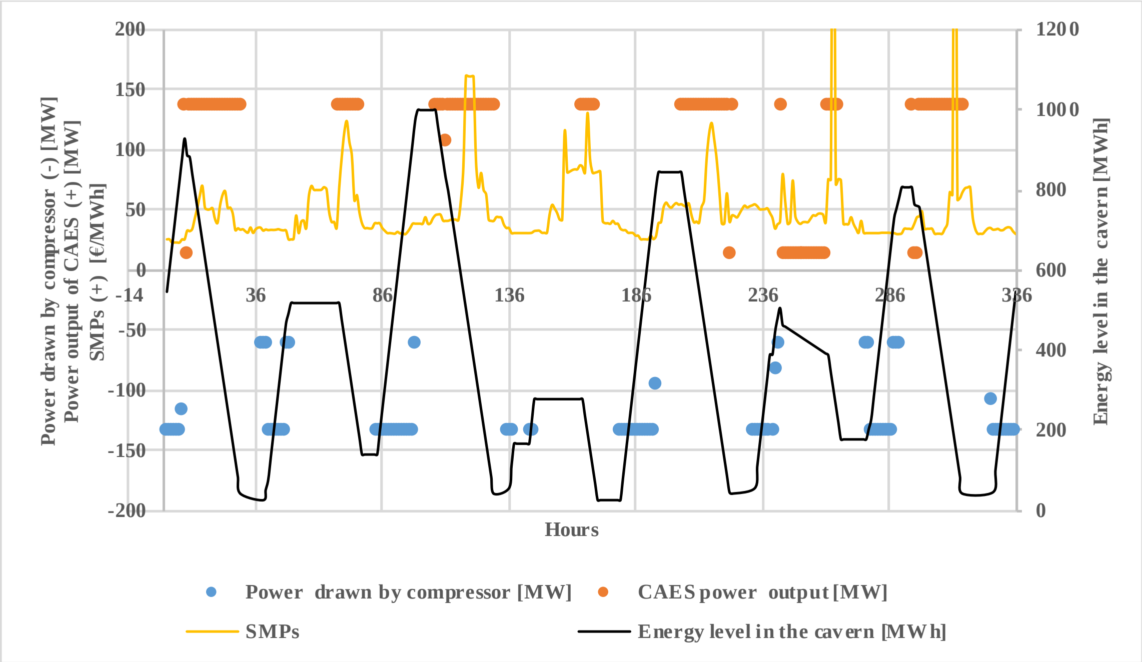

Figure 6-60: One week of CAES simulation (Model: TE, Scenario: High SMPs).

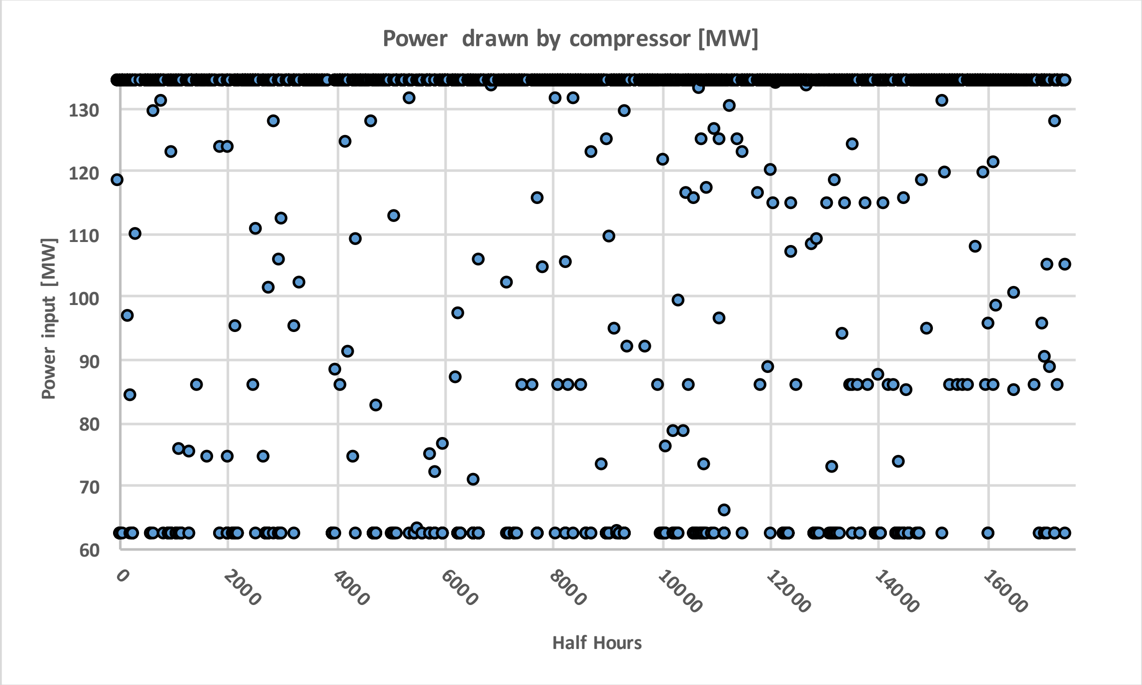

Figure 6-61: Power used for compression at each time increment (half hours) over a period of 52 weeks (Model: FP, Scenario: High SMPs).

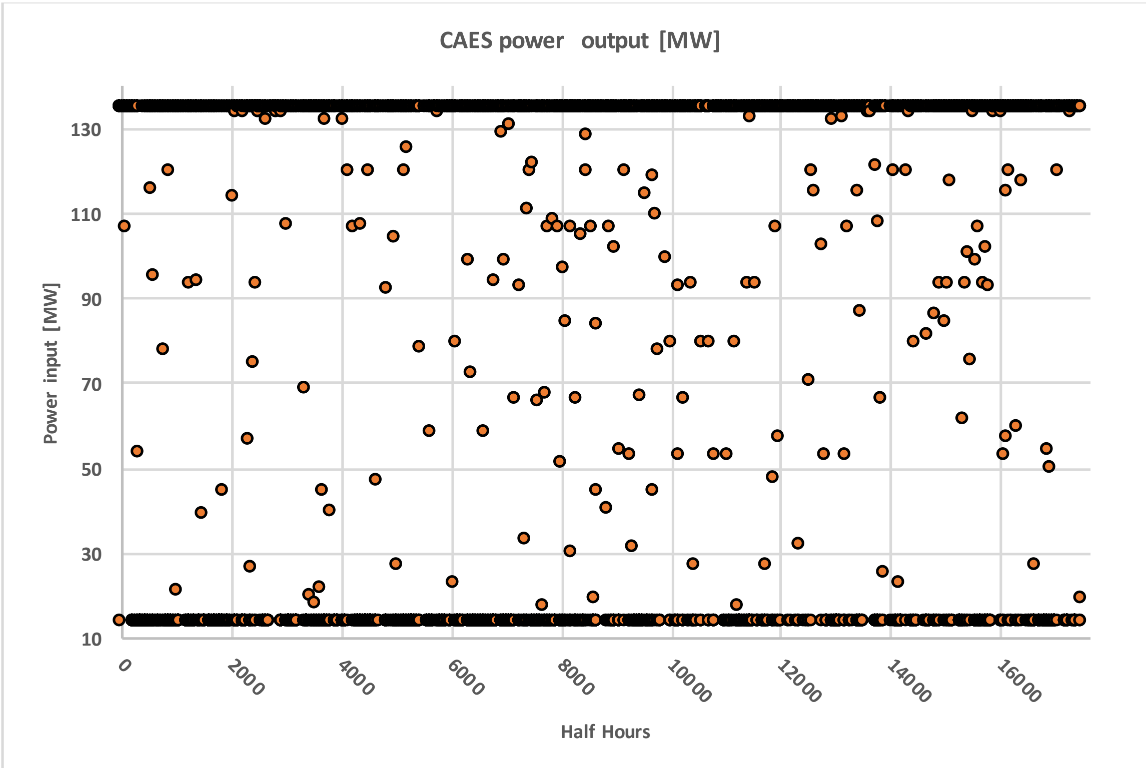

Figure 6-62: CAES power output at each time step (half hours) over a period of 52 weeks (Model: FP, Scenario: SMPs).

- Thermo-Economic model

The total operational profit for the TE model over 52 weeks is €11.5m. Total operating revenues are equal to €28.8m and operating costs are equal to €15.5m. The increase for operating profit, revenues and costs compared to the Base scenario is 41%, 21% and 10% respectively. Revenues are increased compared to the Base case due to higher SMPs. Cost increases are related to higher SMPs that result to higher operational cost of the compressor €34.3/MWh (versus €27.1/MWh in the Base) (see figure 6-65 and 6-66). Compression costs account for around 60% of total costs compared to the Base scenario where compression costs are ~50% of total costs.

The TE model in the High SMPs scenario charges and discharges very similar amounts of energy as in the Base scenario, The TE model exerts -14% less profit, -16% less revenues and -17% less costs compared to the FP model.

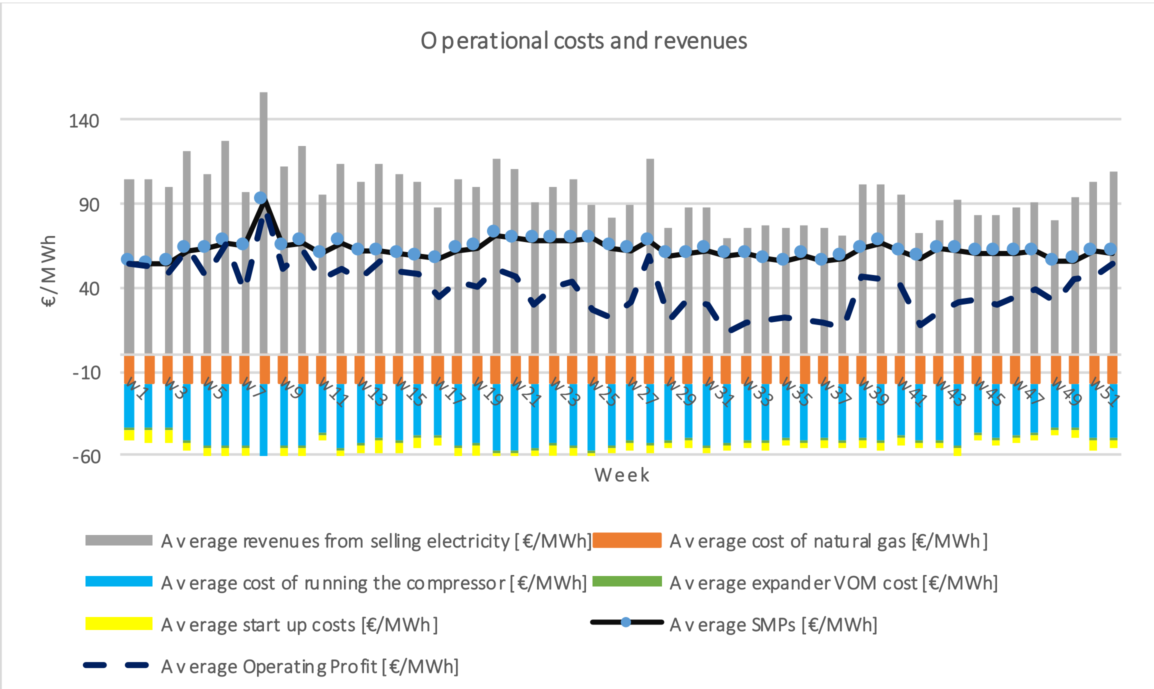

Figure 6-63: Operating profit, main operating costs and revenues expressed as (€/MWh) on a weekly basis (Model: TE, Scenario: High discharge time).

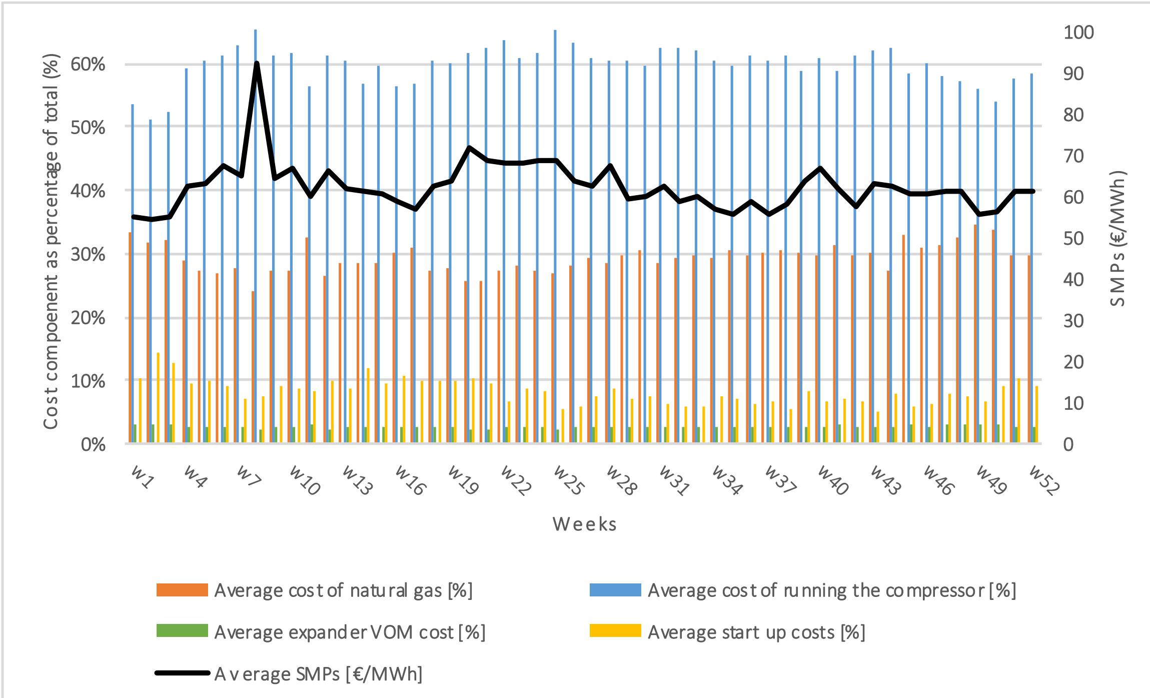

Figure 6-64: Break-down of operating costs as percentage of total operating cost (€/MWh) on a weekly basis (Model: TE, Scenario: High discharge time).

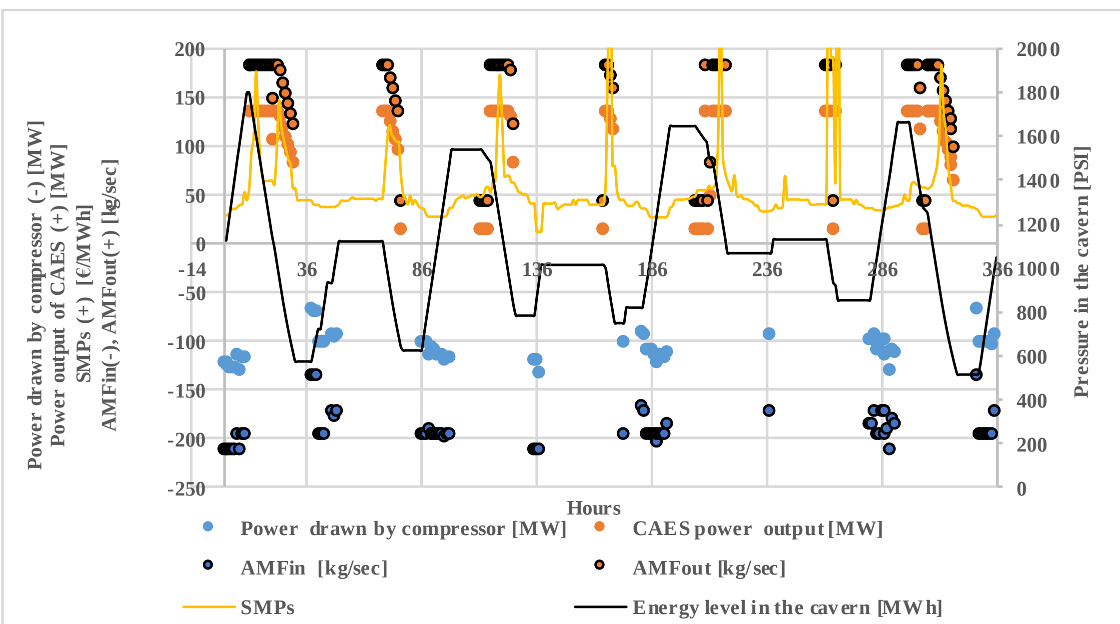

Figure 6-65: One week of CAES simulation (Model: TE, Scenario: High SMPs).

The operational pattern of CAES in the High SMPs scenario is very similar to the Base scenario (see figures 6-67 to 6-71).

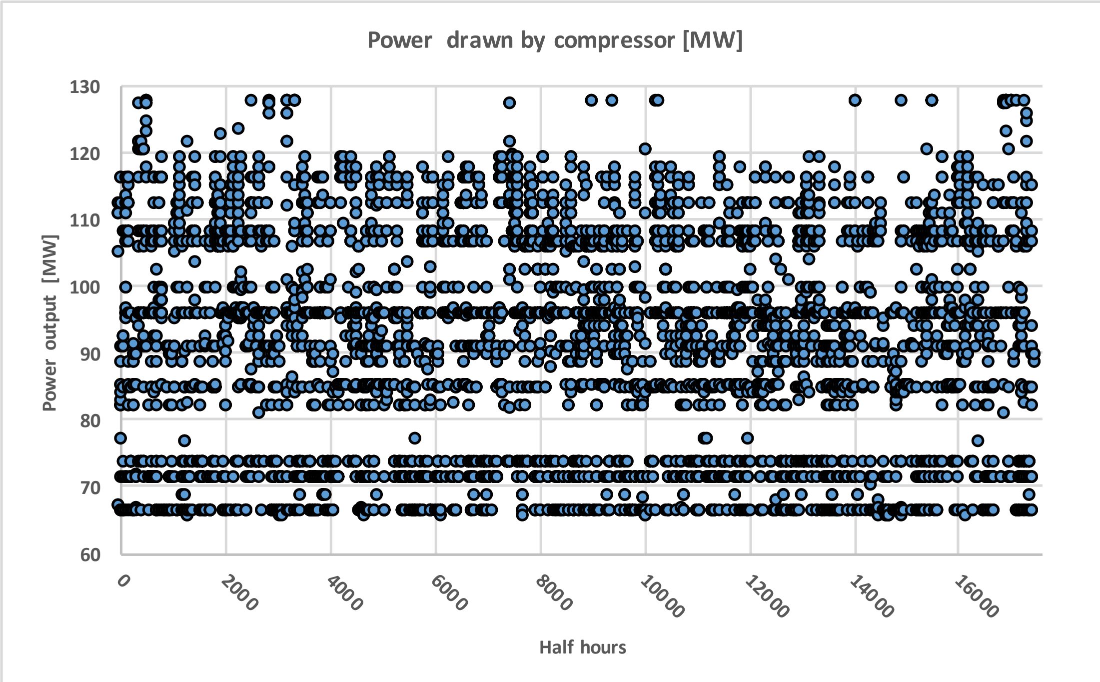

Figure 6-66: Power used for compression at each time increment (half hours) over a period of 52 weeks (Model: TE, Scenario: High discharge time).

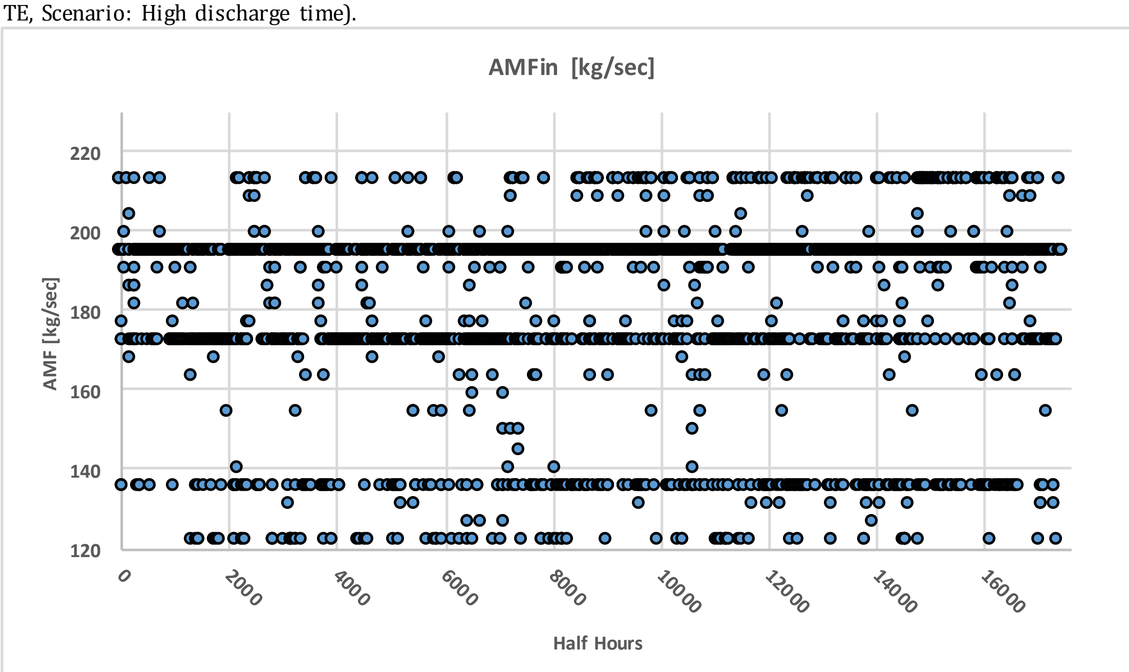

Figure 6-67: Air mass flow for compression during each time increment (half hours) over a period of 52 weeks (Model: TE, Scenario: High discharge time).

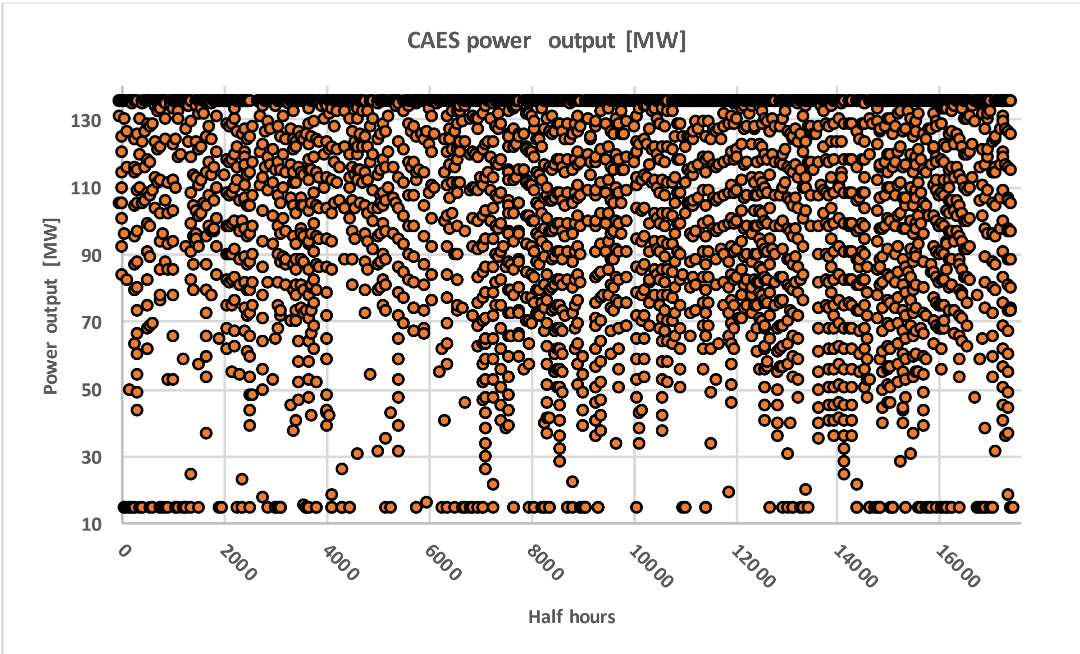

Figure 6-68: CAES power output at each time step (half hours) over a period of 52 weeks (Model: TE, Scenario: High discharge time).

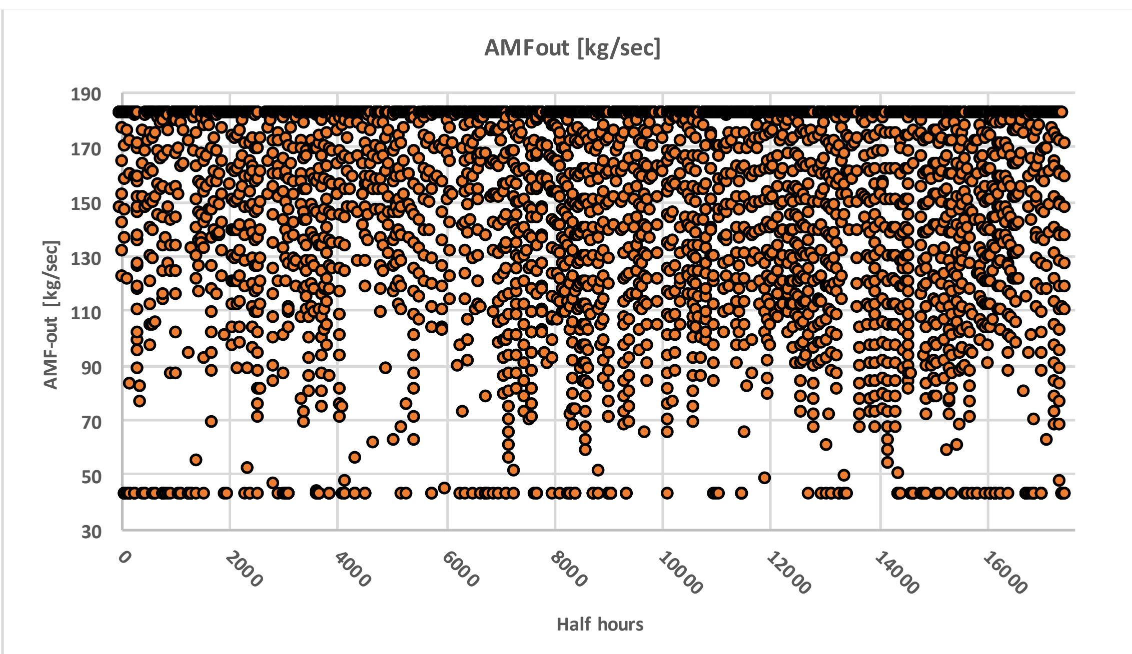

Figure 6-69: Air mass flow for expansion during each time increment (half hours) over a period of 52 weeks (Model: TE, Scenario: High discharge time).

6.3.2.6 Base + Ancillary services scenario

- FP model

If we co-optimize energy arbitrage + ancillary services the operational profit for the FP model over 52 weeks becomes €11.1m (table 6-3). Total operating costs over the 52 week period account for €18.4m while total operating revenues for €29.5m. The absolute increase compared to the Base scenario for profits, revenues and costs is €1.5m, €2.2m and €0.7 m respectively. The same increase expressed as percentages is 16%, 8%, 4% respectively. The cost structure per unit of energy produced is very similar to the Base case as shown in figures 6-72 and 6-73. This was expected as we haven't changed any parameter that would affect cost metrics in this scenario.

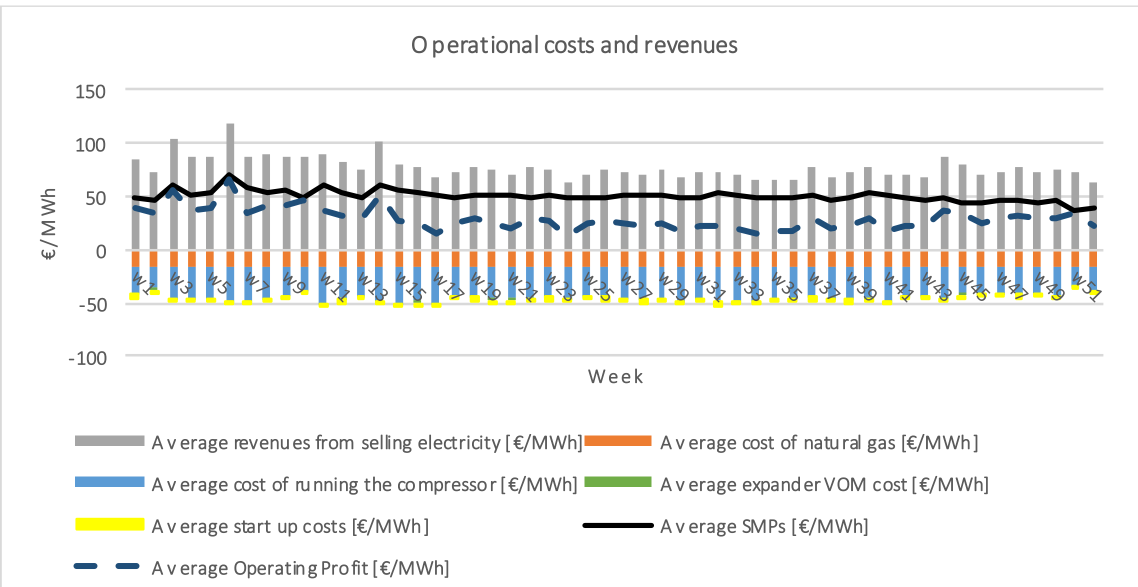

Figure 6-70: Operating profit, main operating costs and revenues expressed as €/MWh-e on a weekly basis (Model: FP, Scenario: High SMPs).

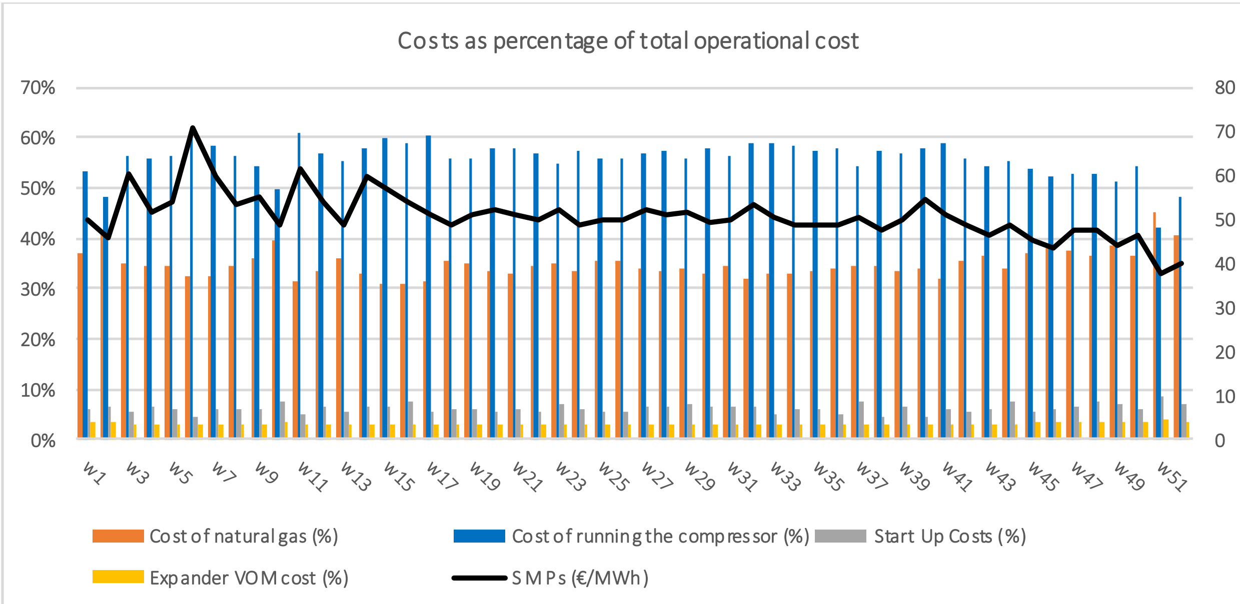

Figure 6-71: Break-down of operating costs expressed in (€/MWh-e) as percentage of total operating cost on a weekly basis (Model: FP, Scenario: High SMPs).

Co-optimizing (energy arbitrage reserve capacity) CAES operation results to different operational patter as shown in figure 6-74. On the top depiction I show 1 week of operation where CAES is performing energy arbitrage and provides reserve capacity. On the bottom depiction I repeat figure 6-6 (Arbitrage only). We observe that in the Base Ancillary services scenarios CAES prefers to operate longer hours at low outputs to preserve spinning capacity and use it to make additional revenues. Same is true for the compressor. CAES operates the compressor for longer hours to be able to make revenues through provision of spinning capacity. The revenues from spinning reserves are €1.5m or 5% of total revenues. Revenues from tertiary (non-spinning) reserves are equal to €0.36m or 1% of total revenues. With revenues from ancillary services being only 6% of total revenues it is clear that the competitiveness of energy storage devices is not greatly increased with the current compensation from the ancillary services markets. The operating range of the compressor and the expander can be also seen in figures 6-76 and 6-77.

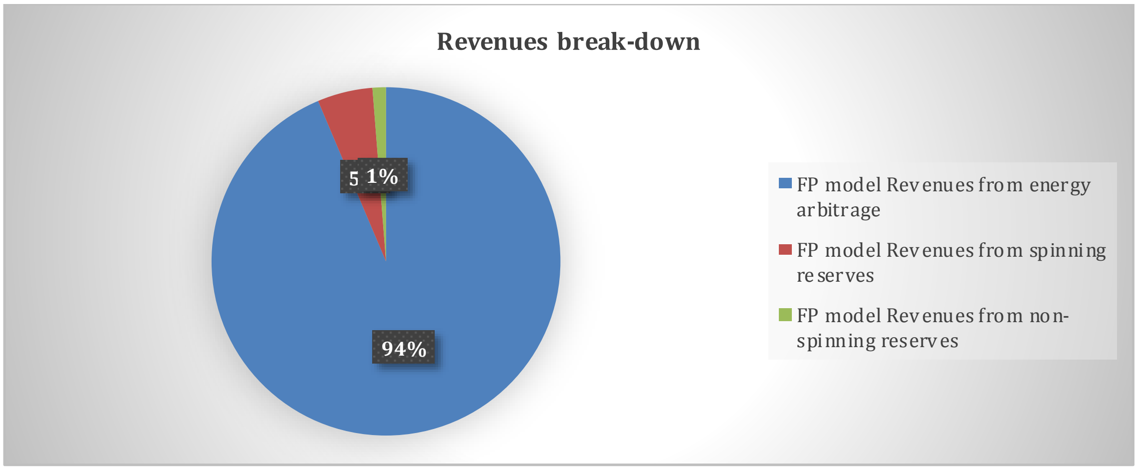

Figure 6-72: Break down of revenue sources (Model: FP, Scenario: Base + Ancillary Services).

Figure 6-73: One week of CAES simulation where at the top depiction CAES is performing energy arbitrage only (Base scenario) while in the bottom depiction CAES is performing arbitrage and provides reserve capacity at the same time(Model: FP)

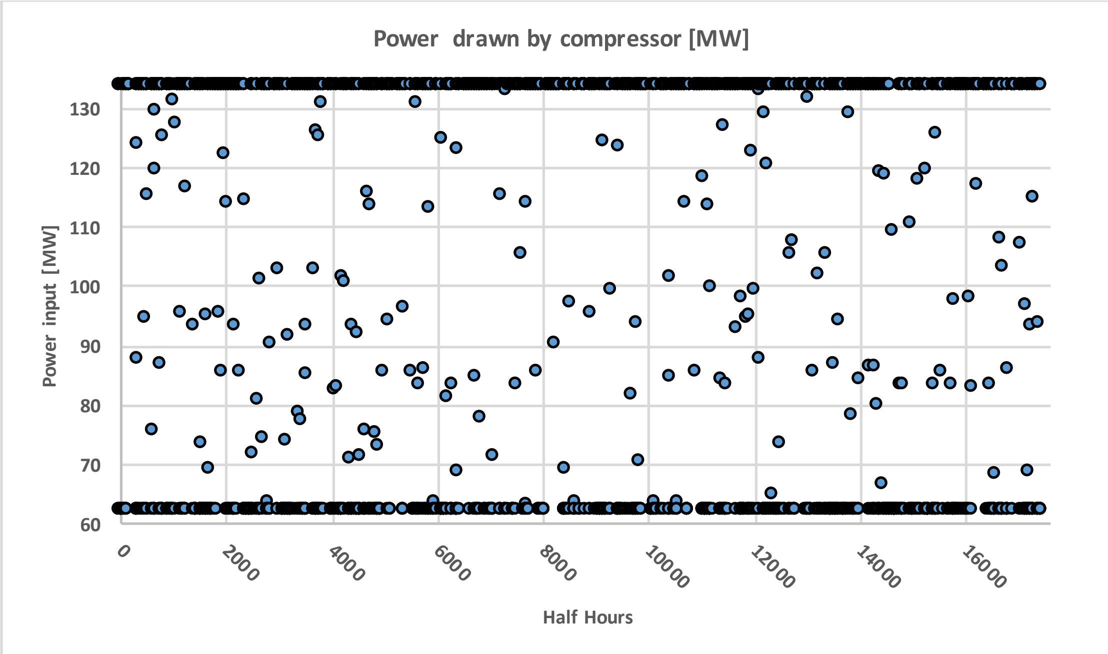

Figure 6-74: Power used for compression at each time increment (half hours) over a period of 52 weeks (Model: FP, Scenario: Base+Ancillary Services)

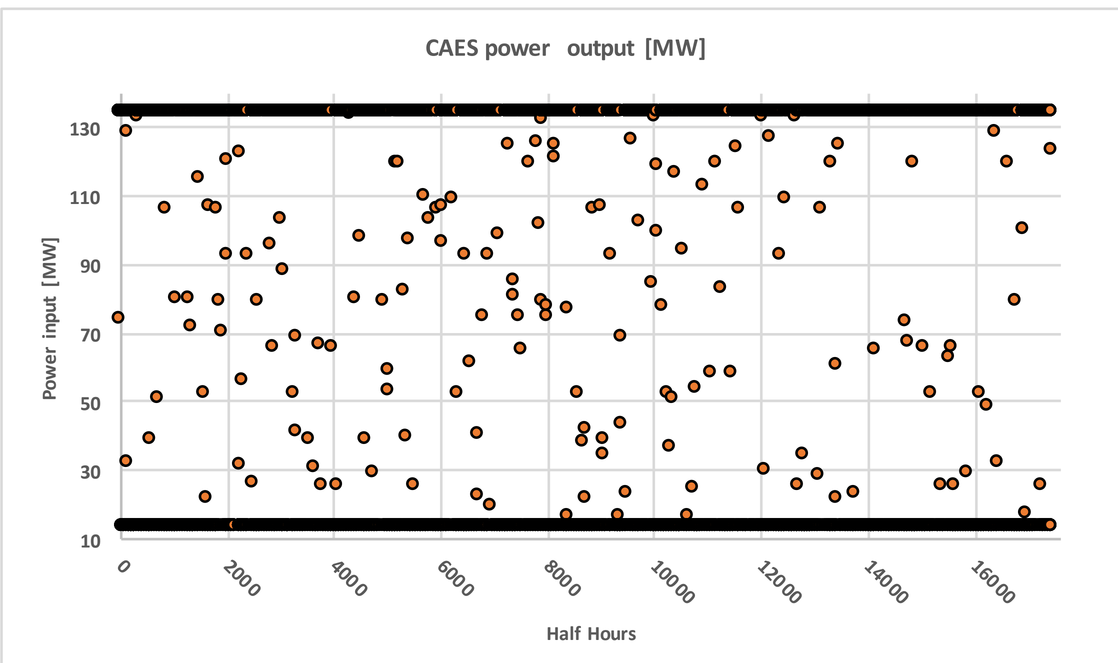

Figure 6-75: CAES power output at each time step (half hours) over a period of 52 weeks (Model: FP, Scenario: Base + Ancillary Services)

- Thermo-Economic model

The total operational profit for the TE model over 52 weeks is €10.4m. Total operating revenues are equal to €26.4m and operating costs are equal to €16m. The increase for operating profit, revenues and costs compared to the Base scenario is 27.4%, 11% and 2.2% respectively. The absolute increase compared to the Base scenario for profits, revenues and costs is €2.2m, €2.6m and €0.3 m respectively. The percent decrease for profits revenues and costs compared to the FP scenario is 9%, 18%, 15% respectively. The cost structure per unit of energy produced is almost identical to the Base case as shown in figures 6-77 and 6-78.

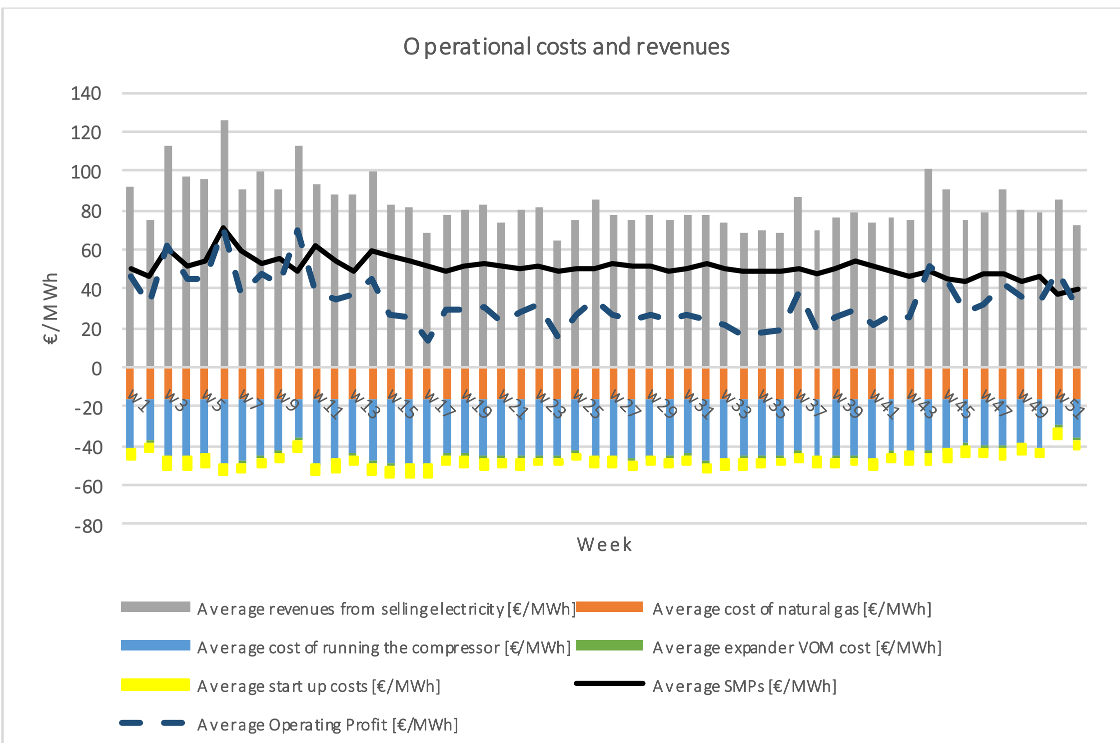

Figure 6-76: Operating profit, main operating costs and revenues expressed as (€/MWh) on a weekly basis (Model: TE, Scenario: Base + Ancillary services).

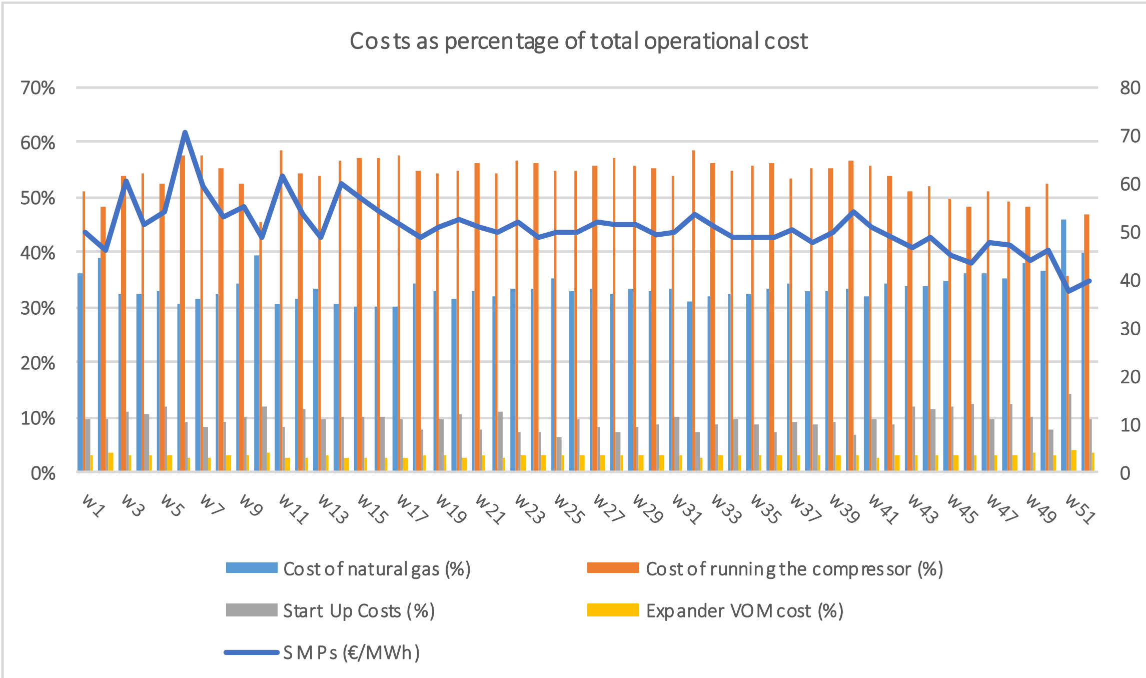

Figure 6-77: Break-down of operating costs as percentage of total operating cost (€/MWh) on a weekly basis (Model: TE, Scenario: Base+Ancillary Services).

Comparing figure 6-80 with figure 6-75 we notice that the TE model doesn't operate CAES as often at low outputs to reserve spinning capacity. The TE model rather prefers to operate CAES similarly as in the arbitrage only scenario (Base) and just makes additional revenues mainly from providing non-spinning (tertiary) reserve capacity. The reason for this is that discharging for long times (even at low outputs) can bring the cavern into low pressure levels and then the actual available reserved capacity is lower than the difference between maximum output and actual output. The FP model doesn't understand that effect and overestimates the revenues from spinning reserves. Total revenues from spinning reserves in the TE model are equal to € 0.7m. Revenues from non-spinning reserves are equal to € 1.5m. The operational pattern of CAES in the High SMPs scenario is very similar to the Base scenario (see figures 6-68 to 6-72).

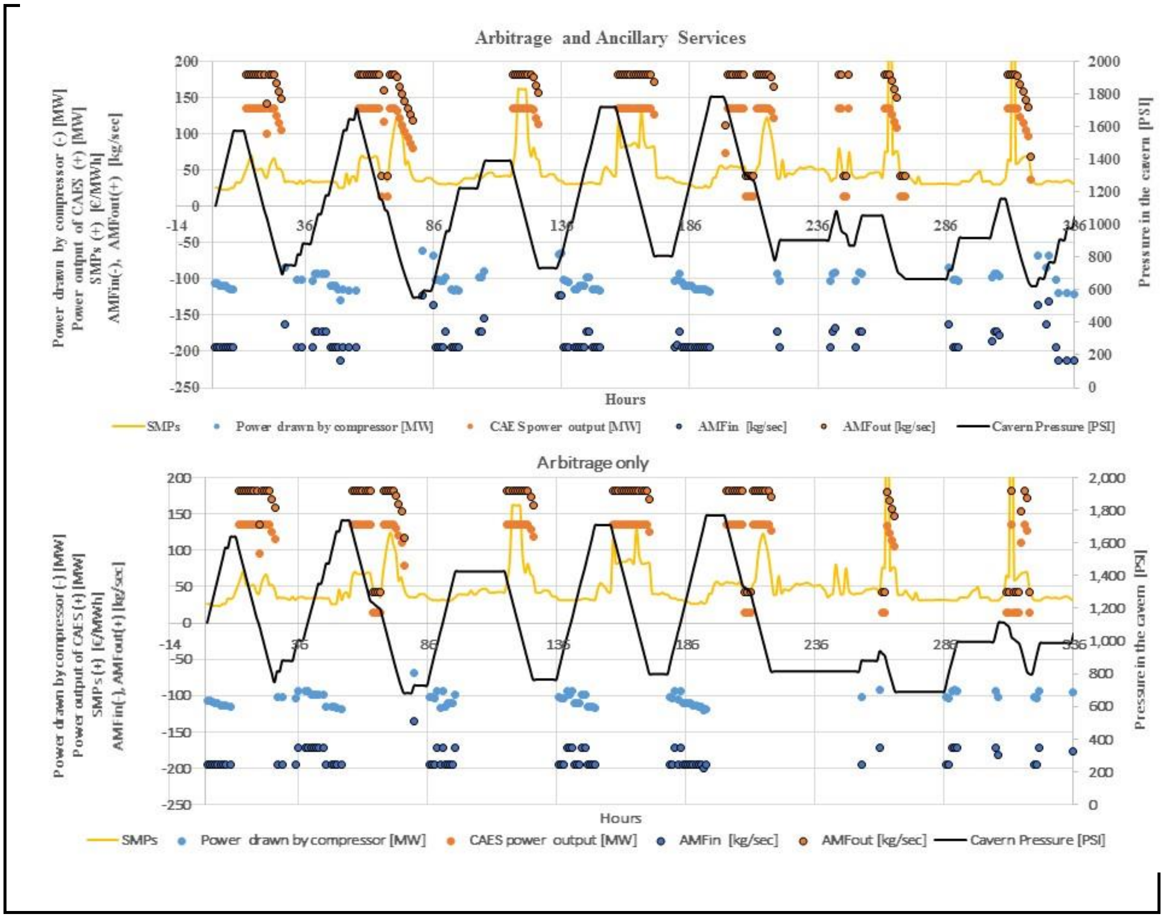

Figure 6-78: One week of CAES simulation with and without providing ancillary services (Model: TE, Scenario: Base + Ancillary Services).

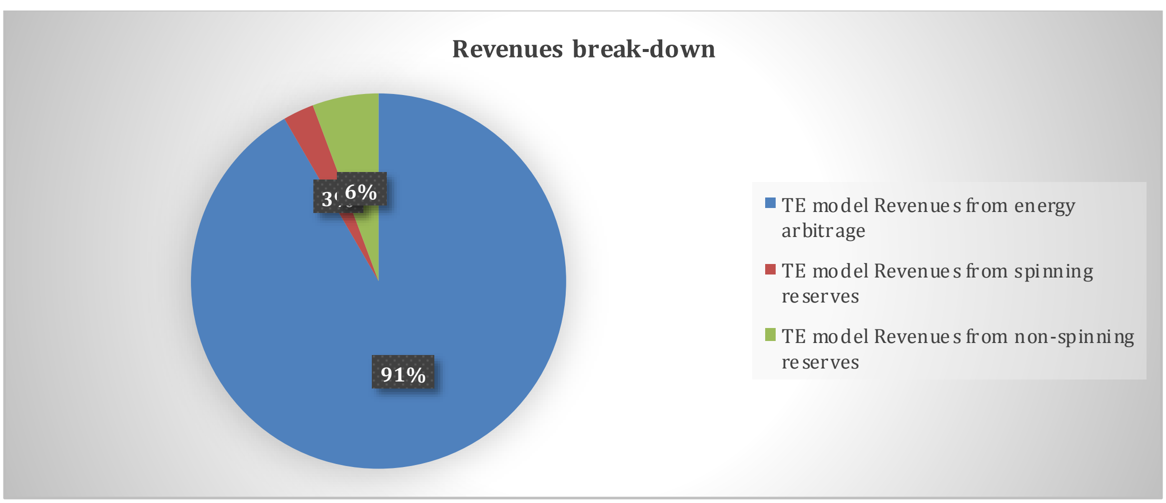

Figure 6-79: Breakdown of revenue sources (Model: TE, Scenario: Base+Ancillary Services).

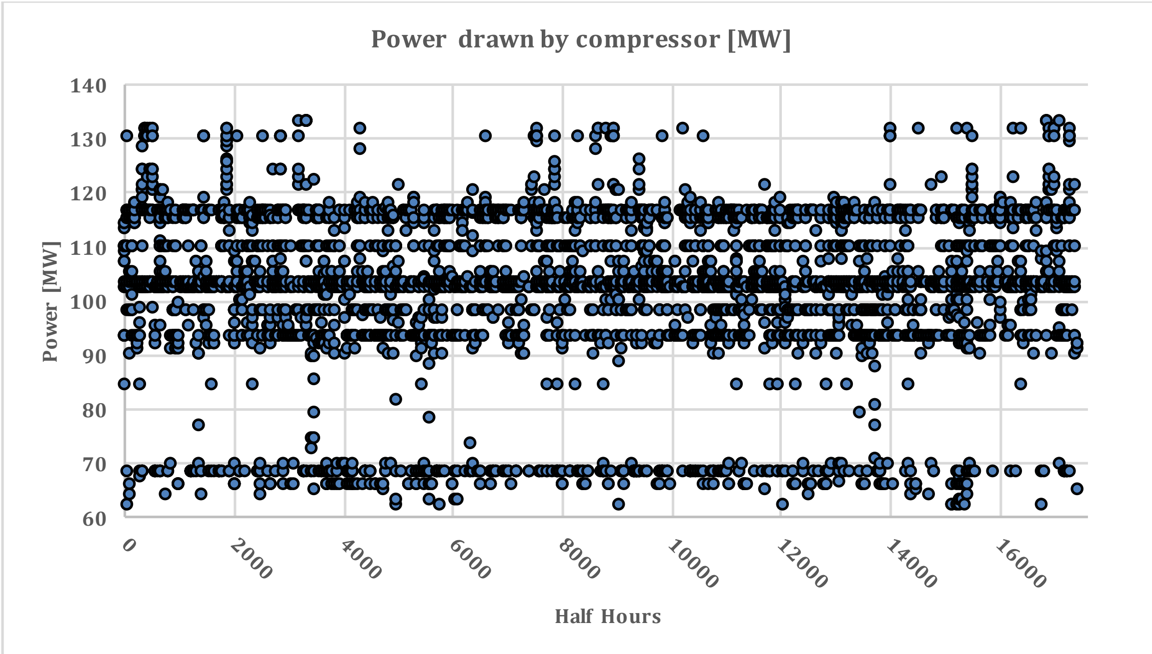

Figure 6-80: Power used for compression at each time increment (half hours) over a period of 52 weeks (Model: TE, Scenario: Base+Ancillary Services)

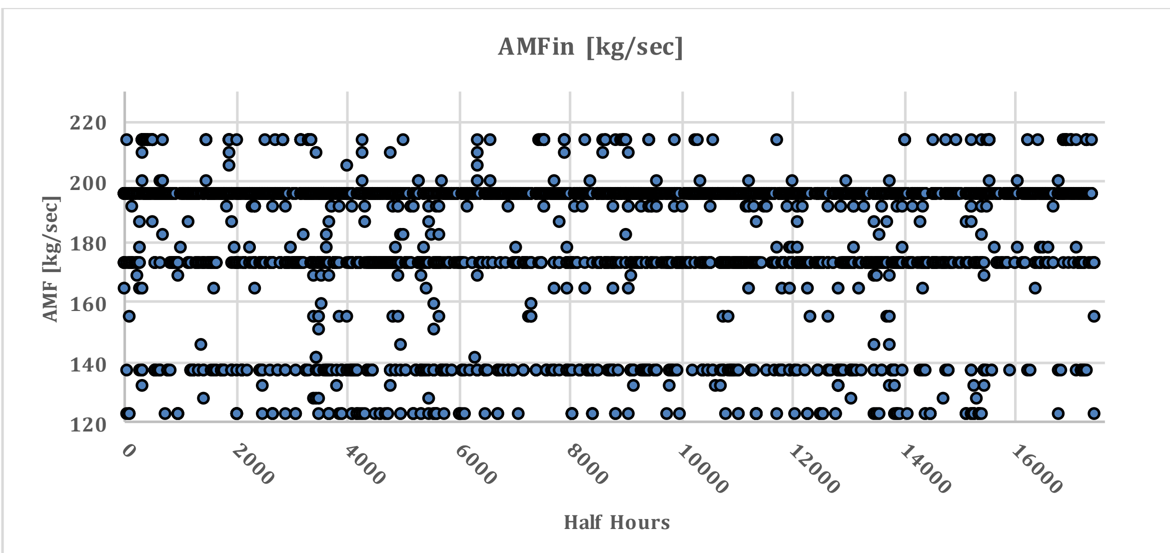

Figure 6-81: Air mass flow for compression during each time increment (half hours) over a period of 52 weeks (Model: TE, Scenario: Base+Ancillary Services)

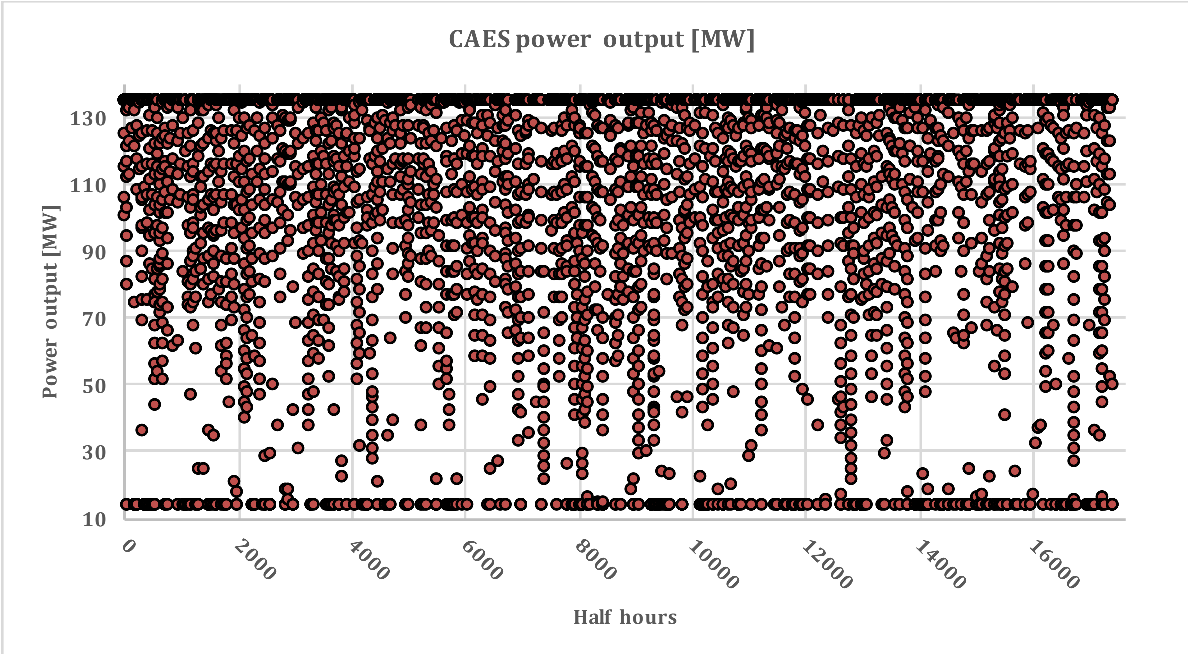

Figure 6-82: CAES power output at each time step (half hours) over a period of 52 weeks (Model: TE, Scenario: Base+Ancillary Services)

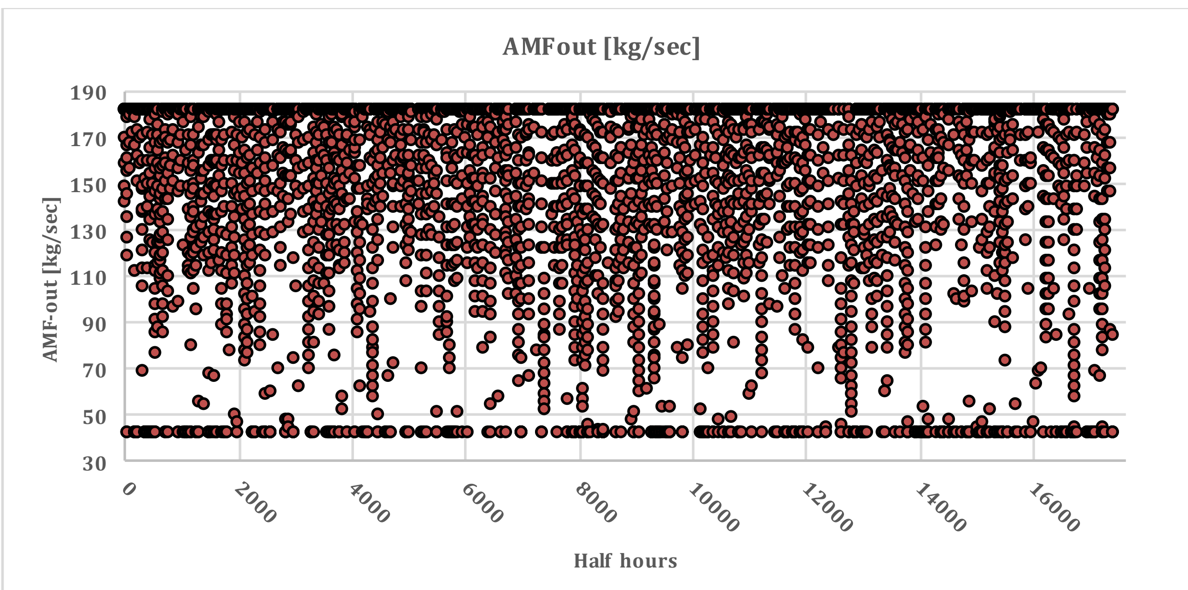

Figure 6-83: Air mass flow for expansion during each time increment (half hours) over a period of 52 weeks (Model: TE, Scenario: Base + Ancillary Services)

Chapter 7 Application of the combined UCED /Thermo-Economic CAES models in Ireland. A 2020 scenario with 40% renewable energy penetration

7.1 Chapter introduction

Ireland has set an ambitious 40% renewable energy (RE) penetration target for each of the RoI and NI grids; the vast majority - 37%- is expected to be wind. In 2014, the installed wind capacity in All Ireland was 2,400MW; the corresponding to this capacity wind energy penetration was 19%. Wind energy penetration in 2015 reached 24% according to EIRGRID and the installed capacity as of September of 2016 was 2,683MW; this is 30% of currently installed thermal capacity of 8689 MW. As of September of 2016, there are 3,083MW of installed wind capacity in All Ireland of which 2,441MW of this capacity being installed in the RoI. By 2020, 1,228MW of wind are expected to be installed in the NI and 3,925MW in the RoI. Such high penetration from variable RE resources would make Ireland one of the leading systems globally with regard to wind energy penetration. At the same time, however, achieving such high share of VRE is challenging. In this chapter a model of the Irish system as expected to be in 2020 is introduced. The magnitude of historic wind output profiles is increased to match the expected wind capacity in 2020. The objective of this part of the current study is to research if the target for 40% RE penetration is technically achievable considering the current instantaneous system non-synchronous penetration (SNSP) limit between 50% and 70%. The system is modeled with and without the addition of a 270MW CAES unit in the NI to identify the impact of CAES on decreasing wind curtailment and the operational cost of the system overall. The TE and

FP CAES models are used to identify the differences in both models and the results of the study are compared with relevant literature.

7.2 Impacts of high levels of wind integration in the Irish power system

Qualitative discussion around main issues arising from VRE integration in AI is presented below and quantitative results are given later in the Results section.

1. Frequency stability issues

The frequency level of a power system is a result of the rotational speed of conventional generators. Frequency can be disturbed if a mismatch between supply and demand occurs. In case of excess generation the generators are accelerated and system frequency increases. The opposite happens if there is shortage of electricity supply, like for example if a major component of the system – like a generator or a transmission line fails. Very high levels of wind penetration introduce into a system increased amounts of variability and uncertainty as explained in chapter 2. As a result the energy balancing process becomes more complex.

All power systems within the EU are required to maintain a frequency of 50Hz, with an error tolerance of no more than ± 0.5Hz. In Ireland frequency regulation under normal operational conditions takes place through an automated control system to a group of generators withholding spinning reserve capacity. Such type of reserve capacity is called dynamic reserve. In case of a contingency, frequency is regulated through different types of operating reserves each type operating at different time scales. The most critical response is provided by primary reserve that is the fastest acting type of reserve. There are two types of primary response:

- **Inertial response**: the inherent response of synchronized generators when a change in its rotational speed and thus kinetic energy occurs.
- **Fast response**: the automated action to increase generation from scheduled plant-for example, in the case of steam cycle plant- by releasing the potential energy stored as steam pressure within the boilers [62].

A primary operating reserve has to respond within 15 seconds after an incident occurred. Other types of contingency reserves that are deployed within longer time scales are the secondary operating reserves and tertiary reserves and have been discussed in chapter 6.

The previous discussion on frequency stability makes a point about the usefulness of synchronous generation on grid stability and issues related to reduced frequency regulating capabilities of power system. In conventional power systems there is a limit with regards to maximum permissible instantaneous level of non-synchronous generation such as wind. The current level of non-synchronous generation in All Ireland is 50%. However, the limit is expected to be increased up 75% by 2020 to facilitate wind penetration. EirGrid is currently designing ancillary services to remunerate providers of synchronous inertia and fast frequency response ($\leq$ 2 s full deployment) to increase SNSP limit [65].

The Irish system's instantaneous non-synchronous penetration limit is defined as [66]:

$$SNSP = \frac{Wind\ power\ [MW] + Electricity\ imports[MW]}{Electricity\ Demand\ [MW] + Electricity\ exports\ [MW] + Storage\ charging\ load[MW]}$$

[eq. 7-1]

If the SNSP level is breached the TSO takes action curtailing the excess amount of wind energy. During 2011, wind curtailment was only 2%[69] however, the level of curtailment is expected to increase as wind penetration grows. So far published estimates for the required installed capacity for AI have been mainly based on estimated wind capacity factors for specific regions and estimates about required operating reserves. However, these estimates do not account for the SNSP limit and therefore underestimate the actual curtailment that will take place and as a result the actual wind capacity required to reach 40% levels of wind penetration [67].

CAES is a technology that can enhance wind integration through (a) shifting time delivery of wind power to better satisfy demand, and (b) using excess wind energy in compression, energy that otherwise it would be curtailed. In this chapter the technical and economic value of CAES in 2020 will be estimated through comparing scenarios with and without CAES. Studies of hypothetical scenarios for an 80% RE penetration are in progress.

[69] It should be noted however, that Moyle was down and the only pumped storage unit being maintained during a high portion of 2011. As a result the system's ability to balance variability on net-demand was reduced

2. Lack of electricity export flexibility

Historical data suggest high correlation factors between wind output in GB and AI [68]. As a result it is likely that surpluses in both grids would happen at the same times, and for the AI would not be able to export surplus wind energy to GB. The reviewed data show that both Moyle and EWIC mainly import electricity from GB to AI and this is what we assumed will be the case in the considered 2020 scenarios.

3. High VRE levels might increase cycling of thermal generators

High wind penetration levels can potentially increase cycling of thermal generators. This is related to the variable nature of wind power. Cycling cost has three components (1) heat rate penalties, (2) cycling damage from ramping continuously and frequent start-ups/shut-downs and (3) the fuel and emission penalties of starting up frequently [69]. The impact of cycling damage is higher for systems that rely heavily on coal-fired and nuclear-fired generation. All-Ireland has a high share of gas-fired units and as a result high level of ramping flexibility. In this chapter we give emphasis on costs implications of wind integration from fuel penalties and changes on start-up patterns of thermal generators. We also report on the emissions increases due to generator cycling and to the benefits due to CAES in both direct costs and emission reductions.

4. **Impact of VRE on emissions**

Increased VRE penetration can cause heat rate penalties on thermal generators as discussed earlier. This has an environmental impact besides the economic one. The assessment of the environmental impact of VRE penetration must consider the net effect by comparing the total CO2 emissions of the system with and without VRE.

7.3 Development of scenarios

Table 7-1: List of scenarios.

	Reference	Reference + CAES FP	Reference + CAES TE	Reference + 25% more wind	Reference 25% more wind and 3x CAES FP	Reference with 25% more wind and 3x CAES TE
Existence of storage in RoI	Turlough Hills Pumped Hydro (292 MW)	Turlough Hills Pumped Hydro (292 MW)	Turlough Hills Pumped Hydro (292 MW)	Turlough Hills Pumped Hydro (292 MW)	Turlough Hills Pumped Hydro (292 MW)+ 2x 270MW CAES	Turlough Hills Pumped Hydro (292 MW)+ 2x 270MW CAES
Existence of storage in NI	No storage	270MW CAES	270MW CAES	No storage	270MW CAES	270MW CAES
Type of CAES model used	[-]	FP	TE	[-]	FP	TE
Wind Energy	15,232 MWh	15,232 MWh	15,232 MWh	19,028 MWh	19,028 MWh	19,028 MWh

The development of scenarios has the following two objectives

1. To study the benefits and impacts of high wind penetration with and without the existence of the proposed 270MW CAES plant in Larne, NI.
2. To research how the benefits of storage change if wind penetration and at the same time the size of storage are increased.

7.3.1 Reference scenario

The main characteristics/assumptions of the Reference scenario are:

1 Thermal generation

- **RoI**

According to EIRGRID's latest capacity statement [28] there is no major decommissioning expected by 2020 in the RoI.

The following two plants are expected to be commissioned before 2020 in the RoI:

1. Dublin waste to energy being 62MW.
2. Mayo biomass CHP 43MW.

- **NI**

The only significant generation currently planned in NI is:

1. Bombardier biomass power plant in 2016 with capacity of 18MW.

The following decommissioning is expected before 2020:

1 Retirement of Ballylumford open cycle gas turbine (OCGT) units 4,5 and 6 of a total capacity of 510MW.

After applying the changes above we get the following capacity mix for thermal generation in 2020 which is used in the 2020 Reference model.

Table 7-2: Capacity mix of thermal generation in All-Ireland in 2020.

	Type of generators (Number of generators)	Installed Thermal Capacity by Fuel and Region (MW)	% of Installed Thermal Capacity by Fuel and Region
ROI	**Natural Gas (17)**	4,234	65%
	Coal (3)	855	13%
	Distillate (6)	324	5%
	Oil (5)	588	9%
	Peat (3)	388	6%
	Waste/Biomass (2)	121	2%
	Total ROI (36)	**6,511**	**98%**
NI	**Natural Gas (7)**	1,182	64%
	Coal (2)	476	26%
	Distillate (4)	142	8%
	Oil (0)	0	0%
	Peat	0	0%
	Waste/Biomass (1)	33	2%
	Total NI (14)	**1,833**	**100%**
All-Island	**Natural Gas (24)**	5,417	66%
	Coal (5)	1,331	16%
	Distillate (10)	466	6%
	Oil (5)	588	7%
	Peat (3)	388	5%
	Waste/Biomass (3)	32	0.4%
	Total All-Island (50)	**8,222**	**100%**

2 Fuel prices

As explained in chapter 5, power stations in AI participate in the European carbon Trading Scheme (ETS). Projections for fuel prices and the price of carbon were obtained from source [70]. Final assumptions for fuel costs for year 2020 are shown on table 7-2. The final fuel prices include the cost of carbon that is shown in table 7-3.

Table 7-3: Fuel prices used in all 2020 scenarios.

Year	Quarter Start Date	Coal ROI (€/GJ)	Coal NI (€/GJ)	Gas ROI (€/GJ)	Gas NI (€/GJ)	Distillate ROI (€/GJ)	Distillate NI (€/GJ)	Oil ROI (€/GJ)	Peat (€/GJ)	Biofuel (€/GJ)
2020	Q1	5.7	6.1	9.3	9.32	19.6	20.0	17.0	7.3	2.7
2020	Q2	5.7	6.1	9.3	9.32	19.6	20.0	17.0	7.3	2.7
2020	Q3	5.7	6.1	9.3	9.32	19.6	20.0	17.0	7.3	2.7
2020	Q4	5.7	6.1	9.3	9.32	19.6	20.0	17.0	7.3	2.7

Table 7-4: Cost of carbon in 2020 and the associated additional cost on various fossil fuels.

Year	Quarter	Carbon (€/t)	*Coal (€/GJ)*	*Gas (€/GJ)*	*Distillate (€/GJ)*	*Oil (€/GJ)*	*Peat (€/GJ)*	*Biomass[a] (€/GJ)*
2020	Q1	41.6	3.90	2.32	3.07	3.20	4.1	0
2020	Q2	41.6	3.90	2.32	3.07	3.20	4.1	0
2020	Q3	41.6	3.90	2.32	3.07	3.20	4.1	0
2020	Q4	41.6	3.90	2.32	3.07	3.20	4.1	0

a: Biomass in not included on the ETS (source: [71])

3 Emission rates

The emissions rates of various fuels used in Ireland are included on the fuel cost calculator being available by CER and published on the SEM-O website. The emissions rates we are using for all 2020 scenarios are presented in table 7-4.

Table 7-5: Emissions rates of fuels used in all 2020 scenarios.

	Coal	*Gas*	*Oil*	*Distillate*	*Peat*[a]	*Biomass*[b]
Final Emission factor (tonne CO2/GJ)	**0.094**	**0.056**	**0.074**	**0.077**	**1**	**0**

a: Emissions rates for peat were obtained from http://www.volker-quaschning.de/index_e.php
b: Emissions rate for biomass are assumed to be zero in this thesis

4 Future demand and renewable penetration

A 2020 demand profile was created through scaling up historical demand data to match the forecasted demand level of around 41TWh. The peak demand for 2020 has been estimated at 7267 MW.

Wind output profiles for both the RoI and NI grids are used in the 2010 reference model were scaled proportionally based on the future wind capacity projections until wind provides 37% of energy production in 2020 for both the RoI and NI without considering potential curtailment. Zero fuel costs and VOM costs of €15MWh are assumed for wind production (see table 5-4).

Hydro capacity has not changed considerably since 2011 and is not expected to change up to 2020 according to EIRGRID. We use historical hydro energy limits for all 2020 scenarios. The UC model dispatches hydro energy based on least-cost principles assuming zero fuel costs and VOM costs of €4.6/MWh (see table 5-4).

5 Interconnections

The capacity of the North South interconnector has been increased to 1,100MW both ways to reflect EIRGRID's and SONI's plans to increase its current capacity of 450MW [72]. In the 2020 model we constraint electricity exports from AI to GB since it is questionable if GB will be able to import electricity during high wind periods as discussed before. The maximum transfer capacity of both Moyle and EWIC towards direction GB->AI is set to 400MW to reflect the need for reserve capacity as per EIRGRID and SONI directions [25].

6 SNSP limit

In the Reference scenario we assume all necessary steps towards increasing the SNSP limit from its current level of 50% to 75% will have been made by 2020. Thus we use a value of 75%.

7 Operating reserve margin

The operating reserve margin of the system from dispatchable sources and electricity import capacity has been imposed at 15% according to international practices [73]. This includes all types of flexible generators (gas and oil/distillate), storage units (CAES+pumped hydro) and 300MW out of the total 1000MW transmission capacity from EWIC and Moyle according to current practice of the AI operators.

8 Cost of wind curtailment

It is difficult to estimate the cost of wind curtailment for the overall system. The loss is high for the wind generators, however curtailment might be necessary if the security of the system is at risk or if wind penetration increases the total operational costs of the system. The cost of curtailment is an input into the UCED model and it is part of the objective function to be minimized. The higher the cost of curtailment the higher the contribution of the rest of the system to minimize curtailment. In this thesis an assumption for a cost of €100/MWh has been made.

7.3.2 Reference + 270MW CAES in NI scenario

Gaelectric[70] - a wind technology company- has proposed the development of a CAES project in NI. The potential of a CAES project has been viewed positively from EIRGRID and SONI [74]. If constructed the project will deliver ancillary services and facilitation of wind penetration. Twenty four-potential sites were initially appraised and a decision was made to go with a deep salt system that exists on Islandmagee, Larne in NI [75].

For the Base scenario we assume a 270MW CAES unit with 13 hours of storage. The technical information of the CAES unit was presented in chapter 6 table 6-2. We assume operation of 2x135MW CAES units in parallel to simulate operation of a 270MW unit.

[70] www.gaelectric.ie

The objective of the Reference+270MW CAES scenario -and for all scenarios that include CAES- is to identify the value/impact of a CAES unit in the overall system. I especially probe the following a) changes on the generation mix, b) environmental impact with a focus on CO2 emissions, c) facilitation of renewables and d) economic impact. Two variations of the Reference plus 270MW CAES in NI scenario are modeled. One with the FP model has been used and another one with the TE model. The objective of such a comparison is to identify the differences on the results when two different CAES models are used.

7.3.3 Reference +25% more wind + 3x 270MW CAES

This scenario explores the benefits/impacts of energy storage when a) wind production increases by 25% and b) as the installed capacity of storage is increased 3 times assuming all other parameters remain the same. The scenario was developed to study a power system with high storage capacity since the assumed total storage capacity is 1100MW or 14% of total AI demand in 2020. Total wind production is assumed to be 19TWh, 25% more compared to the Reference scenario. Out of 810MW of total installed CAES capacity, two thirds (540MW) are assumed to be located in the RoI while 270MW are assumed to be located in the NI. The wind production has been scaled up in the basis of the reference scenario. Two versions of this scenario are studied. One version where the CAES FP model is used and another version where the CAES TE model is used. Both of them are compared with the equivalent Reference scenario which is called Reference+25% more wind (no CAES).

7.4 Results and discussion

7.4.1 Summary of results

Natural gas will continue being the major fuel used for power production in 2020 according to the Reference scenario results. Natural gas contributes with 38.2 % of demand in 2020 compared to 44% in 2014 (see figure 4-17). According to the same scenario actual wind penetration will be ~36% or 14.85TWh. Wind together with biomass and hydro are contributing around 20.5% of total internal demand.

The inclusion of one 270MW CAES unit in NI can help reduce wind curtailment by 22%, CO2 emissions by 150,000 tonnes and system costs by € 6 million per year. If an FP model had been used instead the reductions would be: wind curtailment by 28%, CO2 emissions by 270,000 tonnes and annual system costs by €13 million. Thus, the results show that existing FP models overestimate the benefits of CAES units in a power system and for that reason the more accurate TE model should be used in order to study the effects of CAES on facilitating VRE integration. According to the TE model the major CAES cost reductions come from a) reduction of coal fired generation and b) reduction on wind curtailment compared to the Reference model. A single unit of CAES according to the TE model reduces total coal production by 0.2TWh while increases the usage of imported electricity by 0.1TWh and penetration of wind by another 0.1TWh The results if an FP CAES model was used are similar but magnified since the CAES unit is used for as 5 as time as much time in the FP compared to the TE model. In the FP model coal fired generation reduction reaches 0.4TWh while rest of figures are comparable with the TE model. However, in the FP model CAES operates more time and the resulting expense of natural gas for CAES operation is almost 5 times as much. Any reduction on coal generation is party compensated by natural gas burned in the CAES unit. When only 1 CAES unit is used the effect of the CAES unit on thermal start-ups differs depending on the CAES model. The CAES unit in the FP model leaves the number of start-ups of thermal units unchanged mostly because CAES arbitrages coal based electricity. The CAES unit in the TE model increases start-ups by 20% because it operates for less hour trying to increase system flexibility, albeit allow small flexible oil and gas units operate more often for little time.

As explained earlier, additional scenarios were tested where wind installed capacity was increased by 25% and CAES capacity was tripled to 810MW, with two thirds of CAES capacity being installed in the RoI. This model version also has its Reference version In the Reference + high wind scenario total wind production is ~19TWh. Wind penetration reaches ~42% compared to ~36% in the Reference scenario. Total wind curtailment reaches 1.5TWh or ~8% of total wind energy produced.

If 810MW of CAES were added and the TE model was used all three CAES units would reduce wind curtailment by 36% compared to the Reference scenario (or by 650,000MWh). At the same time total CO2 emissions would be reduced by 550,000 tonnes almost 4 times as much as in the Reference + CAES TE model. What is a striking finding though is that total system costs would be reduced by €86 million which is a much higher number compared to the Reference+270MW CAES scenarios (both TE and FP). The same reductions described above can be expressed on a per 270MW CAES units basis. If we divide the figures by three we are getting 12% reduction on wind curtailment (or 188,000MWh), €29 millions on total system costs and 180,000 tonnes of CO_2 per CAES unit (TE model). The same reductions per 270MW CAES (FP model) are: 14% reduction on wind curtailment (or 217,000MWh), €25.6 million on total system costs and 180,000 tonnes of CO_2. Even though reduction on CO_2 emissions is lower for the high wind+3x CAES scenarios, the reduction on wind curtailment and total system costs significantly increases per unit of storage device (see table 7-11). Thus a major conclusion of the analysis is that the economic benefit of CAES hugely increases with a) increased installed capacity of wind and b) increased usage of storage capacity. One 270MW CAES unit according to the more accurate TE model brings less than half the economic benefit to the system compared to the FP model. However, if the storage capacity is increased considerably each CAES unit -according to the TE model- brings around 10 million Euros more benefit compared to the FP model. It should be noted however, that the positioning of storage in RoI where the majority of supply and demand takes place might have boosted the significance of CAES as well. The following sections present detailed discussion around each of the scenarios modeled.

Table 7-6: Generation based on fuel and region for all 2020 scenarios.

	Generation Coal RoI (MWh)	Generation Coal NI (MWh)	Generation Gas RoI (MWh)	Genration Gas NI (MWh)	Genration Distillate RoI (MWh)	Genration Distillate NI (MWh)	Generation Oil RoI MWh)	Generation biomass (MWh)	Generation Peat (MWh)	Imported electricity (MWh)	Wind (MWh)	Hydro (MW)
Reference	1,068,338	74,366	12,723,898	3,129,986	4,167	3,064	24,926	1,065,582	2,006,915	5,737,947	14,850,991	871,819
Reference +270MW CAES FP (NI)	698,414	30,678	12,736,773	3,043,676	4,667	2,399	16,530	1,065,823	2,008,668	5,849,770	14,958,812	871,819
Reference +270MW CAES TE (NI)	883,922	64,520	12,581,885	3,295,485	6,748	4,834	19,801	1,065,516	2,011,926	5,835,305	14,935,956	871,819
Reference w 25% more wind	936,890	90,235	11,454,535	2,756,591	7,162	4,581	36,418	1,057,216	1,969,335	4,870,315	17,491,419	871,819
Reference w 25% more wind + 3x CAES (540 MW in RoI,	222,472	15,159	10,771,031	2,426,391	3,985	2,355	10,256	1,065,346	2,009,949	5,207,987	18,139,576	871,819
Reference w 25% more wind + 3x CAES (540 MW in RoI, 270MW in NI)	524,791	21,631	11,129,522	2,757,367	11,657	24,403	12,164	1,045,495	1,975,033	5,021,296	18,055,469	871,819

Table 7-7: Energy mix based on fuel and region for all 2020 scenarios.

	Share of Coal ROI (%)	Share of Coal NI (%)	Share of Gas ROI (%)	Share of Gas NI (%)	Share of Distillate ROI (%)	Share of Distillate NI (%)	Share of Oil RoI (%)	Share of Biomass (%)	Share of Peat (%)	Share of Electricity Imports (%)	Share of Wind (%)	Share of Hydro (%)
Reference	2.6%	0.2%	30.7%	7.5%	0.0%	0.0%	0.1%	2.6%	4.8%	13.8%	35.8%	2.1%
Reference +270MW CAES FP (NI)	1.7%	0.1%	30.7%	7.3%	0.0%	0.0%	0.0%	2.6%	4.8%	14.1%	36.1%	2.1%
Reference +270MW CAES TE (NI)	2.1%	0.2%	30.3%	7.9%	0.0%	0.0%	0.0%	2.6%	4.9%	14.1%	36.0%	2.1%
Reference w 25% more wind	2%	0%	28%	7%	0%	0%	0%	3%	5%	12%	42%	2%
Reference w 25% more wind + 3x CAES FP (540 MW in RoI,	1%	0%	26%	6%	0%	0%	0%	3%	5%	13%	44%	2%
Reference w 25% more wind + 3x CAES TE (540 MW in RoI, 270MW in NI)	1%	0%	27%	7%	0%	0%	0%	3%	5%	12%	44%	2%

Table 7-8: Wind penetration and curtailment figures based on geography for all 2020 scenarios.

	Wind penetration RoI (MWh)	Wind penetration NI (MWh)	Total wind penetration	Wind curtailment RoI (MWh)	Wind curtailment NI (MWh)	Total wind curtailment (MWh)	Wind penetration RoI (%)	Wind penetration NI (%)	Total wind penetration (%)	Wind curtailment RoI (%)	Wind curtailment NI (%)	Total wind curtailment (%)
Reference	11,099,127	3,751,865	14,850,991	309,998	70,680	380,678	35.7%	36.2%	35.8%	2.7%	1.8%	2.5%
Reference +270MW CAES FP (NI)	11,166,278	3,792,535	14,958,812	242,847	30,010	272,857	35.9%	36.6%	36.1%	2.1%	0.8%	1.8%
Reference +270MW CAES TE (NI)	11,147,615	3,788,342	14,935,956	261,510	34,203	295,713	35.9%	36.6%	36.0%	2.3%	0.9%	1.9%
Reference w 25% more wind	12,972,020	4,519,400	17,491,419	1,257,142	280,337	1,537,479	41.7%	43.6%	42.2%	8.8%	5.8%	8.1%
Reference w 25% more wind + 3x CAES FP (540 MW in RoI, 270MW in NI)	13,495,305	4,644,270	18,139,576	733,886	155,436	889,321	43.4%	44.8%	43.8%	5.2%	3.2%	4.7%
Reference w 25% more wind + 3x CAES (540 MW in RoI, 270MW in NI) TE	13,421,499	4,633,969	18,055,469	807,692	165,737	973,428	43.2%	44.7%	43.6%	5.7%	3.5%	5.1%

Table 7-9: Break down operational costs of the Irish system for all 2020 scenarios.

	Total System costs [€/MWh]	Total System Costs [€m]	Operational Costs Coal-RoI [€m]	Operational Costs Coal-NI [€m]	Operational Costs Gas-RoI [€m]	Operational Costs Gas-NI [€m]	Operatinal cost of CAES [€m]	Operational Costs Distillate-RoI [€m]	Operational Costs Distillate-NI [€m]	Operational Costs Oil [€m]	Operational Costs Biomass [€m]	Operational Costs Peat [€m]	Operational Costs Wind [€m]	Operational Costs Hydro [€m]	Start-Up Costs [€m]	Cost of wind curtailment [€m]	Cost of electricity imports [€m]
Reference	39.7	1,648	73.6	5.9	821.1	203.3	0.0	1.0	0.9	6.1	3.7	27.9	222.8	3.5	30.7	38.1	209.7
Reference +270MW CAES FP (NI)	39.6	1,635	48.1	2.5	815.7	196.1	41.4	1.2	0.7	4.3	3.7	27.9	224.4	3.5	26.2	27.3	212.3
Reference +270MW CAES TE (NI)	39.5	1,642	60.9	5.2	809.1	214.4	7.3	1.7	1.5	4.9	3.7	28.0	224.0	3.5	33.9	29.6	214.8
Reference w 25% more wind	40.3	1,673	64.6	7.3	751.4	181.1	0.0	1.8	1.3	8.2	3.7	27.4	262.4	3.5	29.7	153.7	177.5
Reference w 25% more wind + 3x CAES FP (540 MW in RoI, 270MW in NI)	39.2	1,597	15.3	1.2	685.9	155.2	129.1	1.0	0.7	2.7	3.7	27.9	272.1	3.5	21.9	88.9	187.3
Reference w 25% more wind + 3x CAES TE (540 MW in RoI, 270MW in NI)	38.3	1,587	36.1	1.7	714.8	180.0	28.6	2.8	6.8	3.0	3.7	27.5	270.8	3.5	26.6	97.3	183.9

Table 7-10: Emissions factors based on fuel, overall emissions factor of the Irish grid and number of start-ups of thermal generators for all 2020 scenarios.

	Total CO2 emissions [million tons]	Average emissions factor of coal (g CO2/kWh)	Average emissions factor of gas (g CO2/kWh)	Average emissions factor of distillate (g CO2 /kWh)	Average emissions factor of oil (g CO2/kWh)	Average emissions factor of peat (g CO2/kWh)	Average Irish grid emissions factor (g CO2/kWh)*	Number of start ups
Reference	9.90	1,025	377	1,031	6,779	954	238	5,784
Reference +CAES FP	9.63	1,016	373	1,033	4,379	954	233	5,492
Reference +CAES TE	9.76	1,025	377	1,063	3,386	954	235	6,914
Reference w 25% more wind	9.23	1,034	384	1,003	5,227	955	222	5,783
Reference w 25% more wind + 3x CAES FP	8.68	1,032	371	1,087	3,267	954	213	5,111
Reference w 25% more wind + 3x CAES TE	8.68	1,010	377	983	1,266	954	209	5,964

Table 7-11: Benefits per 270MW CAES unit for different scenarios*.

	Reference +CAES FP	Reference w 25% more wind + 3x CAES FP	Reference +CAES TE	Reference w 25% more wind + 3x CAES TE
CO2 emissions reduction per 270 MW CAES unit [million tons]	0.27	0.18	0.14	0.18
Wind curtailment reduction per 270MW CAES unit [GWh]	108	216	85	188
Total system cost reduction per 270MW CAES unit [million euros]	12.8	25.6	5.9	28.8

*The reduction refer to the relevant Reference scenario. For example the reductions for the Reference+CAES FP scenario have been calculated by comparing with the Reference scenario. The reductions for the Reference + 25% more wind + 810MW CAES have been calculated by comparing with the Reference + 25% more wind.

7.4.2 Reference scenario

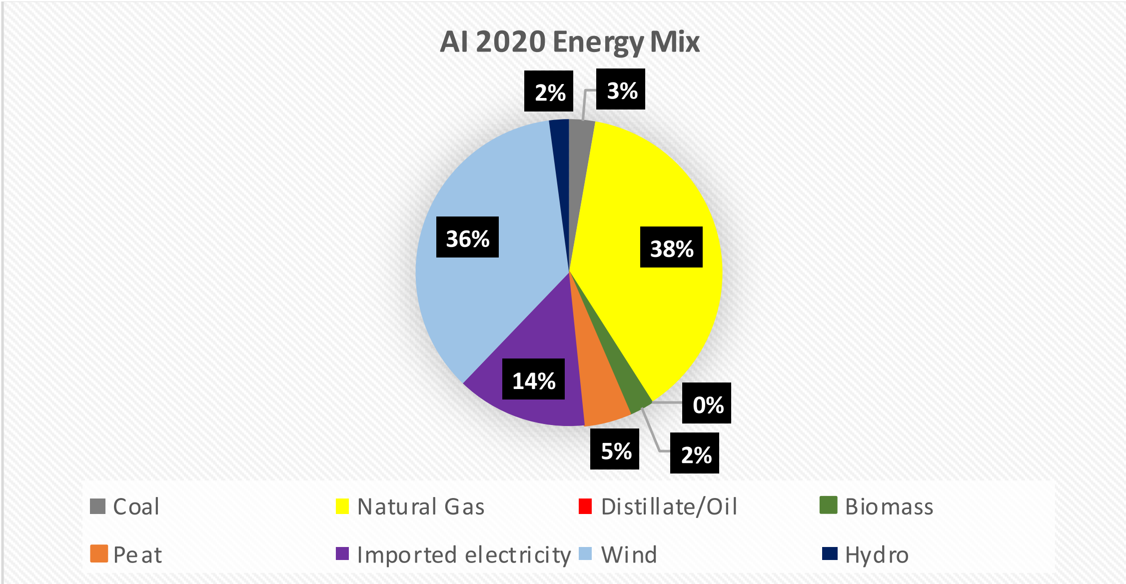

Figure 7-1: Energy mix in AI in 2020. (Scenario: Reference).

In 2020, 36% of total energy will come from wind based on EIRGRIDs and SONI's wind capacity projections. Around 2% of total energy production will be hydro based and another 2% from biofuels so that the total RE generation will be 40% according to AI RE targets. The UCED model results for the Reference scenario show that the balance of the generation will come from natural gas fired units (38%) while coal fired generation will only be 3%. Electricity imports from GB will reach 13% of annual demand. Indigenous peat production will be 5%.

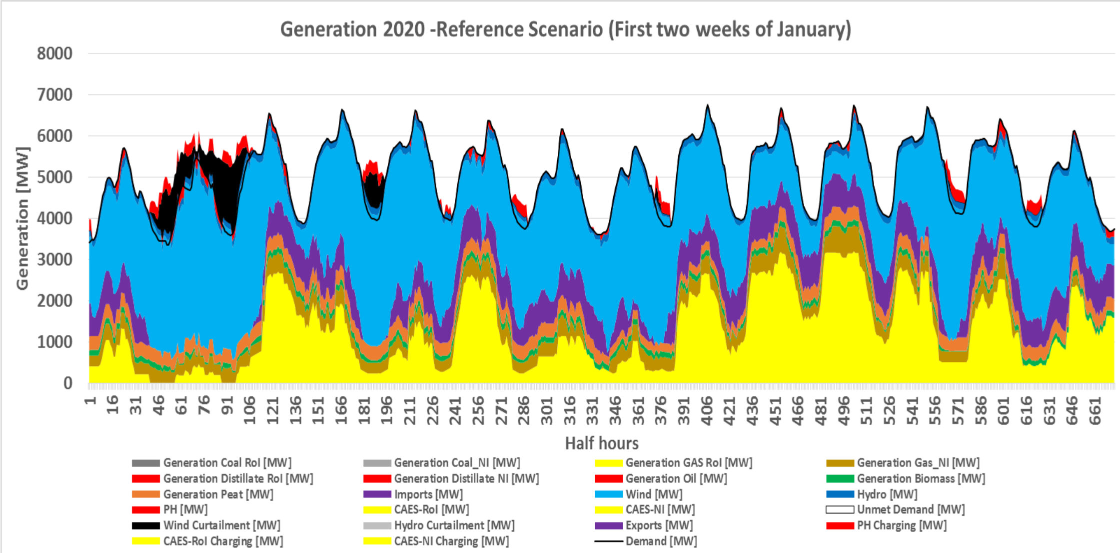

Figure 7-2: Generation per fuel over the first two weeks of January 2020 in AI (Scenario: Reference).

Figures 7-2 and 7-3 show generation over the first two weeks in the beginning of the year (January) and the middle of the year mid-June respectively. Figure 7-2 depicts two weeks with high wind penetration and high demand (6,900MW peak demand for the two week period) while figure 7-3 depicts two weeks with lower wind penetration and lower demand levels (5,500MW peak demand for the two week period). Any output over the demand line represents either wind spillage or additional load created by storage units. Whenever there is additional load there is also additional generation to satisfy this load. The red color corresponding to the pumped hydro units should not be confused with the red color corresponding to oil/distillate fired generation. Pumped hydro related pumping/generating of electricity has been placed adjustment to the demand line. Depiction over the line corresponds to the pumped hydro unit pumping while under the line corresponds to the unit generating. During periods of high wind output there is wind energy spillage unavoidably. The ability of thermal generators to absorb wind output is constrained by the following factors:

1 **The system's NSPS**: Wind penetration can never exceed 75% of demand plus the extra load created when the pumped hydro unit operates. In that respect storage units create additional load, a portion of which[71] can be used to absorb wind energy that otherwise would have been curtailed. It is important that pumped hydro and CAES are both synchronous spinning generators that can contribute on VRE facilitation while other non-synchronous storage devices like batteries cannot.

2 **The system's reserve margin**: At each moment the reserve capacity of thermal units, energy storage units and of Moyle and EWIC[72] needs to be equal to 15% of total system demand. This is the reason, wind penetration can never reach 100% in a system that does not have exporting capabilities. As explained before in this study an assumption has been made that GB won't be able to accept over generation from Ireland due to similar wind resource patterns. An interesting finding of this simulation is that the pumped hydro unit is standby for the most of the time providing spinning reserve[73] rather than pumping during periods of wind curtailment. This happens because the equivalent reserve capacity would otherwise need to be provided by additional thermal generators that unlike pumped hydro units have a minimum operating point. Such a unit would unavoidably need to start-up and provide additional thermal output that will further increase wind curtailment. Thus any benefit of curtailment reduction would be lost. System wide wind curtailment depends on the specified as an input in the model cost of wind curtailment; at the specified value of €100/MWh, there is optimal value

[71] The portion of pumping load that can be used to absorb wind power depends on the NSPS limit according to equation 7-1.
[72] We assume 300MW out of total 1,000MW from regional interconnections is secured as reserve capacity
[73] Unlike thermal generators that require considerable time to synchronize from a cold start, pump hydro units can get loaded almost immediately and for that reason it is assumed they are "spinning" with almost zero output providing reserve capacity.

when the hydro unit provides reserve capacity. When additional storage capacity is available the potential reserve capacity from storage units is increased and their ability to reduce wind curtailment is also increased. This is evident on scenarios that include CAES as well (see section 7.4.3).

3 **The ramp rates and minimum up and down times of thermal generators**: There is limited ability of thermal generators to balance net demand based on their technical characteristics. This is one the main reasons coal generation is greatly reduced compared to 2010 scenario modeled in chapter 5 even though coal is cheaper than gas. Coal generators are not flexible enough to accommodate wind generation and additionally their very high start-up costs renders any possibility for increased cycling uneconomic.

Total wind curtailment in 2020 reaches 524GWh or 3.4% of total wind production of 14.8TWh. This is a good figure for such a high wind penetration and it a result of the 1) the good dispersion of wind farms in AI that reduces wind variability, b) the plans of the operators on increase the SNSP from current levels of 50% to 75% and c) investments on flexible gas capacity over the last decade (for example the 435MW ESB Aghada CCGT that was built in 2014).

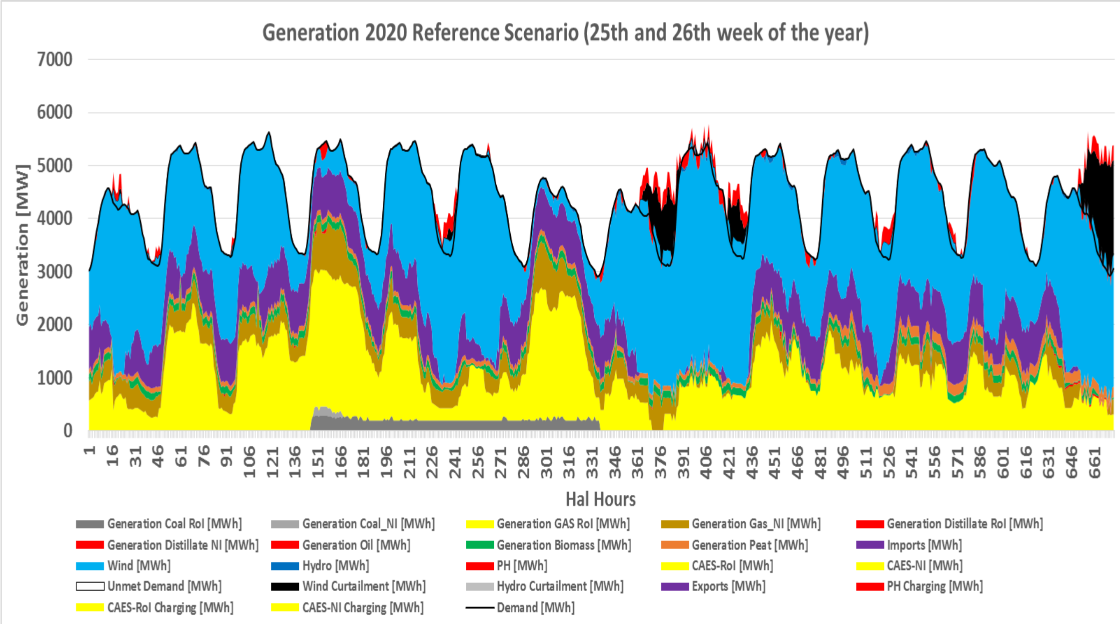

Figure 7-3: Generation per fuel over the 25th and 26th week of 2020 (mid-June) in AI (Scenario: Reference).

The resulting cycling of thermal generators has impact on the emissions trend as shown in figures 7-4 to 7-7. Figures 7-4 and 7-5 correspond to the same period of generation as in figures 7-1 and 7-2 respectively. In figures 7-4 and 7-5 one can observe the following:

a. Gas fired generators emit in the range of 350 to 450grCO2/kWh during normal operation. The lower limit corresponds to operation near optimal point and the higher limit corresponds to part loading conditions. Start-up of gas generators can produce up to ~1000$\frac{gr\ CO2}{kWh}$. It should be noted that in this thesis start-up emissions correspond to emissions from thermal energy required to start-up thermal units and are allocated to the first half-hour of their operation. Emissions from gas-fired generation cycling can be observed better in graph 7-6 which is a copy of figure 7-4 zooming into the emissions range that corresponds to gas generators.

b. Peat and coal related emissions in the RoI don't seem to vary during normal operation since the cycling of the generators corresponding to those fuels is being avoided. However, emissions from the Killroot station (the only coal fired unit in NI) vary a lot due to the thermal characteristics of the generator that have been discussed in chapter 5.

c. Emissions from oil/distillate-fired generators vary. Oil/distillate generators are usually called in to balance rapid variations in demand and for that reason operate most of the time far from their optimal point. Figure 7-8 depicts average emissions per fuel type in a weekly basis. It is evident that oil generators as well the Killroot unit (coal-NI) are the most sensitive to cycling with regards to their emissions levels.

d. Figure 7-7 shows emissions over the whole year and in addition the y-axis range has been increased to 12,000$\frac{gr\ CO2}{kWh}$ to show the level start-up emissions from coal-fired and oil-fired generators that operate on steam cycles. Emissions from such generators can reach up to ~11,000$\frac{gr\ CO2}{kWh}$ due to the vast amount of energy required to heat water and produce steam.

e. The trends explained on a) to d) above are similar for both January and June (and throughout the year). Emissions change according to generation patterns that exist for each month accordingly.

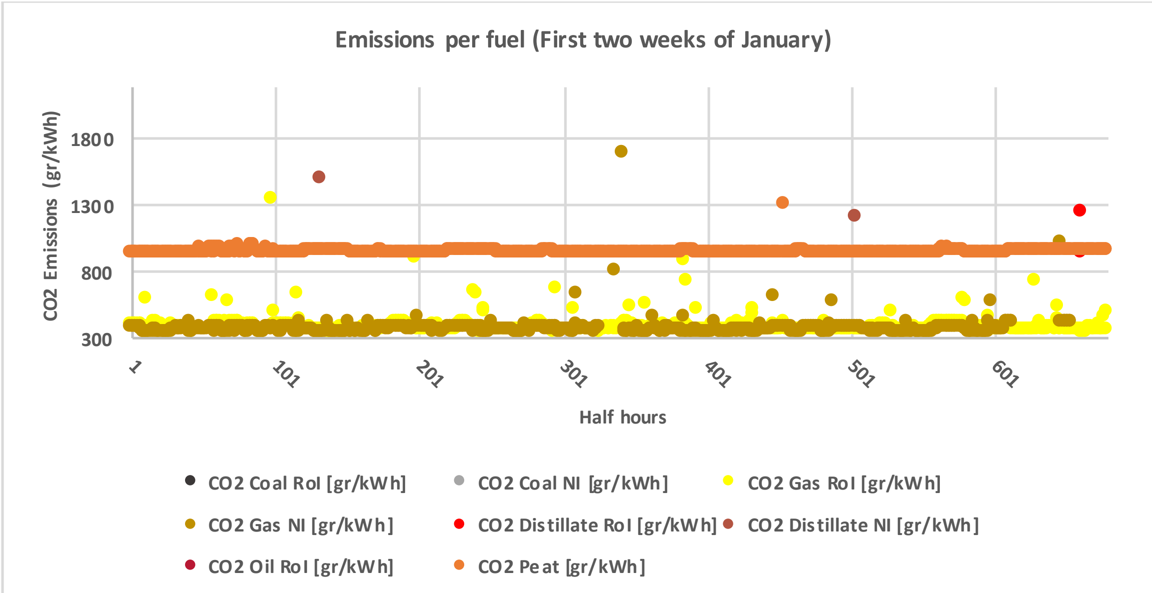

Figure 7-4: CO2 emissions over the first 2 weeks of January (Scenario: Reference).

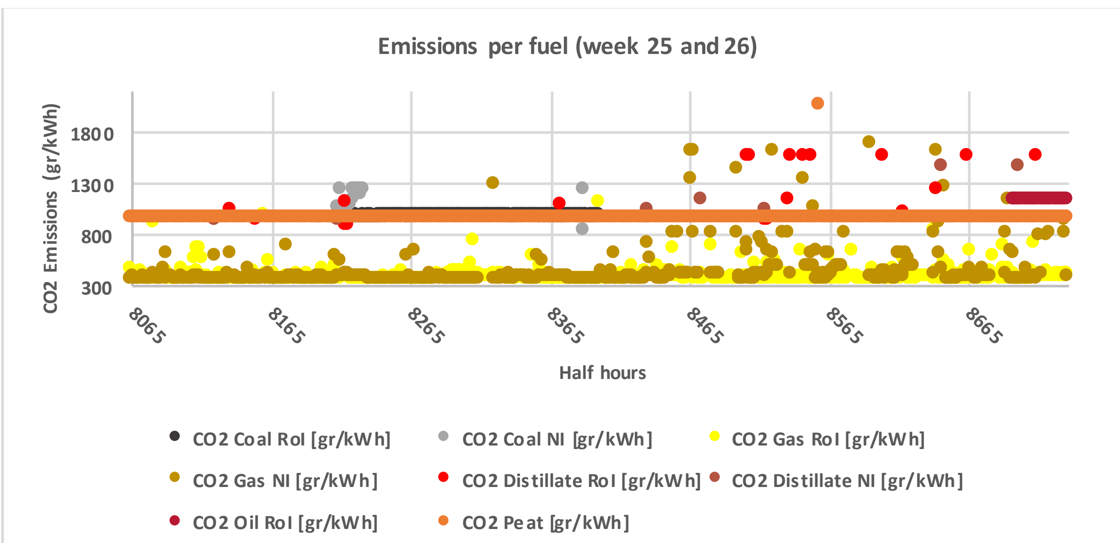

Figure 7-5: CO2 emissions over weeks 25 and 26 (Scenario: Reference).

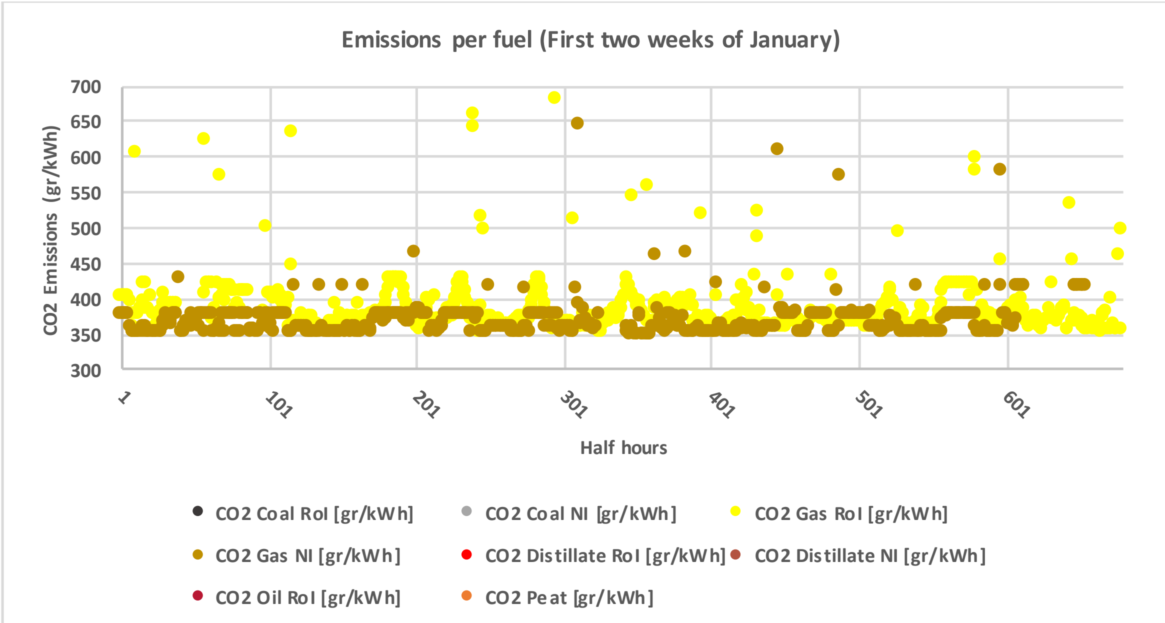

Figure 7-6: CO2 emissions over the first 2 weeks of January (Scenario: Reference).

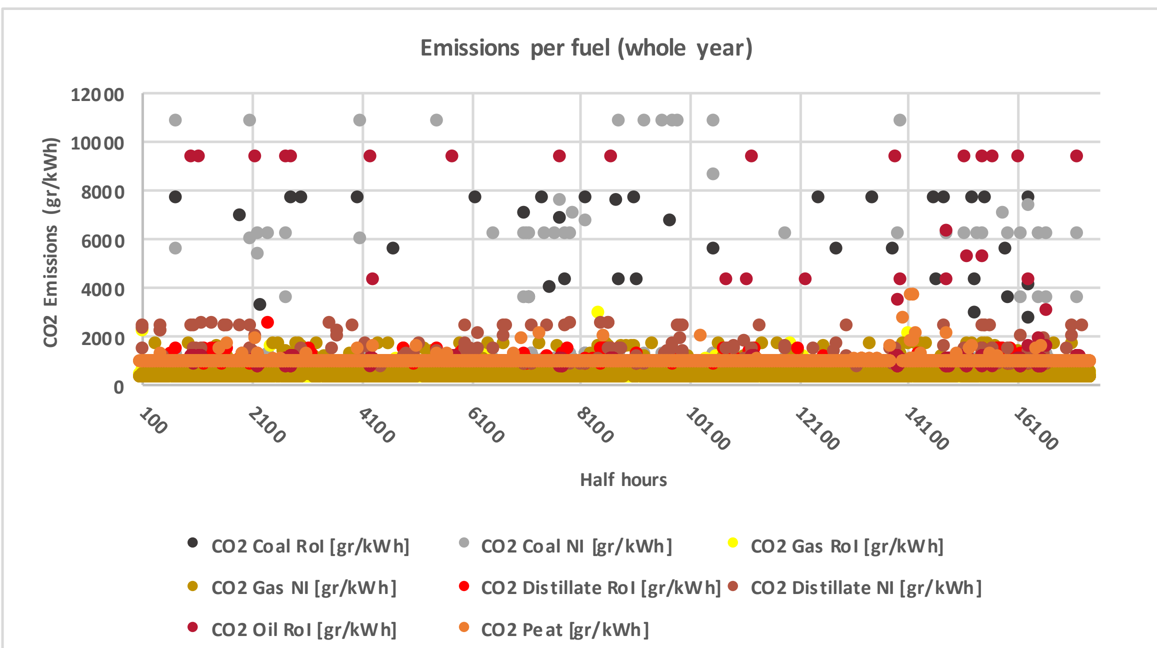

Figure 7-7: CO2 emissions over the whole year (Scenario: Reference).

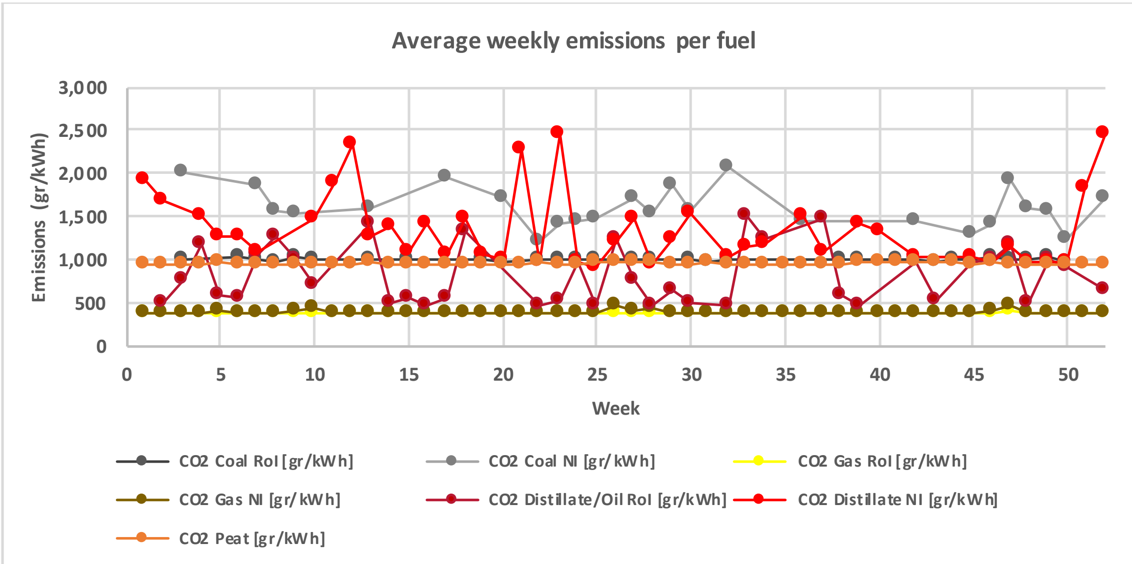

Figure 7-8: Average emission levels per week for various fuel types (Scenario: Reference).

The discussion around emissions trends in AI applies to all scenarios and it won't be repeated from this point and on and will be briefly discussed again in section 7.4.5. Any differences on emissions per unit of energy produced across scenarios are small and related to the levels of wind penetration in the AI system (see table 7-9).

Total average operational cost of the Irish system in 2020 will be €39.7/MWh for the Reference scenario. A breakdown of operational system costs per unit of energy produced is shown in figure 7-9. There is negative correlation between total system cost and wind penetration as expected due to the low production cost of wind power. The most important operational cost components for the Reference scenario are the cost of natural gas and the cost of imported electricity.

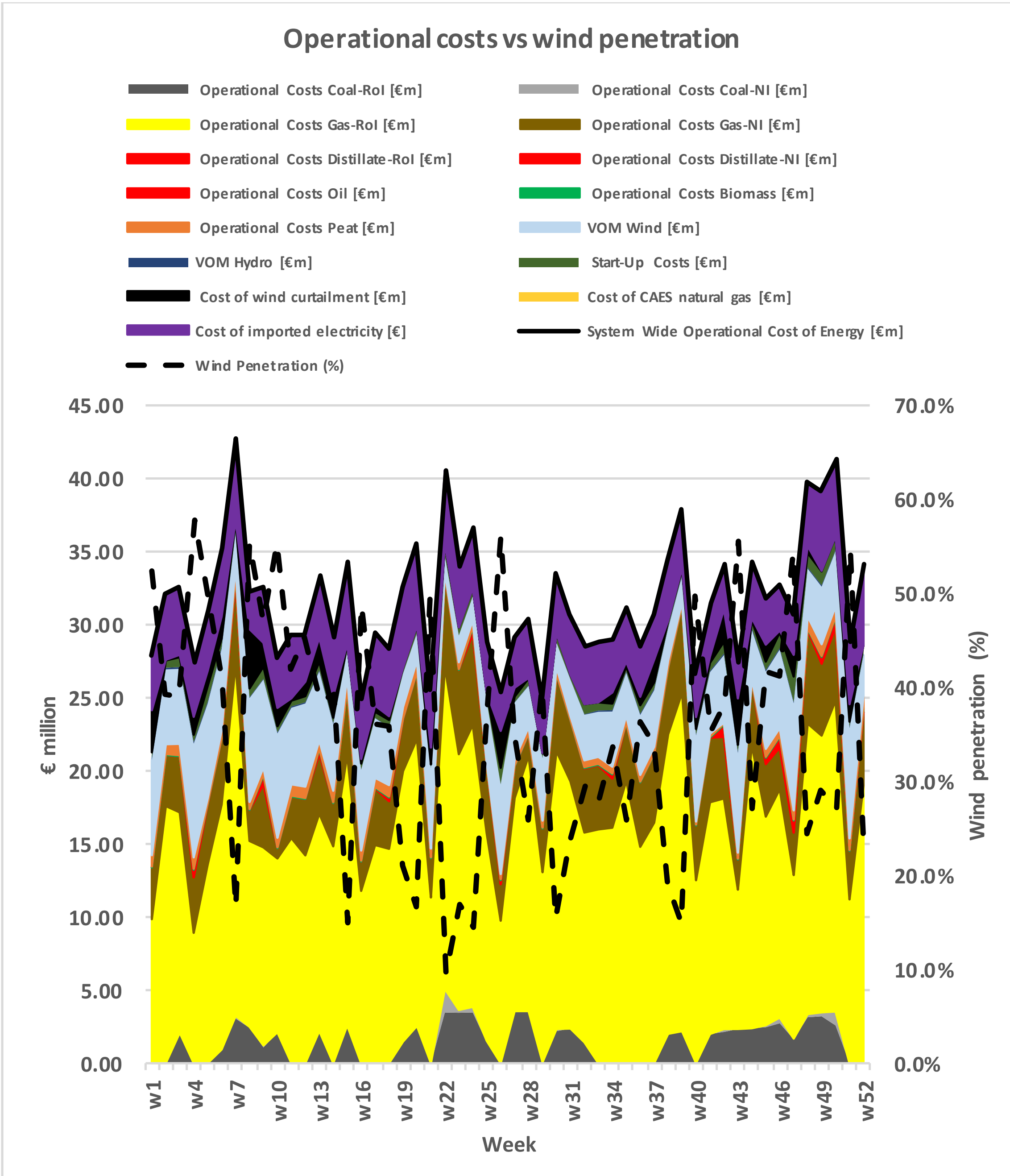

Figure 7-9: Breakdown of operational costs of the Irish system on a weekly basis (€/MWh) (Scenario: Reference).

7.4.3 Scenario: Reference + 270MW CAES in NI (FP model)

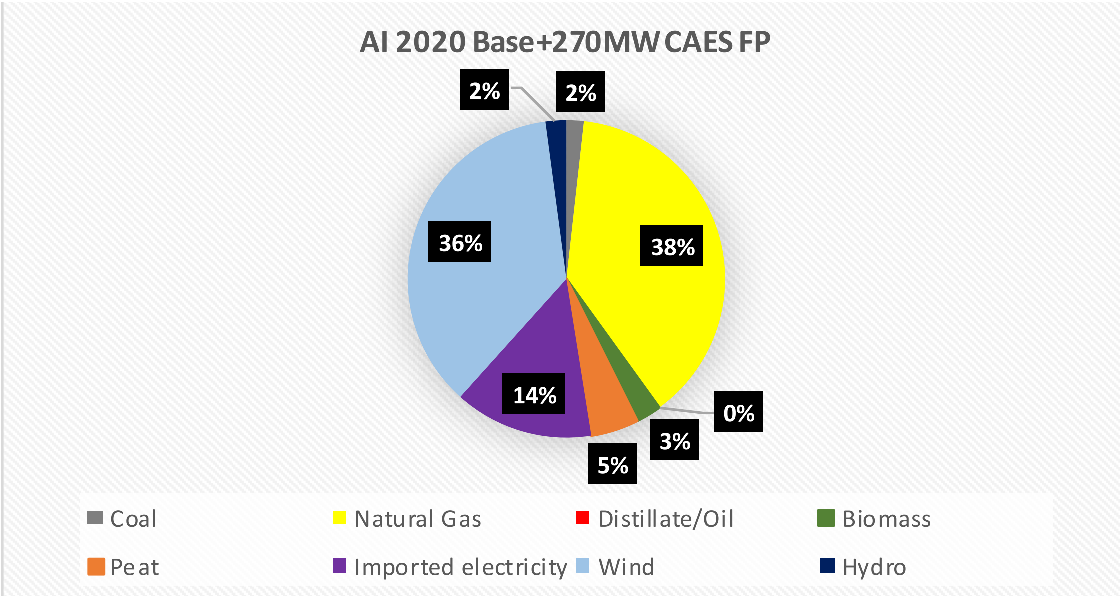

Figure 7-10: Energy mix in AI in 2020. (Scenario: Reference+270MW CAES in NI (FP)).

The main change in the generation mix due to the presence of one 270MW CAES unit in the NI is 30% reduction of coal-fired generation from 1.15TWh to 0.73TWh (the share of coal fired generation drops from 2.8% to 1.7%). The energy difference is mainly balanced through a) increased amounts of imported electricity, b) utilization of 107GWh wind power that would have been otherwise been curtailed by the CAES unit and c) the utilization of the equivalent heat amount of around 4,406 GJ from burning natural gas to operate the CAES unit. Based on the above there is a related reduction on total system emissions by 270,000tons[74] (see table 7-9).

[74] The emissions factor of the GB grid in 2020 has been assumed 400g/kWh and is applied to estimate the contribution of imported electricity on total emissions in this thesis. The current emissions factor of the GB grid is around 500g/kWh. (source: http://www.carboncredentials.com/2015-emissions-factors-released-what-implications-for-201516-crc-forecasting/)

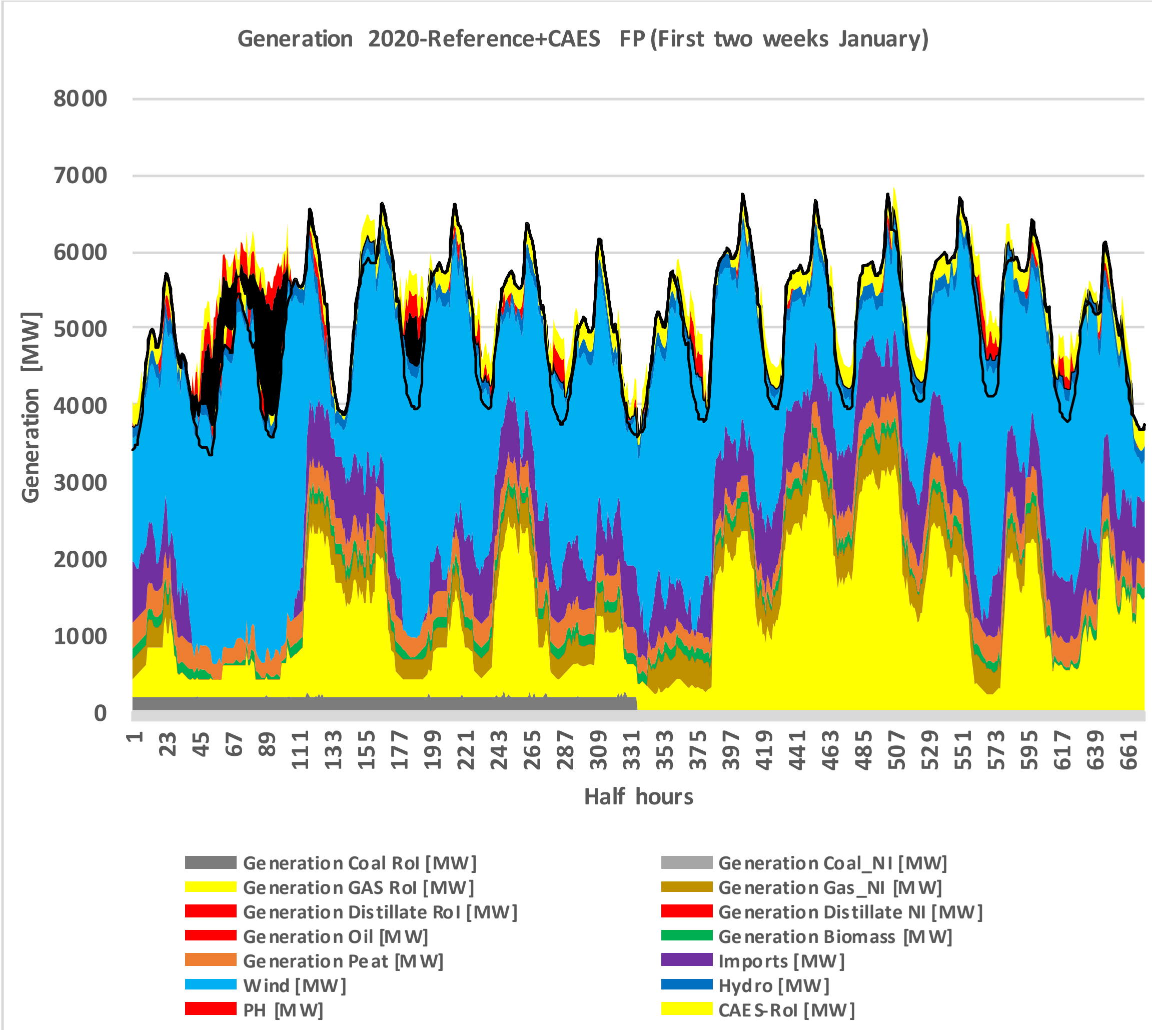

Figure 7-11: Generation per fuel over the first two weeks of January 2020 in AI (Scenario: Reference+270MW CAES in NI (FP)).

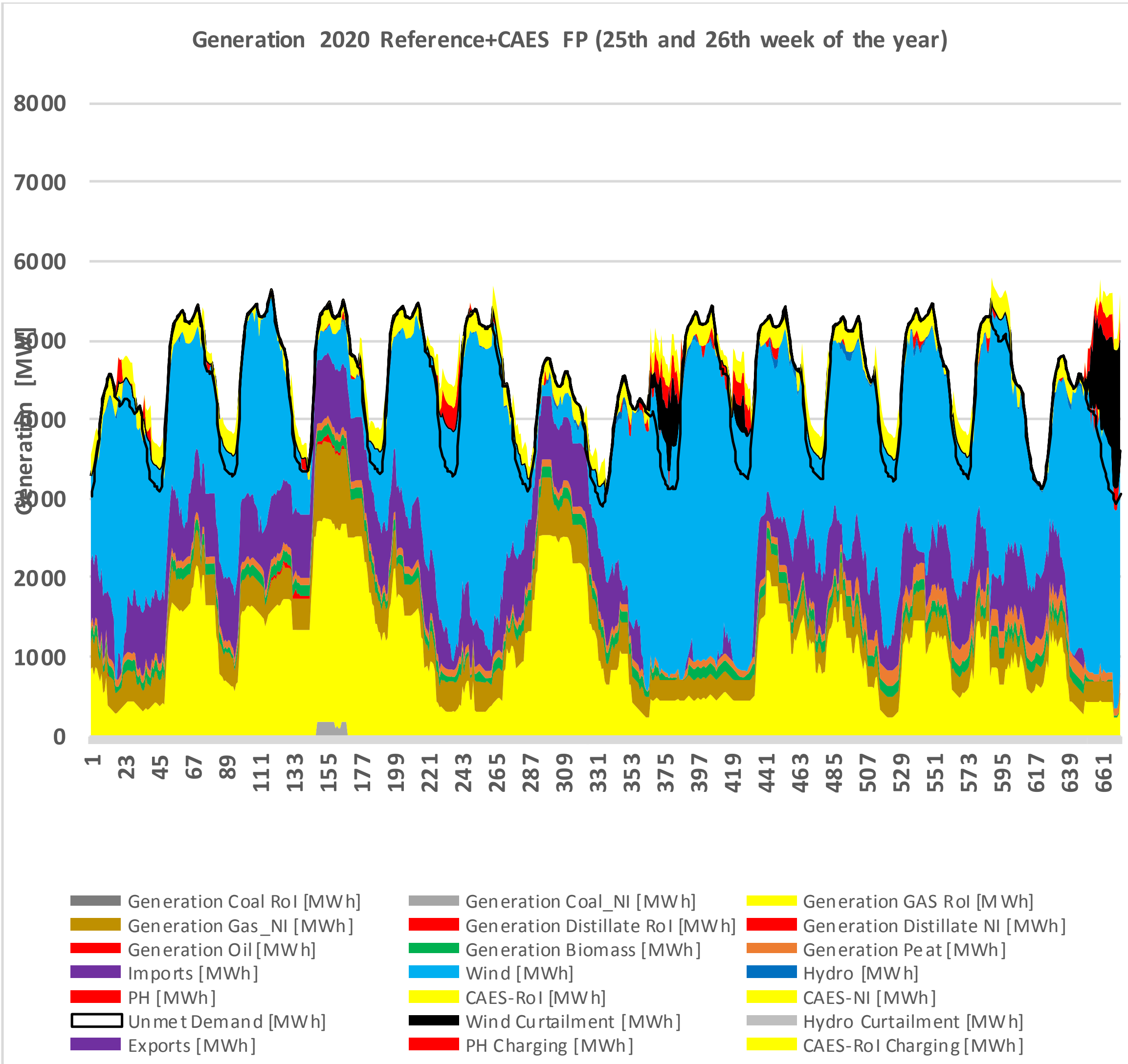

Figure 7-12: Generation per fuel over the 25th and 26th week of 2020 (mid-June) in AI (Scenario: Reference+270MW CAES in NI (FP)).

Figures 7-12 and 7-13 show generation over the same two weeks presented in the Reference scenario (see figures 7-2 and 7-3). Similarly as in the pumped hydro unit, CAES operation is adjacent to the demand line but in yellow color. The yellow color should not be confused with the yellow representing natural gas generation. Operation above the demand line represents charging while below the demand line discharging of the unit. The presence of CAES further increases available capacity for provision of ancillary services.

However, CAES is used mainly for the following purposes: a) reduction of wind curtailment (this is depicted when CAES is charging during high wind output periods) and b) to provide immediate load following services (this is depicted when CAES operates during rapid increase/decrease of the net load and c) peak load reduction (this happens when CAES discharges during peak periods to prevent expensive peak units from coming on line). In addition, the existence of CAES decreases the number of start-ups of thermal generators by 5% (292 less start-ups over the whole year compared to the Reference scenario).

The benefits of CAES presented above can be translated to cost reductions in the overall system. The reduction on total system operational cost is equal to €12 million. The most important cost savings in the system are related to reduction on wind curtailment and on reduction on coal consumption for power generation. Both costs have been reduced by €39 million. The average operational system cost in the "Reference+270MW CAES (FP) in NI" scenario is €39.6/MWh. A break-down of operational system costs in a weekly basis is given in figure 7-13.

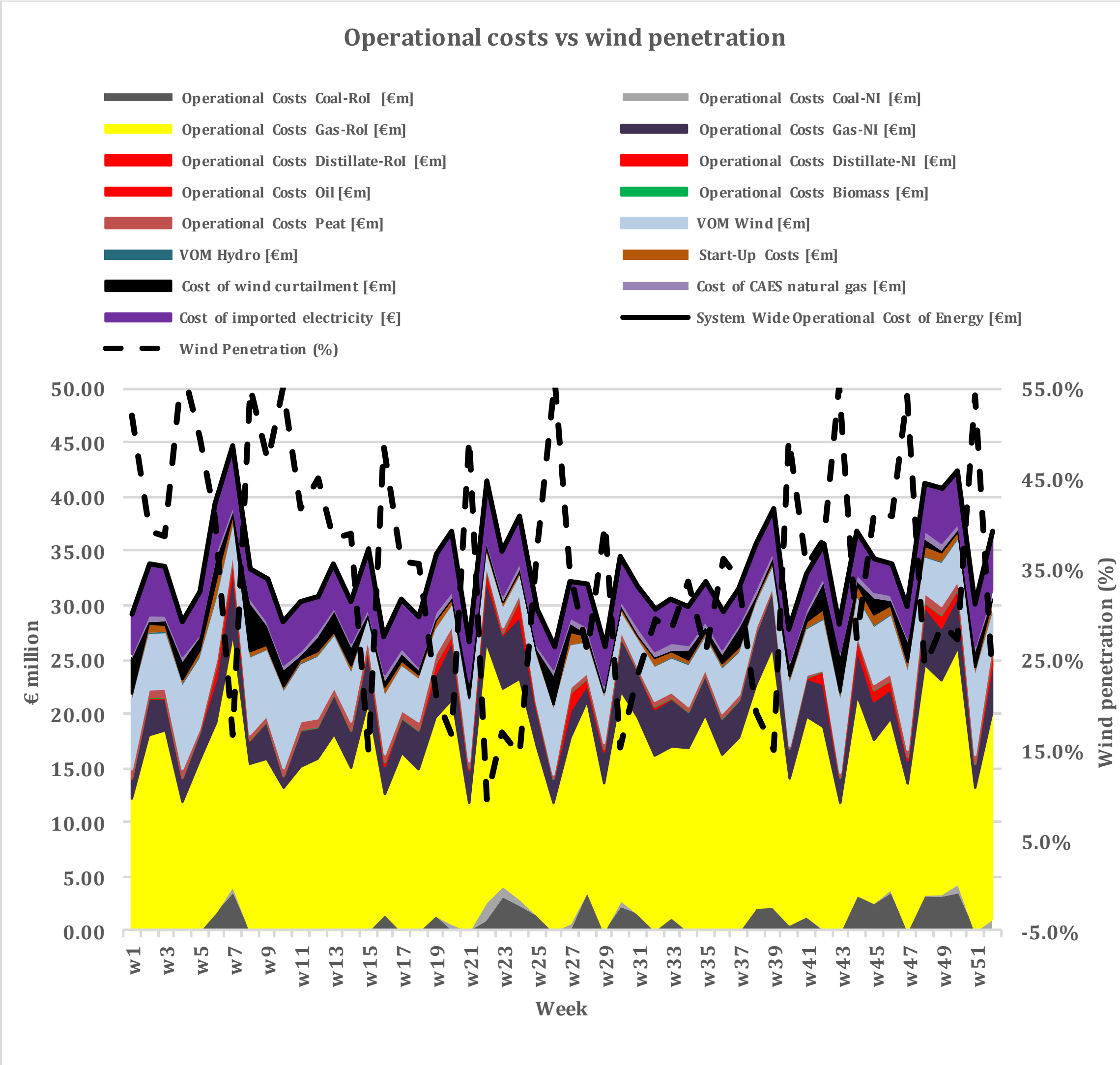

Figure 7-13: Breakdown of operational costs of the Irish system on a weekly basis (€/MWh) (Scenario: Reference+270MW CAES in NI (FP).

7.4.4 Scenario: Reference + 270MW CAES in NI (TE model)

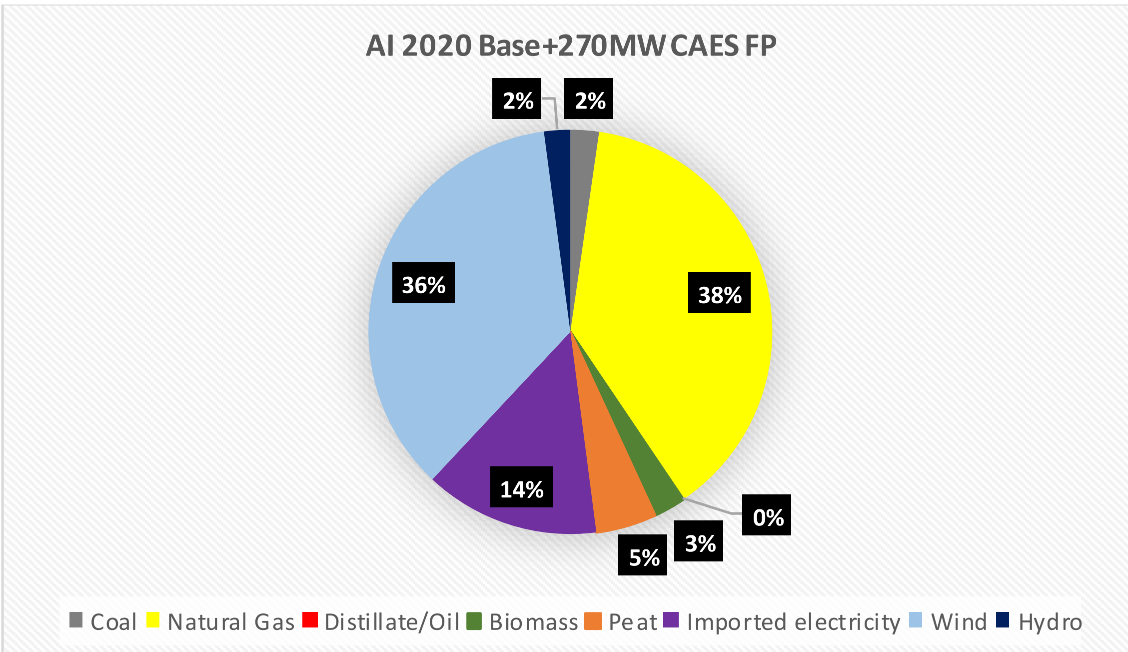

Figure 7-14: Energy mix in AI in 2020. (Scenario: Reference+ 270MW CAES in NI (TE)).

The differences on generation if the CAES TE model is used are not very different compared to the FP model. However, the CAES unit operates for much less time. In the FP model the CAES unit used a for energy arbitraging while in the TE model the CAES unit is used a lot for decreasing wind curtailment and increasing system flexibility (allow more flexible units jump in and accommodate wind variability). Total wind penetration is slightly higher compared to the FP model and imported electricity increases by ~85,0000MWh.

Generation graphs 7-15 and 7-16 represent the Reference+270MW CAES (TE) for the same periods presented before. Comparing with figures 7-12 and 7-13 it is evident that the CAES unit operates for less time in the TE model.

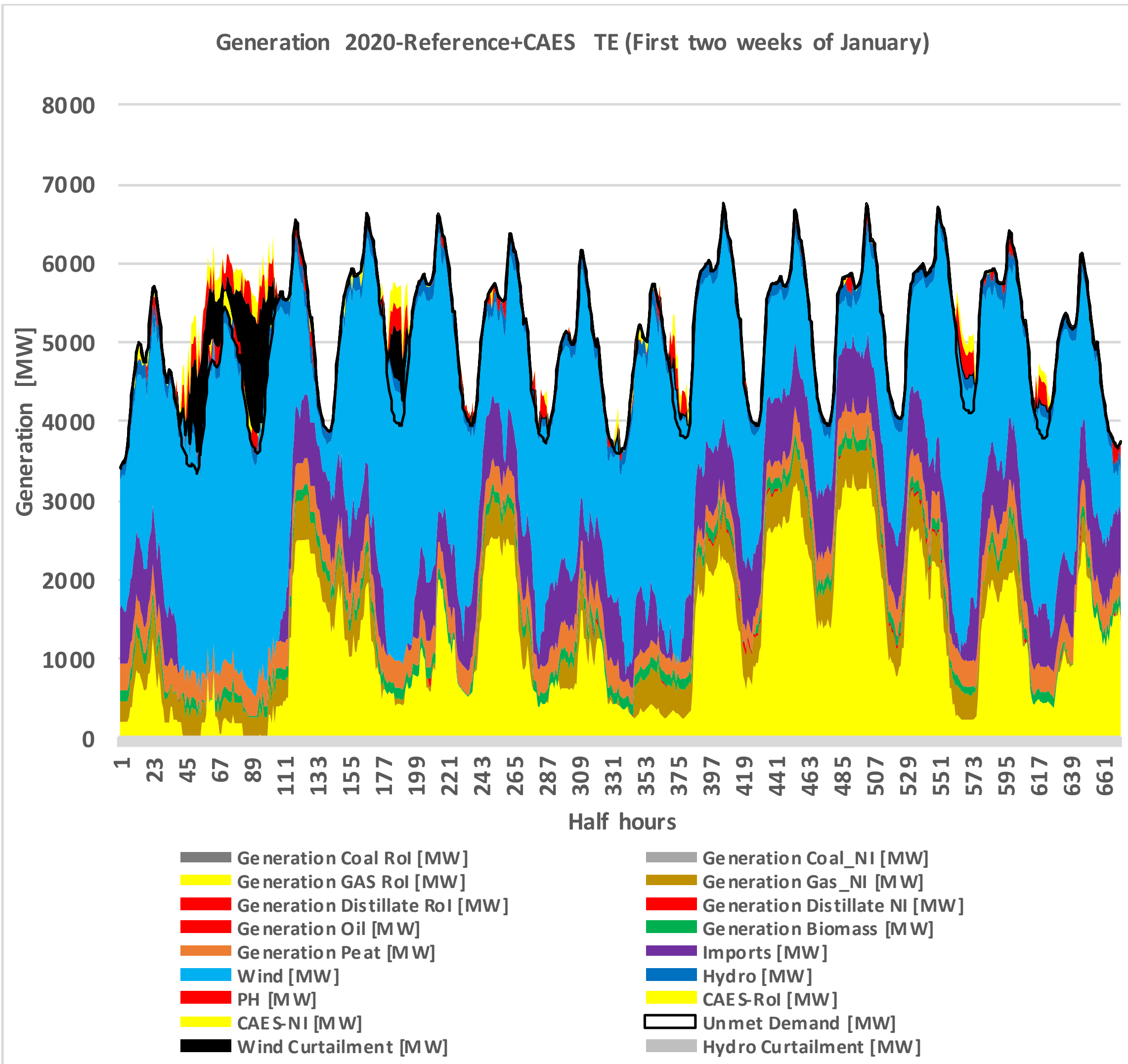

Figure 7-15: Generation per fuel over the first two weeks of January 2020 in AI (Scenario: Reference+270MW CAES in NI (TE)).

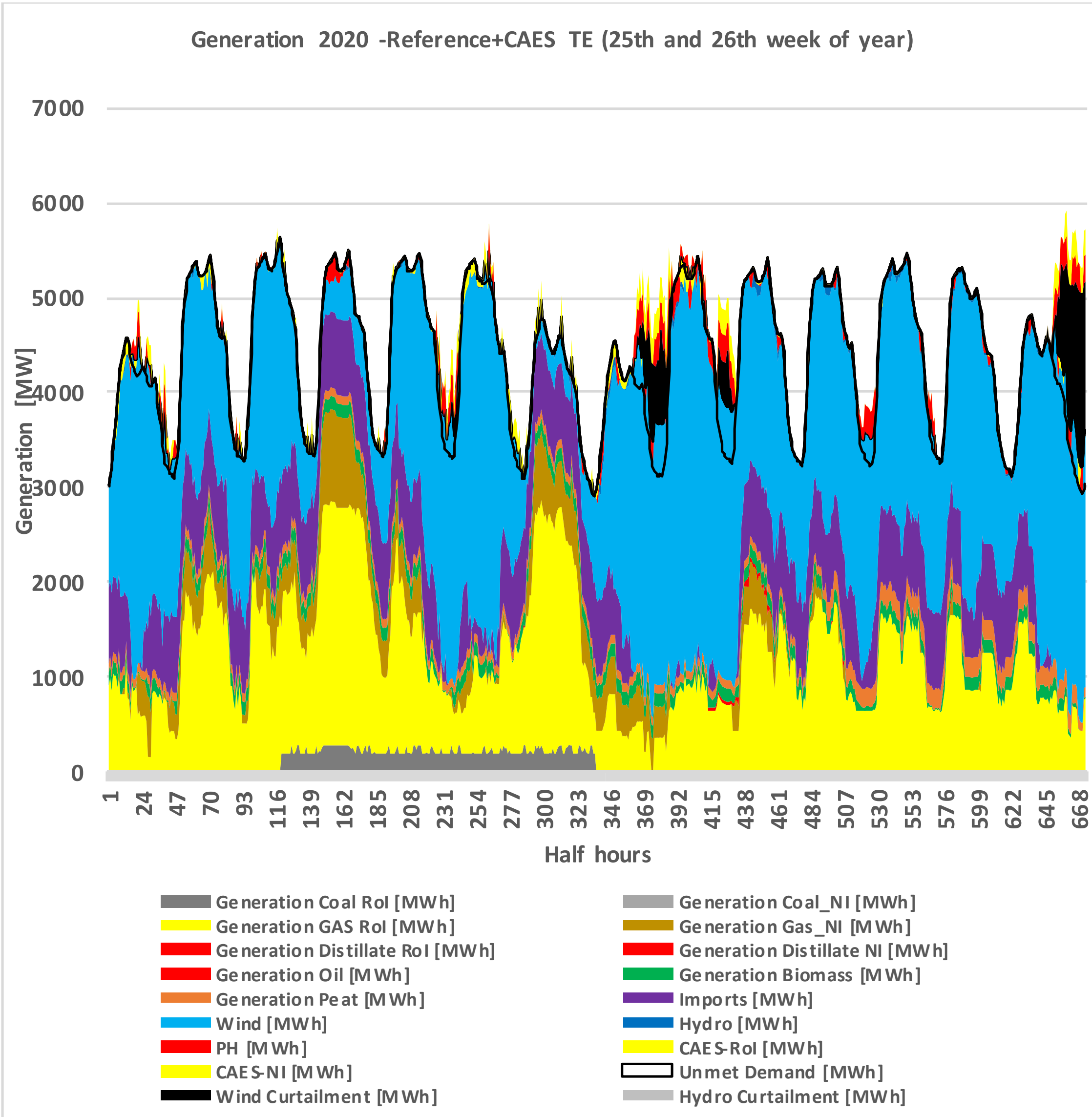

Figure 7-16: Generation per fuel over the 25th and 26th week of 2020 in AI (Scenario: Reference+270MW CAES in NI (TE)).

The economic benefit of the CAES unit using the TE model is much smaller compared to the FP (€6 million compared to €13 million). The most important cost savings in the system are related to reduction on wind curtailment and on reduction on coal consumption for power generation. Both costs have been reduced by €22 million. The average operational system cost in the “Reference+270MW CAES (TE) in NI” scenario is €39.5/MWh. A break-down of operational system costs in a weekly basis is given in figure 7-17.

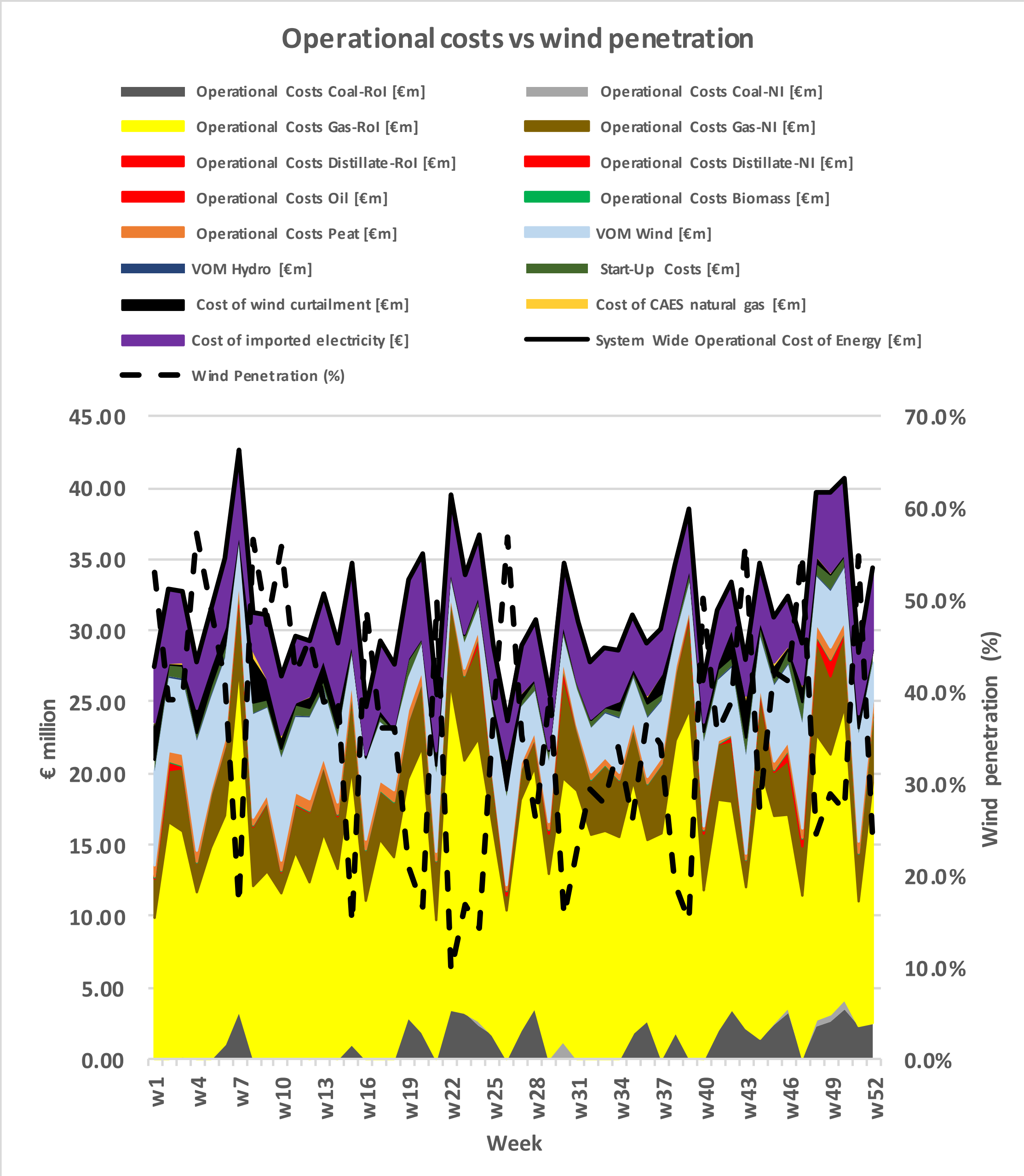

Figure 7-17: Breakdown of operational costs of the Irish system on a weekly basis (€/MWh) (Scenario: Reference+270MW CAES in NI (TE)

7.4.5 Reference scenario + 25% more wind

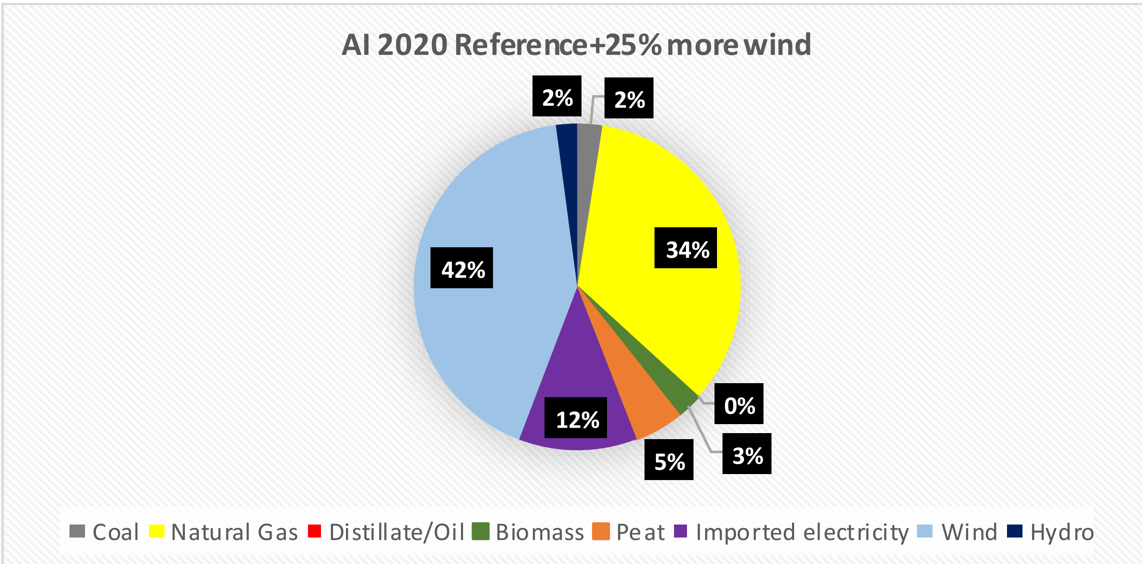

Figure 7-18: Energy mix in AI in 2020. (Scenario: Reference+25% more wind).

If the wind output is scaled up by 25% the energy mix changes. Wind contribution in the energy mix reaches 42% compared to 36% in the Reference scenario. At the same time wind curtailment reaches 8% of the 19TWh of wind produced throughout the year. Natural gas fired generation will only provide 34% of total energy compared to 38% in the Reference scenario. Similarly imported electricity is reduced from 14% to 12% of total internal demand.

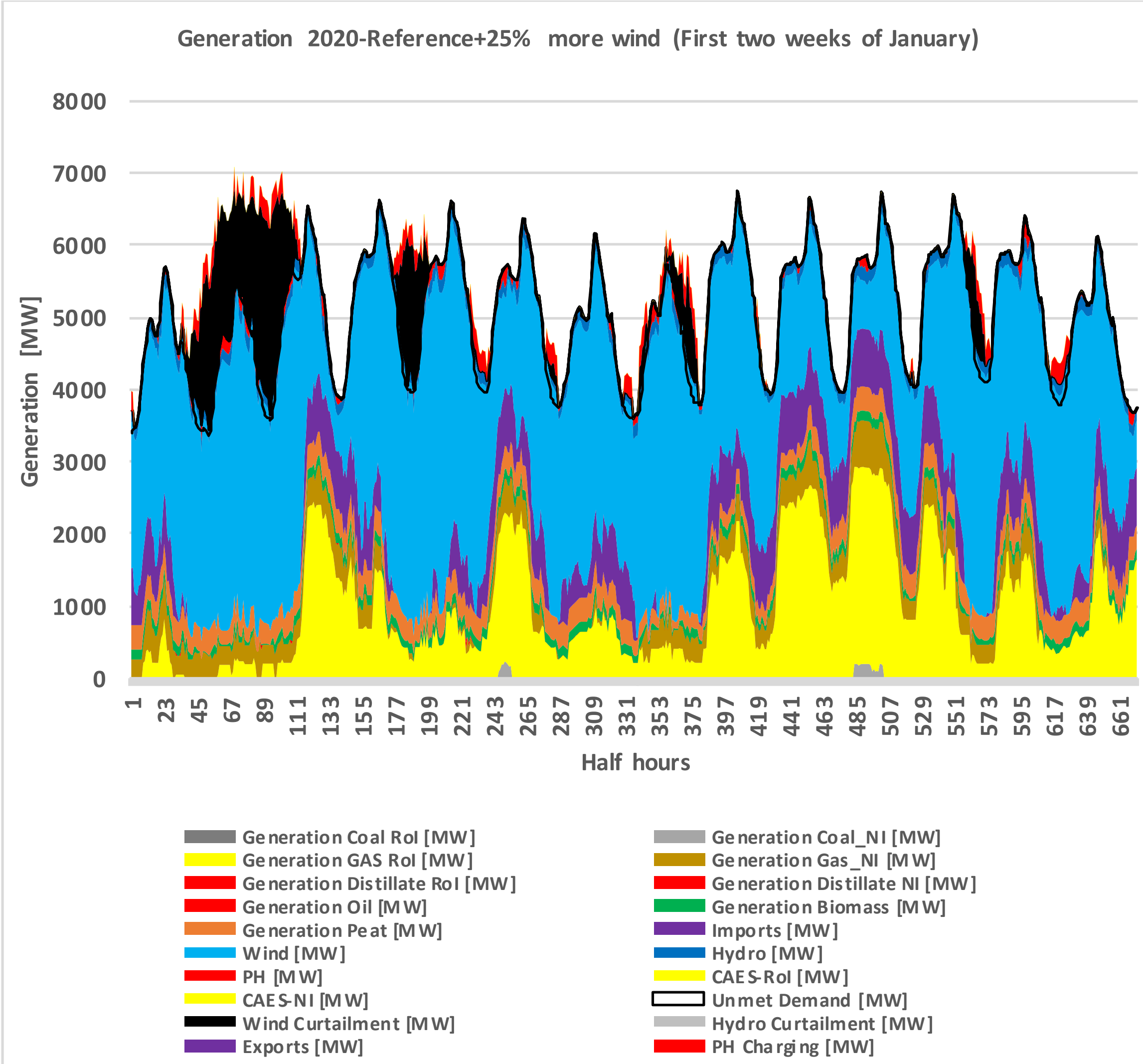

Figure 7-19: Generation per fuel over the first two weeks of January 2020 in AI (Scenario: Reference+25% more wind).

Figures 7-19 and 7-20 show generation over the first two weeks in the beginning of the year (January) and the middle of the year (mid-June) respectively similarly as in the scenarios discussed before. Comparing figures 7-19 and 7-20 with figures 7-2 and 7-3 respectively we observe the following:

1. Wind pushes thermal generator even further down during high wind periods.
2. Events of wind generation exceeding demand become more frequent. The same is true for number of hours with wind curtailment.

3. The pumped storage device operates for longer periods to accommodate wind.

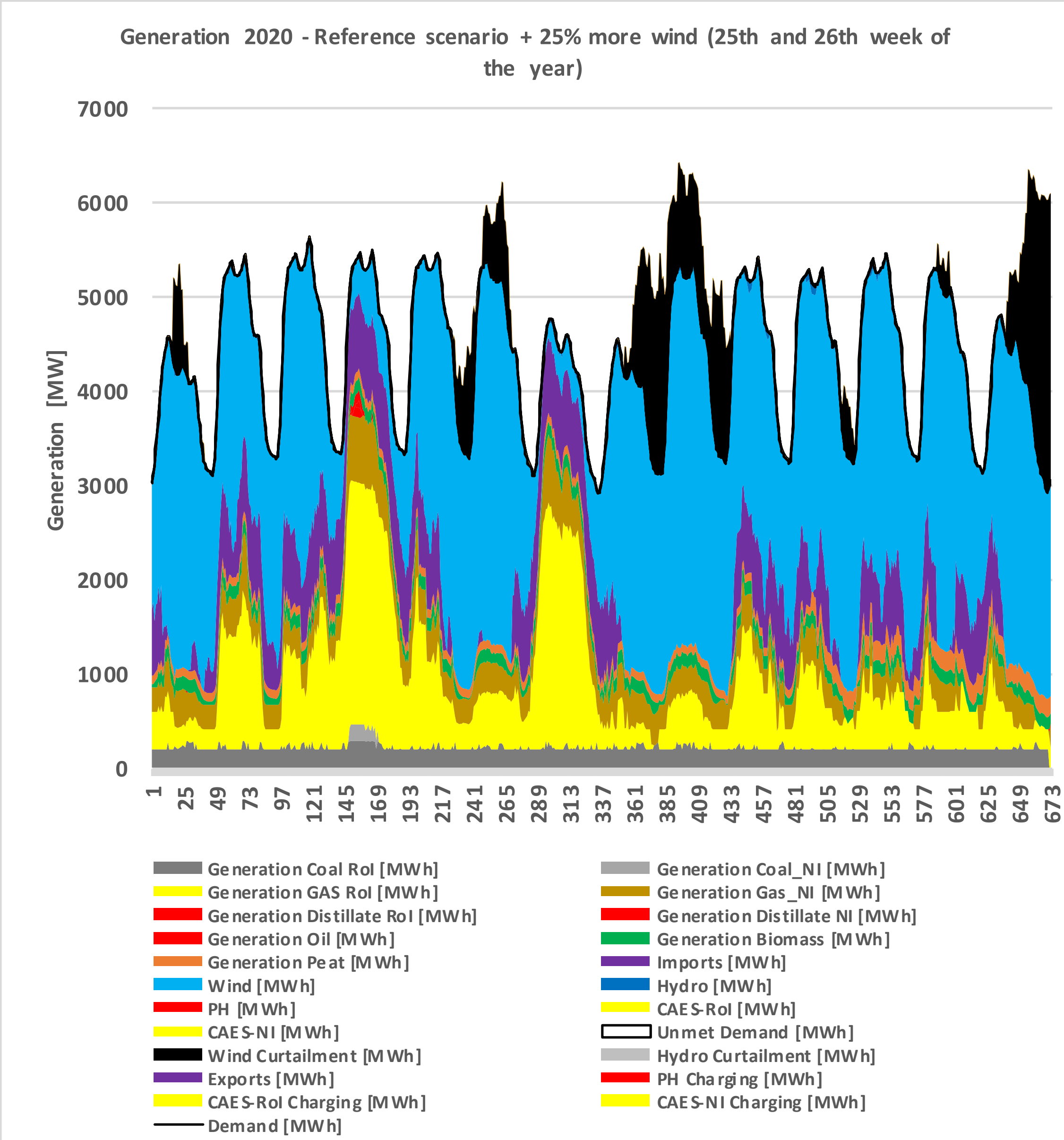

Figure 7-20: Generation per fuel over the 25th and 26th week of 2020 in AI (Scenario: Reference+25% more wind).

Figures 7-21 to 7-23 show the effect of emission from cycling of thermal generators. Comparing figure 7-21 with 7-5 we can observe that higher wind penetration increases the cycling of gas generators and the resulting part-loading emissions. The average weekly emissions for natural gas don't change throughout the year however, emissions from oil change a lot similarly as in the Reference scenario (see figure 7-25).

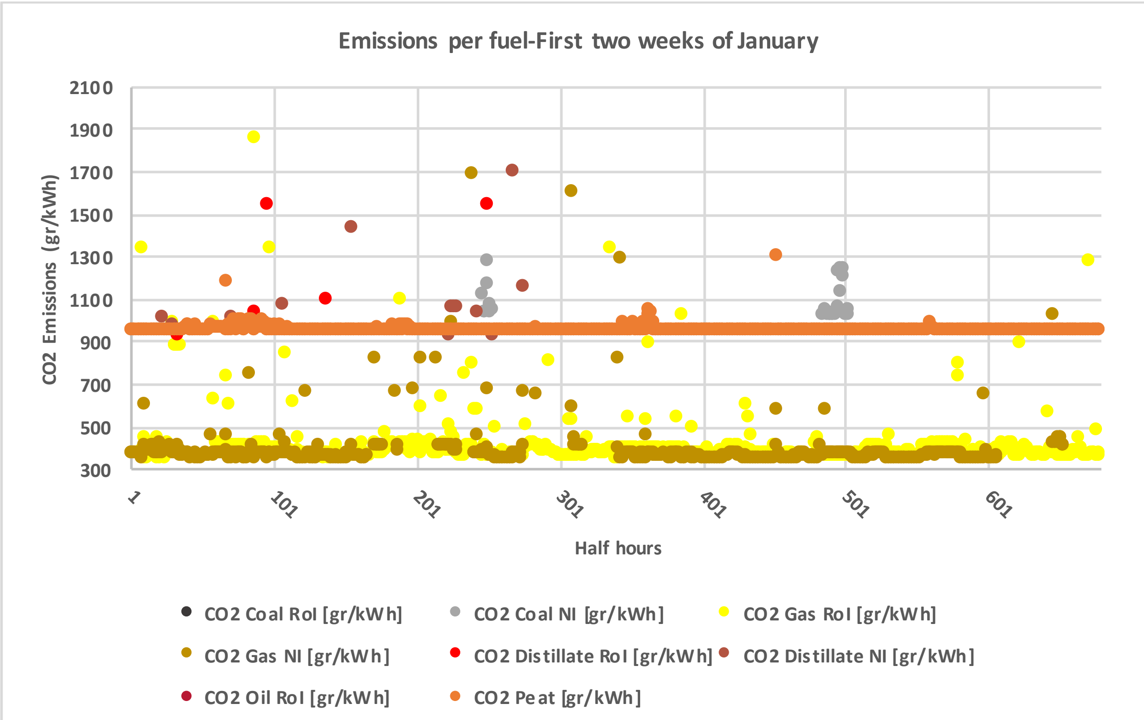

Figure 7-21: CO2 emissions over the first 2 weeks of January (Scenario: Reference+25% more wind).

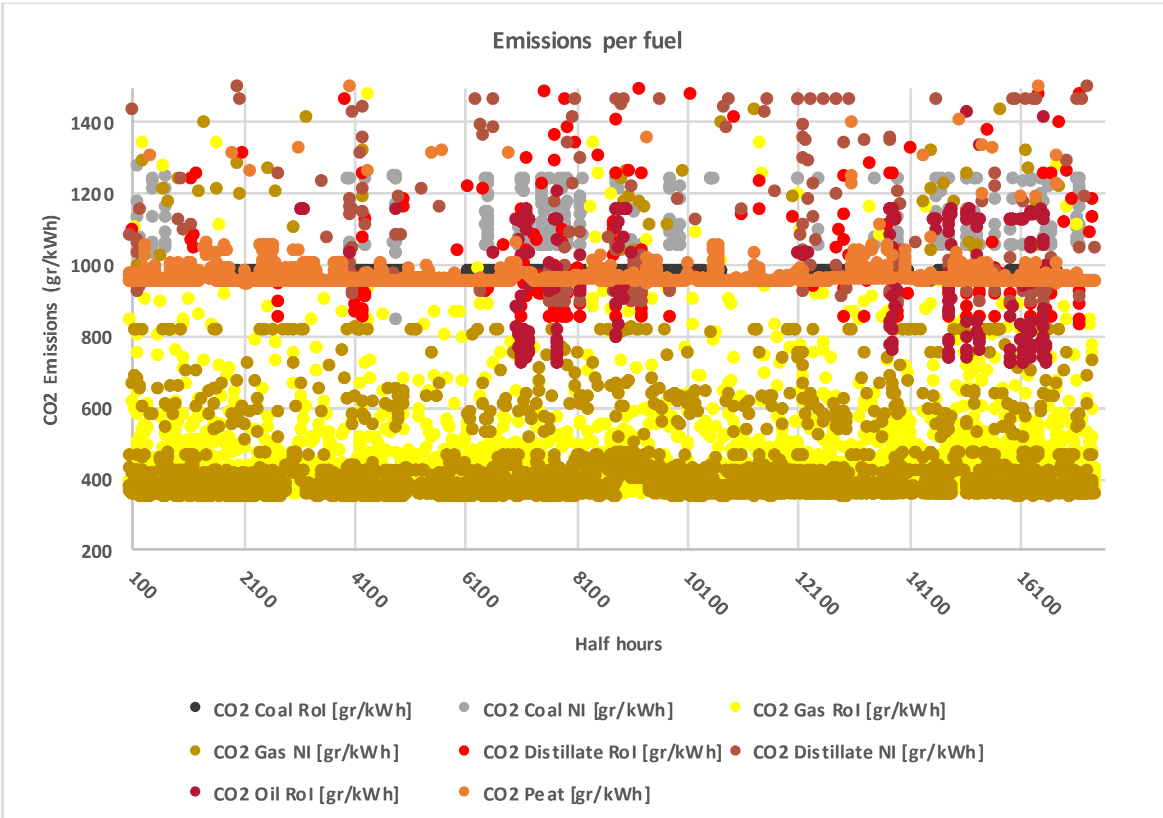

Figure 7-22: CO2 emissions over the whole year (Scenario: Reference+25% more wind).

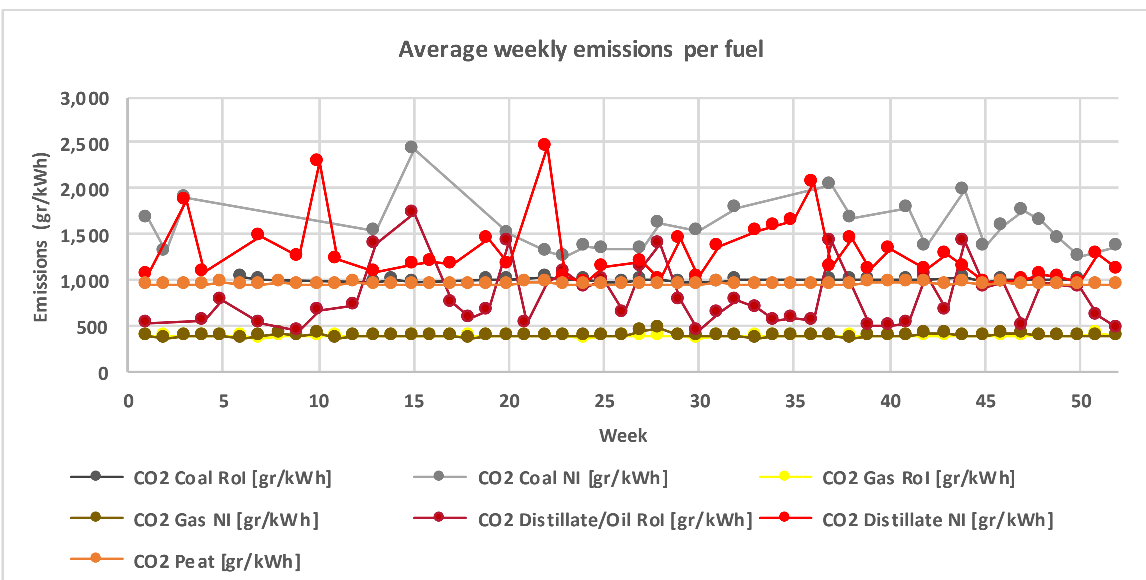

Figure 7-23: Average emission levels per week for various fuel types (Scenario: Reference+25% more wind).

Total average operational cost of the Irish system in 2020 will be €40.3/MWh for the Reference+25% more wind scenario which is higher than the Reference scenario. In the Reference+25% more wind scenario all cost components -but the cost of wind curtailment and the VOM of wind -are lower. However, the resulting high levels of wind spillage make the annual operational costs more expensive by €25 million. A breakdown of operational system costs per unit of energy produced in shown in figure 7-26.

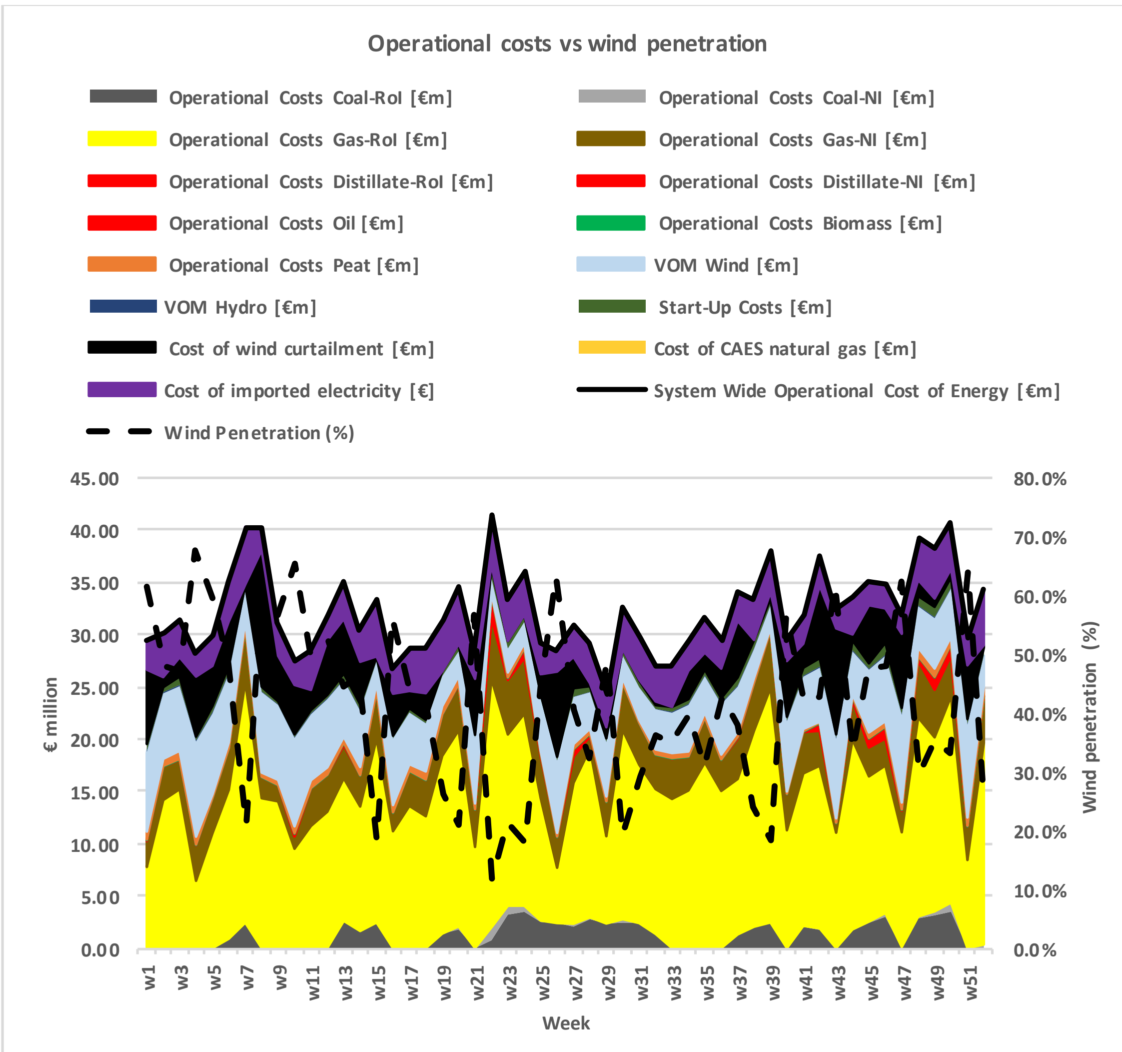

Figure 7-24: Breakdown of operational costs of the Irish system on a weekly basis (€/MWh) (Scenario: Reference+25% more wind.

7.4.6 Scenario: Reference +25% more wind+3x CAES (FP model)

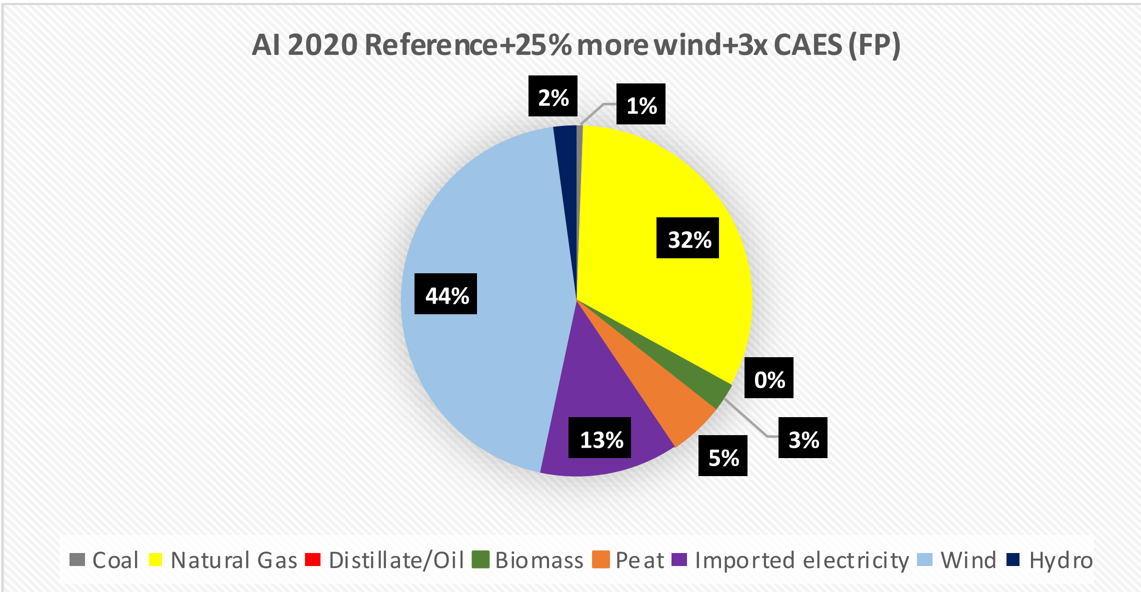

Figure 7-25: Energy mix in AI in 2020. (Scenario: Reference+25% more wind+3x CAES (FP)).

The presence of 810MW of CAES in the Irish system increases wind penetration by 650GWh on an annual basis compared to the Reference+25% more wind scenario. Wind generation reaches 44% of total internal demand over the whole year. At the same time the share of natural gas fired generation drops from 34% to 32% and of coal fired generation from 2% to 1% compared to the Reference+25% more wind scenario. Total wind curtailment drops from 8.1% of total wind generation to 4.7%.

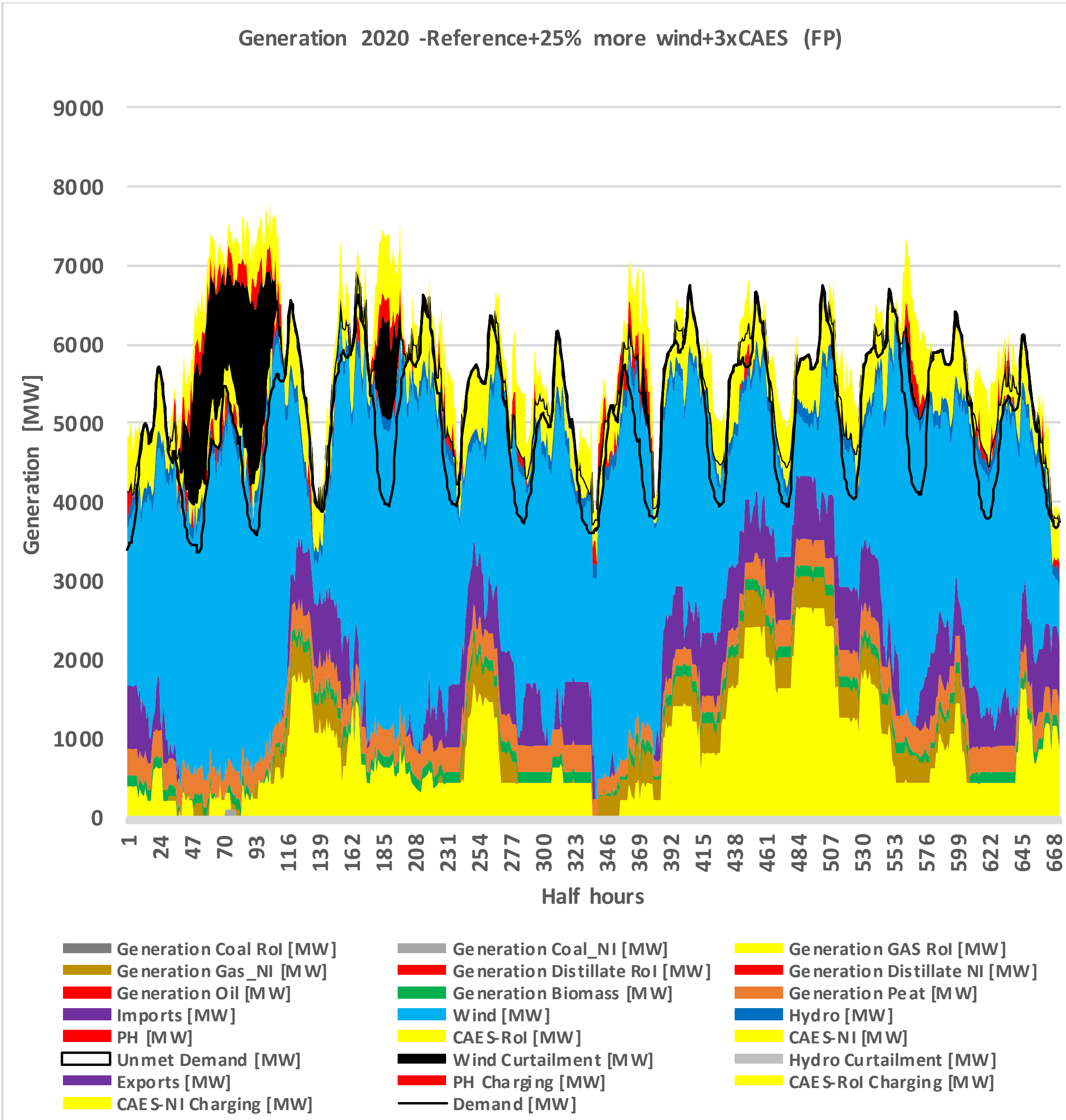

Figure 7-26: Generation per fuel over the first two weeks of January 2020 in AI (Scenario: Reference+25% more wind+3x CAES (FP)).

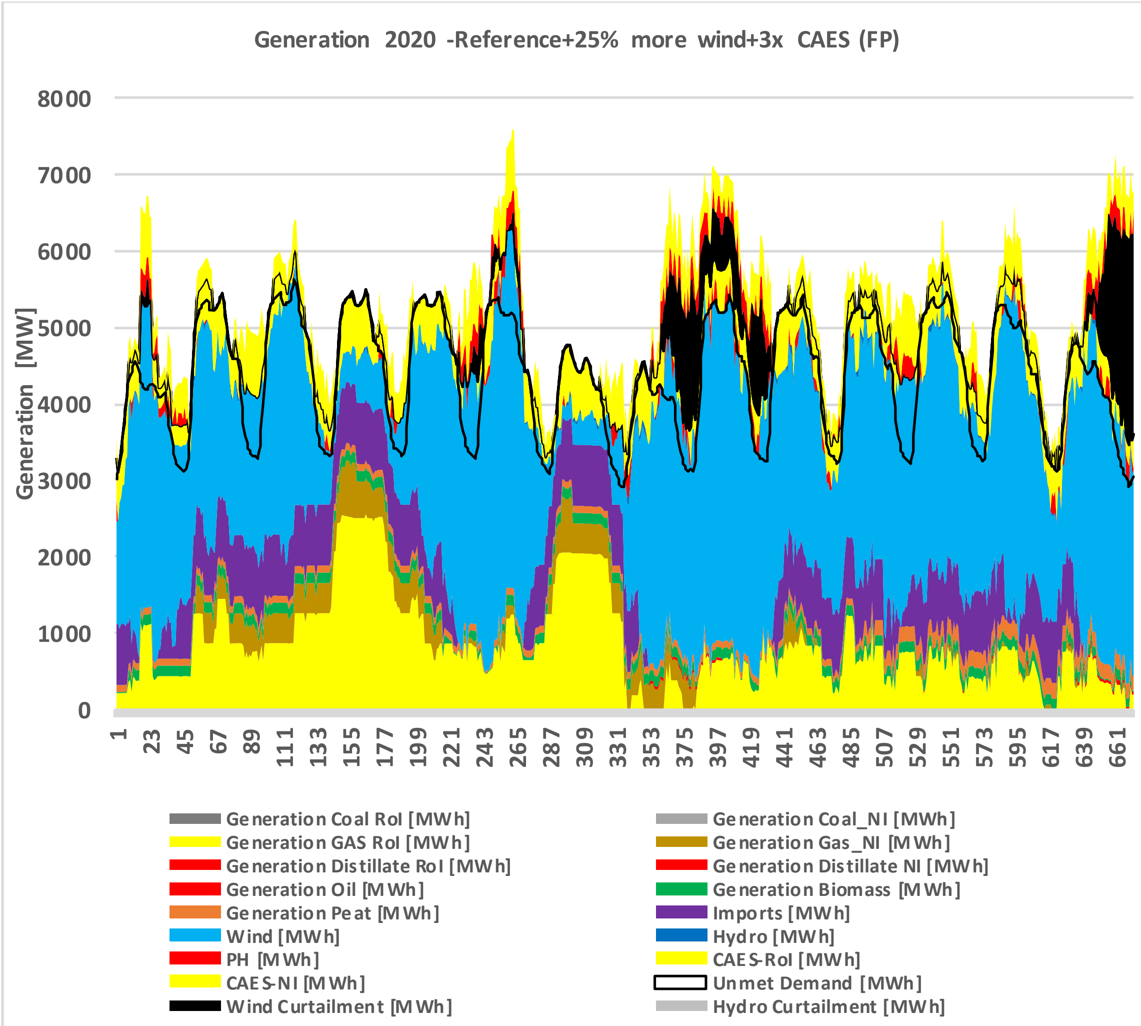

Figure 7-27: Generation per fuel over the 25th and 26th week of 2020 (mid-June) in AI (Scenario: Reference+25% more wind+3x CAES (FP)).

Figures 7-26 and 7-27 show generation over the same two weeks presented (compare with figures 7-19 and 7-20). In the Reference+25% more wind+3x more CAES, the storage capacity reaches ~15% of annual peak demand. As the graphs show the storage units come on line very often to:

1. Reduce effectively wind curtailment (this is depicted when CAES is charging during high wind output periods).

2. To provide immediate load following services (this is depicted when CAES operates during rapid increase/decrease of the net load.
3. Provide peak load reduction (this happens when CAES discharges during peak periods to prevent expensive peak units from coming on line).
4. Effectively reduce the number of thermal start-ups by 11% compared to the Reference+25% more wind scenario.

The system-wide economic benefits of CAES in the Reference+25% more wind +3 CAES (FP) scenario are significantly higher compared to the Reference+270MW CAES (FP). The reduction on total system operational cost is equal to €77 million. The most important cost savings in the system compared to the Reference+25% more wind scenario are related to a) reduction on wind curtailment, b) fuel savings due reduction on coal consumption for power generation resulting from increased penetration of wind energy and c) fuel savings due reduction on natural gas consumption for power generation. All costs together are reduced by €212 million. However the operational system costs for CAES are equal to € 129 million. The average operational system cost in the "Reference+25% more wind+3xCAES (FP)" scenario is €39.2/MWh. A break-down of operational system costs in a weekly basis is given in figure 7-28.

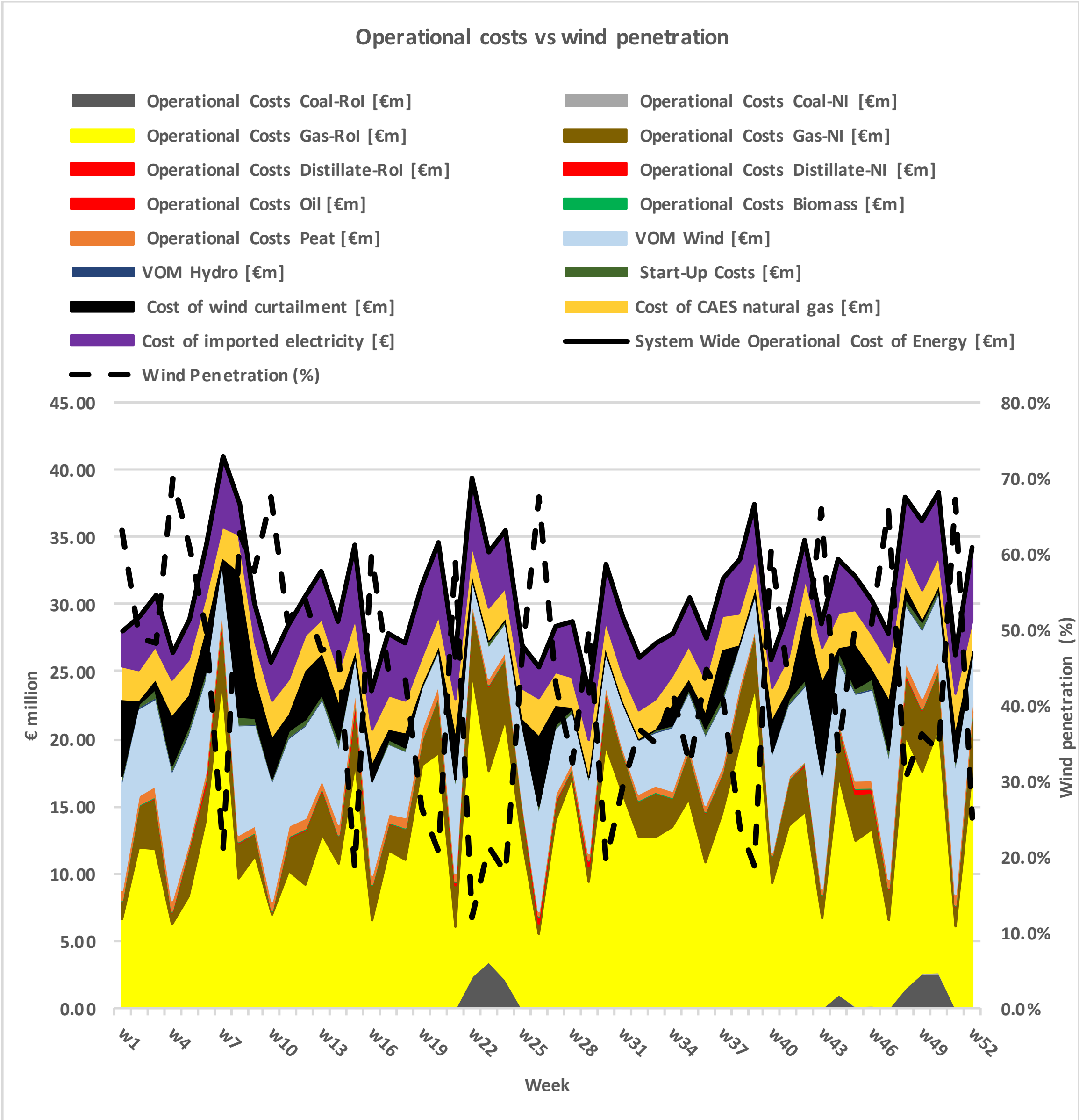

Figure 7-28: Breakdown of operational costs of the Irish system on a weekly basis (€/MWh) (Scenario: Reference+25% more wind+3x CAES (FP)).

7.4.7 Scenario: Reference +25% more wind+3x CAES (TE model)

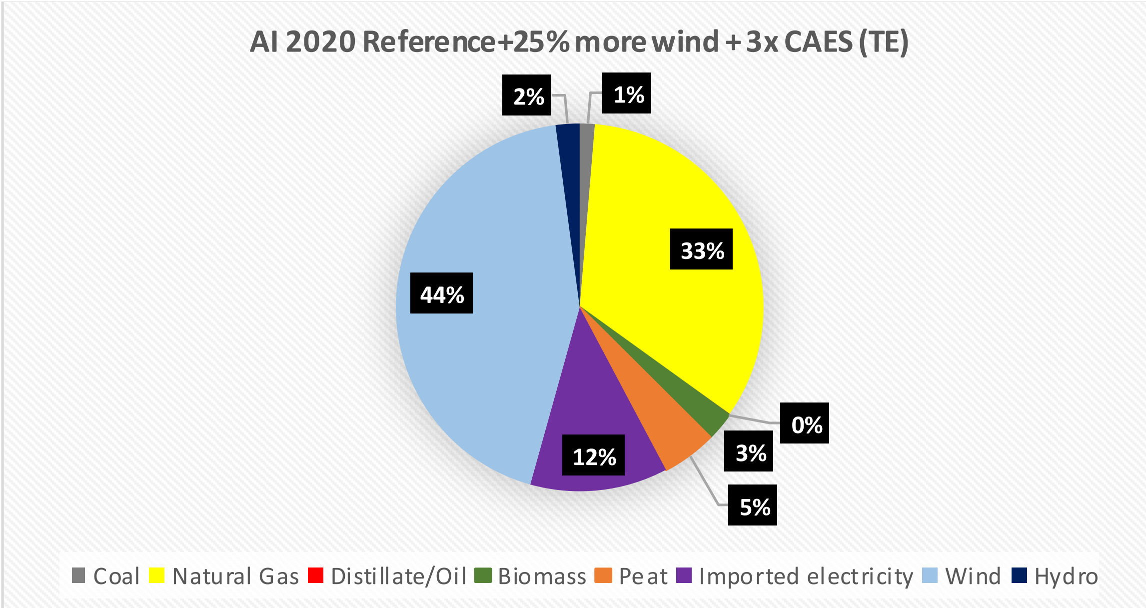

Figure 7-29: Energy mix in AI in 2020. (Scenario: Reference+25% more wind+3x CAES (TE)).

The generation mix results for the CAES TE model are not very different compared to the FP one. The presence of 810MW of CAES in the Irish system increases wind penetration by 564GWh on an annual basis compared to the Reference+25% more wind scenario. Wind generation reaches 44% of total internal demand over the whole year. At the same time the share of natural gas fired generation drops from 34% to 33% and of coal fired generation from 2% to 1% compared to the Reference+25% more wind scenario. Total wind curtailment drops from 8.1% of total wind generation to 5.1%.

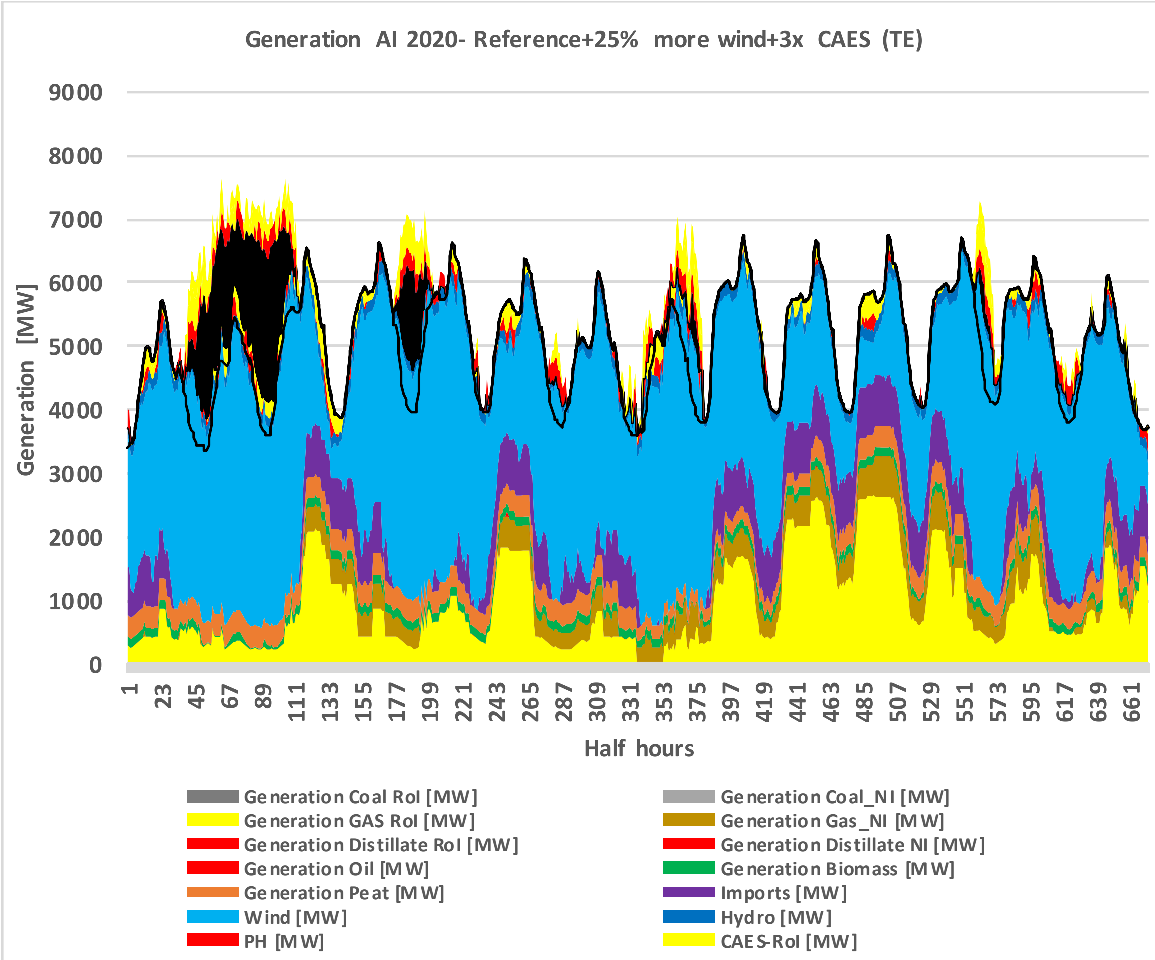

Figure 7-30: Generation per fuel over the first two weeks of January 2020 in AI (Scenario: Reference+25% more wind+3x CAES (TE)).

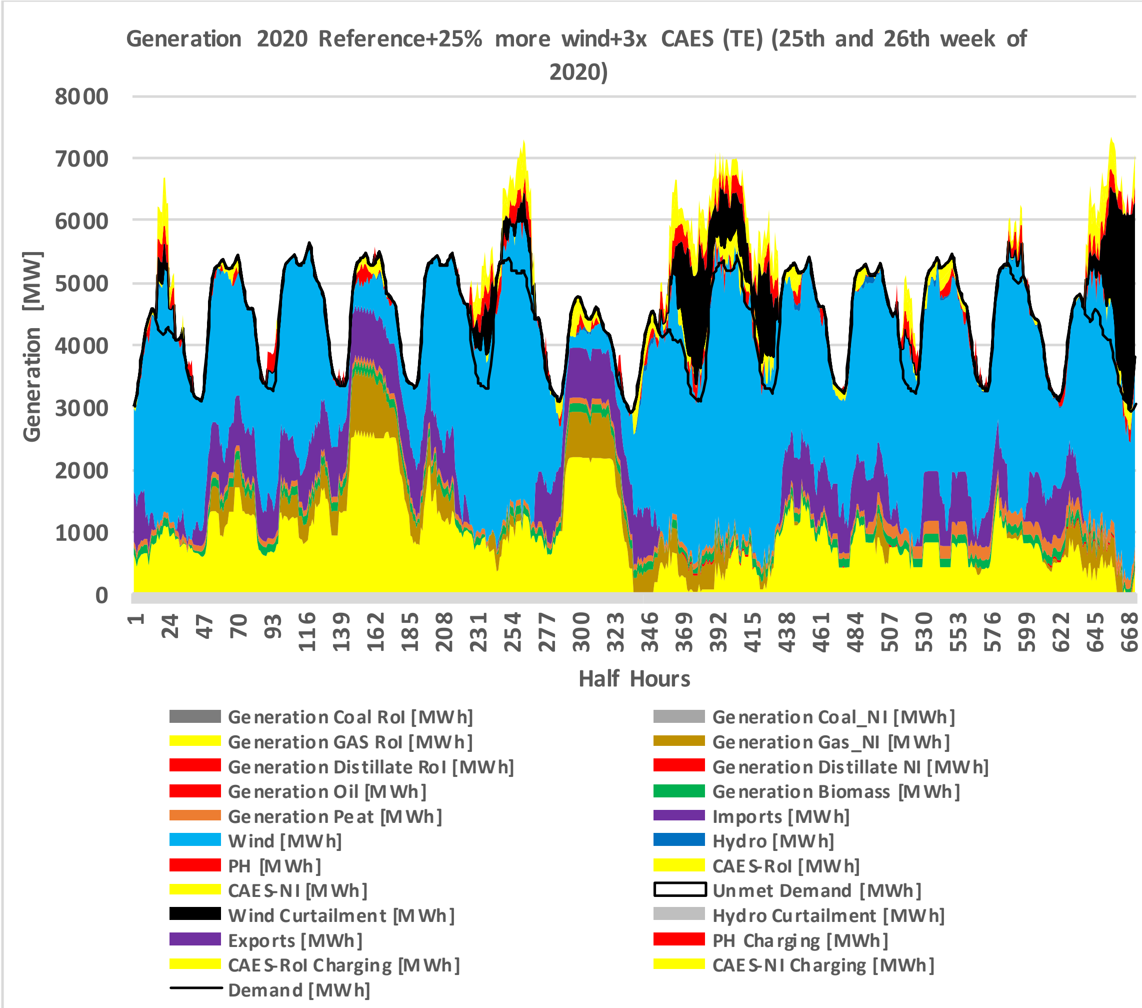

Figure 7-31: Generation per fuel over the 25th and 26th week of 2020 (mid-June) in AI (Scenario: Reference+25% more wind+3x CAES (TE)).

Comparing figures 7-29 and 7-30 with figures 7-26 and 7-27 we observe that the CAES units –when using the TE model- are operated for less time compared to the FP model. Actually the CAES units in the FP model operates 4.6 times as much as in the TE model. The CAES in the TE model operates mainly for reducing wind curtailment and secondarily to increase system flexibility over sudden changes of wind power.

The economic benefits of CAES in the Reference+25% more wind +3 CAES (TE) scenario are significantly higher compared to the Reference+270MW CAES (TE). The reduction on total system operational cost is equal to €86 million on an annual basis compared to €76 million for the FP model. This is an interesting finding considering that the Reference+270MW CAES (TE) scenario results exhibited significantly lower economic benefits compared to the Reference+270MW FP scenario results. Thus, it is evident that the CAES TE returns slightly lower performance on wind curtailment reduction in all cases, however, the economic benefit depends on the size of storage capacity and the total wind production. The economic benefits of CAES TE significantly grow with higher storage capacity and wind production.

The most important cost savings in the system compared to the Reference+25% more wind scenario are related to a) reduction on wind curtailment, b) fuel savings due reduction on coal consumption for power generation and c) fuel savings due reduction on natural gas consumption for power generation . All above costs are reduced by €128 million. As discussed earlier CAES operational costs are 4.6 times compared to the FP model because the CAES unit is used for less time in the TE model. The average operational system cost in the “Reference+25% more wind+3xCAES (FP)” scenario is €38.3/MWh. A break-down of operational system costs in a weekly basis is given in figure 7-32.

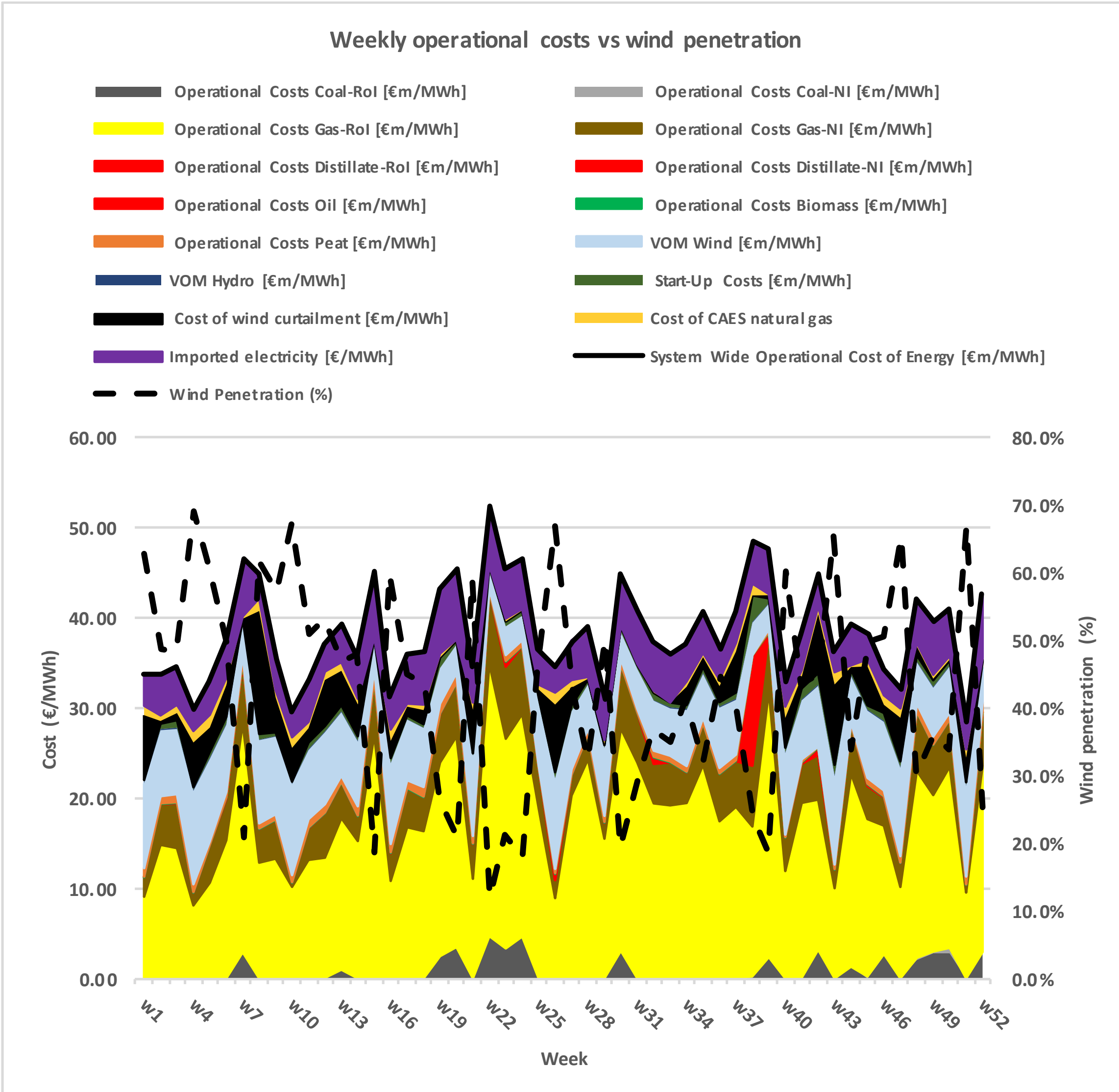

Figure 7-32: Breakdown of operational costs of the Irish system on a weekly basis (€/MWh) (Scenario: Reference+25% more wind+3x CAES (TE)).

BIBLIOGRAPHY

[1] E. Ela, V.Diakov, E. Ibanez and M. Heaney, "Impacts of Variability and Uncertainty in Solar Photovoltain Generation at Multiple Timescales," NREL, 2013.

[2] B. Kirby, "Ancillary Services: Technical and Commercial Insights," WARTSILA, 2007.

[3] P. Denholm, B. K. E Ela and M. Milligan, "The Role of Energy Storage with Renewable Electricity," NREL, 2010.

[4] T. NIkolakakis and V. Fthenakis, "The Optimum Mix of Electricity from Wind and Solar Sources in Conventional Power Systems: Evaluating the Case for New York State," *Energy Policy,* vol. 39, pp. 6972-6980, 2011.

[5] R. Kempener, P. Komor and A. Hoke, "Smart Grids and Renewables. A Guide for Effective Deployment," IRENA, 2013.

[6] A. Mills and R. Wiser, "Implication of Wide-Area Geographic Diversity for Short-Term Variability of Solar Power," LBNL, 2009.

[7] Electricity Storage Association, 2009. [Online]. Available: www.electricitystorage.org. [Accessed 2009].

[8] H. Ibrahim, A. Ilinca and J. Perron, "Energy Storage Systems-Characteristics and Comparisons," *Renewable and Sustainable Energy Reviews,* vol. 12, no. 5, pp. 1221-1250, 2008.

[9] G. P., "Compressed Air Energy Storage Engineering and Economic Study," NYSERDA, 2009.

[10] C. Richter, "Generation Control and Unit Commitment," in *Power Systems Stability and Control*, 2007.

[11] J. Klein, "THE USE OF HEAT RATES IN PRODUCTION COST MODELING AND MARKET MODELING," California Energy Commission , 1998.

[12] M. A. Iqbal, "Analysis and Comparison of Lambda Iteration, Genetic Algorithm and Particle Swarm Optimization to Solve Economic Load Dispatch Problem," *International Journal of Software and Web Sciences (IJSWS),* pp. 60-64, 2012.

[13] J. Zhu, Optimization of Power System Operation, Wiley and Sons, 2015.

[14] A. Wood and B. Wollenberg, Power generation operation and control, Wiley and Sons, 1996.

[15] R. Mallipeddi and P. Suganthan, "Unit commitment - A survey and comparison of conventional and nature inspired algorithms," *International Journal of Bio-Inspired Computation,* vol. 6, no. 2, pp. 71-90, 2014.

[16] J. Zhu, Optimization of Power System Operation, New Jersey: Wiley and Sons, Inc, 2009.

[17] S. Soliman and A. A. Malawy, Modern Optimization Techniques with Applications to Power Systems, New York: Spriger, 2012.

[18] Wikipedia, "CPLEX in Wikipedia," [Online]. Available: https://en.wikipedia.org/wiki/CPLEX.

[19] A. Schoofs, "The Electricity Markets in Ireland," [Online]. Available: http://www.wattics.com/the-electricity-market-in-ireland/.

[20] The Competition Authority, "Competition on Electricity Sector," 2010. [Online].

[21] Commission for Energy Regulation, "CER Factsheet on the Single Electricity Market," April 2011. [Online]. Available: http://www.cer.ie/docs/000262/cer11075.pdf.

[22] R. Turvey, "Interconnector Economics," *Energy Policy,* vol. 34, pp. 1457-1472, 2006.

[23] A. Wilson, "Economically Rational Trading Between the All Island Single Electricity Market and Great Britain; Theory vs Practice," Dublin, 2014.

[24] Mutual Energy A Northern Ireland company working for consumers, "Trading accross the Moyle interconnector," [Online]. Available: http://www.mutual-energy.com/electricity-business/moyle-interconnector/trading-across-the-moyle-interconnector/.

[25] EIRGRID, "The East West Interconnector: Delivering Electricity Trading Between Ireland and Great Britain," [Online]. Available: http://www.eirgridgroup.com/site-files/library/EirGrid/EWICTradingBrochure.pdf.

[26] SONI; EIRGRID, "All-Island Generation Capacity Statement 2016-2025," SONI;EIRGRID, 2016.

[27] EIRGRID and SONI, "All-Island Generation Capacity Statement 2015-2024," 2015.

[28] EIRGRID, "All Island Generation Capacity Statement 2016-2025," 2016.

[29] SONI, EIRGRID, "ALL-ISLAND GENERATION CAPACITY STATEMENT 2014-2015," 2015.

[30] ESB, "Power system overview and RES integration: Ireland. Facilitating energy storage to allow high penetration of intermittent renewable energy," 2013.

[31] EIRGRID and SONI, "All-Island Ten Year Transmission Forecast Statement 2013," 2013.

[32] EIRGRID and SONI, "The Need for a second North-South Electricity Interconnector: North-South 400kV Interconnection Development," 2015.

[33] Utility Regulator, "Natural Gas Market Overview," [Online]. Available: http://www.uregni.gov.uk/gas/market_overview/.

[34] Department of Communications, Energy and Natural Resources, "GAS," [Online]. Available: http://www.dcenr.gov.ie/energy/en-ie/gas/Pages/home.aspx#.

[35] Sustainagle Energy Authority of Ireland, "Energy Security in Ireland: A Statistical Overview," 2016.

[36] International Energy Agency (IEA), "Energy Policies of IEA Countries : Ireland. 2012 Review," Paris, 2012.

[37] J. Clancy, F. Gaffney, J. Deane, J. Curtis and B. O. Gallachoir, "Fossil fuel and CO2 emissions savivgs on a highly renewable electricity system- A single year case study for Ireland," *Energy Policy,* vol. 83, pp. 151-164, 2015.

[38] Accenture Analysis, "From Thermal Coal Production to Marketing and Trading: A Growth Opportunity for Coal Minining Industry in Asia Pacific," Accenture, 2013.

[39] Scotia Howard Weil, "Coal Weekly," 2016. [Online].

[40] argus, "ARGUS COAL DAILY INTERNATIONAL," March 2016. [Online]. Available: http://www.argusmedia.com/coal/argus-coal-daily-international/. [Accessed March 2016].

[41] Arthur Cox, "Overview of the Regulation of the Electricity Sector in Ireland," 2015.

[42] Redpoint Energy, "Validation of market simulation software," 2010.

[43] (CER), Commission for Energy Regulation, "Validation of market simulation software in SEM to end 2012," Dublin, 2011.

[44] EIRGRID, "Grid 25 A Strategy for the Development of Ireland's Electricity Grid for a Sustainable and Competitive Future," 2010.

[45] J. Deane, A. Driscoll and B. O. Gallachoir, "Quantifying the Impacts of National Renewable Electricity Ambitions using a North-West European Electricity Market Model," *Renewable Energy,* vol. 80, pp. 604-609, 2013.

[46] S. Bliss, "the bliss point," 30 December 2013. [Online]. Available: https://theblisspoint.org/2013/12/30/the-eu-emission-trading-scheme-band-aid-for-a-broken-market/.

[47] European Commission, "Quarterly Report on European Gas Markets: Market Observatory for Energy (volume 7, issue 3)," 2017.

[48] European Commission, "The Market for Solid Fuels in the European Union in 2010 and the Outlook for 2011," 2011.

[49] J. Clancy, F. Gaffney, J. Deane, J. Curtis and B. O. Gallachoir, "Fossil fuel and CO2 emissions savings on a high renewable electricity system- A single year case study for Ireland," *Energy Policy,* vol. 83, pp. 151-164, 2015.

[50] OECD, IEA and NEA, "Projected Costs of Generating Electricity," 2010.

[51] IRENA, "RENEWABLE ENERGY TECHNOLOGIES: COST ANALYSIS SERIES," 2012.

[52] P. Denholm, E. Ela, B. Kirby and M. Milligan, "The Role of Energy Storage," National Renewable Energy Laboratory (NREL), 2010.

[53] M. Henderson, "Energy Storage in Deregulated Power Markets," *IEEE SMART GRID,* December 2013.

[54] E. Drury, P. Denholm and R. Sioshansi, "The Value of Compressed Air Energy Storage in Energy and Reserve Markets," NREL, 2010.

[55] Y. Gu, J. McCalley, M. Ni and R. Bo, "Economic Modelling of Compressed Air Energy Storage," *Energies,* vol. 6, pp. 2221-2241, 2013.

[56] G. S. Henrik Lund, "The role of compressed air energy storage (CAES) in future sustainable energy systems," *Energy Conversion and Management,* vol. 50, no. 5, p. 1172–1179, 2009.

[57] D. Wolf, A. Kanngieber, M. Budt and C. Doetch, "Adiabatic Compressed Air Energy Storage co-located with wind energy—multifunctional storage commitment optimization for the German market using GOMES," *Energy Systems,* vol. 3, p. 181–208, 2012.

[58] A. Foley and I. D. Lobera, "Impacts of compressed air energy storage plant on an electricity market with a large renewable portfolio," *Energy,* vol. 57, pp. 85-94, 2013.

[59] B. Cleary, A. Duffy, A. O. Connor, M. Conlon and V. Fthenakis, "Assessing the Economic Benefits of Compressed Air Energy Storage for Mitigating Wind Curtailment," *IEEE TRANSACTIONS ON SUSTAINABLE ENERGY,* vol. 6, no. 3, pp. 1021 - 1028, 2015.

[60] S. Mullendore, "Energy Storage and Electricity Markets: The value of storage to the power system and the importance of electricity markets in energy storage economics," Clean Energy Group, 2015.

[61] E. Ela, M. Milligan, B. Kirby, E. Lannoye, D. Flynn, M. O. Malley and B. Zavadil, "Evolution of Operating Reserve Determination in Wind Power Integration Studies," NREL, 2010.

[62] Sustainable Energy Ireland, "Operating Reserve Requirements as Wind Power Penetration Increases in the Irish Electricity System," Dublin, 2004.

[63] SONI, "Ancillary Services Statement of Payments and Charges: Available from October 1st 2015," SONI, 2015.

[64] DOE, EPRI, "2013 Electricity Storage Handbook in Collaboration with NRECA," Sandia National Laboratories, 2013.

[65] EIRGRID, SONI, "DS3: System Services Review TSO Recommendations," 2013.

[66] EIRGRID plc, "ALL ISLAND TSO FACILITATION OF RENEWABLES STUDIES: Final Report for Lot3/ENQEIR132," 2010.

[67] E. M. Garrigle, J. Deane and P. Leahy, "How much wind energy will be curtailed on the 2020 Irish power system?," *Renewable Energy,* vol. 55, pp. 544-553, 2013.

[68] stoRE, "Does Ireland need more storage? Power system overview and RES integration," 2013.

[69] NREL, "Wind integration cost and cost causation," 2013.

[70] EIRGRID, "Interconnection Economic Feasibility Report," 2009.

[71] European Parliament, "Biomass for Electricity and Heating: Opportunities and challenges," 2015.

[72] EIRGRID;SONI, "The Need for a second North-South Electricity Interconnector," 2015.

[73] California Energy Commission, "California Clean Energy Future Metrics," [Online]. Available: http://www.energy.ca.gov/2011_energypolicy/documents/2011-07-06_workshop/background/Metrics_July_IEPR_Reserve_Margin_v5.pdf.

[74] EIRGRID;SONI, "All Island Generation Capacity Statement 2014-2023," 2014.

[75] Gaelectric, "Gaelectric energy storage: The missing link," 2015.

[76] National Grid, "Large Combustion Plant Directive," 2007.

[77] B. Cleary, "PhD thesis: A Techno-Economic Analysis of Wind Generation in Conjunction with Compressed Air Energy Storage in the Integrated Single Electricity Market," Dublin, 2016.